BINDING SERVICES
Tel +44 (0)29 2087 4949
Fax +44 (0)29 20371921
e-mail bindery@cardiff.ac.uk

GLOBAL VIBRATION ANALYSIS OF SYMMETRIC AND ASYMMETRIC HIGH RISE BUILDINGS

BEHZAD RAFEZY

BSc, MSc

This dissertation is being submitted in partial fulfilment of the requirement for the degree of Doctor of Philosophy

School of Engineering, Cardiff University

2004

ProQuest LLC
789 East Eisenhower Parkway
P.O. Box 1346
Ann Arbor, MI 48106-1346

DECLARATION AND STATEMENTS

Declaration

This work has not previously been accepted in substance for any degree and is not being concurrently submitted in candidature for any degree.

Signed.....B. Rafezy.....(candidate)
Date .....29/9/04.....

STATEMENT 1

This thesis is the result of my own investigations, except where otherwise stated.
Other sources are acknowledged by footnotes giving explicit references. A bibliography is appended.

Signed.....B. Rafezy.....(candidate)
Date .....29/9/04.....

STATEMENT 2

I hereby give consent for my thesis, if accepted, to be available for photocopying and for inter-library loan, and for the title and summary to be made available to outside organisations.

Signed .....B. Rafezy.....(candidate)
Date .....29/9/04.....

ABSTRACT

This thesis presents two global analysis approaches to the calculation of the natural frequencies of high rise buildings. The structures are proportional and their component members are repeated at each storey level unless there is a step change of properties. Within this scope many geometric configurations can be encompassed, ranging from uniform structures with doubly symmetric floor plans to doubly asymmetric ones comprising plane frame and wall structures running in two orthogonal directions.

The first method utilises a continuum element approach in which the structure is divided into segments by cutting through the structure horizontally at those storey levels corresponding to changes in storey properties. A typical segment is then replaced by an appropriate substitute beam that has uniformly distributed mass and stiffness. Subsequently, the governing differential equations of the substitute beam are formulated using the continuum approach and posed in the form of a dynamic member stiffness matrix that is exact to small deflection theory. Since the formulation allows for the distributed mass and stiffness of the member, it necessitates the solution of a transcendental eigenvalue problem. The required natural frequencies are thus determined using a cantilever model in conjunction with the Wittrick-Williams algorithm, which ensures that no natural frequencies can be missed. In addition, a two step process has been developed for certain asymmetric structures in which the natural frequencies corresponding to coupled motion between the planes of vibration can be obtained from the equivalent uncoupled ones through a simple cubic relationship. This enables coupled, three-dimensional vibration problems to be solved very efficiently using a two dimensional approach.

The second method utilises the Principle of Multiples which, when applicable, enables any frame, regardless of the number of storeys or bays, to be simplified to an equivalent one bay frame, that has precisely the same natural frequencies. If the original frame does not fully satisfy the Principle, the same process can still be utilised, but the resulting substitute frame will yield approximate frequencies, although they will normally be

acceptable to engineering accuracy. Like the first method, it can also be used for the vibration analysis of asymmetric, three-dimensional frame and wall-frame structures in a two-step procedure. First the analogous uncoupled system is analysed using substitute frames, then the relationship between the uncoupled and coupled responses is imposed through a cubic equation.

Both of the above methods assume rigid floor diaphragms and require a knowledge of the building's static eccentricity at each storey level. The current methods of calculating this are cumbersome and even the definitions are open to dispute. A practical method of calculation is therefore presented and a small parametric study enables recommendations to be made.

Overall, the proposed methods require little effort, offer clear and concise output and can sometimes yield solutions of sufficient accuracy for definitive checks, but more usually provide engineering accuracy for intermediate checks during tasks such as scheme development or remedial work. This claim is supported by the results of extensive parametric studies undertaken for this thesis. In all examples, the results from the proposed methods have been compared with the results of a full finite element analysis of the original structure obtained using the vibration programme ETABS. The exercise confirms that the proposed methods can yield results of sufficient accuracy for engineering calculations.

To my wife Parinaz

ACKNOWLEDGEMENTS

All praises to my almighty Lord "Allah" for providing me the opportunity and the capability to complete this work.

My first and most earnest acknowledgement must go to my supervisor Dr Paul Howson for his continuous guidance, encouragement and support throughout. In every sense, none of this work would have been possible without him.

I would like to thank Sahand University of Technology and the Ministry of Science, Research and Technology of the Islamic Republic of Iran for their financial support and co-operation.

My gratitude also goes to numerous friends and colleagues for their help and the generous way in which they shared their knowledge. In particular, especial thanks should go to Mr Abdolreza Zare for many beneficial discussions and his enjoyable friendship.

Naturally I owe my parents a great debt of gratitude for being available and supportive when I needed them most.

My final and most heartfelt acknowledgment must go to my wife Parinaz. Her love, support, encouragement and companionship turned my time in Cardiff into a pleasure. I also should mention my lovely son Farbod, for his understanding and tolerance of his father's absence on evenings and weekends that were devoted to this thesis.

CONTENTS

LIST OF FIGURES

CHAPTER 1

INTRODUCTION

1.1 INTRODUCTION

The calculation of the natural frequencies and mode shapes of multi-storey structures has become commonplace due to the widespread availability of powerful desktop computers and a variety of inexpensive finite element software. However, such models often require elaborate data preparation and checking and the voluminous output may well lack clarity. A compelling alternative is to run simple models that require little effort, offer clear and concise output and which can sometimes yield solutions of sufficient accuracy for definitive checks, but more usually provide engineering accuracy for intermediate checks during tasks such as scheme development or remedial work.

A considerable amount of research effort has been expended on developing approximate methods for the frequency analysis of structures over the last thirty years or so. These methods can be classified into two main categories called Continuum and Substitute Frame methods.

1.2 CONTINUUM METHOD

The most widely used approximate methods have utilised a continuum approach, in which the building structure is replaced by a cantilever beam with uniformly distributed mass and stiffness. Research in this area was initially focused on two-dimensional and symmetric, three-dimensional structures, with many authors developing a variety of approximate methods for frames (Bolton 1978; Rafezy and Howson 2003; Roberts and Wood 1981; Williams et al. 1983); shear-walls (Rosman 1974; Rutenberg 1975); wall-frames (Kollar 1991) and three-dimensional symmetric structures comprising frames, coupled walls, wall-frames and braced frames (Delpak et al. 1997; Smith and Crowe 1986). The method has also been successfully applied to the critical load calculation of various structures by many authors, e.g. (Macleod and Zalka 1996; Zalka 1979; Zalka and Macleod 1996). In symmetric, three-dimensional structures the translational and torsional vibrations can be analysed independently. This means that they can be analysed by all of those methods that have been developed for two-dimensional structures. However, in the majority of building structures, the functional and architectural requirements result in an asymmetric location of structural elements. For such structural configurations, the translational and torsional modes of vibration can no longer be treated independently due to coupling between the three components of displacement. This type of coupled vibration characterises building structures with asymmetric floor plans.

More recently approximate methods have been developed that can deal with the coupled vibration of asymmetric, three-dimensional structures. Kuang and Ng (Kuang and Ng 2000; Kuang and Ng 2001) considered the problem of doubly asymmetric, proportional structures in which the motion is dominated by shear walls. For the analysis, the structure is replaced by an equivalent uniform cantilever whose deformation is coupled in flexure and warping torsion. The same authors extended this concept to the case of wall-frame structures by allowing for bending and shear. In this case however, the wall and frame systems are independently proportional, but result in a non-proportional structural form (Ng and Kuang 2000). Wall-frame structures have also been addressed by Wang *et.al.* (Wang *et al.* 2000). They used an equivalent eccentricity technique that is appropriate for non-proportional structures, but the analysis is limited to finding the first two coupled natural frequencies of uniform structures with singly asymmetric plan form.

Hand methods have also received considerable attention and are particularly suitable for check calculations. In a recent paper by Zalka (Zalka 2001), such a method is presented which can deal with the three-dimensional frequency analysis of buildings braced by frameworks, coupled shear-walls and cores. The paper also reviews similar related work in some depth.

The most recent contribution has been made by Potzta and Kollar, who replace the original structure by an equivalent sandwich beam that can model both slender and wide structures consisting of frames, trusses and coupled shear walls (Potzta and Kollar 2003). In a subsequent paper, Tarjan and Kollar (Tarjan and Kollar 2004) present an alternative approach in which the natural frequencies of the replacement beam are solved approximately. This, together with other simplifying assumptions, leads to simple formulae for determining the required natural frequencies. A useful tabulated summary of related work by the following authors is also included (Basu 1983; Kopecsiri and Kollar 1999a; Kopecsiri and Kollar 1999b; Rosman 1974; Rutenberg 1975; Skattum 1971; Smith and Crowe 1986; Smith and Yoon 1991; Zalka 2001).

The methods developed in the references above offer solutions of varying accuracy depending on the assumptions employed. Most of them consider structures with singly symmetric floor plan and surprisingly none of them allows for step changes of properties along the height of the structure, despite the fact that this is almost inevitably the case in practical building structures of reasonable height. This study therefore seeks to present the simplest model that retains the essential characteristics necessary for calculating the natural frequencies of structures ranging from two-dimensional to doubly asymmetric, three-dimensional structures whose members may be uniform throughout the height of the structure or may have step changes of properties at one or more storey levels.

The approach adopted is to dissect the original building structure into segments, by cutting through the structure horizontally at those storey levels corresponding to changes in storey properties. Thus the storeys contained within a segment between any two adjacent cut planes are identical. In the case of three-dimensional structures, it is also assumed that the plan view of a segment comprises two sets of resisting elements running

in orthogonal directions. A typical segment is then considered in isolation. In the case of three-dimensional structures a primary resisting element in one direction is replaced initially by an appropriate substitute beam that has uniformly distributed mass and stiffness, thus utilising the continuum approach. (The various types of substitute beams which can be utilised for the vibration analysis structures are explained in detail in Chapter 2). In turn, each resisting element running in the same direction is replaced by its own substitute beam and the effect of all these beams is summed to model the effect of the original resisting elements. This leads directly to the differential equation governing the sway motion of the segment in the chosen direction. The same procedure is then adopted for those resisting elements running in the orthogonal direction. Once both equations are available it requires little effort to write down the substitute expressions for the coupled torsional motion. The three equations thus formed are subsequently solved precisely and posed in dynamic stiffness matrix form, which relates the harmonically varying forces to the harmonically varying displacements at the nodes of the beam element. The resulting coupled translation-torsion beam element, substitute beam, can then be used to reconstitute the original structure by assembling the dynamic stiffness matrices for the individual segments in the usual manner.

It should be noted that the element formulation accounts for the uniform distribution of mass and stiffness, with the result that the final model has a transcendental dependence upon the frequency parameter. The required natural frequencies are then determined by solving the model using a precise technique, based on the Wittrick-Williams algorithm (Wittrick and Williams 1971), that can be arrested after achieving any desired accuracy and which also ensures that no natural frequencies can be missed. In the following section an historical review of the vibration of beams with symmetric and asymmetric cross-section is given, together with a literature survey of the development of the dynamic stiffness matrix method. This is followed by an explanation of the generalised procedure for the derivation of the dynamic stiffness matrix used in Chapters 2, 5 and 6 of this thesis.

1.2.1 Dynamic stiffness matrix method

1.2.1.1 Historical review of the vibration of beam members

The vibration of beams has been of interest to engineers and mathematicians for many years. As early as 1688, Christiaan Huygens described a series of vibrational experiments carried out on a simple beam. Newton and Leibnitz independently formulated the calculus, while James and Daniel Bernoulli obtained the static bending relationship for a thin beam. In 1743 D'Alembert took a major step forward in vibration theory when he showed that problems in dynamics could be stated in such a way that they could be solved using the rules of statics. In the following year Daniel Bernoulli and Leonard Euler independently presented the partial differential equation for the flexural motion of a slender beam. By 1824 the corresponding equation for longitudinal motion had been developed by Navier. Five years later Poisson presented the equivalent equation for torsion, the third of the three basic equations needed to completely define the small amplitude motion of linearly elastic thin beam.

By 1877 these uncoupled equations had received a good deal of attention. It was during this year that Lord Rayleigh published his famous treatise "Theory of Sound" (Rayleigh 1877). In this exceptional work Rayleigh reported in some depth on the advances in the field of beam vibrations. He showed that the equations of longitudinal and torsional motion were unaffected by the presence of a permanent axial load, but that the equation of flexural had to be modified. In the same work, Rayleigh suggested how the basic flexural equation could be modified to account for the effect of rotary inertia. A more significant effect was pointed out by Timoshenko in 1921 (Timoshenko 1921) when he extended Rayleigh's solution to include the effects of transverse shear deformation. He showed additionally that the effects of rotary inertia and shear deformation are unimportant if the wavelength of the transverse vibration is large compared to the dimensions of the cross-section.

Thus by 1921 the three differential equations used to analyse the flexural motion of beams had been developed. It has since become common practice to classify beams according to the simplest theory which adequately describes their flexural motion. A Bernoulli-Euler beam is therefore one in which only the effect of bending is important, unlike the Rayleigh beam where the effect of rotary inertia must be included. The Timoshenko beam takes its name from sophisticated of the three analysis in which the effects of bending, rotary inertia and shear deflection are all accounted for.

With the advent of the digital computer, matrix methods of problem solution became extremely popular. In the field of structural engineering these are typified by the force and displacement methods of static analysis. However, while it has long been recognised that dynamic problems could be formulated in precisely the same fashion, it is only in the last three decades that they have begun to command appreciable interest.

The overall dynamic stiffness matrix for a structure can be assembled from the dynamic member stiffness matrices in precisely the same way as for the static case. The individual member matrices may be developed in an approximate way or by a method which can be considered to be exact. Undoubtedly the most popular of the approximate methods is the powerful finite element approach. In this method the dynamic stiffness matrix is derived by assuming a static displaced shape for the member. The matrix itself consists of two individual matrices, the static stiffness matrix, defining the elastic properties of the structure, and the mass matrix, which defines the inertial properties. This leads to a set of equations from which the natural frequencies are determined by solving a generalised linear eigenvalue problem. The overall method of approach has been widely reported (Gupta 1970; Peters and Wilkinson 1969) as have the methods of solving the eigenvalue problem itself (Wilkinson 1965).

The exact method of approach, with which this thesis will be solely concerned from now on, consists of deriving the dynamic member stiffness matrix by solving the partial differential equations of motion for each beam exactly. The dynamic member stiffness matrix is then a single matrix and the mass of the member, whose uniform distribution is automatically accounted for, is an inextricable part of it. The overall matrix can then be formed as before and the natural frequencies found by solving the resulting non-linear

eigenvalue problem. The word 'exact' in this method means that the solution is a correct implementation of the governing equations and thus yields exact results in the area of assumptions (Macleod 1990). Consider now the development of this exact method.

1.2.1.2 literature survey of the development of the exact dynamic stiffness method

The concept of dynamic stiffness and dynamic carry-over factors was developed by Veletsos and Newmark and presented in a notable paper in 1955 (Veletsos and Newmark 1955). In this paper the natural frequencies of continuous beam and certain frame structures were obtained using exact expressions, based on Bernoulli-Euler theory, for the rotational stiffness and carry-over factors. In 1969 Bolton (Bolton 1969) used the same rotational stiffness and carry-over factors to determine the natural frequencies of continuous beams. In the absence of joint translations he obtained a simplified dynamic slope deflection equation which is analogous to that used in the static case. The procedure used to determine the natural frequencies then parallels those which are familiar in critical load analysis (Bolton 1955). In the same year (1969) a paper by Armstrong (Armstrong 1969a) extended Bolton's work to cover multi-bay, multi-storey frames, with and without sidesway. He later (Armstrong 1969b) presented a comprehensive set of dynamic stability functions that enable such problems to be solved by hand.

Matrix methods of problem solution started to receive considerable attention in the late 60's. One of the first papers to describe the formulation of a dynamic stiffness matrix was presented by Laursen *et al.*(Laursen et al. 1962). Initially attention is focused on the development of the individual member matrix, which relates the amplitudes of the sinusoidally varying moment and shear forces at the end of a beam member to the corresponding displacements. Subsequently it is shown how these matrices can be formed into an overall dynamic stiffness matrix for a structure. However, the overall matrix used by Laursen *et al* does not account for the rigid body motion of the members. Thus when considering structures in which longitudinal or sway modes are of interest, the overall matrix must be augmented by the relevant inertia matrix. The necessity of having this additional matrix was overcome by Henshell and Warburton (Henshell and Warburton 1969). Their method consisted of forming a more general dynamic stiffness matrix which

included additional stiffness elements to account for both the longitudinal and torsional motion of the member. Cheng (Cheng 1970) and Wang and Kinsman (Wang and Kinsman 1971) also developed the dynamic stiffness matrix for a Timoshenko beam that could be used in the vibration analysis of frameworks. Later Howson and Williams (Howson and Williams 1973) derived the dynamic stiffness matrix of an axially loaded Timoshenko beam that has been used extensively in the eigensolution of plane frames (Howson 1979; Howson 1985; Howson et al. 1983).

In last two decades, research on the dynamic stiffness matrix formulation for beams has grown enormously and has taken numerous turns, including beams on elastic foundations (Capron and Williams 1988; Issa 1988; Williams and Kennedy 1987), tapered beams (Banerjee and Williams 1985) and curved beams (Howson and Jemah 1999a; Howson and Jemah 1999b; Howson et al. 1995; Issa 1988). However, one important area of developing interest is the dynamic stiffness matrix formulation of the bending-torsion coupled beam. In such beams the elastic centre and the centre of mass are not coincident, so the translational and torsional modes are inherently coupled as a result of this offset. The solution for individual beams has been approached in different ways by Gere and Lin (Gere and Lin 1958), Falco and Gasparetto (Falco and Gasparetto 1973) and Dokumaci (Dokumaci 1987). However, development of the dynamic stiffness matrix for coupled beams is relatively new and has been considered by only a few investigators. Hellauer and Liu (Hallauer and Liu 1982) derived the exact dynamic stiffness matrix for a straight, elementary bending-torsion beam where bending translation was restricted to one direction. Friberg (Friberg 1983) formulated a 12x12 element dynamic stiffness matrix for a bending-torsion coupled beam by using Euler-Bernoulli-Saint Venant theory. He later (Friberg 1985) included the effect of axial load and warping rigidity using Vlasov's torsion theory to obtain the 14x14 dynamic stiffness matrix for such a member numerically, whereas Banerjee (Banerjee 1989) derived explicit expressions for each of the dynamic stiffness matrix elements and later included the effect of shear deformation and rotary inertia (Banerjee and Williams 1992). Subsequently, Banerjee *et al* (Banerjee *et al.* 1996) studied the vibration of a bending-torsion beam with singly asymmetric cross-section including warping rigidity and showed that large errors may be incurred in the calculation of natural frequencies of thin walled open section beam assemblies when the effect of warping rigidity is ignored.

In a recent paper Rafezy and Howson (Rafezy and Howson 2004) considered the vibration analysis of shear beams with doubly asymmetric cross-section. This approach can be used very efficiently in the approximate determination of the lower natural frequencies of three-dimensional, multi-storey framed structures (Rafezy and Howson 2003), including those that are doubly asymmetric on plan.

The general procedure for the derivation of dynamic stiffness matrices has been long established and used by many authors, e.g. Banerjee (Banerjee 1997), and is given in the following section.

1.2.2 Dynamic Stiffness Formulation

The first step towards the formulation of the dynamic stiffness matrix of a beam element is to derive its governing differential equations of motion. This can be accomplished in various ways such as applying Newton's laws, D'Alembert's principle, principle of virtual work, etc.

The governing differential equation of motion of a beam element in free undamped vibration can be written as

$$L(\mathbf{u}) = 0 \tag{1.1}$$

where L is a differential operator and $\mathbf{u}$ is the corresponding displacement vector.

The next step is to solve Eq. (1.1) for harmonically varying $\mathbf{u}$, so that the displacement $\mathbf{u}$ may be expressed as

$$\mathbf{u} = \mathbf{U}e^{i\omega t} \tag{1.2}$$

where $\mathbf{U}$ denotes the amplitude of the displacements, ω is the circular frequency, t is time and $i = \sqrt{-1}$.

Substituting Eq. (1.2) into Eq. (1.1) eliminates the time dependent terms in the differential equation to give

$$L_1(\mathbf{U}, \omega) = 0 \tag{1.3}$$

where L_1 is a differential operator.

The general solution of the differential equation (1.3) is obtained in the form

$$\mathbf{U} = \mathbf{AC} \tag{1.4}$$

in which **C** is a vector of constants and **A** is a frequency dependent square matrix.

The boundary conditions for displacements and forces are now applied to eliminate the vector **C** and subsequently to obtain the force-displacement relationship via the dynamic stiffness matrix. First the boundary conditions for nodal displacements are applied to give

$$\mathbf{D} = \mathbf{SC} \tag{1.5}$$

where **D** is the nodal displacement vector and **S** is a square matrix obtained from **A** when the displacement boundary conditions are applied. Next the force boundary conditions are applied and the vector of nodal forces are related to the constant vector **C** by a similar procedure to that of Eq. (1.5) to give

$$\mathbf{F} = \mathbf{BC} \tag{1.6}$$

in which **F** is the vector of amplitudes of nodal forces and **B** is a frequency dependent matrix.

The vector **C** can now be eliminated from Eqs. (1.5) and (1.6) to give

$$\mathbf{F} = \mathbf{BS}^{-1}\mathbf{D} = \mathbf{KD} \tag{1.7}$$

where

$$\mathbf{K} = \mathbf{B}\mathbf{S}^{-1} \tag{1.8}$$

and is the required dynamic stiffness matrix.

In Eq. (1.8), the two steps involved to obtain the dynamic stiffness matrix are: (i) to invert the **S** matrix to obtain $\mathbf{S}^{-1}$, and then (ii) to premultiply the inverted matrix ($\mathbf{S}^{-1}$) by the **B** matrix to give **K**. Implementation of these steps can be accomplished either numerically or algebraically. It is always preferable to derive the elements of the dynamic stiffness matrix explicitly. However, the task of inverting the **S** matrix algebraically and then premultiplying by the B matrix, again algebraically, can be quite formidable(Banerjee and Williams 1994; Banerjee and Williams 1995). In this thesis the numerical approach for obtaining the dynamic stiffness matrix will be used most often.

Once the overall dynamic stiffness matrix of the structure, **K**, is assembled from the dynamic stiffness matrices of all the individual elements, the natural frequencies then correspond to the values of the circular frequency ω which satisfy the matrix equation

$$\mathbf{K}\,\mathbf{D} = \mathbf{0} \tag{1.1}$$

where **D** is the vector of amplitudes of the harmonically varying nodal displacements and **K** is a function of ω. In most cases the required natural frequencies correspond to $|\mathbf{K}|$, the determinant of **K**, being equal to zero. In early formulations (Blaszkowiak and Kaczkowski 1966; Cheng 1970; Henshell and Warburton 1969; Mohsin and Sadek 1968; Wang and Kinsman 1971), the required natural frequencies have mainly been ascertained by simply tracking the value of $|\mathbf{K}|$ and noting the value of ω corresponding to $|\mathbf{K}| = 0$. However when **K** is developed from exact member theory, the determinant is a highly irregular, transcendental function of ω. Additionally, several natural frequencies may be close together or coincident, while others may exceptionally correspond to $\mathbf{D} = \mathbf{0}$. Thus any trial and error method which involves computing $|\mathbf{K}|=0$ and noting when it changes

sign through zero can miss roots. These problems can be overcome by use of the Wittrick-Williams algorithm (Wittrick and Williams 1971) which has received wide attention in the literature (Williams and Wittrick 1983). The algorithm requires the overall dynamic stiffness matrix of the structure, together with information about the clamped-clamped natural frequencies of the constituent members. The use of the algorithm has been frequently discussed in the literature, but for a detailed insight, reference should be made to (Wittrick and Williams 1971). The Wittrick-Williams algorithm then yields the number of natural frequencies of a structure that lie below an arbitrarily chosen trial frequency. This clearly enables a systematic procedure to be developed for converging upon any natural frequency of the structure to any desired accuracy.

In this thesis, the dynamic stiffness matrix of various beam members ranging from two-dimensional shear sensitive beams on continuous rotational elastic supports to three-dimensional beams with doubly asymmetric cross section are developed. These are then used efficiently in the approximate determination of the natural frequencies of two and thee-dimensional, asymmetric frame and wall-frame structures with step changes of properties along the height of the structure. The Wittrick-Williams algorithm is used for the solution of the transcendental non-linear eigenvalue problems, which ensures that no natural frequencies are missed.

1.3 SUBSTITUTE FRAME METHOD

The Substitute Frame method has already been used in the buckling and vibration analysis of braced and unbraced plane frame structures. See the next section. The method utilises the Principle of Multiples which, when applicable, enables any frame, regardless of the number of storeys or bays, to be simplified to an equivalent one bay frame, having the same displacements, buckling loads or natural frequencies as the original frame. If the original multi-bay frame does not obey the Principle of Multiples, the same procedure may be adopted, but the resulting frame only yields approximate frequency results for the original structure. The accuracy of the results is dependent on how close the frame is to satisfying the Principle of Multiples, but will normally yield results of acceptable accuracy for engineering calculations.

The basis of Principle of Multiples is that, if the beams and columns have such stiffness ratios that the joint rotations at any storey level would be the same, then a multi-storey, multi-bay frame can be split up into several single bay frames all of which would have the same response. The application of the Principle of Multiples for a two-bay frame is illustrated in Figure 1.1 and will be explained in detail in Chapter 2 of this thesis.

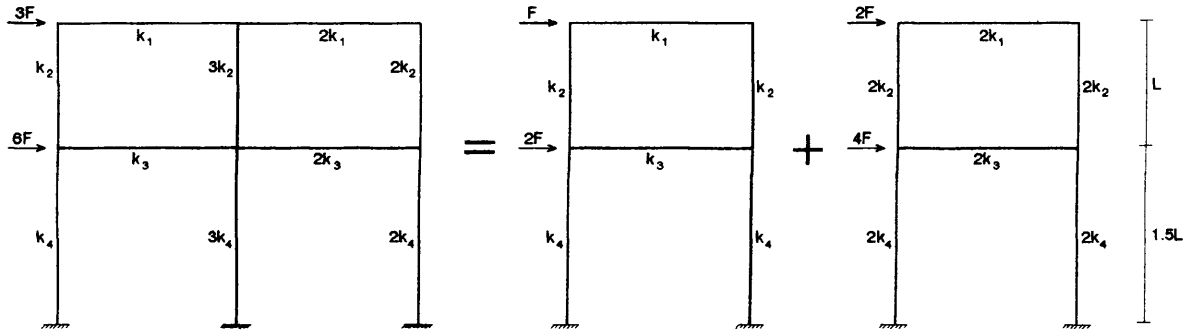

Figure 1.1 The Principle of Multiples applied to a two-bay frame (the k's indicate the stiffness of the columns and beams)

1.3.1 Literature Survey for the Substitute Frame Method

Numerous authors have dealt with the use of the Principle of Multiples and associated simple methods for lateral loading, buckling calculations and vibration of plane sway frames with and without cladding. The specific use of substitute frames is probably attributable to Grinter (Grinter 1937), with the techniques being developed by Lightfoot and others (Horne and Merchant 1965; Lightfoot 1956a; Lightfoot 1956b; Lightfoot 1957; Lightfoot 1958; Williams 1977; Williams 1979; Williams and Butler 1988) and through Wood's significant contribution (Wood 1974a; Wood 1974b; Wood 1974c) finally being adopted as an appropriate design method in current Codes of Practice. The extension of simplified methods to the calculation of natural frequencies (Bolton 1978; Delpak et al. 1997; Roberts and Wood 1981; Williams et al. 1983) and critical buckling loads (Bolton 1976; Horne 1975; Williams and Howson 1977) of framed structures has developed steadily over the last twenty-five years. In a recent paper, Howson and Williams (Howson

and Williams 1999) have applied the substitute frame method to the vibration analysis of plane braced and unbraced frames on the assumption of both inextensible and extensible member theory. They have shown that, for unbraced frames, the substitute frame gives acceptable accuracy for most practical engineering structures.

The earliest attempt to account for torsional deformation under static loads, using only a plane frame program, was given by Coull and Smith (Coull and Smith 1973). In a recent development Howson and Rafezy (Howson and Rafezy 2002) have succesfully applied the substitute frame method when determining the nodal deflections of multi-bay, multi-storey asymmetric proportional building structures subjected to static loads. This was probably the first time that the substitute frame was used for the analysis of asymmetric structures.

In this thesis, the substitute frame technique will be extended to cover the calculation of the natural frequencies of three-dimensional, symmetric and asymmetric frame and wall-frame structures, which appears not to have received any direct attention before. The method is best suited to regular, doubly symmetric structures, although asymmetric plan forms can be treated with equal accuracy so long as the structural properties of parallel primary frames and walls are proportional. Buildings that do not fulfil these ideal requirements can usually be analysed to sufficient accuracy for scheme development. Each substitute frame is a single bay, multi-storey frame that has the same number of storeys and the same storey heights as the original frame but is symmetric, allows for the uniform distribution of mass in its members and comprises only in-plane stiffnesses. The method is based on the Principle of Multiples; requires only the use of a standard plane frame computer program and can yield almost exact solutions for certain combinations of structural topology and member properties. In asymmetric structures, the proposed method will be applied in a two-step procedure. First the analogous uncoupled system will be analysed then the relation between the uncoupled and coupled responses will be imposed through a cubic equation.

1.4 VERIFICATION OF RESULTS

A theory cannot be considered correct in an absolute sense (Macleod 1990; Popper 1977). It can only be shown to be 'not false' to some degree. In this study the results are usually verified by comparing them with equivalent results obtained from a finite element analysis using the vibration programme ETABS (Wilson et al. 1995), which is widely used in engineering analysis. The main assumptions inherent in using ETABS will be given whenever it is used. In Chapter 2 the results from developed models are compared with results obtained using exact buckling and vibration programme called BUNVIS-RG (Anderson and Williams 1986). The main assumptions for this programme have been given in Section 2.4.1.

In this thesis, the description 'good' means that the results represent the real behaviour of the structures fairly accurately and 'acceptable' means that the results may be used for most engineering purposes. When the description 'exact' is used, it only means that the solution is a correct implementation of the governing equations, as there are no basic assumptions that can be described as 'exact' (Macleod 1990).

1.5 BASIC ASSUMPTIONS

The following assumptions are assumed in this thesis

1. The simplest model has been developed for each type of building. In certain cases two models with different complexities have been considered and the validity limits of each model have been determined e.g. In Chapter 2, elastic support and shear beam models have been compared.

2. The in-plane stiffness of the floor systems used in most building structures is extremely large compared to the stiffness of the framing members. Thus the theory in which rigid floor diaphragms are assumed has been maintained in the thesis. As a result, the in-plane deformations of beams can often be neglected, and columns

and walls connected to a given diaphragm will be constrained to move as one single unit in the lateral directions.

3. Inextensible member theory has been assumed in the whole thesis. It means that the full height bending deformation of buildings as a whole has been neglected. The reason for this is to avoid any unnecessary complexity when developing simple substitute models which can model structures satisfactorily. A small parametric study has been undertaken to assess the effect of this assumption when determining the natural frequencies of a series of three-dimensional, asymmetric, multi-storey buildings and the results have been given in Section 5.4.1.

1.6 OUTLINE OF THE THESIS

The contents of this thesis are presented in seven chapters. The outline of each chapter is briefly given as follows:

Chapter 1 describes the aims and objectives of the thesis and gives a brief literature survey for the proposed methods classified as continuum and substitute frame methods.

Chapter 2 deals with the vibration problem of two-dimensional frame and wall-frame structures. Two substitute beam models, namely elastic support and shear beam models, are proposed for finding the natural frequencies of plane structures.

Chapter 3 extends the continuum and substitute frame approach to three-dimensional structures with symmetric floor plans. It is shown that symmetric structures can be analysed using the same approximate methods that were developed for planar structures. The appropriate transformations for converting a symmetric structures to three planar substitute structures are given.

Chapter 4 presents a practical method for locating the centres of rigidity and shear and hence the static eccentricity of asymmetric structures. The method is based on the use of a plane frame computer programme and utilises the flexibility matrix of each resisting plane

element to establish a matrix relation between the loading on the elements and the total lateral loading on the building.

Chapter 5 derives the governing differential equations of a three-dimensional shear beam with doubly asymmetric cross-section in the form of a dynamic stiffness matrix. This is subsequently used successfully for the vibration analysis of asymmetric frame structures in conjunction with the Wittrick-Williams algorithm. This chapter further extends the substitute frame technique to cover the calculation of the natural frequencies of three-dimensional, asymmetric frame structures

Chapter 6 extends both substitute beam and frame methods to three-dimensional wall-frame structures with an asymmetric arrangement of frames and walls. The plane frames that run in two orthogonal directions are assumed to be proportional to each other in any one direction, as are the walls, but the proportionality is not necessarily the same in both directions.

Finally Chapter 7 provides a summary of the thesis, draws conclusions and suggests those areas of this thesis that could be usefully extended.

CHAPTER 2

LATERAL VIBRATION ANALYSIS OF PLANE FRAME AND WALL-FRAME STRUCTURES

2.1 INTRODUCTION

This chapter presents two methods of analysis for determining the lateral frequencies of planar structures, in which the structure is simplified prior to analysis. Such an approach leads to simple models that can be solved easily, either by the use of short computer programs or by hand. Each method is able to analyse plane frame and wall-frame structures i.e. a combination of shear walls and frames whose members may be uniform throughout the height of the structure or may have step changes of properties at one or more storey levels.

The first method utilises a continuum approach so that a plane frame or wall-frame structure is divided into segments, by cutting through the structure horizontally at those storey levels corresponding to changes in storey properties. Thus the storeys contained within a segment between any two adjacent cut planes are identical. Then a typical segment is replaced by an appropriate substitute beam that has uniformly distributed mass

and stiffness, thus utilising the continuum approach. Two types of substitute beams that can be used for the vibration analysis of plane frame and wall-frame structures will be developed. Each are derived from a study of the vibration of a shear sensitive Bernoulli-Euler beam on continuous rotational elastic support. These will be called the elastic support model and shear beam model respectively. Both models lead to a dynamic stiffness formulation that necessitates the solution of a transcendental eigenvalue problem. The eigenvalues correspond to the required natural frequencies and can be determined to any desired accuracy using the Wittrick-Williams algorithm (Wittrick and Williams 1971) with the certain knowledge that none have been missed.

The second method utilises the Principle of Multiples which, when applicable, enables any frame, regardless of the number of storeys or bays, to be simplified to an equivalent one bay frame, having the same natural frequencies of vibration as the original frame. If the original multi-bay frame does not obey the Principle of Multiples, the same procedure is adopted, but the resulting frame only yields approximate frequency results for the multi-bay case. Then, using the results of the elastic support model, the method is extended and applied to the frequency analysis of wall-frame structures.

In order to validate the use of the proposed methods, it was deemed necessary to carry out a parametric study to ascertain the accuracy that might be expected from the proposed methods.

2.2 CONTINUUM METHOD

The continuum approach will be used to develop two simple models for calculating the lower natural frequencies of plane sway frames. These will be called, the elastic support and shear beam model, respectively. It will be necessary to derive a dynamic stiffness matrix for each model, both of which represent transcendental eigenvalue problems in which the eigenvalues correspond to the required natural frequencies. The detailed development of the models will be presented in the following sections, but first it is necessary to derive the governing differential equation of a Bernoulli-Euler beam on a rotational elastic support, including the effect of shear deformation.

2.2.1 Bernoulli-Euler beam on a rotational elastic support allowing for shear deformation

The member considered is a basic Bernoulli beam enhanced by taking the following effects into account

- shear deformation
- continuous rotational elastic support

The deflection of the beam results not only from the longitudinal extension and contraction of the fibres due to the normal bending stresses, as assumed by Bernoulli, but also from transverse displacements of cross-section due to the shear stresses. When deformed by bending (Figure 2.1b) with the effect of shear neglected, the deflection of the beam axis is $u_b(z,t)$ and the rotation of the tangent to the axis is the angle $\theta(z,t)$. When the effect of shear is added (Figure 2.1c) the deflection is increased by $u_s(z,t)$ with the rotation increased by $\gamma(z,t)$. The total deflection and the total rotation of the beam axis are then

$$u(z,t) = u_b(z,t) + u_s(z,t) \tag{2.1}$$

$$\partial u(z,t)/\partial z = \theta(z,t) + \gamma(z,t) \tag{2.2}$$

Where γ, the shear slope (strain), related to the shearing force through elementary bending theory as

$$Q = \gamma GA_s \tag{2.3}$$

in which GA_s is the shear rigidity of the cross section including the section shape factor and Q is the transverse force in the cross section.

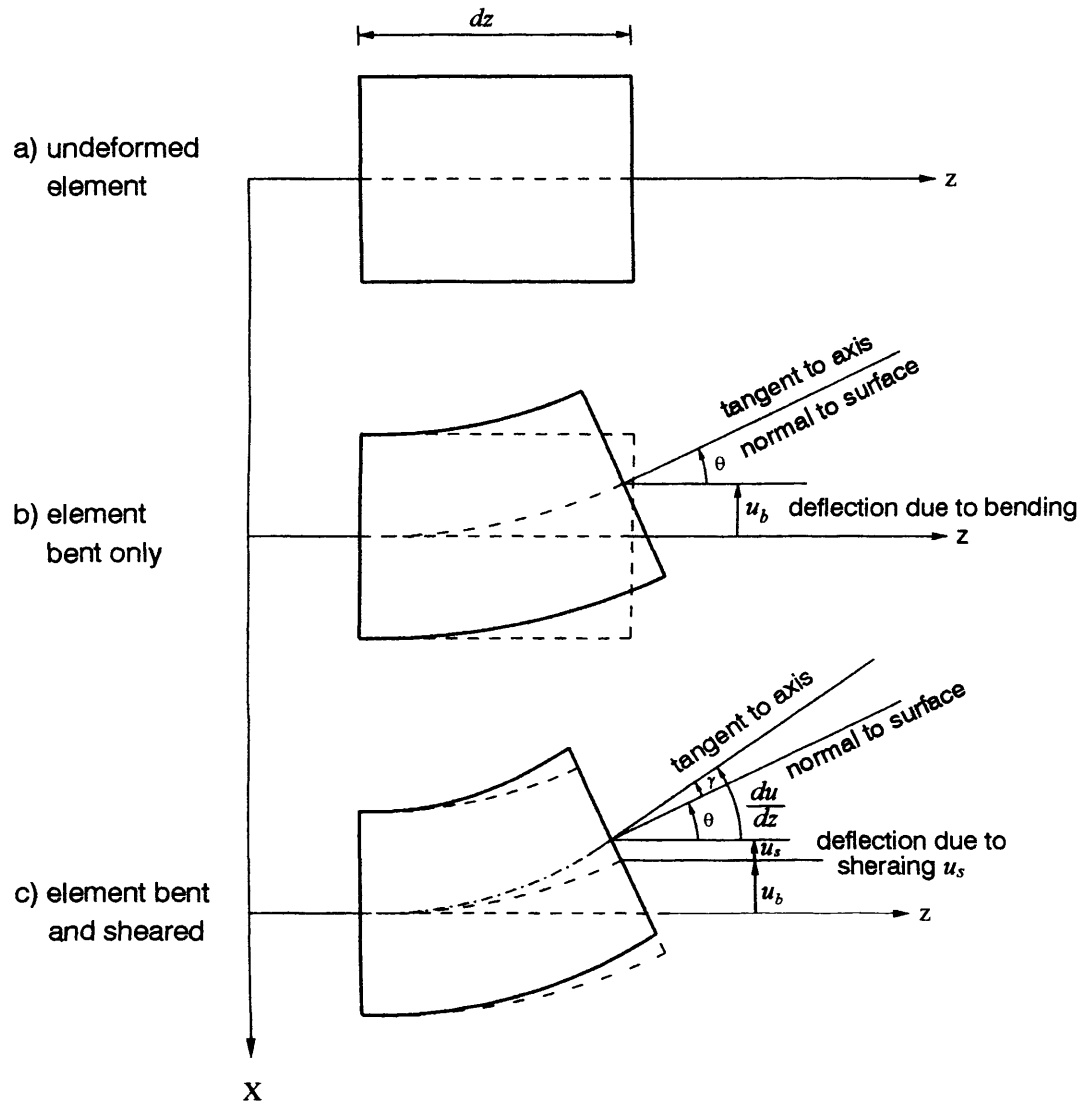

Figure 2.1 Deformation of beam element

Figure 2.2(a) shows a member of mass/unit length m undergoing flexural vibrations in the z-x plane and subjected to a rotational stiffness per unit length k^*. Using the following notation and considering a typical element of the member as shown in Figure 2.2(b), Eqs. (2.4)-(2.7) are easily obtained, as follows

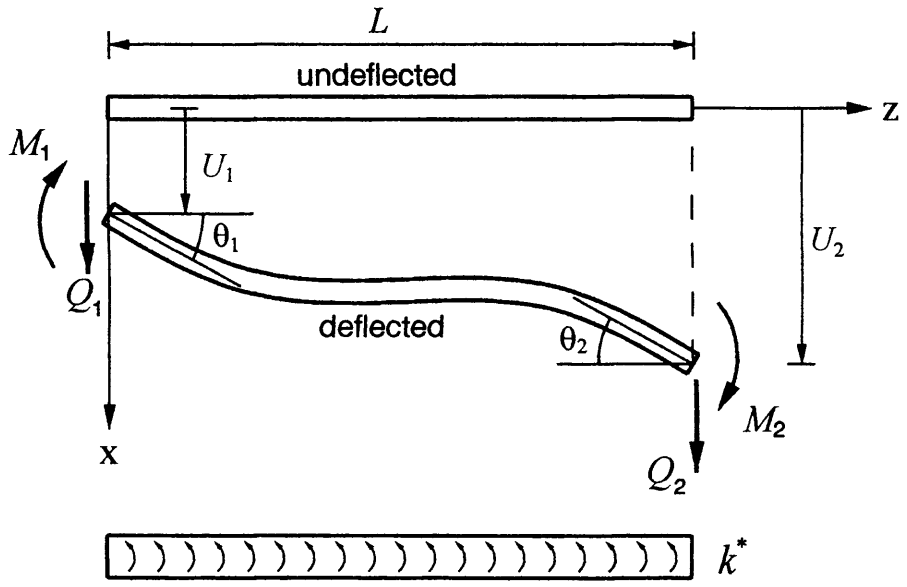

Figure 2.2(a) Forces and displacements in member coordinates in the z-x plane. All the forces and displacements vary sinusoidally with time.

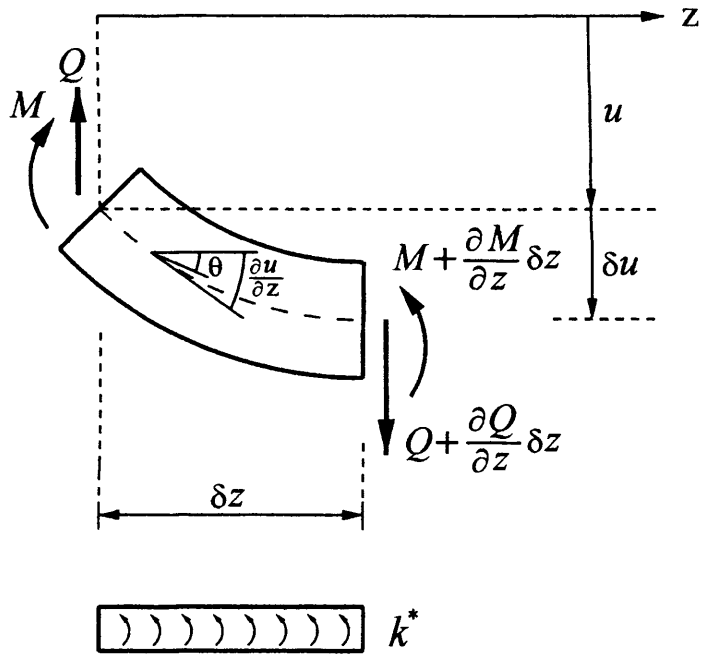

Figure 2.2(b) Positive forces and displacements on an elemental length of the member in local coordinates

a) dynamic equilibrium in the x direction

$$\left[Q+(\frac{\partial Q}{\partial z})\delta z\right]-Q-\left[m\frac{\partial^2 u}{\partial t^2}\right]\delta z=0 \tag{2.4}$$

where Q is the transverse force.

b) dynamic moment equilibrium

$$Q\delta z+M-\left[M+(\frac{\partial M}{\partial z})\delta z\right]-(k^*\theta)\delta z=0 \tag{2.5}$$

where M is the bending moment.

c) bending theory

$$M=-EI\frac{\partial \theta}{\partial z} \tag{2.6}$$

where E is Young's modulus and I is the second moment of area for bending in the z-x plane.

d) Consideration of the shearing of the element gives

$$\frac{\partial u}{\partial z}=\theta+\frac{Q}{GA_s} \tag{2.7}$$

Eqs. (2.3) to (2.7) can be rewritten as

$$\frac{\partial Q}{\partial z}-m\frac{\partial^2 u}{\partial t^2}=0 \tag{2.8}$$

$$Q-\frac{\partial M}{\partial z}-k^*\theta=0 \tag{2.9}$$

$$M = -EI\frac{\partial\theta}{\partial z} \tag{2.10}$$

$$Q = GA_s\left(\frac{\partial u}{\partial z} - \theta\right) \tag{2.11}$$

Substituting Eq. (2.11) and the derivative of Eq. (2.10) in terms of z in Eq. (2.9) gives

$$GA_s\left(\frac{\partial u}{\partial z} - \theta\right) + EI\frac{\partial^2\theta}{\partial z^2} - k^*\theta = 0 \tag{2.12}$$

and differentiating gives

$$GA_s\left(\frac{\partial^2 u}{\partial z^2} - \frac{\partial\theta}{\partial z}\right) + EI\frac{\partial^3\theta}{\partial z^3} - k^*\frac{\partial\theta}{\partial z} = 0 \tag{2.13}$$

Substituting Eq. (2.11) in Eq. (2.8) gives

$$GA_s\left[\frac{\partial^2 u}{\partial z^2} - \frac{\partial\theta}{\partial z}\right] - m\frac{\partial^2 u}{\partial t^2} = 0 \tag{2.14}$$

Then

$$\frac{\partial\theta}{\partial z} = \frac{\partial^2 u}{\partial z^2} - \frac{m}{GA_s}\frac{\partial^2 u}{\partial t^2} \tag{2.15}$$

and

$$\frac{\partial^2\theta}{\partial z^2} = \frac{\partial^3 u}{\partial z^3} - \frac{m}{GA_s}\frac{\partial^3 u}{\partial z\partial t^2} \tag{2.16}$$

$$\frac{\partial^3\theta}{\partial z^3} = \frac{\partial^4 u}{\partial z^4} - \frac{m}{GA_s}\frac{\partial^4 u}{\partial z^2\partial t^2} \tag{2.17}$$

Substituting Eq. (2.15) to Eq. (2.17) in Eq. (2.13) gives

$$GA_s\left(\frac{m}{GA_s}\frac{\partial^2 u}{\partial t^2}\right)+EI\left(\frac{\partial^4 u}{\partial z^4}-\frac{m}{GA_s}\frac{\partial^4 u}{\partial z^2\partial t^2}\right)-k^*\left(\frac{\partial^2 u}{\partial z^2}-\frac{m}{GA_s}\frac{\partial^2 u}{\partial t^2}\right)=0 \qquad (2.18)$$

which, on rearranging, gives

$$EI\frac{\partial^4 u}{\partial z^4}+\left(m+k^*\frac{m}{GA_s}\right)\frac{\partial^2 u}{\partial t^2}-k^*\frac{\partial^2 u}{\partial z^2}-m\frac{EI}{GA_s}\frac{\partial^2 u}{\partial z^2\partial t^2}=0 \qquad (2.19)$$

Eq. (2.19) is the governing differential equation for free vibration of the member .

If a sinusoidal variation of u with circular frequency ω is assumed then

$$u(z,t)=U(z)\sin\omega t \qquad (2.20)$$

where $U(z)$ is the amplitude of the sinusoidally varying displacement.

$$\frac{d^4U}{dz^4}+\left(\frac{\omega^2 m}{GA_s}-\frac{k^*}{EI}\right)\frac{d^2U}{dz^2}-\frac{\omega^2 m}{EI}\left(1+\frac{k^*}{GA_s}\right)U=0 \qquad (2.21)$$

Introducing the non-dimensional parameter

$$\xi=z/L \qquad (2.22)$$

Eq. (2.21) can be written as

$$\frac{d^4U(\xi)}{d\xi^4}+L^2\left(\frac{\omega^2 m}{GA_s}-\frac{k^*}{EI}\right)\frac{d^2U(\xi)}{d\xi^2}-L^4\frac{\omega^2 m}{EI}\left(1+\frac{k^*}{GA_s}\right)U(\xi)=0 \qquad (2.23)$$

where L is the length of the member.

In the following sections Eq. (2.23) will be used for the derivation of the dynamic stiffness matrix of two different element types, each of which can be used for the free vibration analysis of plane frame and wall-frame structures.

2.2.2 Elastic Support Model

2.2.2.1 Plane rigid frame structures

A rigid high-rise frame structure typically comprises parallel or orthogonally arranged bents consisting of columns and girders with moment resistant joints. Resistance to horizontal loading is provided by the bending resistance of the columns, girders and joints. The continuity of the frame also contributes to resisting gravity loading, by reducing the moment in the girders. The advantage of rigid frames are the simplicity and convenience of its rectangular form. Its unobstructed arrangement, clear of bracing members and structural walls, allows freedom internally for the layout and externally for the fenestration. Rigid frames are considered economical for buildings of up to about 25 storeys, above which their drift resistance is costly to control. If however, a rigid frame is combined with shear walls or cores, the resisting structure is very much stiffer so that is its height potential may extend up to 50 storeys or more(Smith and Coull 1991).

The total deformation of a rigid frame can be determined by superimposing its three component parts(Zalka 2001): i.e. the full-height bending deformation of the structure as a whole, the full-height bending deformation of the individual columns and the shear deformation of the structure, see Figures 2.3(a)-2.3(c).

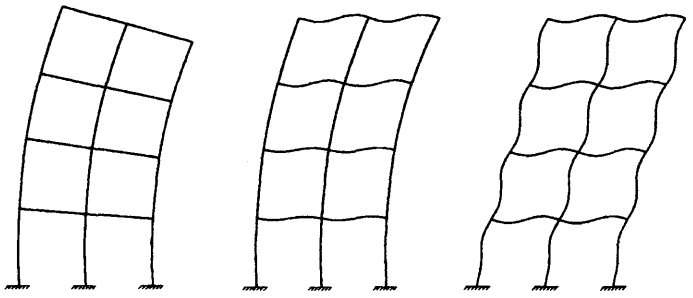

Figure 2.3 Components of frame deformation (Zalka 2001) (a) The full height bending deformation of the structure as a whole (b) The full height bending deformation of the individual columns (c) Shear deformation of the structure

The elastic support model incorporates components (b) and (c) of the total deformation and the motion is governed by a fourth order differential equation. When posed in dynamic stiffness form it accounts for both lateral translation and rotation at each node and is generally applicable to any kind of frame structure. The resulting member stiffness matrix (exact finite element) can be assembled to form the dynamic structure stiffness matrix, **K**, in the usual way and can therefore be used for the analysis of frames with step changes of properties along the height of the structure. The required natural frequencies then correspond to those values of ω, the circular frequency, that satisfy the equation

$$\mathbf{K}\ \mathbf{D} = \mathbf{0} \tag{2.24}$$

where **D** is the vector of amplitudes of the harmonically varying nodal displacements and **K** is a function of ω. Convergence to the required natural frequencies is achieved using the Wittrick-Williams algorithm(Howson and Williams 1973), which guarantees that no natural frequencies can be missed.

The first step in developing the elastic support model is to establish a substitute frame corresponding to the original frame structure. This process is well documented (Howson and Rafezy 2002) and results in a symmetric, single bay frame with the same number of storeys as the original frame and members whose properties are adjusted to replicate the behaviour of the original frame, see Figure 2.4(a). Such substitute frames can yield precise results for certain combinations of structure topology and member properties and will be explained in detail in following Sections under the title of Principle of Multiples. However, the substitute frame technique more regularly offers results of engineering accuracy when the original frame is irregular.

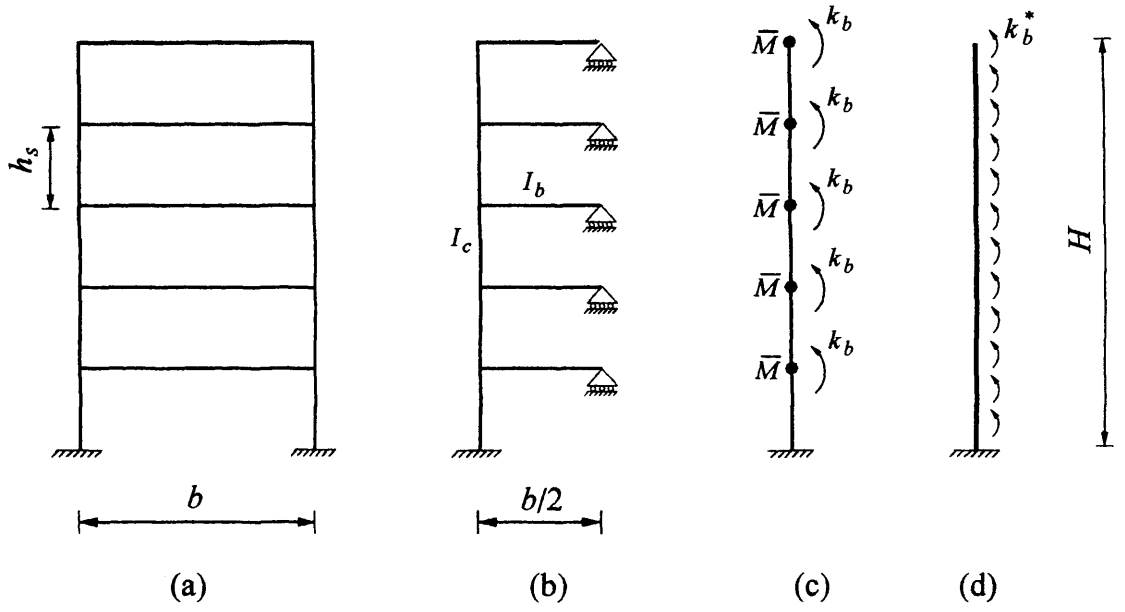

Figure 2.4 Development of the elastic support model.

Since the substitute frame is symmetric, it can only vibrate in a symmetric or anti-symmetric mode, of which only the anti-symmetric mode is of interest when considering the lower natural frequencies. Hence the substitute frame can be replaced by the model of Figure 2.4(b). This can be further simplified by replacing it with a bending cantilever that carries a lumped mass and rotational spring stiffness at each floor level to represent the beams, see Figure 2.4(c). The spring could be a dynamic stiffness, resulting in virtually no loss of accuracy, or more conveniently the equivalent static beam stiffness which, for the lower natural frequencies, yields negligibly small errors. The mass to be added to the cantilever at each floor level is then $\overline{M}$, where $\overline{M}$ is half the mass of a beam on Figure 2.4(a) and, assuming inextensible member theory, the required static stiffness is easily determined from the slope deflection equations to be

$$k_b = 6EI_b/b$$

where b is the bay width, and I_b is the second moment of area of a beam. The final simplification is to smear the mass and stiffness of the beams along the column so that they become uniformly distributed. When consecutive storeys are identical, their smeared properties define a new member, which together with other members form the final model. This leads to the uniform, single member cantilever of Figure 2.4(d) when

all storeys are identical. The model then corresponds to a 2 x 2 dynamic stiffness matrix developed from the original substitute frame column, but carrying the added distributed mass, m^*, and distributed stiffness, k_b^*, respectively, which are given by

$$m^* = \overline{M}/h_s \quad \text{and} \quad k_b^* = k_b/h_s = 6EI_b/bh_s \tag{2.25}$$

where h_s is the storey height.

Now consider only the single member idealisation of Figure 2.4(d). It is clear that the smeared beam stiffness k_b^* becomes infinite when the original beam stiffnesses become infinite. Hence the model of Figure 2.4(d) yields only infinite natural frequencies. However, in identical circumstances the model of Figure 2.4(c) would yield those sway frequencies corresponding to double curvature of the columns between nodes. This form of sway deformation has therefore been lost, but can be accounted for as follows.

Consider the shear deformation of two adjacent storeys as shown in Figure 2.5, in which the beams of the frame are restricted from bending. It is clear that applying the slope deflection equations between the points of contra-flexure yields the shear stiffness k_c and the equivalent smeared stiffness k_c^* as

$$k_c = M_A/\theta_A = 12EI_c/h_s \qquad \text{and} \qquad k_c^* = k_c/h_s = 12EI_c/h_s^2 \tag{2.26}$$

where I_c is the second moment of area of a column and M_A and θ_A are defined in Figure 2.5 . The smeared bending and shear stiffnesses can now be combined into a single stiffness k^* using the Foppl-Papkovich theorem(Tarani 1999), such that

$$\frac{1}{k^*} = \frac{1}{k_b^*} + \frac{1}{k_c^*} \quad \text{or} \quad k^* = k_b^* \frac{k_c^*}{k_b^* + k_c^*} \tag{2.27}$$

i.e. the initial beam stiffness should be factored by $k_c^*/(k_b^* + k_c^*)$, which is always less than one. The equation also shows that the local sway of columns can be ignored when

the frame has relatively stiff columns. e.g. in the case of coupled shear walls. Substituting Eqs. (2.25) and (2.26) in Eq. (2.27) gives

$$k^* = \frac{12EI_bI_c}{h(2I_cb + I_bh)} \tag{2.28}$$

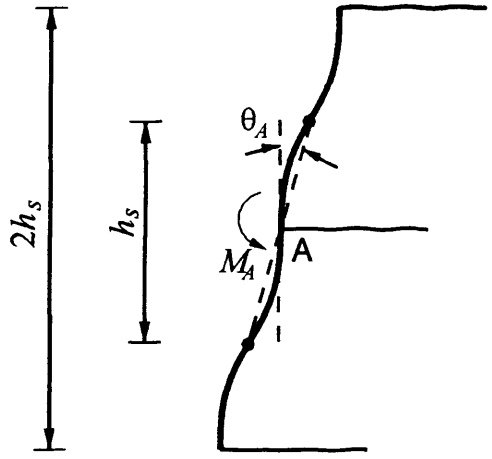

Figure 2.5 Development of column shear stiffness.

k^* equals half the effective shear rigidity of the frame (GA_s), which has been defined in reference(Smith and Coull 1991). This parameter expresses the racking stiffness of frame on a storey-height average basis. The composite symbol (GA_s) is used because it corresponds to the shear rigidity of an analogous shear cantilever of sectional area A and modulus of rigidity G. A storey-height segment of such a cantilever maybe compared (Figure 2.6a) with a corresponding portion of a rigid frame as Figure 2.6b.

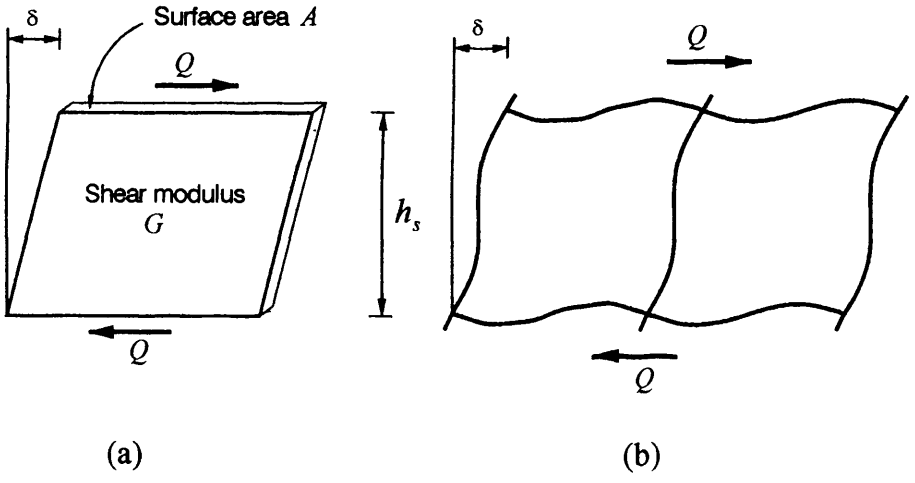

Figure 2.6 a) storey-height segment of analogous shear wall b) single storey of rigid frame (Smith and Coull 1991)

Stafford Smith and Coull (Smith and Coull 1991) have shown that the effective shear rigidity of a frame at floor level i, $(GA_s)_i$, can be obtained as follows. This is based on the assumption that the points of contraflexure occur in the frame at the mid-storey level of the columns and at the mid-span of the beams. This is a reasonable assumption for high-rise rigid frames for all stories near the top and bottom.

$$(GA)_i = \frac{12E}{h_s(\frac{1}{G}+\frac{1}{C})_i} \tag{2.29}$$

in which h_s is the storey height, $G = \sum(I_{bj}/b_j)$ for all beams of span b_j across floor level i and $C = \sum(I_{cj}/h_s)$ for all columns in storey level i of the bent. E is the Young's modulus of elasticity and I_{bj} and I_{cj} are the second moments of area of the columns and beams, respectively.

It can be concluded that when consecutive storeys of a frame are identical, their smeared properties define a new member, which together with other members form the final model. The second moment of area of the member equals the sum of the second moment of area of the columns and the rigidity of the rotational elastic support equals the effective shear rigidity of the frame, which can be obtained from Eq. (2.29). Finally the uniformly distributed mass of the element equals the sum of the distributed mass of the columns plus the smeared mass of the beams. In fact the fixing effect of the columns and beams as well as the mass in the beams is distributed downwards, which is clearly an approximation that will remain in the continuum model. In the following section the governing differential equation of the elastic support model is simply obtained from Eq. (2.23). It will then be used to formulate the required element stiffness matrix which has a transcendental dependence upon ω.

2.2.2.1.1 Governing equation of free vibration – elastic beam model

Eq. (2.23) represents the governing differential equation of a Bernoulli-Euler beam with shear rigidity GA_s on a rotational elastic support k^*. It will be used for the derivation of

the differential equation of the elastic support model, on the assumption that the shear deflection of the columns is ignored by putting $GA_s = \infty$. The governing differential of the elastic support model can then be written as follows

$$\frac{d^4U(\xi)}{d\xi^4} - L^2\frac{k^*}{EI}\frac{d^2U(\xi)}{d\xi^2} - L^4\frac{\omega^2 m}{EI}U(\xi) = 0 \tag{2.30}$$

in which k^* equals the effective shear rigidity of the frame as described in Eq. (2.29), I is the sum of the second moment area of the columns on a floor level and m is the smeared mass of the frame along the height of the structure.

Eq. (2.30) can be written in the following non-dimensional form

$$U''''(\xi) - \alpha^2 U''(\xi) - \beta^2\omega^2 U(\xi) = 0 \tag{2.31}$$

in which $\alpha^2 = k^* L^2/EI$ and $\beta^2 = mL^4/EI$ (2.32)

The solution of the Eq. (2.31) can be obtained by substituting the trial solution $U(\xi) = e^{s\xi}$ to give the characteristic equation

$$s^4 - \alpha^2 s^2 - \beta^2\omega^2 = 0 \tag{2.33}$$

The solution of Eq. (2.33) in terms of s^2 is

$$s^2 = \frac{\alpha^2}{2} \mp \sqrt{\beta^2\omega^2 + \frac{\alpha^4}{4}} \tag{2.34}$$

It is evident that s^2 has one positive and one negative solution so the roots of characteristic equation i.e. s_1-s_4 are

$$s_{1,2} = \mp\lambda_1 \text{ and } s_{3,4} = \mp i\lambda_2 \tag{2.35}$$

in which $i = \sqrt{-1}$ and

$$\lambda_1 = \sqrt{\sqrt{\beta^2\omega^2 + \frac{\alpha^4}{4}} + \frac{\alpha^2}{2}} \quad \text{and} \quad \lambda_2 = \sqrt{\sqrt{\beta^2\omega^2 + \frac{\alpha^4}{4}} - \frac{\alpha^2}{2}} \tag{2.36}$$

It follows that the solution of Eq. (2.31) is of the form

$$U(\xi) = C_1 \cosh\lambda_1\xi + C_2 \sinh\lambda_1\xi + C_3 \cos\lambda_2\xi + C_4 \sin\lambda_2\xi \tag{2.37}$$

Following the sign convention of Figures 2.2(b) and 2.2(c), the expression for the bending slope $\theta(\xi)$, shear force $Q(\xi)$ and bending moment $M(\xi)$ can be obtained from Eq. (2.7), Eq. (2.9) and Eq. (2.10) as follows

$$\theta(\xi) = (1/L)U'(\xi) = (1/L)(C_1\lambda_1 \sinh\lambda_1\xi + C_2\lambda_1 \cosh\lambda_1\xi - C_3\lambda_2 \sin\lambda_2\xi + C_4\lambda_2 \cos\lambda_2\xi) \tag{2.38}$$

$$Q(z) = \frac{dM(z)}{dz} + k^*\theta(z) = -EI\frac{d^2\theta(z)}{dz^2} + k^*\theta(z) = -EI\frac{d^3U(z)}{dz^3} + k^*\frac{dU(z)}{dz}$$

$$Q(\xi) = -\frac{EI}{L^3}U'''(\xi) + \frac{k^*}{L}U'(\xi)$$

$$Q(\xi) = -\frac{EI}{L^3}[C_1\lambda_1^3 \sinh\lambda_1\xi + C_2\lambda_1^3 \cosh\lambda_1\xi + C_3\lambda_2^3 \sin\lambda_2\xi - C_4\lambda_2^3 \cos\lambda_2\xi]$$

$$+\frac{k^*}{L}[C_1\lambda_1 \sinh\lambda_1\xi + C_2\lambda_1 \cosh\lambda_1\xi - C_3\lambda_2 \sin\lambda_2\xi + C_4\lambda_2 \cos\lambda_2\xi] \tag{2.39}$$

$$M(z) = -EI\frac{d^2U(z)}{dz^2}$$

$$M(\xi) = -\frac{EI}{L^2}U''(\xi)$$

$$M(\xi) = -\frac{EI}{L^2}[C_1\lambda_1^2 \cosh\lambda_1\xi + C_2\lambda_1^2 \sinh\lambda_1\xi - C_3\lambda_2^2 \cos\lambda_2\xi - C_4\lambda_2^2 \sin\lambda_2\xi] \tag{2.40}$$

where a prime now denotes differentiation with respect to ξ.

The end conditions for displacements and forces of the beam based on the sign convention Figures 2.2(b) and 2.2(c) are respectively,

At end 1 (ξ=0) $U = U_1$ and $\theta = \theta_1$

At end 2 (ξ=1) $U = U_2$ and $\theta = \theta_2$ (2.41)

and

At end 1 (ξ=0) $Q = -Q_1$ and $M = M_1$

At end 2 (ξ=1) $Q = Q_2$ and $M = -M_2$ (2.42)

Substituting Eq. (2.41) into Eqs. (2.37) and (2.38) gives

$$\begin{bmatrix} U_1 \\ \theta_1 \\ U_2 \\ \theta_2 \end{bmatrix} = \begin{bmatrix} 1 & 0 & 1 & 0 \\ 0 & \lambda_1/L & 0 & \lambda_2/L \\ Ch_{\lambda 1} & Sh_{\lambda 1} & C_{\lambda 2} & S_{\lambda 2} \\ \lambda_1 Sh_{\lambda 1}/L & \lambda_1 Ch_{\lambda 1}/L & -\lambda_2 S_{\lambda 2}/L & \lambda_2 C_{\lambda 2}/L \end{bmatrix} \begin{bmatrix} C_1 \\ C_2 \\ C_3 \\ C_4 \end{bmatrix} \tag{2.43}$$

i.e.

$$\mathbf{d = s\,c} \tag{2.44}$$

Where $Ch_{\lambda 1} = \cosh \lambda_1$, $Sh_{\lambda 1} = \sinh \lambda_1$, $C_{\lambda 1} = \cos \lambda_1$ and $S_{\lambda 1} = \sin \lambda_1$ and the same abbreviation applies for λ_2. (2.45)

Substituting Eq. (2.42) into Eqs. (2.39) and (2.40) gives

$$\begin{bmatrix} Q_1 \\ M_1 \\ Q_2 \\ M_2 \end{bmatrix} = \begin{bmatrix} 0 & \frac{EI}{L^3}\lambda_1^3 - \frac{k^*}{L}\lambda_1 & 0 & -\frac{EI}{L^3}\lambda_2^3 - \frac{k^*}{L}\lambda_2 \\ -\frac{EI}{L^2}\lambda_1^2 & 0 & \frac{EI}{L^2}\lambda_2^2 & 0 \\ \lambda_1(-\frac{EI}{L^3}\lambda_1^2 + \frac{k^*}{L})Sh_{\lambda 1} & \lambda_1(-\frac{EI}{L^3}\lambda_1^2 + \frac{k^*}{L})Ch_{\lambda 1} & \lambda_2(-\frac{EI}{L^3}\lambda_2^2 - \frac{k^*}{L})S_{\lambda 2} & \lambda_2(\frac{EI}{L^3}\lambda_2^2 + \frac{k^*}{L})C_{\lambda 2} \\ \frac{EI}{L^2}\lambda_1^2 Ch_{\lambda 1} & \frac{EI}{L^2}\lambda_1^2 Sh_{\lambda 1} & -\frac{EI}{L^2}\lambda_2^2 C_{\lambda 2} & -\frac{EI}{L^2}\lambda_2^2 S_{\lambda 2} \end{bmatrix} \begin{bmatrix} C_1 \\ C_2 \\ C_3 \\ C_4 \end{bmatrix} \tag{2.46}$$

i.e.

$$\mathbf{f} = \mathbf{b}\,\mathbf{c} \tag{2.47}$$

Eqs. (2.44) and (2.47) give

$$\mathbf{f} = \mathbf{k}\,\mathbf{d} \tag{2.48}$$

i.e

$$\begin{bmatrix} Q_1 \\ M_1 \\ Q_2 \\ M_2 \end{bmatrix} = \begin{bmatrix} K_{1,1} & K_{1,2} & K_{1,3} & K_{1,4} \\ & K_{2,2} & K_{2,3} & K_{2,4} \\ Sym. & & K_{3,3} & K_{3,4} \\ & & & K_{4,4} \end{bmatrix} \begin{bmatrix} U_1 \\ \theta_1 \\ U_2 \\ \theta_2 \end{bmatrix} \tag{2.49}$$

where $\mathbf{k} = \mathbf{b}\,\mathbf{s}^{-1}$ (2.50)

is the required dynamic stiffness matrix of the member.

2.2.2.1.2 Wittrick-Williams Algorithm

The dynamic stiffness matrix, **K**, when assembled from the member stiffness matrices yields the required natural frequencies as solutions of the equation

$$\mathbf{K}\,\mathbf{D} = \mathbf{0} \tag{2.50}$$

where **D** is the vector of amplitudes of the harmonically varying nodal displacements and **K** is a function of ω, the circular frequency. In most cases the required natural frequencies correspond to $|\mathbf{K}|$, the determinant of **K**, being equal to zero. Traditionally the required values have been ascertained by simply tracking the value of $|\mathbf{K}|$ and noting the value of

ω corresponding to $|\mathbf{K}|=0$. However when **K** is developed from exact member theory, defined in Chapter 1, the determinant is a highly irregular, transcendental function of ω.

Additionally, several natural frequencies maybe close together or coincident, while others may exceptionally correspond to **D** = **0**. Thus any trial and error method which involves computing $|\mathbf{K}|=0$ and noting when it changes sign through zero can miss roots. This can be overcome by use of Wittrick-Williams algorithm (Wittrick and Williams 1971) which has received wide attention in the literature(Williams and Wittrick 1983). The algorithm states that

$$J = J_0 + s\{\mathbf{K}\} \tag{2.51}$$

where J is the number of natural frequencies of the structure exceeded by some trial frequency, ω^*, J_0 is the number of natural frequencies which would still be exceeded if all members were clamped at their ends so as to make **D** = **0** and s{**K**} is the sign count of the matrix **K**. s{**K**} is defined in Ref. (Wittrick and Williams 1971)and is equal to the number of negative elements on the leading diagonal of the upper triangular matrix obtained from **K**, when $\omega = \omega^*$, by the standard form of Gauss elimination without row interchanges.

The knowledge of J corresponding to any trial frequency makes it possible to develop a method for converging upon any required natural frequency to any desired accuracy. However, while s{**K**} is easily computed, the value of J_0 is sometimes more difficult to determine, as in the present case. A procedure for the calculation of J_0 i.e. the sum of the clamped-clamped natural frequencies of each member in the structure which is the below the trial frequency ω^*, is described below. (Note that J_0 can also be interpreted as the number of natural frequencies of the structure corresponding to **D** = **0** which is below the trial frequency ω^*).

Calculation of J_0

From the definition of J_0 it can be seen that (Williams and Wittrick 1983; Wittrick and Williams 1971)

$$J_0 = \sum J_m \tag{2.52}$$

where J_m is the number of natural frequencies of an element, with its end clamped, which has been exceeded by ω^*, and the summation extends over all elements. In some cases it is possible to determine the value of J_m for a structural member symbolically using a direct approach (Howson 1979) which gives an analytical expression for J_m. However this is impractical in the present case due to the algebraic complicity of the expression. Instead, the result (i.e. the calculation of J_m) is achieved by an argument based on Eq. (2.51) and applies the Wittrick-Williams algorithm (Wittrick and Williams 1971) in reverse. The procedure corresponds to the one originally proposed by Howson and Williams (Howson and Williams 1973) and is described as follows.

Consider an element which has been isolated from its neighbours by clamping its ends. Treating this members as a complete structure, it is evident that the required value of J_m could be evaluated if its natural frequencies were known. Unfortunately this simple structure can rarely be solved easily. We therefore seek to establish a different set of boundary conditions (other than clamped-clamped) which admit a simple solution from which the solution for the clamped-clamped case can be deduced. This is most easily achieved by imposing pin-pin support conditions at the ends of the member, which prevent lateral displacements but allow rotational displacements.

The stiffness relationship for this single member with simply supported ends can be obtained by deleting appropriate rows and columns from Eq. (2.49) give

$$\begin{bmatrix} M_1 \\ M_2 \end{bmatrix} = \begin{bmatrix} K_{2,2} & K_{2,4} \\ K_{2,4} & K_{4,4} \end{bmatrix} \begin{bmatrix} \theta_1 \\ \theta_2 \end{bmatrix} \tag{2.53}$$

or

$$\mathbf{m_{ss}} = \mathbf{k_{ss}}\, \boldsymbol{\theta}_{\mathbf{ss}} \tag{2.54}$$

where $\mathbf{k}_{ss}$ is the required 2×2 stiffness matrix of this simple one-member structure. Application of the Wittrick-Williams algorithm (Wittrick and Williams 1971) to this simple structure gives

$$J_{ss} = J_m + s\{\mathbf{k}_{ss}\} \tag{2.55}$$

where J_{ss} is the number of natural frequencies for the simply supported case that lie below the trial frequency ω^*, J_m is the required number of clamped-clamped natural frequencies of the member lying between $\omega = 0$ and $\omega = \omega^*$, $s\{\mathbf{k}_{ss}\}$ is the number of negative elements on the leading diagonal of $\mathbf{k}_{ss}^{\Delta}$; and $\mathbf{k}_{ss}^{\Delta}$ is the upper triangular matrix obtained by applying the usual form of Guess elimination to $\mathbf{k}_{ss}$. Thus clearly (Banerjee and Williams 1994)

$$s\{\mathbf{k}_{ss}\} = \frac{1}{2}\left(2 - \mathrm{sgn}[K_{2,2}] - \mathrm{sgn}[K_{4,4} - K_{2,4}^2/K_{2,2}]\right) \tag{2.56}$$

where sgn[ ] is +1 when the content of the brackets [ ] is positive and is –1 when the content of the brackets [ ] is negative. Hence from Eq. (2.55),

$$J_m = J_{ss} - s\{\mathbf{k}_{ss}\} \tag{2.57}$$

$s\{\mathbf{k}_{ss}\}$ can then be easily obtained.

Evaluation of J_{ss} is more difficult, but relates to boundary conditions that yield a simple solution, as explained below.

For the pin-pin support, the boundary conditions are defined for

$$\xi = 0 \text{ and } \xi = 1 \quad \text{as} \quad U = M = 0 \tag{2.58}$$

These conditions are satisfied by assuming a solution for the displacement $U(\xi)$ of the form(Timoshenko et al. 1974).

$$U(\xi) = C_i \sin(i\pi\xi) \qquad (i = 1,2,3,\ldots,\infty) \tag{2.59}$$

where C_i are constants.

Substituting Eq. (2.59) into.Eq. (2.31) gives

$$\left((i\pi)^4 + \alpha^2(i\pi)^2 - \beta^2\omega^2\right) = 0 \tag{2.60}$$

and yields one possible value for ω for each value of i as follows

$$\omega_i^{ss} = \frac{i\pi}{\beta}\sqrt{\alpha^2 + (i\pi)^2} \tag{2.61}$$

where ω_i^{ss} increases monotonically with i. Therefore, J_{ss} can be calculated from

$J_{ss}=i$

where i is the highest value of i for which ω_i^{ss} lies below ω^*. Once J_{ss} is known, J_m can be calculated from Eq. (2.57).

2.2.2.2 Plane wall-frame structures

A wall-frame structure is the combination of shear walls and rigid frames, or in the case of a steel structure, the combination of braced bents with rigid frames. Since walls tend to deflect in a flexural configuration and frames tend to deflect in a shear mode, where they are constrained to adopt a common deflected shape by the horizontal rigidity of the floor slabs, they interact horizontally, especially at the top, thus a stiffer and stronger structure is provided.

Another advantage of the wall-frame structure is that, in a carefully designed structure, the shear in the frame can be made approximately uniform over the height. Allowing the floor framing to be repetitive.

A further understanding of the interaction between the wall and the frame in a wall-frame structure is given by the deflected shapes of a shear wall and a rigid frame, subjected separately to horizontal loading, as shown in Figure 2.6(a) and (b)(Smith and Coull 1991). The wall deflects in a flexural mode with concavity downwind and a maximum slope at the top, while the frame deflects in a shear mode with concavity upwind and a maximum slope at the base. When the wall and frame are connected together by pin-ended links and subjected to horizontal loading, the deflected shape of the composite structure has a flexural profile in the lower part and a shear profile in the upper part (Figure 2.6c). Axial forces in the connecting links cause the wall to restrain the frame near the base and the frame to restrain the wall at the top. Illustration of the effects of wall-frame interaction are given by the curves for deflection, moment, and shear for a typical wall-frame structure, as shown in figure 2.7(a), (b) and (c), respectively. The deflection curve (Figure 2.7(a)) and the wall moment curve (Figure 2.7(b)) indicate a reversal in curvature with a point of inflexion, above which the wall moment is opposite in sense to that of a free cantilever. Figure 2.7(c) shows the shear as approximately uniform over the height of the frame, except near the base where it reduces to a negligible amount. At the top, where the external shear is zero, the frame is subjected to a significant positive shear, which is balanced by an equal negative shear at the top of the wall.

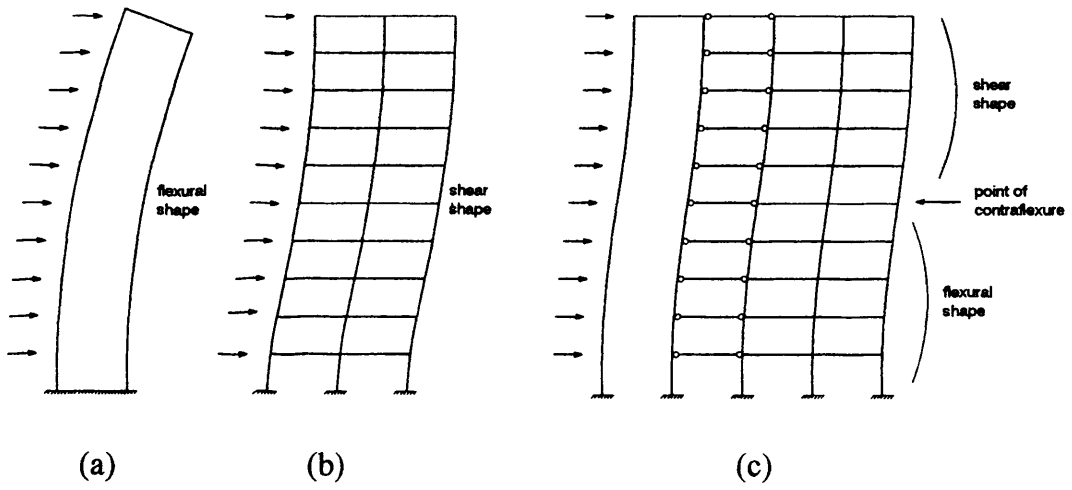

Figure 2.6 (a) wall subjected to uniformly distributed horizontal loading; (b) frame subjected to uniformly distributed horizontal loading; (c) wall-frame structure subjected to uniformly distributed horizontal loading(Smith and Coull 1991).

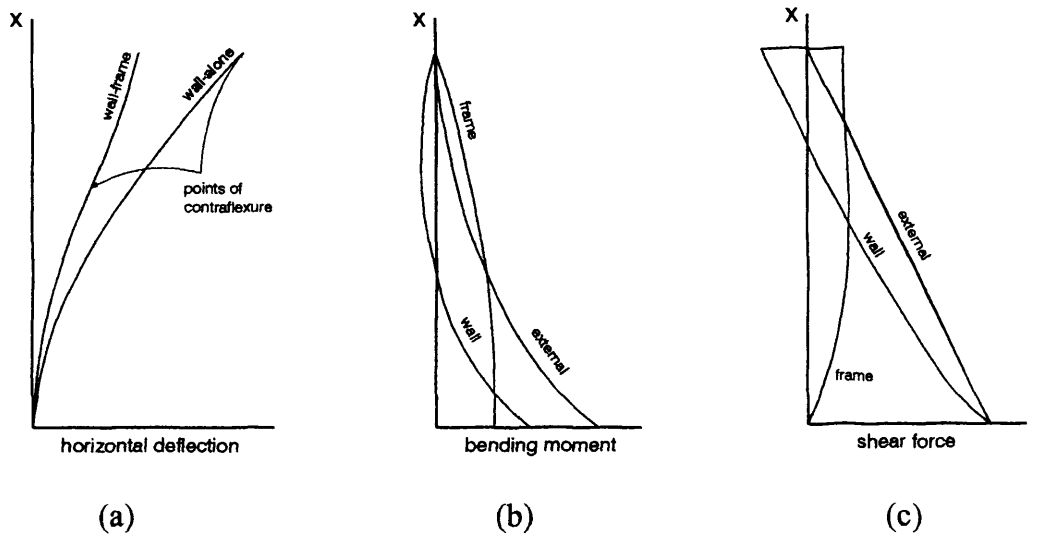

Figure 2.7 - (a) Typical deflection diagram of laterally loaded wall-frame structure (b) typical moment diagrams for components of wall-frame structure (c) typical shear diagram for components of wall-frame structure(Smith and Coull 1991).

2.2.2.2.1 Governing equation of free vibration

Stafford Smith (Smith and Coull 1991) derived the differential equation governing the static displacement of a plane wall-frame structure subjected to lateral distributed load using the continuum method. In this study, his work is extended to cover the vibration analysis of plane wall-frame structures. It is assumed that the properties of the wall and frame members are uniform, but subject to step wise change over the height of the structure.

The plane wall-frame in Figure 2.8(a) may be taken to represent either a structure with walls and frames interacting in the same plane, or one with walls and frames in parallel planes(Smith and Coull 1991). This is possible since, in a non-twisting structure, parallel walls and frames translate identically and may therefore be simulated by a plane linked model.

The governing differential equation of motion can be obtained by cutting the wall-frame through the structure horizontally at those storey levels corresponding to changes in storey properties and considering the equilibrium of a typical segment. However, for simplicity the governing equation of motion will be obtained by considering a uniform cantilever as shown in Figure 2.8 and writing the equation of equilibrium for shear forces in an arbitrary cross section. The following assumptions are adopted to achieve this:

1. The properties of the wall and the frame members are uniform along the height of the structure.
2. The wall may be represented by a flexural cantilever, i.e., one which deforms in bending only.
3. The frame may be represented by a continuous shear cantilever, which deforms in shear only. This implies that the frame deflects only by reverse bending of the columns and girders and that the columns are axially rigid (Figure 2.3(c)).
4. The connecting members (pin ended links) may be represented by a horizontally rigid connecting medium that transmits horizontal forces only and that causes the flexural and shear cantilevers to deflect identically.

Consider the wall and frame separately, as in Figure 2.8(c), $w(z)$ and $q(z)$ are, respectively, the distributed external loading and the distributed internal interactive force, whose intensities vary with height. Q_H is a concentrated horizontal force that acts between the top of the wall and the frame. m_w and m_f are the uniformly distributed mass per unit length of the wall and the frame, respectively.

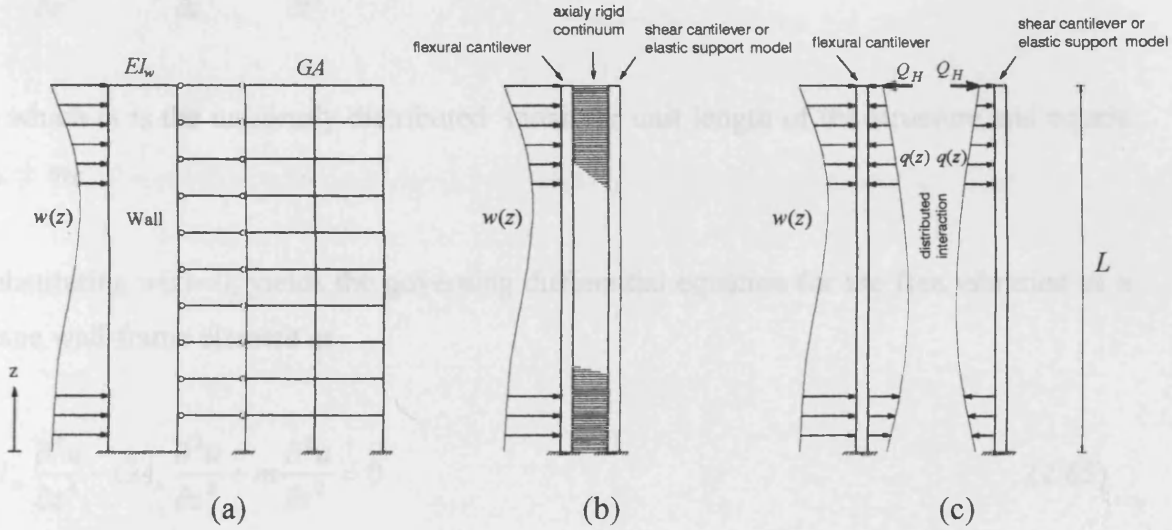

Figure 2.8 –(a) Planar wall-frame structure (b) continuum method for wall-frame (c) free body diagrams for wall and frame (Smith and Coull 1991)

The differential equation for shear in the flexural member is

$$-EI_w \frac{\partial^3 u}{\partial z^3} = \int_z^L m_w \frac{\partial^2 u}{\partial t^2} dz + \int_z^L [w(z) - q(z)] dz - Q_H \tag{2.62}$$

and, for shear in the shear cantilever is

$$GA_s \frac{\partial u}{\partial z} = \int_z^L m_f \frac{\partial^2 u}{\partial t^2} dz + \int_z^L q(z) dz + Q_H \tag{2.63}$$

in which L is the height of the structure, EI_w is the flexural rigidity of the walls and the parameter GA_s represents the storey-height averaged shear rigidity of the frame, as though it were a shear member with an effective shear area A and a shear modulus G. Note that G is not the shear modulus of the frame material nor is A the area of its members.

Differentiating and summing Eqs (2.62) and (2.63) gives

$$EI_w \frac{\partial^4 u}{\partial z^4} - GA_s \frac{\partial^2 u}{\partial z^2} + m\frac{\partial^2 u}{\partial t^2} = w(z) \tag{2.64}$$

in which m is the uniformly distributed mass per unit length of the structure and equals $m_w + m_f$.

Substituting $w(z)=0$, yields the governing differential equation for the free vibration of a plane wall-frame element as

$$EI_w \frac{\partial^4 u}{\partial z^4} - GA_s \frac{\partial^2 u}{\partial z^2} + m\frac{\partial^2 u}{\partial t^2} = 0 \tag{2.65}$$

If a sinusoidal variation of u with circular frequency ω is assumed, then

$$u(z,t) = U(z)\sin \omega t \tag{2.66}$$

where U(z) is the amplitude of the sinusoidally varying displacement. Substituting the non dimensional parameter

$$\xi = z / L \tag{2.67}$$

Eq. (2.65) can be written as.

$$\frac{d^4 U}{d\xi^4} - L^2 \frac{GA_s}{EI_w}\frac{d^2 U}{d\xi^2} - L^4 \frac{\omega^2 m}{EI_w} U(\xi) = 0 \tag{2.68}$$

Clearly Eq. (2.68) is directly comparable with Eq. (2.30), so the elastic support model can be used for the vibration analysis of wall-frame structures that can be modelled in planar form. It further means that the derived dynamic stiffness matrix of Eq. (2.49) can be used for the frequency analysis of plane wall-frame structures when EI and k^* are replaced by the flexural rigidity of the wall and GA_s of the frame, respectively.

This conclusion can also be reached from physical arguments based on the fact that the flexural deformation of the wall occurs in the same form as the full-height bending deformation of the individual columns of the frame (Figure 2.3(b)).

Plane wall-frame structures can also be analysed more accurately if the shear cantilever of Figure 2.8(b) is replaced with an elastic support model. If this is the case Eq. (2.63) can be substituted with the following equation

$$-EI_c\frac{d^4u}{dz^4}+GA_s\frac{d^2u}{dz^2}=m_f\frac{d^2u}{dt^2}+q(x) \tag{2.69}$$

in which I_c is the sum of the second moment of area of individual columns.

With a similar procedure it can be shown that the governing differential equation of the free vibration of such a model can be written in the following form

$$\frac{d^4U}{d\xi^4}-L^2\frac{GA_s}{(EI_c+EI_w)}\frac{d^2U}{d\xi^2}-L^4\frac{\omega^2 m}{(EI_c+EI_w)}U(\xi)=0 \tag{2.70}$$

Therefore substituting EI with EI_c+EI_w in the formulation of the elastic support model can give better result for the frequency analysis of wall-frame structures.

2.2.3 Shear Beam Model

The second model proposed, like the first, is a continuum model of a cantilever, but allows only for shear deformation and therefore is only applicable to the free vibration analysis of rigid frame structures. Thus, for the regular frame considered in previous sections, the equivalent model would require only one degree of freedom. The motion is governed by a second order differential equation that is easily developed from first principles or can be deduced from any published beam theory which allows for shear deformation e.g. the theory developed in Section 2.2.1 of this study. The latter course would require the bending rigidity to be set to infinity, elastic support stiffness to be set to

zero and the shear rigidity to be set to an equivalent shear frame rigidity(Zalka 2001). The effective shear rigidity was previously explained in detail in section 2.2.2. As the full height bending stiffness of the individual columns (Figure 2.3(b)) is ignored in this model, the model will be more accurate for tall buildings with relatively weak columns.

2.2.3.1 Governing differential equation – shear beam model

Eq. (2.23) represents the governing differential equation of a beam with shear rigidity GA_s on a continuous rotational elastic support k^* and can be used to obtain the governing differential equation of the shear beam model. On ignoring the elastic support ($k^* = 0$) and setting the bending rigidity to infinity ($EI=\infty$, θ=0), the required differential equation can be obtained from Figures 2.2(a) and 2.2(b) as follows

Dynamic equilibrium in the x direction gives

$$\frac{\partial Q}{\partial z} - m\frac{\partial^2 u}{\partial t^2} = 0 \tag{2.71}$$

Substituting $\theta=0$ in Eq. (2.7) gives

$$\frac{\partial u}{\partial z} = \frac{Q}{GA_s}$$

Therefore

$$Q = GA_s\frac{\partial u}{\partial z} \text{ and hence } \frac{\partial Q}{\partial z} = GA_s\frac{\partial^2 u}{\partial z^2} \tag{2.72}$$

Substituting Eq. (2.71) in Eq. (2.72) gives

$$\frac{\partial^2 u}{\partial z^2} - \frac{m}{GA_s}\frac{\partial^2 u}{\partial t^2} = 0 \tag{2.73}$$

If a sinusoidal variation of u with circular frequency ω is assumed then

$$u(z,t) = U(z)\sin\omega t \tag{2.74}$$

where $U(z)$ is the amplitude of the sinusoidally varying displacement.

Substituting Eq. (2.74) in Eq (2.73) results

$$\frac{d^2U}{dz^2} + \frac{m\omega^2}{GA_s}U(z) = 0 \tag{2.75}$$

Using the non-dimensional parameter $\xi=z/L$, the governing differential equation of a shear beam can be written as follows.

$$\frac{d^2U}{d\xi^2} + \lambda^2\omega^2 U(\xi) = 0 \tag{2.76}$$

in which $\lambda^2 = \frac{mL^2}{GA_s}$ (2.77)

The solution of the differential Eq. (2.76) can be obtained by substituting the trial solution $U(\xi) = e^{s\xi}$ to give the characteristic equation

$$s^2 + \lambda^2\omega^2 = 0 \tag{2.78}$$

with the result that

$$s = \pm i\lambda\omega \tag{2.79}$$

It follows that the solution of Eq. (2.76) is of the form

$$U(\xi) = C_1\cos\lambda\omega\xi + C_2\sin\lambda\omega\xi \tag{2.80}$$

Following the sign convention of Figures 2.2(a) and 2.2(b), the expression for the shear force $Q(\xi)$ can be obtained from Eq. (2.72) as follows

$$Q = GA_s \frac{dU}{dz} \tag{2.81}$$

Thus

$$Q(\xi) = \frac{GA_s}{L}\frac{dU}{d\xi} = \frac{GA_s}{L}(-C_1 \lambda\omega \sin \lambda\omega\xi + C_2 \lambda\omega \cos \lambda\omega\xi) \tag{2.82}$$

The boundary conditions for displacements and forces of the beam, based on the sign conventions of Figures 2.2(a) and 2.2(b), are respectively

At end 1 (ξ=0) $U = U_1$

At end 2 (ξ=1) $U = U_2$ (2.83)

and

At end 1 (ξ=0) $Q = -Q_1$

At end 2 (ξ=1) $Q = Q_2$ (2.84)

Substituting Eq. (2.83) into Eq. (2.80) gives

$$\begin{bmatrix} U_1 \\ U_2 \end{bmatrix} = \begin{bmatrix} 1 & 0 \\ \cos \lambda\omega & \sin \lambda\omega \end{bmatrix} \begin{bmatrix} C_1 \\ C_2 \end{bmatrix} \tag{2.85}$$

or

$$\begin{bmatrix} C_1 \\ C_2 \end{bmatrix} = \frac{1}{\sin \lambda\omega} \begin{bmatrix} \sin \lambda\omega & 0 \\ -\cos \lambda\omega & 1 \end{bmatrix} \begin{bmatrix} U_1 \\ U_2 \end{bmatrix} \tag{2.86}$$

Substituting Eq. (2.84) into Eq. (2.82) gives

$$\begin{bmatrix} Q_1 \\ Q_2 \end{bmatrix} = \frac{GA_s}{L} \begin{bmatrix} 0 & -\lambda\omega \\ -\lambda\omega \sin\lambda\omega & \lambda\omega\cos\lambda\omega \end{bmatrix} \begin{bmatrix} C_1 \\ C_2 \end{bmatrix} \tag{2.87}$$

Eqs. (2.86) and (2.87) gives

$$\begin{bmatrix} Q_1 \\ Q_2 \end{bmatrix} = \frac{GA_s\lambda\omega}{(\sin\lambda\omega)L} \begin{bmatrix} \cos\lambda\omega & -1 \\ -1 & \cos\lambda\omega \end{bmatrix} \begin{bmatrix} U_1 \\ U_2 \end{bmatrix} \tag{2.88}$$

or

$$\mathbf{f = k\,d} \tag{2.89}$$

where **k** is the dynamic stiffness matrix for the shear beam model.

2.2.3.2 Wittrick-Williams Algorithm

The dynamic stiffness matrix, **K**, when assembled from the member stiffness matrices, yields the required natural frequencies as solutions of the equation

$$\mathbf{K\,D = 0} \tag{2.90}$$

The Wittrick-Williams algorithm can then be used again to solve this transcendental eigenvalue problem. As was explained in Section 2.2.2.1.2, Eq. (2.51) yields the number of natural frequencies of the structure exceed by the trial frequency ω^*. In this case it is possible to determine the value of J_m for a structural member symbolically, using a direct approach as follows.

The governing differential equation of a shear beam and its general solution are written here again for convenience

$$\frac{d^2U}{d\xi^2} + \lambda^2\omega^2 U(\xi) = 0 \tag{2.91}$$

$$U(\xi) = C_1 \cos\lambda\omega\xi + C_2 \sin\lambda\omega\xi \tag{2.92}$$

The end displacement conditions for a clamped-clamped member are

At end 1 (ξ=0) $U(0) = 0$ (2.93)

At end 2 (ξ=1) $U(1) = 0$ (2.94)

Substituting Eqs. (2.93) and (2.94) in Eq. (2.92) gives C_1=0 and

$$C_2 \sin\lambda\omega = 0 \quad \text{or} \quad \lambda\omega = i\pi \quad \text{and} \quad (i=1,2,3,\ldots) \tag{2.95}$$

or

$$\omega = \frac{i\pi}{\lambda} \tag{2.96}$$

so J_m for any trial frequency ω^* can be given as follows

$$J_m = \text{int}\left[\frac{\omega^*}{(\pi/\lambda)}\right] \tag{2.97}$$

in which int represents the image integer function i.e. the greatest integer < $\omega^*/(\pi/\lambda)$.

It should be noted that when all storeys of a frame are identical, the whole frame can be modelled with one element which is free at one end and clamped at the other. Imposing these boundary conditions on Eq. (2.88) gives the frequency equation of such a frame as

$$\cos\lambda\omega = 0 \quad \text{where} \quad \lambda^2 = mL^2/GA \tag{2.98}$$

As the structure compromises only one element, L can be replaced by H, the height of the whole frame. Thus

$$\lambda^2 = mH^2/GA$$

in which m and H are the mass per unit length and height of the substitute column, respectively, and GA is the shear rigidity of the frame. The required natural frequencies are therefore given by

$$\lambda\omega = (2j-1)\pi/2 \quad \text{or} \quad \omega = \frac{(2j-1)\pi}{2}\sqrt{\frac{GA}{mH^2}} \quad \text{where} \quad j=1,2,3,... \qquad (2.99)$$

It should be noted from Section 2.2.2.1 that m, the mass per unit length of the substitute beam, equals the sum of distributed mass of columns plus the smeared mass of the beams between floors. Moreover, the mass in the beams is distributed downwards, which will produce small errors in the model. Also, as the full height bending stiffness of the individual columns (Figure 2.3(b)) is ignored here, the model will be more accurate for tall buildings with relatively weak columns and short storey height.

2.3 SUBSTITUTE FRAME METHOD

2.3.1 The Principle of Multiples

The Principle of Multiples (Howson and Williams 1999) was first applied to unbraced, rigidly jointed, multi-bay, multi-storey plane frames and is exact on the basis of inextensible member theory. It can be used to prove that the frames of Figures 2.9 (a)-(d) share the same horizontal deflections for static or harmonic response calculations when F $\neq$ 0, that they share the same critical value of W for buckling problems when F = 0 and W $\neq$ 0 and that they share the same natural frequencies when F = 0. In general the response

and natural frequency calculations will be performed with W = 0, but non-zero values of W can be used when it is required to allow for the magnifying effect that compressive vertical loads have on horizontal deflections caused by lateral loading or the corresponding reduction in natural frequencies. The static response has been dealt with elsewhere (Howson and Rafezy 2002) and can be modified easily to deal with harmonic response by incorporating the dynamic stiffness matrix defined in(Howson and Williams 1973). The arguments that follow therefore relate only to natural frequency calculations for which F = 0.

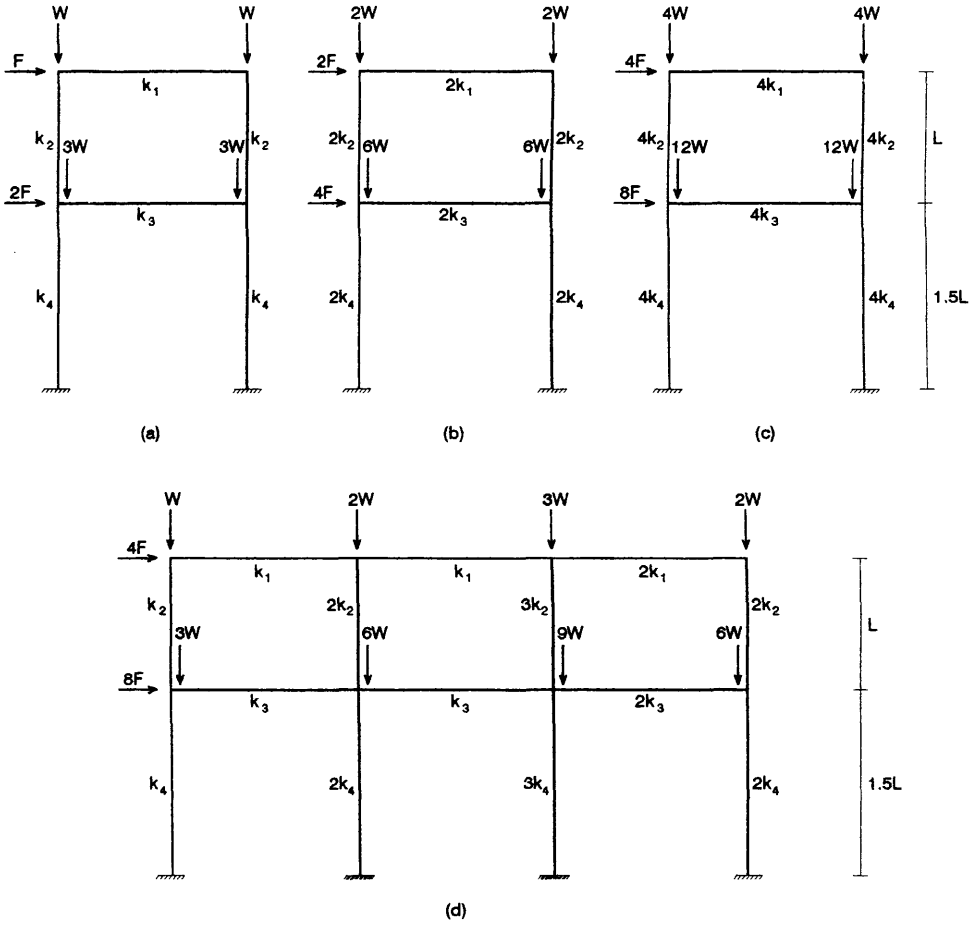

Figure 2.9 Frames (a) – (d) comply with the Principle of Multiples

In Figure 2.9, the k's are values of *EI/L* for the members, where *EI* is the flexural rigidity and *L* is the length. Additionally, values are identical when the subscripts are identical, so

that the frame of Figure 2.9(a) is symmetrical. Note also that any vertical loading is symmetric and therefore the frame must vibrate with a symmetric or an anti-symmetric mode and it is easily proved that the anti-symmetric mode gives the lowest possible natural frequency. Thus, it is clear that any frame which is identical to frame (a) must have the same natural frequency and the same deflected shape. Therefore any frame obtained by superposing N such frames (where N need not be integer), in the sense implied by frames (b) and (c), must also share the natural frequency and the deflected shape of frame (a), even if the frames are all clamped together. Hence putting N=2 and N=4 gives the required proofs for frames (b) and (c), respectively. Moreover, frame (d) can be obtained by fastening together two frame (a)'s and a frame (b) that are situated side by side in the appropriate way. Since frames (a) and (b) share the same natural frequencies and sway with an anti-symmetric deflection pattern, the process of fastening them together to form frame (d) leaves the natural frequencies and the deflections unaltered.

It is evident, however, that most frames do not obey the Principle of Multiples. Fortunately, a well established method exists for reducing multi-bay, multi-storey frames to single bay, multi-storey 'substitute' frames that can then be used to obtain approximate results for the multi-bay case. The substitute frame has the same number of storeys and the same storey heights as the original frame, but differs in that it has only one bay, is symmetric and may only be loaded symmetrically. The required details of the substitute frame are found from the actual frame as follows: the substitute column k (mass/unit length) is equal to half the sum of the k's (mass/unit length) for all actual columns at the same storey level; the substitute beam k (mass/unit length) is equal to the sum of the k's (mass/unit length) for all beams at the same storey level.

Applying the above rules to the frame of 2.9(d) gives the frame of Figure 2.9(c) and hence it can be deduced that when a frame obeys the Principle of Multiples the rules yield a substitute frame which gives correct results for the actual frame, remembering that inextensible member theory is assumed.

However, there are some practical problems that need to be addressed. For the current purpose it is assumed that 'exact' member theory is used in the sense that the distributed mass of the members and the attached walls and floors are incorporated when calculating

the dynamic member stiffness matrices, which are therefore transcendental functions of both frequency and load per unit length. Hence, there are two additional restrictions that apply to the application of the Principle of Multiples to vibration. These are that members sharing the same subscript on Figure 2.9 must have the same mass per unit length as well as the same value of k and that all bays must have identical spans. The second requirement occurs because, whereas in the static case a beam (because it is in contraflexure) contributes 6k to the overall stiffness matrix of the half substitute frame analysed, in vibration problems the stiffness contributed depends both on k and on a dynamic stability function which is a transcendental function of both the beam span and the mass per unit length.

Therefore rules must be adopted to establish the values of L and μ for the beams of the substitute frame where μ is the distributed mass of the beam per unit length. The rules adopted herein are that L is taken as the average value of the bay widths of the actual frame, so that EI can be calculated from the rules given in the previous section for calculating the substitute beam k, and μ for the substitute beam is obtained by dividing its L into the total mass of all beams at the same storey level of the actual frame(Howson and Williams 1999).

2.3.2 Application of the Substitute Frame method in plane frame structures

It was explained in Section 2.3.1 that, by the application of the Principle of Multiples, any frame, regardless of number of storeys or bays, maybe simplified to an equivalent one bay frame, having the same natural frequencies of vibration as the original frame if the conditions of the Principle of Multiples are adhered to. If the conditions of the Principle of Multiples are not achieved, the substitute frame method can still be applied for the frequency analysis of plane frame structures and the results will normally achieve acceptable engineering accuracy. The substitute frame has many fewer design variables than the actual frame. Therefore, parametric studies undertaken with the substitute frame can give the designer insights into the behaviour of the full range of possible actual frames, i.e. the full range of multi-storey, multi-bay frames, with very small

computational effort and without the designer overload referred to in the introduction occurring.

2.3.3 Application of the Substitute Frame method in plane wall-frame structures

In Section 2.2.2.2.1 it was shown that the governing differential equation of free vibration of a plane wall-frame structure is directly comparable to the differential equation of free vibration of a frame. This means that if the sum of the second moment of area of the columns in a frame structure equals the sum of the second moment of area of the columns and walls of a wall-frame structure, the governing differential equations will be same for both structures. This can also be explained by comparing Figures 2.10(a) and 2.10(c), in which I_i is the second moment of area of the individual columns of the wall-frame structure and I_{sub} is the second moment of area of columns of one-bay substitute frame. If I_{sub} equals $(\sum I_i + I_w)/2$ then the continuum models of the plane wall-frame in Figure 2.10(a) and the substitute frame in Figure 2.10(c) will be same. Therefore the substitute frame for a plane wall-frame structure can be defined by the aforementioned rule. This simplification can also be justified by a study of the behaviour of frame and wall-frame structures. A comparison of Figure 2.7(a) and Figure 2.3(b) shows that the flexural behaviour of the wall in a wall-frame structure is identical to the full-height bending deformation of the individual columns in a frame structure, so applying the elastic support model will result in a unique structure for both a wall-frame structure and its substitute frame obtained by the above rule.

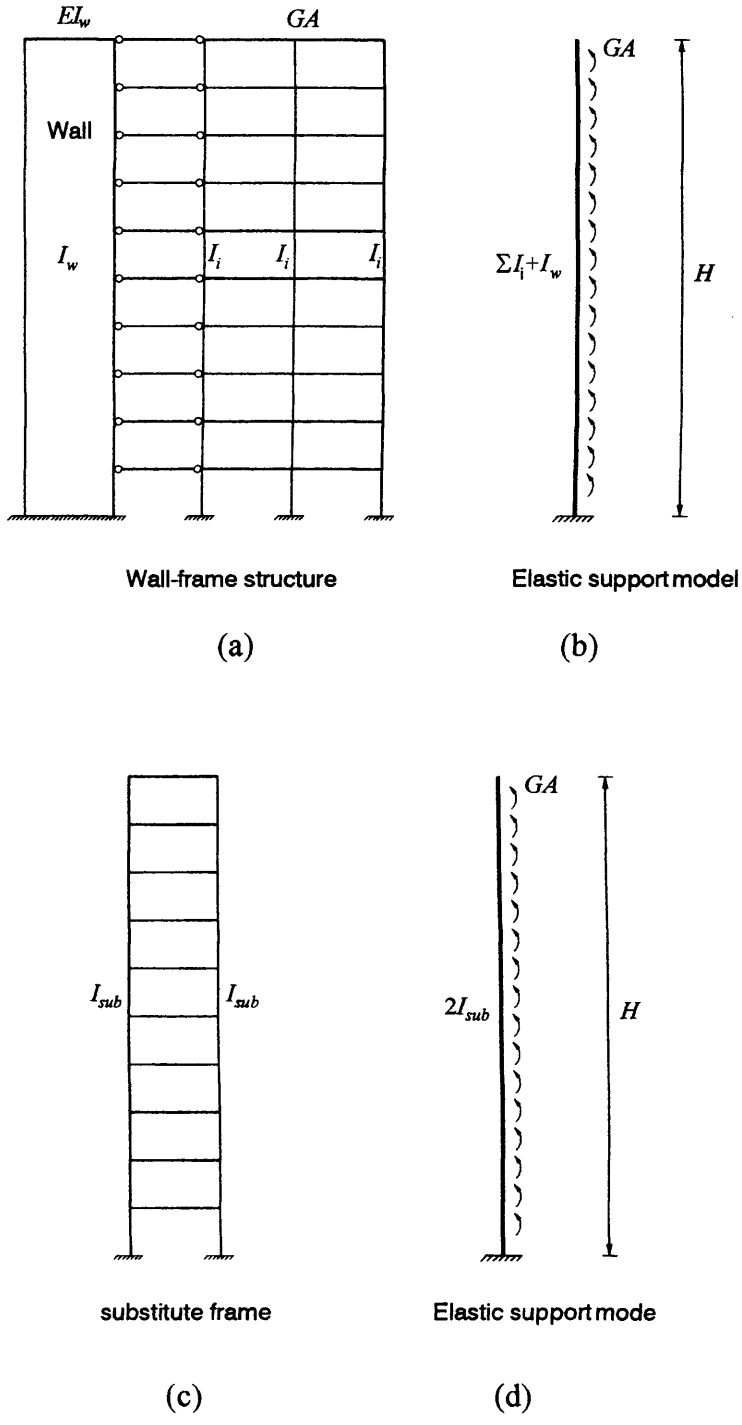

Figure 2.10 (a) and (b) a plane wall-frame and its elastic support model (c) and (d) a one bay substitute frame and its elastic support model

2.4 NUMERICAL RESULTS

In order to validate the use of the proposed methods it was deemed necessary to carry out a parametric study to ascertain the accuracy that might be expected from the proposed methods. These have been achieved by developing two computer programs for the vibration analysis of shear beam and elastic support models in Qbasic language.

2.4.1 Example 2.1

The results from the "elastic support" and "shear beam" models are now compared with results obtained using exact buckling and vibration programme called BUNVIS-RG (Anderson and Williams 1986) by analysing four concrete plane frames comprising 5, 7, 10 and 20 storeys, respectively. Each frame has equal storey heights of 4.0m and three equal bays of width 7.5m, as shown in Figure 2.11(a). Young's modulus for all members is taken as $E=2\text{x}10^{10}$ N/m^2. The column and beam properties are as follows.

Column properties:	external (1)	$I_c = 0.0026\text{m}^4$	$m = 300$ kg/m
	internal (2)	$I_c = 0.0052\text{m}^4$	$m = 600$ kg/m
Beam properties:	roof (3)	$I_b = 0.0026\text{m}^4$	$m = 300$ kg/m
	floor (4)	$I_b = 0.0052\text{m}^4$	$m = 600$ kg/m

All frames obey the Principle of Multiples and assume inextensible member theory. Therefore the results will only show the errors that are inherent in the application of the proposed methods. If the frames don't obey the Principle of Multiples the error will increase as there will be an extra error due to reducing multi-bay frames to single bay substitute frames.

Each method has been applied in two different ways. In the first case, termed "Lump mass", every storey has been considered as an element and the mass of the beams has been lumped at the nodes (Figure 2.11(b)). In the second case, termed "Dist. mass", the whole frame has been considered as a single element and the mass of the beams at each storey level has been distributed along the height of the structure and added to the mass of

the columns (Figure 2.11(c)). It is obvious that the application of the second case is much simpler and the solution can sometimes be obtained by hand methods.

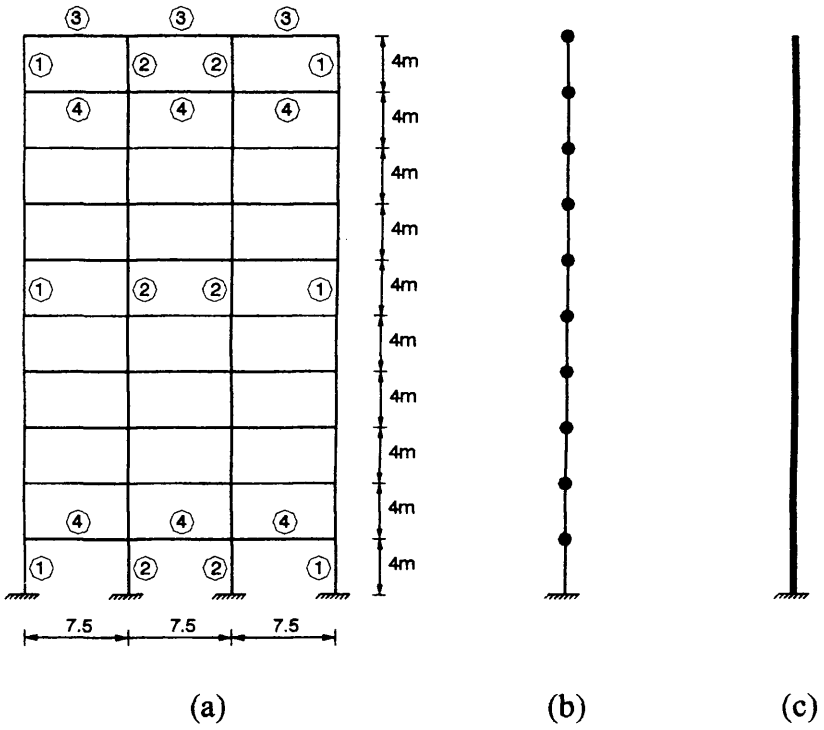

Figure 2.11 (a) Frame of Example 2.1 and its continuum model with lumped (b) and distributed mass (c)

Columns 2 and 4 of Table 2.1 show the natural frequencies (Hz.) of the frames obtained from the shear model with the beam mass lumped and distributed, respectively (case1 and 2). Columns 6 and 8 likewise show the natural frequencies obtained from the elastic support model. The last column in the table shows the result obtained using an exact buckling and vibration programme called BUNVIS-RG(Anderson and Williams 1986). Finally columns 3, 5, 7 and 9 show the difference between the results of the substitute beam models and BUNVIS-RG. When analysing frames with BUNVIS-RG it is assumed that beams and columns obey Bernoulli-Euler theory and therefore don't allow for shear deformation and rotary inertia. Additionally the following assumptions have been made when modelling buildings with BUNVIS-RG

- No $P-\Delta$ effect
- No reduction in the stiffness of columns due to compressive axial loads (no geometric rigidity)

- Inextensible member theory is imposed by multiplying the cross-sectional area of the beams and columns by a factor, typically 10^3.

Table 2.1 - Natural frequencies for the frames of Example 2.1 obtained using the SB and ES models, compared with BUNVIS-RG results

N=5 storeys	Shear Beam model (SB)				Elastic Support model (ES)				BUNVIS-RG
	Lump mass		Dist. mass		Lump mass		Dist. mass		
frequencies	f(Hz.)	diff.%	f(Hz.)	diff.%	f(Hz.)	diff.%	f(Hz.)	diff.%	f(Hz.)
1	1.56	15.68	1.57	15.14	1.73	6.49	1.75	5.41	1.85
2	4.48	22.09	4.7	18.26	5.2	9.56	5.61	2.43	5.75
3	6.87	31.70	7.84	22.07	9.19	8.65	10.45	3.88	10.06
4	8.94	38.26	10.97	24.24	14.32	1.10	16.7	15.33	14.48
5	10.66	47.17	14.11	30.08	19.68	2.48	24.62	22.00	20.18
Average (1^{st},2^{nd},3^{rd})		23.16		18.49		8.23		3.91	

N=7 storeys	Shear Beam model (SB)				Elastic Support model (ES)				BUNVIS-RG
	Lump mass		Dist. mass		Lump mass		Dist. mass		
frequencies	f(Hz.)	diff.%	f(Hz.)	diff.%	f(Hz.)	diff.%	f(Hz.)	diff.%	f(Hz.)
1	1.12	11.11	1.12	11.11	1.21	3.97	1.21	3.97	1.26
2	3.29	14.99	3.36	13.18	3.66	5.43	3.77	2.58	3.87
3	5.29	21.28	5.60	16.67	6.27	6.70	6.73	0.15	6.72
4	7.02	28.73	7.84	20.41	9.35	5.08	10.29	4.47	9.85
5	8.58	38.27	10.08	27.48	13.05	6.12	14.58	4.89	13.90
Average (1^{st},2^{nd},3^{rd})		15.79		13.65		5.36		2.23	

N=10 storeys	Shear Beam model (SB)				Elastic Support model (ES)				BUNVIS-RG
	Lump mass		Dist. mass		Lump mass		Dist. mass		
frequencies	f(Hz.)	diff.%	f(Hz.)	diff.%	f(Hz.)	diff.%	f(Hz.)	diff.%	f(Hz.)
1	0.78	8.24	0.78	8.24	0.83	2.35	0.83	2.35	0.85
2	2.33	9.69	2.35	8.91	2.50	3.10	2.53	1.94	2.58
3	3.83	13.54	3.92	11.51	4.26	3.84	4.38	1.13	4.43
4	5.24	18.38	5.49	14.49	6.16	4.05	6.47	0.78	6.42
5	6.53	23.80	7.05	17.74	8.30	3.15	8.85	3.27	8.57
Average (1^{st} – 5th)		14.73		12.18		3.30		1.89	

N=20 storeys	Shear Beam model (SB)				Elastic Support model (ES)				BUNVIS-RG
	Lump mass		Dist. mass		Lump mass		Dist. mass		
frequencies	f(Hz.)	diff.%	f(Hz.)	diff.%	f(Hz.)	diff.%	f(Hz.)	diff.%	f(Hz.)
1	0.39	4.88	0.39	4.88	0.40	2.44	0.40	2.44	0.41
2	1.18	3.28	1.18	3.28	1.21	0.82	1.21	0.82	1.22
3	1.96	4.85	1.96	4.85	2.04	0.97	2.04	0.97	2.06
4	2.74	5.84	2.74	5.84	2.89	0.69	2.91	0.00	2.91
5	3.53	7.35	3.53	7.35	3.77	1.05	3.81	0.00	3.81
Average (1^{st} – 5^{th})		5.24		5.24		1.19		0.85	

As expected, the results from the shear model are poor for low numbers of storeys, whereas the results from the elastic support model generally show good agreement with BUNVIS results. To get a general idea of the magnitude of the difference, the average of the differences of the 1st, 2nd and 3rd natural frequencies of the 5 and 7 storey frames and also the average of the differences of first 5 natural frequencies of the 10 and 20 storey frames have been calculated and recorded in the last rows of the Table 2.1. The graph of the average differences in each case is presented in Figure 2.12.

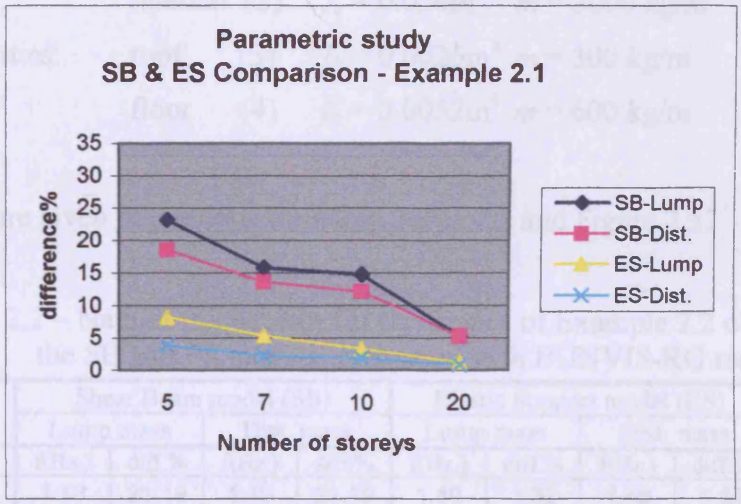

Figure 2.12 The graph of the difference in each model of Example 2.1

The following results can be obtained from the graph.

- The differences in all models decrease with increasing number of storeys.
- All models give acceptable results for frames with 20 storeys or more.
- Both forms of the elastic support model give acceptable results (difference < 10%) for any number of storeys.
- The difference between the lumped and distributed mass models is small and can be safely ignored

2.4.2 Example 2.2

This example investigates the accuracy of the proposed methods when applied to frames with strong columns and weak beams. The data and assumptions of Example 2.1 are used again, except that the second moment of area and the mass per unit length of columns is increased by a factor of 5. The data are as follows.

Column properties:	external (1)	$I_c = 0.013\text{m}^4$	$m = 1500$ kg/m
	internal (2)	$I_c = 0.026\text{m}^4$	$m = 3000$ kg/m
Beam properties:	roof (3)	$I_b = 0.0026\text{m}^4$	$m = 300$ kg/m
	floor (4)	$I_b = 0.0052\text{m}^4$	$m = 600$ kg/m

The results are given in previous format in Table 2.2 and Figure 2.13.

Table 2.2 – Natural frequencies for the frames of Example 2.2 obtained using the SB and ES models, compared with BUNVIS-RG results

N=5 storeys	Shear Beam model (SB)				Elastic Support model (ES)				BUNVIS-RG
	Lump mass		Dist. mass		Lump mass		Dist. mass		
frequencies	f(Hz.)	diff.%	f(Hz.)	diff.%	f(Hz.)	diff.%	f(Hz.)	diff.%	f(Hz.)
1	1.19	21.19	1.19	21.19	1.49	1.32	1.49	1.32	1.51
2	3.40	32.27	3.58	28.69	5.13	2.19	5.19	3.39	5.02
3	5.35	46.07	5.97	39.82	10.66	7.46	10.96	10.48	9.92
4	7.37	59.55	8.35	54.17	18.43	1.15	19.33	6.09	18.22
5	9.32	65.22	10.74	59.93	27.61	3.02	30.47	13.69	26.80
Average (1^{st},2^{nd},3^{rd})		33.18		29.90		3.66		5.06	

N=7 storeys	Shear Beam model (SB)				Elastic Support model (ES)				BUNVIS-RG
	Lump mass		Dist. mass		Lump mass		Dist. mass		
frequencies	f(Hz.)	diff.%	f(Hz.)	diff.%	f(Hz.)	diff.%	f(Hz.)	diff.%	f(Hz.)
1	0.85	15.84	0.85	15.84	1.00	0.99	1.00	0.99	1.01
2	2.51	23.01	2.56	21.47	3.28	0.61	3.30	1.23	3.26
3	4.04	35.67	4.26	32.17	6.40	1.91	6.47	3.03	6.28
4	5.49	44.66	5.97	39.82	10.63	7.16	10.84	9.27	9.92
5	6.98	56.02	7.67	51.67	16.07	1.26	16.56	4.35	15.87
Average (1^{st},2^{nd},3^{rd})		24.84		23.16		1.17		1.75	

N=10 storeys	Shear Beam model (SB)				Elastic Support model (ES)				BUNVIS-RG
	Lump mass		Dist. mass		Lump mass		Dist. mass		
frequencies	f(Hz.)	diff.%	f(Hz.)	diff.%	f(Hz.)	diff.%	f(Hz.)	diff.%	f(Hz.)
1	0.60	10.45	0.59	11.94	0.66	1.49	0.66	1.49	0.67
2	1.78	15.64	1.78	15.64	2.11	0.00	2.11	0.00	2.11
3	2.93	23.70	2.98	22.40	3.89	1.30	3.90	1.56	3.84
4	4.02	33.55	4.17	31.07	6.14	1.49	6.19	2.31	6.05
5	5.08	42.53	5.37	39.25	8.97	1.47	9.08	2.71	8.84
Average (1^{st} – 5th)		25.17		24.06		1.15		1.62	

N=20 storeys	Shear Beam model (SB)				Elastic Support model (ES)				BUNVIS-RG
	Lump mass		Dist. mass		Lump mass		Dist. mass		
frequencies	f(Hz.)	diff.%	f(Hz.)	diff.%	f(Hz.)	diff.%	f(Hz.)	diff.%	f(Hz.)
1	0.30	3.23	0.30	3.23	0.31	0.00	0.31	0.00	0.31
2	0.89	5.32	0.89	5.32	0.96	2.13	0.96	2.13	0.94
3	1.49	8.59	1.49	8.59	1.64	0.61	1.66	1.84	1.63
4	2.08	12.24	2.09	11.81	2.40	1.27	2.43	2.53	2.37
5	2.66	17.90	2.68	17.28	3.26	0.62	3.31	2.16	3.24
Average (1^{st} – 5^{th})		9.45		9.25		0.92		1.73	

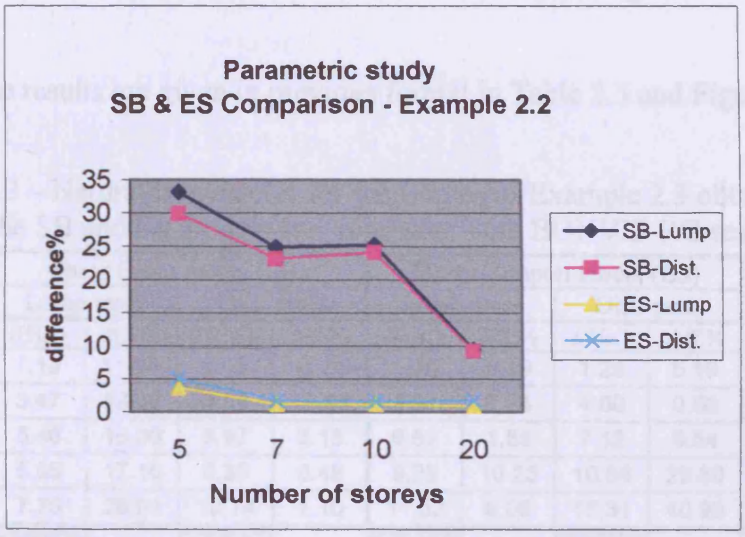

Figure 2.13 The graph of the difference in each model of Example 2.2

The graph clearly shows that the difference in the shear beam model has now increased in comparison with Example 2.1. This can be explained as follows.

The full height bending deformation of the individual columns of such a frame (Figure 2.3(b)) now plays a considerable role in the total deformation of the frame (Figure 2.3). The shear beam model ignores this component of the total deformation, so it was

anticipated that the results would be poor. On the other hand, the accuracy of the elastic support model has improved.

2.4.3 Example 2.3

The final example considers the case of strong beams and weak columns. As before, the data and assumptions of Example 2.1 are used again but this time the second moment of area and the mass per unit length of the beams are increased by a factor of 5. The data are as follows.

Column properties:	external	(1)	$I_c = 0.0026\text{m}^4$	m = 300 kg/m
	internal	(2)	$I_c = 0.0052\text{m}^4$	m = 600 kg/m
Beam properties:	roof	(3)	$I_b = 0.013\text{m}^4$	m = 1500 kg/m
	floor	(4)	$I_b = 0.026\text{m}^4$	m = 3000 kg/m

Once more, the results are given in previous format in Table 2.3 and Figure 2.14.

Table 2.3 – Natural frequencies for the frames of Example 2.3 obtained using the SB and ES models and compared with BUNVIS-RG results

N=5 Storeys	Shear Beam model (SB)				Elastic Support model (ES)				BUNVIS-RG
	Lump mass		Dist. mass		Lump mass		Dist. mass		
Frequencies	f(Hz.)	diff.%	f(Hz.)	diff.%	f(Hz.)	diff.%	f(Hz.)	diff.%	f(Hz.)
1	1.19	11.85	1.19	11.85	1.28	5.19	1.28	5.19	1.35
2	3.47	13.68	3.58	10.95	3.91	2.74	4.00	0.50	4.02
3	5.46	16.00	5.97	8.15	6.62	1.85	7.12	9.54	6.50
4	6.95	17.16	8.35	0.48	9.25	10.25	10.89	29.80	8.39
5	7.75	28.64	10.74	1.10	11.52	6.08	15.31	40.98	10.86
Average (1^{st},2^{nd},3^{rd})		13.84		10.32		3.26		5.07	

N=7 storeys	Shear Beam model (SB)				Elastic Support model (ES)				BUNVIS-RG
	Lump mass		Dist. mass		Lump mass		Dist. mass		
frequencies	f(Hz.)	diff.%	f(Hz.)	diff.%	f(Hz.)	diff.%	f(Hz.)	diff.%	f(Hz.)
1	0.85	8.60	0.85	8.60	0.90	3.23	0.90	3.23	0.93
2	2.52	9.68	2.56	8.24	2.73	2.15	2.75	1.43	2.79
3	4.08	11.30	4.26	7.39	4.64	0.87	4.76	3.48	4.60
4	5.46	13.47	5.97	5.39	6.62	4.91	7.01	11.09	6.31
5	6.58	15.21	7.67	1.16	8.60	10.82	9.58	23.45	7.76
Average (1^{st},2^{nd},3^{rd})		9.86		8.08		2.08		2.71	

N=10 storeys	Shear Beam model (SB)				Elastic Support model (ES)				BUNVIS-RG
	Lump mass		Dist. mass		Lump mass		Dist. mass		
frequencies	f(Hz.)	diff.%	f(Hz.)	diff.%	f(Hz.)	diff.%	f(Hz.)	diff.%	f(Hz.)
1	0.60	4.76	0.59	6.35	0.62	1.59	0.62	1.59	0.63
2	1.78	6.32	1.78	6.32	1.87	1.58	1.87	1.58	1.90
3	2.92	7.59	2.98	5.70	3.16	0.00	3.19	0.95	3.16
4	4.00	9.09	4.17	5.23	4.51	2.50	4.59	4.32	4.40
5	5.00	10.71	5.37	4.11	5.91	5.54	6.12	9.29	5.60
Average (1^{st} – 5th)		7.70		5.54		2.24		3.54	

N=20 storeys	Shear Beam model (SB)				Elastic Support model (ES)				BUNVIS-RG
	Lump mass		Dist. mass		Lump mass		Dist. mass		
frequencies	f(Hz.)	diff.%	f(Hz.)	diff.%	f(Hz.)	diff.%	f(Hz.)	diff.%	f(Hz.)
1	0.30	0.00	0.30	0.00	0.30	0.00	0.30	0.00	0.30
2	0.89	2.20	0.89	2.20	0.91	0.00	0.91	0.00	0.91
3	1.48	2.63	1.49	1.97	1.53	0.66	1.53	0.66	1.52
4	2.06	3.74	2.09	2.34	2.15	0.47	2.16	0.93	2.14
5	2.63	3.66	2.68	1.83	2.79	2.20	2.81	2.93	2.73
Average (1^{st} – 5th)		2.45		1.67		0.66		0.90	

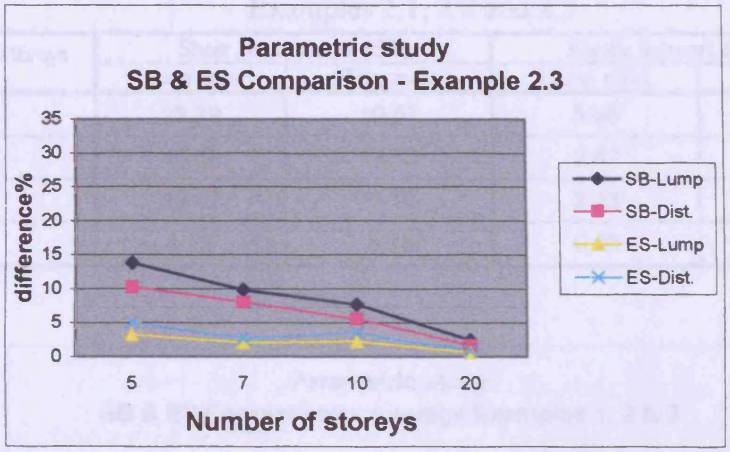

Figure 2.14 The graph of the difference in each model of Example 2.3

The graph clearly shows that the difference in the shear beam model has been reduced to its lowest values of all examples for the converse reasons to those described in Example 2.2.

2.4.4 Conclusions

Table 2.4 shows the average difference for the application of the shear beam and elastic support models in Examples 2.1, 2.2 and 2.3. Figure 2.15 has been drawn from the

information in the table and can be used to draw the final conclusion of the parametric study as follows

- The differences in all models decrease and converge on each other as the number of storeys increases.
- Shear beam models give acceptable results for 20 storey frames and higher. It can also be used for the frames with 10 or more storeys if the frame does not comprise very strong columns relative to the beams. However more investigation is necessary to define more precisely the limitations of the shear beam model.
- The elastic support model gives acceptable results (difference < 10%) for any type of frame in the range of the solved examples
- The difference between the results for the lumped and distributed mass models is small and can safely be ignored.

Table 2.4 - The average difference (%) for the application of SB and ES models in Examples 2.1, 2.2 and 2.3

Number of Storeys	Shear Beam model (SB)		Elastic Support model (ES)	
	Lump mass	Dist. mass	Lump mass	Dist. mass
5	23.39	19.57	5.05	4.68
7	16.83	14.96	2.87	2.23
10	15.87	13.93	2.23	2.35
20	5.71	5.38	0.93	1.16

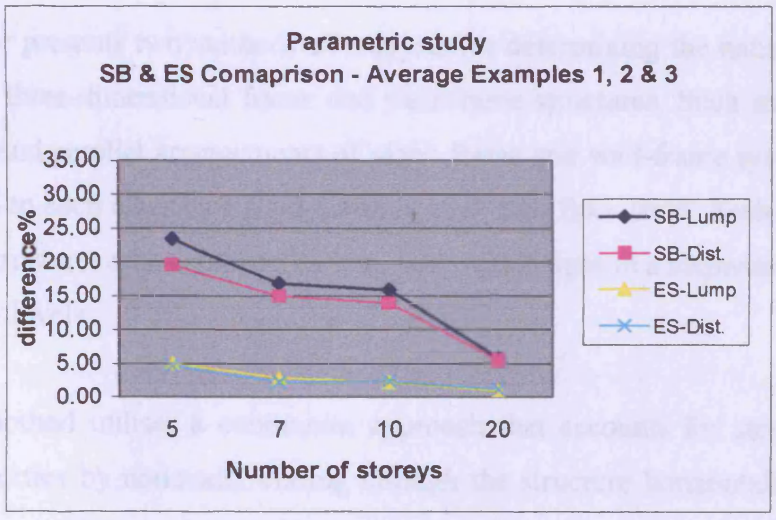

Figure 2.15 The graph of the average difference in each model

CHAPTER 3

VIBRATION ANALYSIS OF SYMMETRIC THREE-DIMENSIONAL FRAME AND WALL-FRAME STRUCTURES

3.1 INTRODUCTION

This chapter presents two methods of analysis for determining the natural frequencies of symmetric, three-dimensional frame and wall-frame structures. Such structures comprise symmetric and parallel arrangements of plane frame and wall-frame systems, which have been joined to each other by a rigid diaphragm at each floor level. Each method is able to deal with structures whose properties may vary with height in a stepwise fashion at one or more storey levels.

The first method utilises a continuum approach that accounts for stepwise changes in storey properties by notionally cutting through the structure horizontally at those storey levels corresponding to changes in storey properties. A typical segment of the structure thus formed is then considered in isolation. Initially, a primary frame or wall-frame in one direction is replaced by an appropriate substitute beam that has uniformly distributed

mass and stiffness, thus utilising the continuum approach. In turn, each frame or wall-frame running in the same direction is replaced by its own substitute beam and the effect of all such beams is summed to model the effect of the original frames. This leads directly to the differential equation governing the sway motion of the segment in the chosen direction. The same procedure is then adopted for those frames running in the orthogonal direction. Once both equations are available it requires little effort to write down the substitute expressions for the torsional motion. Both elastic support and shear substitute beams will be used here to model plane frame and wall-frame structures running in two orthogonal directions.

The second method utilises the Principle of Multiples and extends its application to three-dimensional structures. This is achieved by defining three different substitute frames corresponding to the three uncoupled modes of vibration, namely torsional motion and sway in the two lateral directions.

3.2 CONTINUUM METHOD

3.2.1 Elastic Support Model

3.2.1.1 Symmetric three-dimensional rigid frame structures

Consider a typical floor plan of a symmetric, three-dimensional frame structure idealised as a set of orthogonal plane frames, as shown in Figure 3.1. The coordinate system is fixed at the centre of symmetry, C, with the x and y axes running parallel to the axes of symmetry and z defining the height of the structure. It is assumed that the plane frames are connected by a rigid diaphragm (slab) at each floor level, so that the structure will have two pure translational modes and one pure torsional mode of vibration as shown in

Figures 3.2(a), (b) and (c). These uncoupled modes can therefore be studied separately. Since the aim is to find the natural frequencies of the structure, the external forces $\mathbf{P}_x$ and $\mathbf{P}_y$ that act through the centre of pressure, CP, are zero.

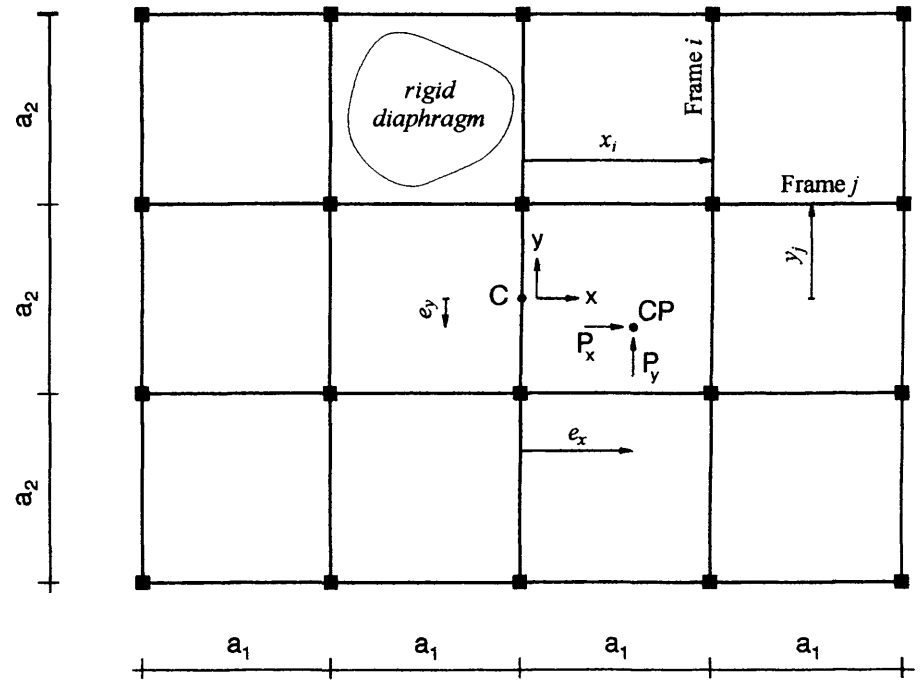

Figure 3.1 Typical floor plan of a symmetric three-dimensional frame structure

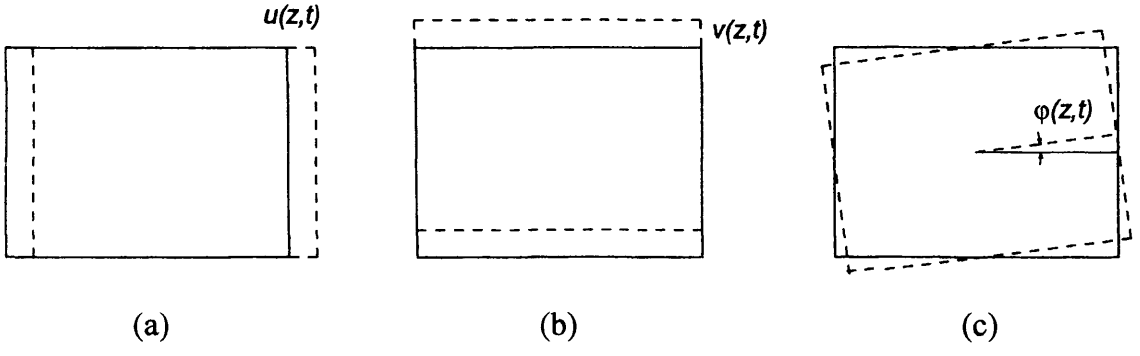

Figure 3.2 Three uncoupled modes of vibration of a symmetric structure (a) and (b) are the translational modes in the x and y directions; (c) is the torsional mode about the z axis

3.2.1.1.1. Translational vibration

The structure is now divided into segments along the z axis by notionally cutting the structure along horizontal planes at those storey levels corresponding to changes in storey properties. Figure 3.3 shows a typical segment formed by cutting the structure through planes $E_kF_kG_kH_k$ and $E_{k+1}F_{k+1}G_{k+1}H_{k+1}$ that correspond to the k^{th} and $k+1^{th}$ changes in storey properties. The number of storeys in any one segment can vary from one, to the total number of storeys in the structure if it is uniform throughout its height. However, in any one segment each storey must have the same properties.

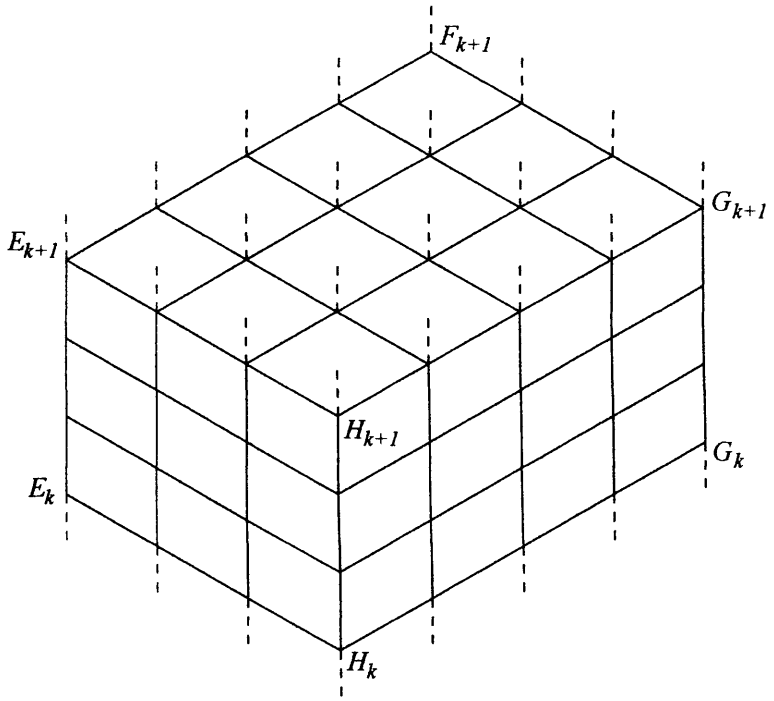

Figure 3.3 Typical segment formed by cutting the structure through planes $E_kF_kG_kH_k$ and $E_{k+1}F_{k+1}G_{k+1}H_{k+1}$ that correspond to the k^{th} and $k+1^{th}$ changes in storey properties. (Some column and beam members have been omitted for clarity.)

We now consider a typical segment in isolation and seek to replace each primary frame by a substitute elastic support beam that replicates its in-plane motion. We start by considering a typical frame, frame i, that runs parallel to the y-z plane, see Figure 3.1. This whole frame is replaced by the single substitute beam, beam i, shown in Figure 3.4. This beam is a two-dimensional elastic support beam of length L and has uniformly distributed mass m_{yi}, flexural rigidity EI_{yi} and rotational elastic support stiffness equal to GA_{yi}/unit length. The mass and elastic axes therefore coincide with the local z-axis and the

elastic axis is permitted deformation $v_i(z,t)$ in the y direction, where z and t denote distance from the local origin and time, respectively.

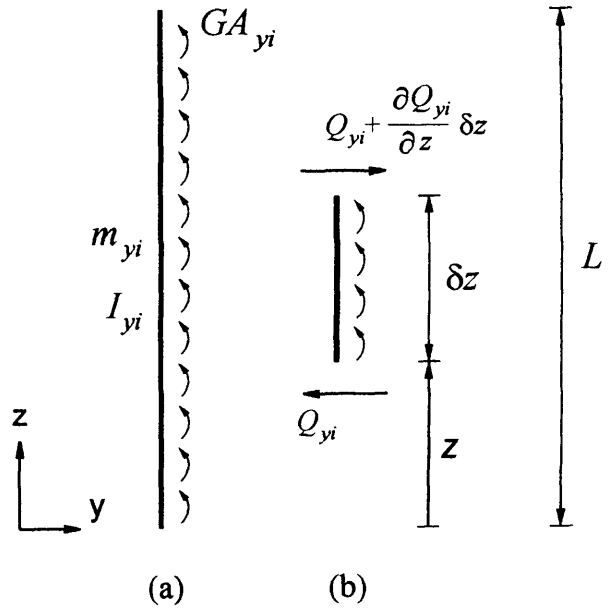

Figure 3.4 Elastic support substitute beam of plane frame i a) substitute beam b) shear force on a typical element length of beam (internal moments have been omitted for clarity)

Using Eqs (2.7) to (2.11), the following equation can be written for the transverse force in the substitute elastic support model.

$$Q_{yi} = -EI_{yi}\frac{\partial^3 v_i(z,t)}{\partial z^3} + GA_{yi}\frac{\partial v_i(z,t)}{\partial z} \tag{3.1}$$

in which $Q_{yi}(z,t)$ is the shear force on the element.

Dynamic equilibrium of the element in the y direction gives

$$\frac{\partial Q_{yi}}{\partial z}\delta z = m_{yi}\frac{\partial^2 v_i(z,t)}{\partial t^2}\delta z \tag{3.2}$$

Substituting Eq. (3.1) into Eq. (3.2) gives

$$EI_{yi}\frac{\partial^4 v_i(z,t)}{\partial z^4} - GA_{yi}\frac{\partial^2 v_i(z,t)}{\partial z^2} + m_{yi}\frac{\partial^2 v_i(z,t)}{\partial t^2} = 0 \tag{3.3}$$

This is the governing differential equation for the elastic support substitute beam of frame *i*. It was shown in Figure 3.2(b) that, because of the rigid diaphragm, all frames running parallel to the y direction share the same deflection ($v(z,t)$), so the dynamic equilibrium in the y direction for all frames can be written as follows

$$\frac{\partial}{\partial z}(\sum_{i=1}^{n_y} - EI_{yi}\frac{\partial^3 v(z,t)}{\partial z^3} + \sum_{i=1}^{n_y} GA_{yi}\frac{\partial v(z,t)}{\partial z})\delta z = \sum_{i=1}^{n_y} m_{yi}\frac{\partial^2 v(z,t)}{\partial t^2}\delta z \tag{3.4}$$

in which n_y is the number of frames running parallel to the y direction.

Noting that EI_{yi} and GA_{yi} are constant along the length of the member gives

$$EI_y\frac{\partial^4 v(z,t)}{\partial z^4} - GA_y\frac{\partial^2 v(z,t)}{\partial z^2} + m_y\frac{\partial^2 v(z,t)}{\partial t^2} = 0 \tag{3.5}$$

in which

$$EI_y = \sum_{i=1}^{n_y} EI_{yi} \tag{3.6a}$$

$$GA_y = \sum_{i=1}^{n_y} GA_{yi} \tag{3.6b}$$

$$m_y = \sum_{i=1}^{n_y} m_{yi} \tag{3.6c}$$

and $v(z,t)$ is the common deformation of frames in the y direction.

Eqs (3.5) and (3.6a-c) define an elastic support model for the frequency analysis of a three-dimensional frame in the y direction, so the dynamic stiffness matrix obtained in Chapter 2 for an elastic support model can also be used for the frequency analysis of symmetric three-dimensional frame structures.

It should be noted that the contribution from frames running in the x direction to the vibration of the structure in the y direction should be taken into account. The shear rigidity of frames in the x direction does not have any effect on the vibration of the structure in the y direction, but the distributed mass of the beams should be considered by smearing it over the height of the model. Also, if any column of a plane frame running in the x direction does not belong to a plane frame in the y direction, its mass and second moment of area about the x axis should be added to the corresponding properties of the column of the elastic support model, since such a column deflects like a flexural cantilever in the y direction.

An identical argument enables us to define an elastic support substitute beam for vibration of the structure in the x direction. The analogous differential equation for the elastic support beam in the x direction can be written as

$$EI_x \frac{\partial^4 u(z,t)}{\partial z^4} - GA_x \frac{\partial^2 u(z,t)}{\partial z^2} + m_x \frac{\partial^2 u(z,t)}{\partial t^2} = 0 \tag{3.7}$$

in which

$$EI_x = \sum_{j=1}^{n_x} EI_{xj} \tag{3.8a}$$

$$GA_x = \sum_{j=1}^{n_x} GA_{xj} \tag{3.8b}$$

$$m_x = \sum_{j=1}^{n_x} m_{xj} \tag{3.8c}$$

where n_x is the number of plane frames running in the x direction and $u(z,t)$ is the common deformation of frames in the x direction.

3.2.1.1.2. Torsional vibration

It was shown in Figure 3.2 that the pure torsional mode of vibration is one of the three basic modes of vibration in symmetric structures. Consider two typical frames, i in the y direction and j in the x direction, whose distance from the centre of torsion are x_i and y_j, respectively (Figure 3.1). Replacing these frames with their elastic support substitute beams and writing the equation for torsional equilibrium about C, gives

$$\sum_{i=1}^{n_y} -EI_{yi}x_i\frac{\partial^4 v_i(z,t)}{\partial z^4}+\sum_{i=1}^{n_y} GA_{yi}x_i\frac{\partial^2 v_i(z,t)}{\partial z^2}-(\sum_{j=1}^{n_x} -EI_{xj}y_j\frac{\partial^4 u_j(z,t)}{\partial z^4}+\sum_{j=1}^{n_x} GA_{xj}y_j\frac{\partial^2 u_j(z,t)}{\partial z^2})=$$

$$\sum_{i=1}^{n_y} m_{yi}x_i\frac{\partial^2 v_i(z,t)}{\partial t^2}-\sum_{j=1}^{n_x} m_{xj}y_j\frac{\partial^2 u_j(z,t)}{\partial t^2} \qquad (3.9)$$

Because of the rigid diaphragm at each floor level (Figure 3.2c), there is a linear relation between $u_j(z,t)$, $v_i(z,t)$ and $\varphi(z,t)$, which is given by

$$u_j(z,t)=-y_j\varphi(z,t) \qquad (3.10)$$

$$v_i(z,t)=x_i\varphi(z,t) \qquad (3.11)$$

where $\varphi(z,t)$ is the torsional deflection of the structure about C.

Differentiating Eqs. (3.10) and (3.11) and substituting into Eq. (3.9) gives

$$\left(\sum_{i=1}^{n_y} EI_{yi}x_i^2+\sum_{j=1}^{n_x} EI_{xj}y_j^2\right)\frac{\partial^4\varphi(z,t)}{\partial z^4}-\left(\sum_{i=1}^{n_y} GA_{yi}x_i^2+\sum_{j=1}^{n_x} GA_{xj}y_j^2\right)\frac{\partial^2\varphi(z,t)}{\partial z^2}+$$

$$\left(\sum_{i=1}^{n_y} m_{yi}x_i^2+\sum_{j=1}^{n_x} m_{xj}y_j^2\right)\frac{\partial^2\varphi(z,t)}{\partial t^2}=0 \qquad (3.12)$$

or

$$EI_{wf}\frac{\partial^4\varphi(z,t)}{\partial z^4}-GJ\frac{\partial^2\varphi(z,t)}{\partial z^2}+I_{gf}\frac{\partial^2\varphi(z,t)}{\partial t^2}=0 \qquad (3.13)$$

in which

$$EI_{wf} = \left(\sum_{i=1}^{n_y} EI_{yi} x_i^2 + \sum_{j=1}^{n_x} EI_{xj} y_j^2 \right) \tag{3.14a}$$

$$GJ = \left(\sum_{i=1}^{n_y} GA_{yi} x_i^2 + \sum_{j=1}^{n_x} GA_{xj} y_j^2 \right) \tag{3.14b}$$

$$I_{gf} = \left(\sum_{i=1}^{n_y} m_{yi} x_i^2 + \sum_{j=1}^{n_x} m_{xj} y_j^2 \right) \tag{3.14c}$$

Eqs. (3.13) and (3.14a-c) define an elastic support model for the torsional frequency analysis of symmetric, three-dimensional frame structures.

As every frame in the x and y directions was replaced by its elastic support model in its plane of symmetry, the out of plane effect (stiffness and inertia) of the frames in torsion was lost. Therefore if any column in frame i does not belong to any frame in the x direction, its out of plane stiffness and inertia should be taken into account. As such a column behaves like a flexural cantilever, its out of plane stiffness (EI) should be multiplied by the square of its distance from the x axis and added to EI_{wf}. This also applies to any column in frame j which does not belong to any frame in the y direction.

Eq. (3.14c) clearly shows that I_{gf} is the polar second moment of mass about the z axis, so it would be more accurate to calculate I_{gf} based on the distribution of mass in the real structure rather than the elastic support models. Simple formulae for calculating I_{gf} for the case in which the mass is uniformly distributed in the beams or rigid diaphragms (slabs) can be found in handbooks.

3.2.1.2 Symmetric three-dimentional wall-frame structures

A symmetric three-dimensional wall-frame structure is the combination of shear walls and rigid frames in which both the walls and the frames are located symmetrically on plan and

connected to each other by a rigid diaphragm at floor levels (Figure 3.5). The behaviour of plane wall-frame structures was discussed in Section 2.2.2.2 and it is extended here to calculate the natural frequencies of symmetric, three-dimensional wall-frame structures using the elastic support substitute beam.

3.2.1.2.1. Translational vibration

Figure 3.4. shows a typical floor plan of a symmetric, three-dimensional wall-frame structure. Consider a typical wall, wall i, running in the y direction with second moment of area I_{wyi} and uniformly distributed mass m_{wyi}, together with a typical wall, wall j, running in the x direction with second moment of area of I_{wxj} and uniformly distributed mass m_{wxj} acting with the system of planar frames considered before (Figure 3.5).

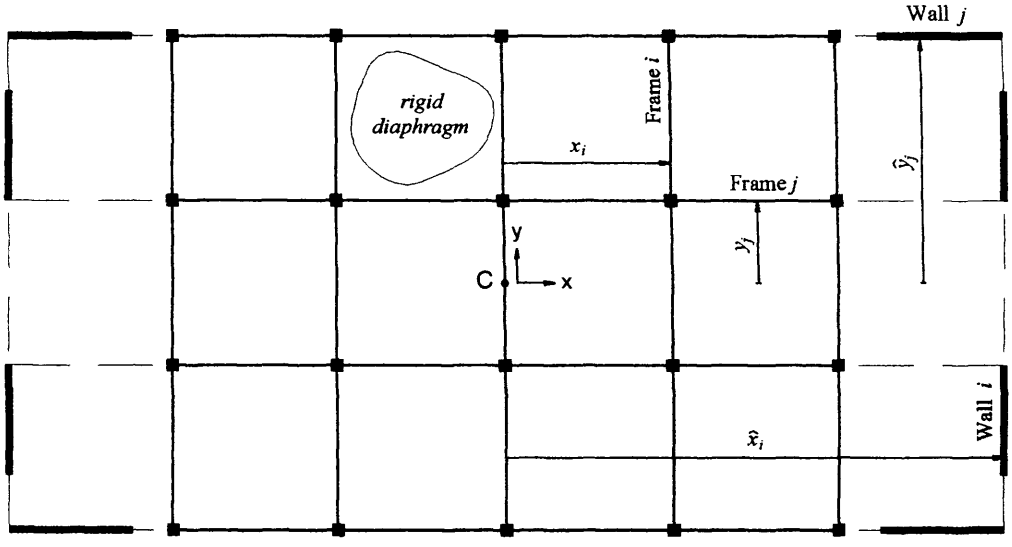

Figure 3.5 Typical floor plan of a symmetric three-dimensional wall-frame structure

Based on the continuum theory explained in Chapter 2, all walls may be replaced with flexural substitute beams and all frames with their elastic support substitute beams, so that the dynamic equilibrium in the y dirction for the combination of walls and frames can be written using Eqs. (2.65) and (2.69) as

$$\sum_{i=1}^{n_{wy}} -EI_{wyi}\frac{\partial^4 v_i(z,t)}{\partial z^4} + \sum_{i=1}^{n_{wy}} -EI_{yi}\frac{\partial^4 v_i(z,t)}{\partial z^4} + \sum_{i=1}^{n_{wy}} GA_{yi}\frac{\partial^2 v_i(z,t)}{\partial z^2} =$$

$$\sum_{i=1}^{n_{wy}} m_{wyi}\frac{\partial^2 v_i(z,t)}{\partial t^2} + \sum_{i=1}^{n_{wy}} m_{yi}\frac{\partial^2 v_i(z,t)}{\partial t^2} \qquad (3.15)$$

or

$$(EI_{wy} + EI_y)\frac{\partial^4 v(z,t)}{\partial z^4} - GA_y\frac{\partial^2 v(z,t)}{\partial z^2} + (m_{wy} + m_y)\frac{\partial^2 v(z,t)}{\partial t^2} = 0 \qquad (3.16)$$

in which

$$EI_{wy} = \sum_{i=1}^{n_{wy}} EI_{wyi} \qquad (3.17a)$$

and

$$m_{wy} = \sum_{i=1}^{n_{wy}} m_{wyi} \qquad (3.17b)$$

where n_{wy} is the number of walls in the y direction and EI_y, GA_y and m_y were defined in Eqs. (3.6a-c).

Here again the contribution of the walls in the x direction to the behaviour of the structure in the y direction should be taken into account. The out-of-plane stiffness of the walls can safely be ignored, but their uniformly distributed mass should be considered by adding it directly to the continuum model. Eq. (3.16) is in the form of the governing differential equation of an elastic support model so it can be concluded that an elastic support model may be defined for the vibration analysis of symmetric wall-frame structures in the y direction.

An identical argument enables us to define an elastic support substitute beam for the vibration of the structure in the x direction. The analogous differential equation may be written as

$$(EI_{wx} + EI_x)\frac{\partial^4 u(z,t)}{\partial z^4} - GA_x \frac{\partial^2 u(z,t)}{\partial z^2} + (m_{wx} + m_x)\frac{\partial^2 u(z,t)}{\partial t^2} = 0 \tag{3.18}$$

in which

$$EI_{wx} = \sum_{j=1}^{n_{wx}} EI_{wxj} \tag{3.19a}$$

$$m_{wx} = \sum_{j=1}^{n_{wx}} m_{wxj} \tag{3.19b}$$

where EI_x, GA_x and m_x were defined in Eqs. (3.8a-c) and n_{wx} is the number of walls in the x direction.

3.2.1.2.2. Torsional vibration

The governing differential equation for torsional vibration of a symmetric wall-frame structure can be achieved by replacing walls with flexural substitute beams and plane frames with elastic support substitute beams and writing the torsional equilibrium about C as follows

$$\begin{aligned}
&\sum_{i=1}^{n_{wy}} -EI_{wyi}\hat{x}_i \frac{\partial^4 v_i(z,t)}{\partial z^4} + \sum_{i=1}^{n_y} -EI_{yi}x_i \frac{\partial^4 v_i(z,t)}{\partial z^4} - (\sum_{j=1}^{n_{wx}} -EI_{wxj}\hat{y}_j \frac{\partial^4 u_j(z,t)}{\partial z^4} + \sum_{j=1}^{n_x} -EI_{xj}y_j \frac{\partial^4 u_j(z,t)}{\partial z^4}) \\
&+ \sum_{i=1}^{n_y} GA_{yi}x_i \frac{\partial^2 v_i(z,t)}{\partial z^2} - \sum_{j=1}^{n_x} GA_{xj}y_j \frac{\partial^2 u_j(z,t)}{\partial z^2} = \sum_{i=1}^{n_{wy}} m_{wyi}\hat{x}_i \frac{\partial^2 \hat{v}_i(z,t)}{\partial t^2} + \sum_{i=1}^{n_y} m_{yi}x_i \frac{\partial^2 v_i(z,t)}{\partial t^2} \\
&- (\sum_{j=1}^{n_{wx}} m_{wxj}\hat{y}_j \frac{\partial^2 \hat{u}_j(z,t)}{\partial t^2} + \sum_{j=1}^{n_x} m_{xj}y_j \frac{\partial^2 u_j(z,t)}{\partial t^2})
\end{aligned} \tag{3.20}$$

in which

$\hat{x}_i$ is the distance of wall i from the centre of symmetry C,

$\hat{y}_j$ is the distance of wall j from the centre of symmetry C,

$\hat{v}_i(z,t)$ is the deflection of wall i in the y direction

and

$\hat{u}_j(z,t)$ is the deflection of wall j in the x direction.

Because of the rigid diaphragm, there is a linear relation between $\hat{u}_j(z,t)$, $\hat{v}_i(z,t)$ and $\varphi(z,t)$, which is given by

$$\hat{u}_j(z,t) = -\hat{y}_j\varphi(z,t) \tag{3.21}$$

$$\hat{v}_i(z,t) = \hat{x}_i\varphi(z,t) \tag{3.22}$$

Substituting Eqs (3.10), (3.11), (3.21) and (3.22) and their derivatives in Eq. (3.20) gives

$$(EI_{ww} + EI_{wf})\frac{\partial^4\varphi(z,t)}{\partial z^4} - GJ\frac{\partial^2\varphi(z,t)}{\partial z^2} + (I_{gw} + I_{gf})\frac{\partial^2\varphi(z,t)}{\partial t^2} = 0 \tag{3.23}$$

in which

$$EI_{ww} = \left(\sum_{i=1}^{n_{wy}} EI_{wyi}\hat{x}_i^2 + \sum_{j=1}^{n_{wx}} EI_{wxj}\hat{y}_j^2\right) \tag{3.24a}$$

$$I_{gw} = \left(\sum_{i=1}^{n_{wy}} m_{wyi}\hat{x}_i^2 + \sum_{j=1}^{n_{wx}} m_{wxj}\hat{y}_j^2\right) \tag{3.24b}$$

where EI_{wf}, GJ and I_{gf} were defined in Eqs. (3.14a-c).

Eqs (3.23) and (3.24) define an elastic support substitute beam for the torsional frequency analysis of symmetric, three-dimensional wall-frame structures.

Here again the out of plane rigidity and moment inertia of the frames and walls should be taken into account in a similar way to that of Section 3.2.1.1.2.

3.2.2 Shear Beam Model

3.2.2.1 Symmetric three-dimensional frame structures

In Section 3.2.1.1, the natural frequencies of symmetric, three-dimensional frames were calculated using the elastic support model. In this section a similar approach will be developed using the shear beam model. Consider Figure 3.1 again with the characteristics described in Section 3.2.1.1. Substituting any frame in both the x and y directions by its substitute shear beam and writing the dynamic equilibrium for the x, y and torsional directions will provide the governing differential equations for translational and torsional vibration of the structure.

3.2.2.1.1. Translational vibration

For the substitute shear beam of frame i shown in Figure 3.6, the transverse load can be obtained using Eq. (2.72) as follows

$$Q_{yi} = GA_{yi}\frac{\partial v_i(z,t)}{\partial z} \tag{3.25}$$

in which $Q_{yi}(z,t)$ is the shear force on the element.

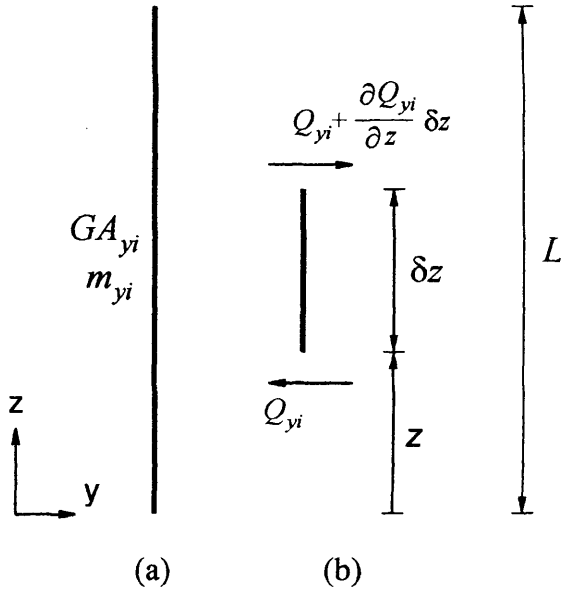

Figure 3.6 Shear substitute beam of frame *i* a) substitute shear beam b) shear force on element

Dynamic equilibrium of the element in the y direction gives

$$\frac{\partial Q_{yi}}{\partial z}\delta z = m_{yi}\frac{\partial^2 v_i(z,t)}{\partial t^2}\delta z \tag{3.2r}$$

Sustituting Eq. (3.25) into Eq. (3.2r) gives

$$GA_{yi}\frac{\partial^2 v_i(z,t)}{\partial z^2} = m_{yi}\frac{\partial^2 v_i(z,t)}{\partial t^2} \tag{3.26}$$

which is the governing differential equation of the shear substitute beam of frame *i*. It was shown in Figure 3.2(b) that, because of the rigid diaphragm, all frames in the y direction share the same deflection ($v(z,t)$), so the dynamic equilibrium in the y direction for all frames can be written as follows

$$\sum_{i=1}^{n_y} GA_{yi}\frac{\partial^2 v_i(z,t)}{\partial z^2} - \sum_{i=1}^{n_y} m_{yi}\frac{\partial^2 v_i(z,t)}{\partial t^2} = 0 \tag{3.27}$$

or

$$GA_y \frac{\partial^2 v(z,t)}{\partial z^2} - m_y \frac{\partial^2 v(z,t)}{\partial t^2} = 0 \tag{3.28}$$

in which

$$GA_y = \sum_{i=1}^{n_y} GA_{yi} \tag{3.29a}$$

$$m_y = \sum_{i=1}^{n_y} m_{yi} \tag{3.29b}$$

The contribution of frames running in the x direction to the vibration of the structure in the y direction should be taken into account in the same way as for the elastic support substitute beam in Section 3.2.1.1.1.

An identical argument enables us to define a shear substitute beam for the vibration of the structure in the x direction. The analogous differential equation may be written as

$$GA_x \frac{\partial^2 u(z,t)}{\partial z^2} - m_x \frac{\partial^2 u(z,t)}{\partial t^2} = 0 \tag{3.30}$$

in which

$$GA_x = \sum_{j=1}^{n_x} GA_{xj} \tag{3.31a}$$

$$m_x = \sum_{j=1}^{n_x} m_{xj} \tag{3.31b}$$

3.2.2.1.2. Torsional vibration

The governing differential equation for torsional vibration of a symmetric frame structure can be achieved by replacing any frame in both the x and y directions with its shear substitute beam and writing the torsional equilibrium about the z axis as follows

$$\sum_{i=1}^{n_y} GA_{yi}x_i \frac{\partial^2 v_i(z,t)}{\partial z^2} + \sum_{j=1}^{n_x} GA_{xj}y_j \frac{\partial^2 u_j(z,t)}{\partial z^2} - \sum_{i=1}^{n_y} m_{yi}x_i \frac{\partial^2 v_i(z,t)}{\partial t^2} - \sum_{j=1}^{n_x} m_{xj}y_j \frac{\partial^2 u_j(z,t)}{\partial t^2} = 0 \qquad (3.32)$$

Substituting Eqs (3.10) and (3.11) and their derivatives into Eq. (3.32) gives

$$GJ \frac{\partial^2 \varphi(z,t)}{\partial z^2} - I_{gf} \frac{\partial^2 \varphi(z,t)}{\partial t^2} = 0 \qquad (3.33)$$

in which

$$GJ = \left(\sum_{i=1}^{n_y} GA_{yi}x_i^2 + \sum_{j=1}^{n_x} GA_{xj}y_j^2 \right) \qquad (3.34a)$$

$$I_{gf} = \left(\sum_{i=1}^{n_y} m_{yi}x_i^2 + \sum_{j=1}^{n_x} m_{xj}y_j^2 \right) \qquad (3.34b)$$

GJ is the torsional rigidity of all frames about the centre of torsion and I_{gf} is the polar second moment of mass about the centre of symmetry.

Finally it should be noted that the shear beam model, as in the case of two-dimensional frames, can not be used for the frequency analysis of wall-frame structures.

3.2.3 Conclusions (Continuum Models)

It has been shown that the free vibration of a symmetric, three-dimensional frame and wall-frame structure can be modelled by three plane continuum models in the x, y and torsional directions. On the assumption that the translational and torsional modes of the original structure are all uncoupled, it was shown that the two continuum models for the

vibration of the structure in the x and y directions can be analysed using the methods of Chapter 2 to yield the lower eigenvalues of the original structure in each of its two orthogonal planes. It was further shown that, with little additional effort, the torsional properties of the structure could be set in the same context to yield the torsional eigenvalues of the structure.

3.3 SUBSTITUTE FRAME METHOD

3.3.1 Application of the Substitute Frame Method to the Static and Dynamic Analysis of Symmetric Three-dimensional Frame Structures

It was explained in Section 2.3.1 that, by the application of the Principle of Multiples, any two-dimensional frame, may be simplified to an equivalent one bay frame, having the same natural frequencies of vibration as the original frame if the conditions of Principle of Multiples are adhered to. If the conditions of the Principle of Multiples are not achieved, the substitute frame method can still be applied in most cases for the frequency analysis of any plane frame structure although the results will be approximate, but will normally have sufficient accuracy for engineering purposes.

Howson and Rafezy (Howson and Rafezy 2002) have extended the application of the substitute frame method from two dimensional structures to calculating the static nodal displacements of doubly plan asymmetric, three-dimensional, multi-bay, multi-storey skeletal sway frames. In this section their method will be extended to calculate the natural frequencies of such frames. The solution to this three dimensional problem will be achieved using a single substitute plane frame for each of the three uncoupled modes of vibration corresponding to torsion and the two orthogonal sway directions. Each substitute frame is a single bay, multi-storey frame that has the same number of storeys and the same storey heights as the original frame, but is symmetric and comprises only in plane stiffnesses. Thus a plane frame computer programme can be used to calculate the

lower sway frequencies in the two orthogonal directions together with the torsional frequencies. In the next section, the theory will be further extended to include the equivalent wall-frame structures.

At this stage it is assumed that the structure is doubly symmetric and that the centre of rigidity and mass, C, are coincident and lie in a common vertical line. The centre of pressure CP, the point at which the resultant horizontal load acts at each floor level, does not need to be coincident with the centre of symmetry but should lie on a vertical line through the building. It is also assumed that inextensional member theory is used.

3.3.1.1 Substitute frame for translation

Consider Figure 3.1 again. It shows the plan view of a multi-storey structure idealised as a set of plane frames running in the x and y directions. If we consider only a typical frame, frame *i*, running in the y direction, it is clear that we can determine the material and geometric properties of each individual member of the equivalent substitute plane frame using the procedure described in Section 2.3.1. The substitute frame stiffness $\mathbf{s}_{yi}$ can then be assembled in the usual way from the member stiffness relationship given in Figures 3.7(a) and (b), where the stiffness elements are defined for both buckling and vibration theory in references(Howson 1979; Howson et al. 1983).

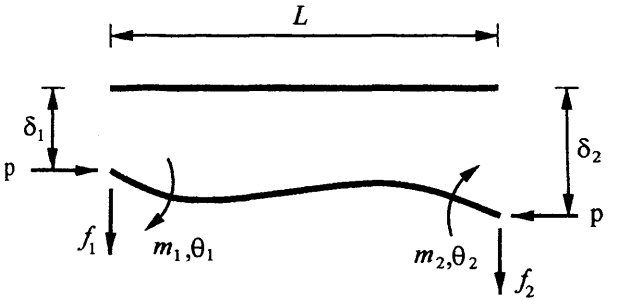

(a)

$$\begin{bmatrix} f_1 \\ m_1 \\ f_2 \\ m_2 \end{bmatrix} = \frac{EI}{L} \begin{bmatrix} \gamma/L^2 & \nu/L & -\varepsilon/L^2 & \delta/L \\ \nu/L & \alpha & -\delta/L & \beta \\ -\varepsilon/L^2 & -\delta/L & \gamma/L^2 & -\nu/L \\ \delta/L & \beta & -\nu/L & \alpha \end{bmatrix} \begin{bmatrix} \delta_1 \\ \theta_1 \\ \delta_2 \\ \theta_2 \end{bmatrix}$$

(b)

Figure 3.7 (a) Member end forces and displacements; (b) Member stiffness relationship.

Hence the stiffness relationship for the typical frame i is given by

$$\mathbf{p}_{yi} = \mathbf{s}_{yi}\mathbf{d}_{yi} \tag{3.25}$$

where $\mathbf{p}_{yi}$ is the vector of external forces and $\mathbf{d}_{yi}$ is the corresponding vector of nodal displacements. Based on the assumption of a rigid diaphragm at each floor level, it is clear that we can add together the substitute frames arising from all such frames running in the y direction to obtain a further substitute frame whose stiffness is given by

$$\mathbf{S}_y = \sum_{i=1}^{n_y} \mathbf{s}_{yi} \tag{3.26}$$

where n_y is the number of plane frames running in the y direction i.e. the individual substitute frames have been clamped together as described in Section 2.3.1. The corresponding force vector is given by

$$\mathbf{P}_y = \sum_{i=1}^{n_y} \mathbf{p}_{yi} \tag{3.27}$$

It should be noted that the contribution from frames running in the x direction to the behaviour of the structure in the y direction should be taken into account. The shear rigidity of frames in the x direction does not have any effect on the stiffness of the structure in the y direction, but the distributed mass of the beams should be considered by adding them to the mass of the beam in the substitute frame. Also, if any column in a plane frame in the x direction does not belong to a plane frame in the y direction, its mass and second moment of area about the x-axis should be halved and added to the corresponding properties of each column of the substitute frame.

An identical argument enables us to write the equivalent expressions for the stiffness and force vector of the n_x frames running in the the x direction as

$$\mathbf{S}_x = \sum_{j=1}^{n_x} \mathbf{s}_{xj} \tag{3.28}$$

and

$$\mathbf{P}_x = \sum_{j=1}^{n_x} \mathbf{p}_{xj} \tag{3.29}$$

The stiffness relationships in the x and y directions, respectively, can therefore be written as

$$\mathbf{P}_x = \mathbf{S}_x \mathbf{D}_x . \tag{3.30}$$

and

$$\mathbf{P}_y = \mathbf{S}_y \mathbf{D}_y \tag{3.31}$$

where $\mathbf{D}_x$ and $\mathbf{D}_y$ are the corresponding nodal displacement vectors. Noting that $\mathbf{P}_x = \mathbf{P}_y = \mathbf{0}$ when calculating natural frequencies, Eqs. (3.30) and (3.31) can be solved using the Wittrick-Williams algorithm (Wittrick and Williams 1971) which guarantees that no required eigenvalues can be missed. The modal vectors $\mathbf{D}_x$ and $\mathbf{D}_y$ then follow directly. A suitable computer program for such solution is freely available in the literature(Howson et al. 1983).

The modal displacements at points on the original frame can then be retrieved from $\mathbf{D}_x$ and $\mathbf{D}_y$ in a straightforward manner. If the torsional deformation of the original structure is deemed to be negligible, this completes the analysis.

3.3.1.2 Substitute frame for torsion

The moment resisted by a typical substitute frame running in the y direction, shown in Figure (3.8) as AB, is

$$\mathbf{p}_{yi}x_i = \mathbf{s}_{yi}\mathbf{d}_{yi}x_i \tag{3.32}$$

where $\mathbf{p}_{yi}$ is the external force vector acting on the substitute frame corresponding to the original plane frame i, $\mathbf{s}_{yi}$ and $\mathbf{d}_{yi}$ are the corresponding stiffness matrix and displacement vector, respectively, and x_i is the distance of the substitute frame from the centre of symmetry, C.

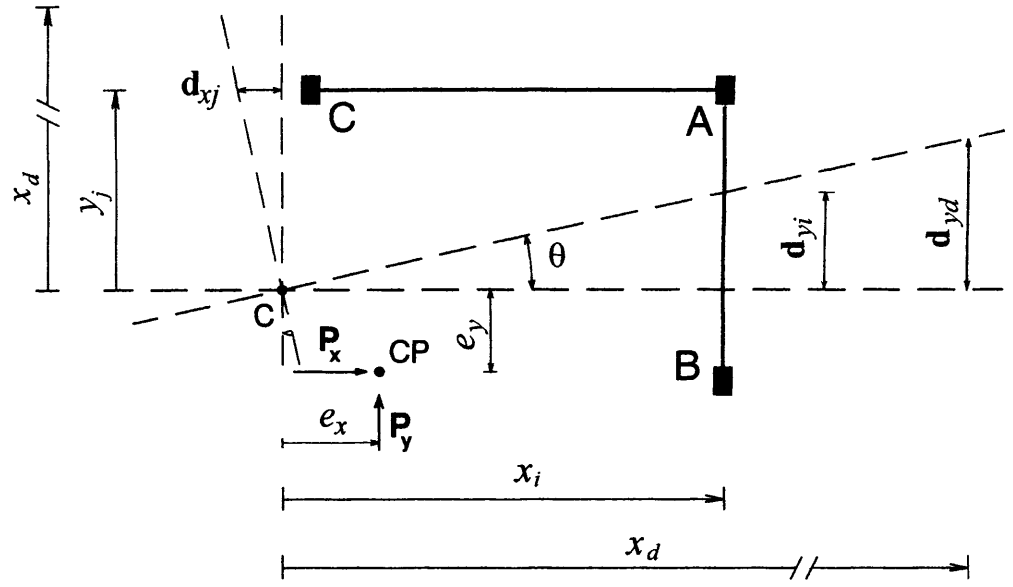

Figure 3.8 Two typical orthogonal substitute frames

It is now desirable to refer this substitute frame to a more convenient datum location at a distance x_d from the centre of resistance along the the x axis. Since its effect must remain unchanged we may write

$$\mathbf{s}_{yi}\mathbf{d}_{yi}x_i = \mathbf{s}'_{yi}\mathbf{d}_{yd}x_d \tag{3.33}$$

where $\mathbf{s}'_{yi}$ is the equivalent stiffness at location x_d and $\mathbf{d}_{yd}$ is the corresponding displacement vector.

Now since the floor diaphragms (slabs) are assumed to be rigid in their plane

$$\mathbf{d}_{yd}x_i = \mathbf{d}_{yi}x_d \tag{3.34}$$

Substituting Eq. (3.34) into Eq. (3.33) gives

$$\mathbf{s}'_{yi} = \mathbf{s}_{yi}\left(\frac{x_i}{x_d}\right)^2 \tag{3.35}$$

Thus the effective stiffness of all such substitute frames running in the y direction is given by

$$\mathbf{S}'_y = \frac{1}{x_d^2}\sum_{i=1}^{n_y} \mathbf{s}_{yi}\, x_i^2 \tag{3.36}$$

In an exactly similar way, a typical substitute frame running in the x direction, i.e. frame *j* in Figure 3.1 and shown in Figure 3.8 as AC, resists a moment

$$\mathbf{p}_{xj} y_j = \mathbf{s}_{xj}\mathbf{d}_{xj} y_j \tag{3.37}$$

where the symbols have the equivalent meaning to the previous derivation.

Again we refer the substitute frame to an equivalent datum location distance x_d from the centre of resistance, but this time along the y axis. The equivalent stiffness is then given by

$$\mathbf{s}'_{xj} = \mathbf{s}_{xj}\left(\frac{y_j}{x_d}\right)^2 \tag{3.38}$$

and the effective stiffness of all such substitute frames is given by

$$\mathbf{S}'_x = \frac{1}{x_d^2}\sum_{j=1}^{n_x} \mathbf{s}_{xj}\, y_j^2 \tag{3.39}$$

Since both sets of frames resist the applied moment and their effective stiffnesses have been calculated for the same effective datum, they can be added directly to give the total effective stiffness as

$$\mathbf{S}' = \mathbf{S}'_y + \mathbf{S}'_x = \frac{1}{x_d^2}\left\{\sum_{i=1}^{my} \mathbf{s}_{yi}\, x_i^2 + \sum_{j=1}^{nx} \mathbf{s}_{xj}\, y_j^2\right\} \tag{3.40}$$

The vector of applied moments, **M**, can then be written down as

$$\mathbf{M} = \mathbf{S}'\,\mathbf{D}\,x_d \tag{3.41}$$

where **D** is the vector of in-plane substitute frame displacements corresponding to **S**′. In turn it can be seen from Figure 3.8 that

$$\mathbf{M} = \mathbf{P}_y e_x - \mathbf{P}_x e_y \tag{3.42}$$

where e_x and e_y are the eccentricities of the applied force vectors.

Noting that

$$\frac{\mathbf{D}}{x_d} = \boldsymbol{\theta} \tag{3.43}$$

where $\boldsymbol{\theta}$ is the required vector of torsional displacements and substituting Eqs. (3.40), (4.42) and (3.43) into Eq. (3.41) gives

$$\mathbf{P}_y e_x - \mathbf{P}_x e_y = \left\{\sum_{i=1}^{my} \mathbf{s}_{yi}\, x_i^2 + \sum_{j=1}^{nx} \mathbf{s}_{xj}\, y_j^2\right\}\boldsymbol{\theta} \tag{3.44}$$

Once more $\mathbf{P}_x = \mathbf{P}_y = \mathbf{0}$ when calculating natural frequencies, hence Eq. (3.44) can be solved for the required eigenvalues in the same way as Section 3.3.1.1.

The modal displacements at points on the original frame can then be retrieved from $\mathbf{D}_x$, $\mathbf{D}_y$ and $\boldsymbol{\theta}$ in a straightforward manner.

Since every frame running in the x and y directions was replaced by a one-bay substitute plane frame, the out of plane contribution of the original frames to the torsional behaviour of the structure was lost. Furthermore, if any column in frame *i* does not belong to any frame running the in the x direction, its out of plane stiffness and inertia should be taken into account. This is because such a column behaves as a flexural cantilever and its out of plane rigidity (I) should therefore be multiplied by the square of its distance from the x axis and added to the second moment area of the columns of the substitute frame for torsion. This also applies to any column in frame *j* that does not belong to any frame that runs in the y direction.

In similar view to Section 3.2.1.1.2, it can be seen that the total mass of the beam and columns of the torsional substitute frame equals the polar second moment of mass of the beams (or rigid diaphragm) and columns of the original frame.

Finally it can be concluded that the natural frequencies of a symmetric, three-dimensional frame structure in both the translational and torsional directions can be obtained by replacing it with three one-bay, multi-storey, substitute plane frames with the properties given by Eqs (3.30), (3.31) and (3.44). The complete analysis can be undertaken using only a plane frame programme.

3.3.2 Application of the Substitute Frame Method in the Static and Dynamic Analysis of Symmetric Three-Dimensional Wall-Frame Structures

In this section it will be shown that the static nodal displacements or the sway and torsional natural frequencies of a symmetric three-dimensional wall-frame structure may be estimated by replacing the original wall-frame structure with an appropriate substitute plane wall-frame structure of the type shown in Figure 3.9.

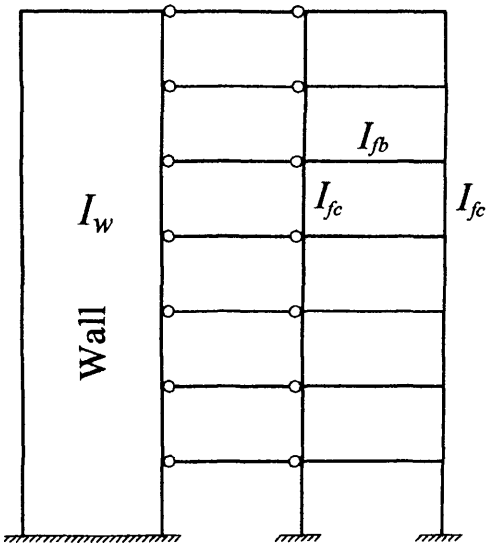

Figure 3.9 Characteristics of a typical substitute wall-frame

3.3.2.1 Substitute wall-frame for translation

Consider a typical floor plan of a doubly symmetric three-dimentional jhgj wall-frame structure, such as shown in Figure 3.5. If we consider only a typical wall, wall *i*, running in the y direction, it is clear that we can determine the material and geometric properties of its equivalent continuum model as a flexural member. The dynamic stiffness matrix $\hat{\mathbf{s}}_{yi}$ of such a member can be assembled in the usual way from the member stiffness relationship given in Figures 3.7(a) and (b).

Hence the stiffness relationship for the typical wall *i* is given by

$$\hat{\mathbf{p}}_{yi} = \hat{\mathbf{s}}_{yi}\hat{\mathbf{d}}_{yi} \tag{3.45}$$

where $\hat{\mathbf{p}}_{yi}$ is the vector of external forces and $\hat{\mathbf{d}}_{yi}$ is the corresponding vector of nodal displacements. Based on the assumption of a rigid diaphragm at each floor level, it is clear

that we can add together the stiffness arising from all frames and walls running in the y direction to obtain a further substitute wall-frame whose stiffness is given by

$$\mathbf{S}_y = \sum_{i=1}^{n_y} \mathbf{s}_{yi} + \sum_{i=1}^{n_{wy}} \hat{\mathbf{s}}_{yi} \tag{3.46}$$

where n_{wy} is the number of walls running in the y direction. The corresponding force vector is given by

$$\mathbf{P}_y = \sum_{i=1}^{n_y} \mathbf{p}_{yi} + \sum_{i=1}^{n_{wy}} \hat{\mathbf{p}}_{yi} \tag{3.47}$$

It should be noted that the contribution of the frames and walls running in the x direction to the behaviour of the structure in the y direction should be taken into account by using the method explained in Section 3.3.1.1

An identical argument enables us to write the equivalent expressions for the stiffness and force vectors of the n_x frames and n_{wx} walls running in the x direction as

$$\mathbf{S}_x = \sum_{j=1}^{n_x} \mathbf{s}_{xj} + \sum_{j=1}^{n_{wx}} \hat{\mathbf{s}}_{xj} \tag{3.48}$$

and

$$\mathbf{P}_x = \sum_{j=1}^{n_x} \mathbf{p}_{xj} + \sum_{j=1}^{n_{wx}} \hat{\mathbf{p}}_{xj} \tag{3.49}$$

The stiffness relationships in the x and y directions, respectively, can therefore be written as

$$\mathbf{P}_x = \mathbf{S}_x \mathbf{D}_x \tag{3.51a}$$

$$\mathbf{P}_y = \mathbf{S}_y \mathbf{D}_y \tag{3.51b}$$

where $\mathbf{D}_x$ and $\mathbf{D}_y$ are the corresponding nodal displacement vectors. Noting that $\mathbf{P}_x = \mathbf{P}_y = \mathbf{0}$ when calculating natural frequencies, Eqs. (3.50) and (3.51) can be solved using the Wittrick-Williams algorithm (Wittrick and Williams 1971) which guarantees that no required eigenvalues can be missed. The modal vectors $\mathbf{D}_x$ and $\mathbf{D}_y$ then follow directly. A suitable computer program for such solution is freely available in the literature(Howson et al. 1983).

The modal displacements at points on the original frame can then be retrieved from $\mathbf{D}_x$ and $\mathbf{D}_y$ in a straightforward manner. If the torsional deformation of the original structure is deemed to be negligible, this completes the analysis.

3.3.2.2 Substitute wall-frame for torsion

Considering the assumptions of Section 3.3.2.1 and noting the method of finding the substitute frame for torsion in Section 3.3.1.2, the corresponding stiffness relation for the torsional substitute wall-frame can be written as follows

$$\mathbf{P}_y e_x - \mathbf{P}_x e_y = \left\{ \sum_{i=1}^{ny} \mathbf{s}_{yi} x_i^2 + \sum_{i=1}^{mxy} \hat{\mathbf{s}}_{yi} \hat{x}_i^2 + \sum_{j=1}^{nx} \mathbf{s}_{xj} y_j^2 + \sum_{j=1}^{mwx} \hat{\mathbf{s}}_{xj} \hat{y}_j^2 \right\} \boldsymbol{\theta} \qquad (3.52)$$

Once more $\mathbf{P}_x = \mathbf{P}_y = \mathbf{0}$ when calculating natural frequencies, hence equation (3.52) can be solved for the required eigenvalues in the same way as the previous section.

The modal displacements at points on the original frame can then be retrieved from $\mathbf{D}_x$, $\mathbf{D}_y$ and $\boldsymbol{\theta}$ in a straightforward manner.

The out of plane rigidity and mass inertia of planar frames and walls in the torsional behaviour of the structure can be taken into account by using the method explained in Section 3.3.1.2.

Finally it can be concluded that the natural frequencies of a symmetric three-dimentional wall-frame structure in x, y and torsional directions can be obtained by replacing it with three, one-bay, multi-storey substitute plane wall-frames with the properties given by Eqs. (3.50), (3.51) and (3.52).

The final substitute wall-frames can be further simplified using the theory of Section 2.3.3 and be replaced with a one-bay multi-storey substitute frame. The characteristics of final substitute frame is shown in Figure 3.10 in which

I_w is the second moment of area of the wall in the substitute wall-frame
I_{fc} is the second moment or area of columns of the frame in the substitute wall-frame
I_{fb} is the second moment or area of beam of the frame in the substitute wall-frame

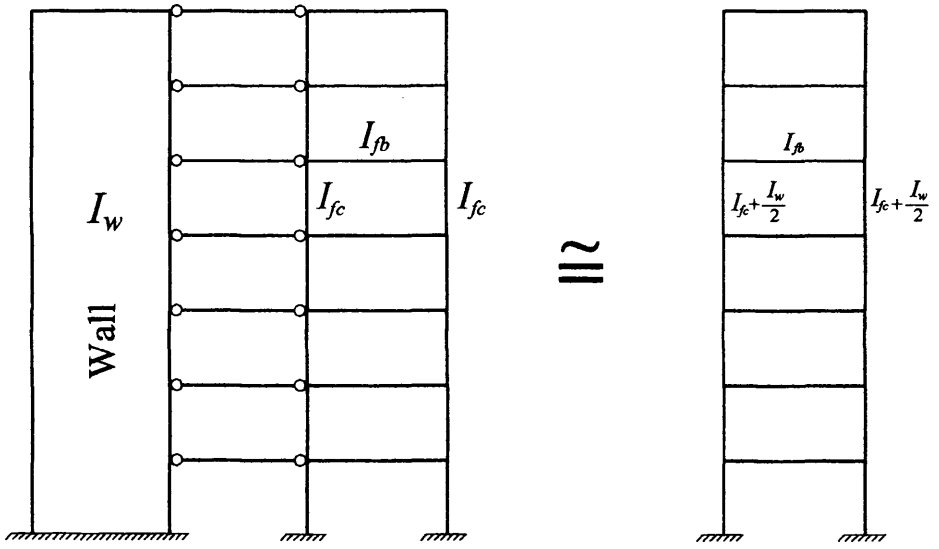

Figure 3.10 (a) Substitute wall-frame (b) Corresponding substitute frame

3.4 NUMERICAL RESULTS

In order to verify the proposed methods, it was deemed necessary to carry out a parametric study to ascertain the accuracy that might be expected from the proposed methods. The translational behaviour of symmetric three-dimensional frame and wall-frame structutres can be transformed directly to a planar problem, so the accuracy achieved in the parametric study of Chapter 2 can be anticipated here too. Thus, in the following examples, only torsional modes of the structures will be considered.

3.4.1 Example 3.1

Consider a series of 5, 7, 10 and 20 storey buildings, each of which have equal storey heights of 3m. The structures consist of 5 plane frames in the y direction (F1-F5) and 4 plane frames in the x direction (F6-F9), which have been connected to each other by typical rigid diaphragms at each floor level with the arrangement shown in Figure 3.11.

Young's modulus for all members is taken as $E=2\times10^{10}$ N/m^2 and the intensity of distributed mass on the diaphragms is assumed to be m=360 Kg/m^2. This incorporates the distributed mass in the beams and columns. Table 3.1 shows the second moment of area of the columns about the x and y axes. The second moment of area of all beams is assumed to be 0.003m^4 and inextensible member theory is assumed.

Table 3.1 - Column properties

Column	1,5,10,14,15,16	2,3,4,13	6,11	7,8,9,12
I_y	0.0035	0.007	0.0035	0.007
I_x	0.0035	0.0035	0.007	0.007

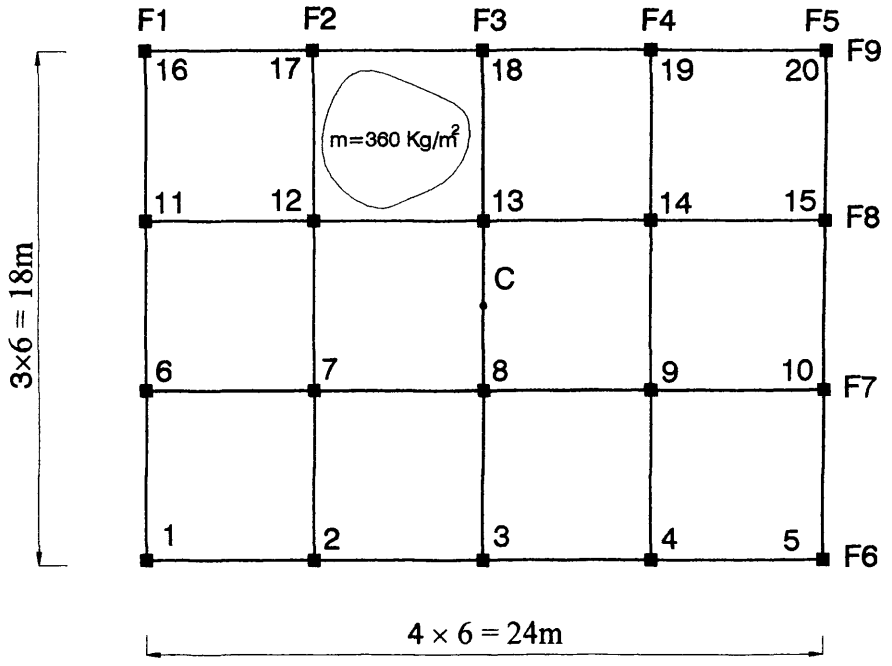

Figure 3.11 Floor plan of the structures considerd in Example 3.1

3.4.1.1 Torsional natural frequencies

3.4.1.1.1. Elastic support model

The characteristics of the equivalent elastic support model for torsional vibration of the structure can be calculated using Eqs (3.14a-c). For this purpose it is necessary to calculate the shear rigidity of a typical frame in the y and x directions using Eq. (2.29).

$GA_{yi} = 98.824 \times 10^6$ N (Frames F1-F5)

$GA_{xj} = 131.764 \times 10^6$ N (Frames F6-F9)

Substituting the properties of the columns (Table 3.1) in Eq. (3.14a) gives

$$EI_{wf} = 2\times10^{6}\times12.6 \text{ Nm}^4$$

and substituting the shear rigidity of the plane frames in the x and y directions in Eq. (3.14b) gives

$$GJ = 59294.16\times10^{6} \text{ Nm}^2$$

The polar second moment of the rigid diaphragm assuming uniformly distributed mass (about the centre of symmetry) can be calculated using the closed form formula given as follows

$$I_{gf} = \left(\frac{18\times24^3}{12}+\frac{24\times18^3}{12}\right)\times360 = 11664000 \text{ Kg.m}^2$$

It should be noted that this allows for the distributed mass in the columns and beams.

3.4.1.1.2. Shear beam model

The properties of the equivalent shear beam model for torsional vibration of the structures can be calculated using Eqs (3.34a-b) as follows

$$GJ = 59294.16\times10^{6} \text{ Nm}^2$$

$$I_{gf} = \left(\frac{18\times24^3}{12}+\frac{24\times18^3}{12}\right)\times360 = 11664000 \text{ Kg.m}^2$$

3.4.1.1.3. Substitute frame method

With a similar procedure, the characteristics of the substitute frame for torsional vibration of the structure can be obtained as follows

$I_{column} = 6.3\ \text{m}^4$

$I_{beam} = 5.4\ \text{m}^4$

$m_{beam} = 11664000\ \text{Kg}$

3.4.1.1.4. Results

Columns 2 and 4 of Table 3.2 show the torsional natural frequencies (Hz.) of the structure obtained from the shear beam model when the beam mass is lumped and distributed along the height of substitute beam, respectively. Columns 6 and 8 likewise show the natural frequencies obtained from the elastic support model and column 10 shows the torsional natural frequencies of the structure obtained by the application of substitute frame method. The last column in the table shows the results from a finite element analysis (FEM) of the whole frame, obtained using the vibration programme ETABS(Wilson et al. 1995). Finally, columns 3, 5, 7, 9 and 11 show the difference between the results of the substitute beam and frame methods with those of ETABS. The following assumptions have been made in modelling buildings with ETABS.

- The floor diaphragm at each storey level is assumed to be rigid and its mass is uniformly distributed.
- The mass of the beams, columns and shearwalls is distributed into the floor diaphragm.
- No allowance has been made for the shear deformation and rotary inertia of beams, columns and shearwalls
- No $P-\Delta$ effect
- No reduction in the stiffness of columns due to compressive axial loads (no geometric rigidity)
- Inextensible member theory is imposed by multiplying the cross-sectional area of the beams and columns by a factor, typically 10^3.

Table 3.2 - Torsional natural frequencies of the structures of Example 3.1 obtained using SB, ES and SF models, compared with the corresponding FEM results (NS stands for number of storeys, SB for shear beam model, ES for elastic support model, SF for substitute frame method and Diff for difference between the results of substitute frame and FEM methods)

N.S. 5	Shear Beam model (SB)				Elastic Support model(ES)				Substitute Frame Method		FEM ETABS
	Lump mass		Dist. mass		Lump mass		Dist mass				
Freq.	f(Hz.)	Diff.%	f(Hz.)	Diff.%	f(Hz.)	Diff.%	f(Hz.)	Diff.%	f(Hz.)	Diff.%	f(Hz.)
1	1.86	13.49	2.05	4.65	2.15	0.00	2.41	12.09	2.15	0.00	2.15
2	5.44	22.95	6.17	12.61	6.84	3.12	8.05	14.02	7.06	0.00	7.06
3	8.58	36.54	10.29	23.89	13.33	1.41	15.89	17.53	13.52	0.00	13.52
Av.		24.32		13.72		1.51		14.55		0.00	

NS 7	Shear Beam model (SB)				Elastic Support model(ES)				Substitute Frame Method		FEM ETABS
	Lump mass		Dist. mass		Lump mass		Dist mass				
Freq.	f(Hz.)	Diff.%	f(Hz.)	Diff.%	f(Hz.)	Diff.%	f(Hz.)	Diff.%	f(Hz.)	Diff.%	f(Hz.)
1	1.37	9.87	1.47	3.29	1.52	0.00	1.64	7.89	1.52	0.00	1.52
2	4.05	15.80	4.41	8.32	4.74	1.46	5.27	9.56	4.81	0.00	4.81
3	6.55	25.74	7.35	16.67	8.66	1.81	9.81	11.22	8.83	0.11	8.82
Av.		17.14		9.42		1.09		9.56		0.04	

NS 10	Shear Beam model (SB)				Elastic Support model(ES)				Substitute Frame Method		FEM ETABS
	Lump mass		Dist. mass		Lump mass		Dist mass				
Freq.	f(Hz.)	Diff.%	f(Hz.)	Diff.%	f(Hz.)	Diff.%	f(Hz.)	Diff.%	f(Hz.)	Diff.%	f(Hz.)
1	0.98	6.67	1.03	1.90	1.05	0.00	1.11	5.71	1.05	0.00	1.05
2	2.91	10.74	3.09	5.21	3.24	0.61	3.46	6.13	3.25	0.31	3.26
3	4.79	16.70	5.15	10.43	5.69	1.04	6.16	7.13	5.75	0.00	5.75
Av.		11.37		5.85		0.55		6.33		0.10	

NS 20	Shear Beam model (SB)				Elastic Support model(ES)				Substitute Frame Method		FEM ETABS
	Lump mass		Dist. mass		Lump mass		Dist mass				
Freq.	f(Hz.)	Diff.%	f(Hz.)	Diff.%	f(Hz.)	Diff.%	f(Hz.)	Diff.%	f(Hz.)	Diff.%	f(Hz.)
1	0.5	3.85	0.51	1.92	0.52	0.00	0.53	1.92	0.52	0.00	0.52
2	1.5	4.46	1.54	1.91	1.57	0.00	1.62	3.18	1.57	0.00	1.57
3	2.49	6.74	2.57	3.75	2.67	0.00	2.75	3.00	2.67	0.00	2.67
Av.		5.02		2.53		0.00		2.70		0.00	

As expected, the results from the shear beam model are poor for small numbers of storeys, whereas the results of the elastic support model generally show good agreement with ETABS results. The results of the substitute frame method are very accurate and show that the substitute frame method can be used with almost no loss of accuracy when the plane frames are proportional. To get a general idea about the magnitude of the differences, the average difference of the natural frequencies of the structures has been calculated and recorded in the last row of each component of Table 3.2. The corresponding diagram is shown in Figure 3.12.

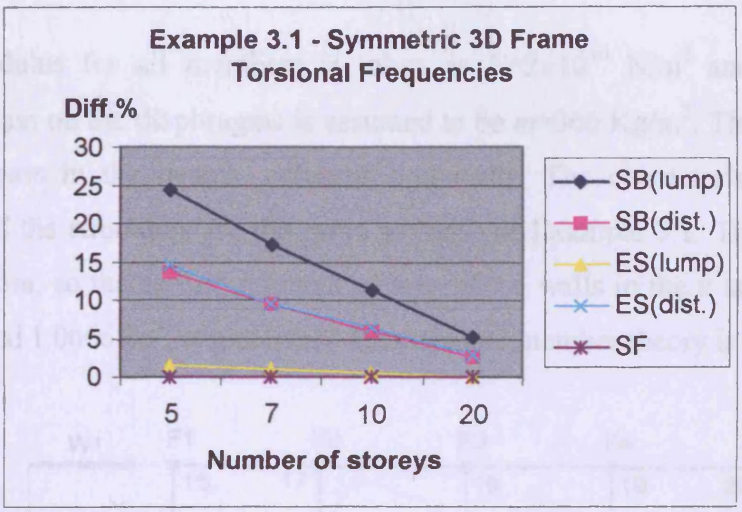

Figure 3.12 The difference graph for example 3.1. SB stands for shear beam model, ES for elastic support model and SF substitute frame method

The following conclusions can be obtained from the graph.

- The difference between the results of substitute frame and FEM methods are almost zero.
- The differences in both the SB and ES models when compared with FEM method decrease and converge on each other as the number of storeys increases.
- All models give acceptable results for 20 storeys and higher.
- The elastic support model gives acceptable results for any number of storeys.
- The difference between the results for lump and distributed mass is considerable, so it is necessary to assess when it is appropriate to use these models.

3.4.2 Example 3.2

Consider a series of 5, 7, 10 and 20 storey wall-frame buildings that have equal storey heights of 3m. The structures consist of 5 plane frames in the y direction (F1-F5), 4 plane frames in the x direction (F6-F9), 4 shear walls in the y direction (W2) and 4 shear walls in the x direction (W1), which are connected to each other by rigid diaphragms at the floor levels with the arrangement shown in Figure 3.13.

Young's modulus for all members is taken as $E=2\times10^{10}$ N/m^2 and the intensity of distributed mass on the diaphragms is assumed to be m=360 Kg/m^2. This incorporates the distributed mass in the beams, columns and walls. The characteristics of the frame component of the structures are the same as those of Example 3.1. The thickness of the walls are 0.25m, so the second moment of area of the walls in the x and y directions are 1.51875m^4 and 1.06667m^4, respectively. Inextensible member theory is assumed.

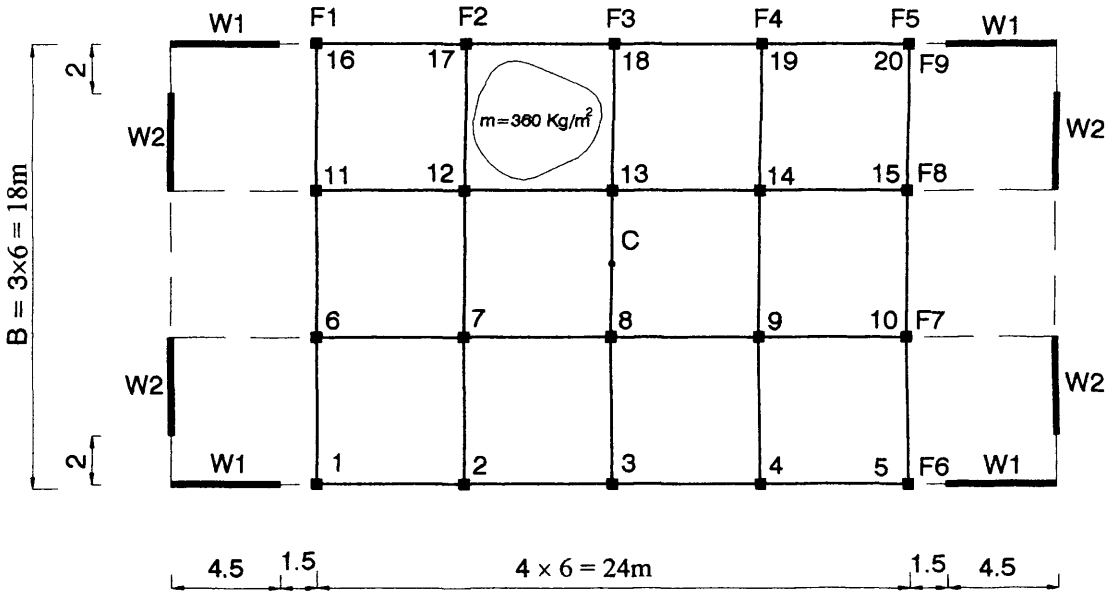

Figure 3.13 Floor plan of the structures considerd in Example 3.2

3.4.2.1 Torsional natural frequencies

3.4.2.1.1. Elastic support model

The characteristics of the equivalent elastic support model for torsional vibration of the structures can be calculated using Eqs (3.14a-c) and Eqs. (3.24a-b).

$EI_{wf} = 2\times10^{10}\times12.6\ \text{Nm}^4$

$EI_{ww} = 2\times10^{10}\times1874.48\ \text{Nm}^4$

$GJ = 59294.16\times10^{6}\ \text{Nm}^2$

$$I_{gf} + I_{gw} = \left(\frac{18\times36^3}{12} + \frac{36\times18^3}{12}\right)\times360 = 31492800\ \text{Kg.m}^2$$

It should be noted that this allows for the distributed mass in the columns, beams and walls.

3.4.2.1.2. Substitute wall-frame for torsion

With a similar procedure, the characteristics of the substitute wall-frame for torsional vibration of the structures can be obtained as follows

$I_{column} = 6.3\ \text{m}^4$

$I_{beam} = 5.4\ \text{m}^4$

$I_{wall} = 1874.48\ \text{m}^4$

$m_{beam} = 31492800\ \text{Kg}$

3.4.2.1.3. Substitute frame for torsion

With additional simplification, a one-bay substitute frame can be defined for torsional vibration analysis of the structures by the rules of Figure 3.10.

$$I_{column} = 6.3 + \frac{1874.48}{2} = 943.54\ \text{m}^4$$

$I_{beam} = 5.4\ \text{m}^4$

$m_{beam} = 31492800\ \text{Kg}$

3.4.2.1.4. Results

Columns 2 and 4 of Table 3.3 show the torsional natural frequencies (Hz.) of the structure obtained from the elastic support model with the beam mass lumped and distributed, respectively. Columns 6 and 8 show the torsional natural frequencies of the structure obtained by the application of substitute wall-frame and frame method respectively. Finally, the last column in the table shows the result obtained from a finite element analysis of the whole wall-frame, using the vibration programme ETABS(Wilson et al. 1995).

Table 3.3 – Torsional natural frequencies of the structures of Example 3.2 obtained using, ES, substitute wall-frame and substitute frame methods, compared with FEM results

NS 5	Elastic Support model (ES)				Substitute Wall-Frame		Substitute Frame		FEM ETABS
	Lump mass		Dist. mass						
	f(Hz.)	Diff.%	f(Hz.)	Diff.%	f(Hz.)	Diff.%	f(Hz.)	Diff.%	f(Hz.)
1	4.18	1.21	5.02	21.55	4.13	0.00	4.13	0.00	4.13
2	25.34	13.99	29.9	34.50	22.44	0.94	21.01	5.49	22.23
3	71.2	34.44	83.04	56.80	53.87	1.72	47.75	9.84	52.96
Av.		16.55		37.62		0.89		5.11	

NS 7	Elastic Support model (ES)				Substitute Wall-Frame		Substitute Frame		FEM ETABS t
	Lump mass		Dist. mass						
	f(Hz.)	Diff.%	f(Hz.)	Diff.%	f(Hz.)	Diff.%	f(Hz.)	Diff.%	f(Hz.)
1	2.36	0.00	2.69	13.98	2.36	0.00	2.39	1.27	2.36
2	13.61	7.25	15.44	21.67	12.76	0.55	12.3	3.07	12.69
3	37.85	18.24	42.51	32.80	32.37	1.12	29.87	6.69	32.01
Av.		8.50		22.82		0.56		3.68	

NS 10	Elastic Support model (ES)				Substitute Wall-Frame		Substitute Frame		FEM ETABS
	Lump mass		Dist. mass						
	f(Hz.)	Diff.%	f(Hz.)	Diff.%	f(Hz.)	Diff.%	f(Hz.)	Diff.%	f(Hz.)
1	1.32	0.75	1.45	9.02	1.33	0.00	1.37	3.01	1.33
2	7.05	3.37	7.72	13.20	6.84	0.29	6.74	1.17	6.82
3	19.23	9.01	20.98	18.93	17.75	0.62	16.95	3.91	17.64
Av.		4.38		13.72		0.31		2.70	

NS 20	Elastic Support model (ES)				Substitute Wall-Frame		Substitute Frame		FEM ETABS
	Lump mass		Dist. mass						
	f(Hz.)	Diff.%	f(Hz.)	Diff.%	f(Hz.)	Diff.%	f(Hz.)	Diff.%	f(Hz.)
1	0.48	0.00	0.50	4.17	0.48	0.00	0.51	6.25	0.48
2	2.06	0.49	2.16	5.37	2.05	0.00	2.1	2.44	2.05
3	5.21	2.16	5.46	7.06	5.11	0.20	5.08	0.39	5.1
Av.		0.88		5.53		0.07		3.03	

To get a general idea about the magnitude of the differences, i.e. the difference between the results of proposed and FEM methods, the average differences have been calculated

and recorded in the last row of each component of Table 3.3. The corresponding diagram is given in Figure 3.12. In the diagram ES stands for elastic support model, SWF stands for substitute wall-frame method and SF stands for substitute frame method.

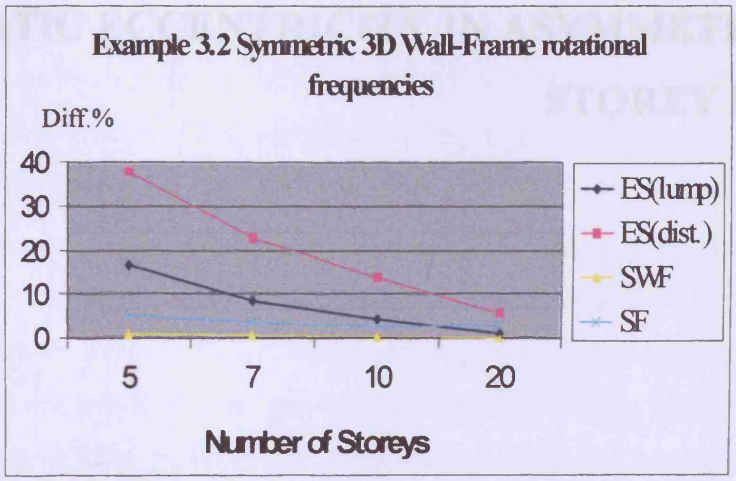

Figure 3.14 The difference graph for Example 3.2

The following conclusions can be obtained from the graph.

- The difference between the results of substitute wall-frame and FEM methods are almost zero.
- The substitute frame method gives acceptable result for all structures. (Diff.%<5%)
- The ES model is not suggested for low rise structures. (less than 7 storeys)
- The differences of the ES model decrease with increase in the number of storeys.
- All models give acceptable results for 20 storeys and higher.
- The elastic support model (Lump mass) gives acceptable results for structures with 7 storeys or higher.
- The difference between the results for the lump and distributed mass models is considerable, so it is necessary to assess when it is appropriate to use these models.

CHAPTER 4

STATIC ECCENTRICITY IN ASYMMETRIC MULTI-STOREY BUILDINGS

4.1 INTRODUCTION

Buildings subjected to lateral loads caused by, for example, wind or earthquake ground motions may undergo torsional as well as lateral displacements. In buildings with doubly symmetric floor plans it could be due to the rotational component in the ground motion or unforeseen conditions such as asymmetric distribution of mass in the floors etc. Coupled translational-torsional motion could also arise due to asymmetry in geometry, stiffness or mass distribution in the plan of asymmetric buildings. In both cases, lateral loading leads to torsional response in addition to the lateral response. Therefore, the structure should be designed for the additional torques that may be induced simultaneously due to lateral forces. The applied torque at each floor level is calculated as the product of lateral load and structural static eccentricity at that floor level. Static eccentricity at a floor level is commonly defined as the distance between its centre of mass (or axis of applied load) and the centre of rigidity. Thus, assuming that the line of action of the resultant lateral load at

each floor level is known, the problem of determining the structural eccentricity reduces to locating the centre of rigidity at each floor level.

The determination of the location of centres of rigidity of buildings has two major applications. Firstly, it is required in the wind or static earthquake analysis of buildings when using formulae typically adopted by codes of practice in which the increment of torque at each floor level needs to be evaluated. Secondly it is a key step in the application of building code provisions, since the classification criteria are typically based on the concept of static eccentricity (Paz 1994). Moreover, even if a three-dimensional analysis is performed, some codes account for dynamic amplification by increasing the static eccentricity by a magnifying factor, which requires calculation of the centres of rigidity. However, most building codes do not provide clear definitions of centres of rigidity or give practical procedures to determine their locations. For this reason there is still some confusion about what exactly is meant by centres of rigidity of multi-storey buildings and whether the location of these centres are inherent properties of the building or if they are a function of lateral loads.

Several investigators have studied this over the last three decades, giving different definitions of the centres. Most of these studies are restricted to structures with resisting elements running in two orthogonal directions. Different terms have been used in the literature for defining centres of rigidity of structures, sometimes implying that these are different terms for the same point. Some of the terms that have been used are; centres of rigidity, centres of resistance, centres of stiffness, shear centres, load (or pressure) centres, centres of twist and centres of torsion.

Poole (Poole 1977) defines the centre of rigidity of a floor as the location of the resultant of the shear forces of various resisting elements in that floor when the building is subjected to a static lateral loading that causes no torsion in any of the storeys. In other words, centres of rigidity are defined as the shear centres of the building. Humar and Award (Humar and Awad 1983) define the centre of rigidity of a floor as that point in the floor through which a static horizontal force should be applied to cause the floor to translate without rotating, other floors however may rotate.

The work of Cheung and Tso (Cheung and Tso 1986) distinguishes between centres of rigidity, shear centres and centres of twist of a multi-storey building. They have extended the concept of eccentricity from single-storey buildings to multi-storey buildings and have shown that all terms used for centres of resistance are interchangeable when referring to a single-storey structure. Mathematical expressions are then presented for the locations of the centres of rigidity and centres of twist of multi-storey buildings. Also an alternative procedure to locate the centres of rigidity, and hence floor eccentricity, has been given that does not require the explicit use of the global stiffness matrix of the structure and is therefore more suitable for use in the design context. This procedure is explained below and will be referred to as Cheung and Tso's method later on.

The approach is based on the interpretation of the centre of rigidities as "load centres" at each floor level. Therefore, if the loading on each resisting structural element at each floor is known under the assumption of no rotational deformation, the load centre at each floor can be obtained by dividing the first moment of the element loads by the total loading at that floor level. Assuming the building is restrained from rotation, the lateral floor displacement in one direction, e.g. the x direction, and the inter-storey shear of all elements under loading in the same direction, can readily be obtained by means of a standard plane frame programme. The global stiffness of the structure in the assumed direction, x, can be simulated by joining all the resisting elements spanning in the x direction by rigid beam elements with pinned ends at floor levels. Therefore, the inter-storey shear force of each resisting element can be calculated by analysing the simulated structure under total lateral loading of the structure. The floor loads for the individual elements then follow directly. The y coordinate of the load centres, i.e. rigidity centres, is then given by the ratio of the first moment of these floor loads about reference axis z and the total floor load at that level. An identical procedure can then be followed to calculate the x coordinate of the rigidity centres.

Cheung and Tso (Cheung and Tso 1986) also showed that the centres of twist do not generally coincide with the centres of rigidity or shear centres. For a special class of buildings, in which the lateral stiffness matrices of all resisting frames are proportional, the location of the centres of twist and rigidity were shown to be coincident, independent of the lateral forces and to lie on a vertical line through the height of the structure. Hejal (Hejal and Chopra 1987) extended Cheung and Tso's work (Cheung and Tso 1986) to

multi-storey buildings with a generalised floor plan comprising plane frames, columns, shear walls and cores and investigated the conditions that must be satisfied for the centres to be coincident and uniquely defined.

Riddell and Vasquez (Riddell and Vásquez 1984) concluded that the centres of resistance exist only for a particular class of structures and that for a general multi-storey building such concepts are meaningless. This particular class is referred to as "compensable buildings" and are shown to have centres of resistance that lie on a vertical line and are not load dependent. The conditions satisfied by this class of building are in agreement with those identified by Cheung (Cheung and Tso 1986). For buildings that are nearly "compensable" two approaches are given to determine approximate locations of the centres of rigidity, all of which lie on a vertical line.

This review of existing studies shows that there is inconsistency in the definitions given for centres of rigidity. However most studies (Cheung and Tso 1986; Hejal and Chopra 1987; Jiang et al. 1993; Riddell and Vásquez 1984; Smith and Vezina 1985) identify a class of buildings in which the centre of rigidity of each floor is independent of the lateral load and lies on a vertical line through the height of the structure. In this study this class of buildings will be referred to as proportional structures.

The objective of this study is to investigate further the definition of each of the centres mentioned earlier. A practical method is then presented for locating centres of rigidity and shear centres and hence the static eccentricity. The method is based on the use of a plane frame computer programme and utilises the flexibility matrix of resisting plane elements to form a matrix relation between loading on the elements and total lateral loading of the building. The centres of rigidity of the building are then obtained using the fact that they can be interpreted as the load centres at each floor level under the assumption of no rotational deformation. A number of examples are included to illustrate the method.

4.2 STATIC ECCENTRICITY IN MULTI-STOREY BUILDINGS

4.2.1 Basic concepts

In a multi-storey building, the resultant lateral load at each floor level passes through the centre of mass in the case of seismic ground motion and the centre of pressure when the building is subjected to wind loads. Thus the problem of calculating floor eccentricities reduces to the problem of determining the centre of rigidity at each floor level. The following definitions are accepted for different centres of buildings that are generally called the centres of reference in this study.

The centre of rigidity at each floor of a building is that point on the floor diaphragm through which the resultant of any set of static horizontal forces at that level causes no rotation or twisting of any of the floors.

The shear centre of a floor is that point on the floor diaphragm through which the resultant of the inter-storey shear forces at that level experienced by all resisting elements passes when the resultant of applied lateral force passes through the centre of rigidity.

The centres of twist of the floors of a building are the points on the floor diaphragms which do not translate when floor levels are subjected to any set of static torsional moments.

The centre of mass at each floor is the point on the floor through which the resultant of the inertia forces of the floor passes. If the masses of individual resisting elements are assumed to be distributed uniformly over the floor diaphragms, or are negligible compared to the masses of the floors, the centres of mass of a building coincide with the geometric centres of the floors.

The static eccentricity of the j^{th} floor, e_j, is defined as the distance between its centre of mass and centre of rigidity. In some building codes (Japan Earthquake Code; Hejal and

Chopra 1987), the static eccentricity of a floor is defined as the distance between its centre of mass and the shear centre.

Tso (Tso 1984) has shown that the different "centres" described above are coincident in the case of single-storey buildings. The approach uses the work-energy principle of mechanics and is explained below.

Consider a single-storey building that is subjected to a torque T and a horizontal point load P, whose line of action passes through the centre of rigidity. When load P is applied first, the floor diaphragm experiences a pure translation, δ. The work done by P is

$$W = P\delta/2 \tag{4.1}$$

The torque T is then applied and the diaphragm rotates an angle θ about the centre of twist. Assuming that the centre of rigidity does not coincide with the centre of twist, the centre of rigidity will move a further distance equal to $c\theta$, where c is the distance between the centres of rigidity and twist. The total work done by the forces is

$$W_1 = P\delta/2 + T\theta/2 + Pc\theta \tag{4.2}$$

If the load sequence is reversed, i.e. T is applied first, followed by P, the total work done will be

$$W_2 = T\theta/2 + P\delta/2 \tag{4.3}$$

For a linear elastic structure, the total strain energy in the structure is independent of the sequence of load application.

Comparing Eqs (4.2) and (4.3) gives

$$Pc\theta = 0 \tag{4.4}$$

Since $P \neq 0$ and $\theta \neq 0$, this leads to

$$c = 0 \tag{4.5}$$

Thus the centre of rigidity is coincident with the centre of twist for a single-storey building. Also, based on the definition of the shear centre, it is obvious that the shear centre of the building is coincident with the rigidity centre, since inter-storey shear force and lateral loading of resisting elements are equal in the case of single-storey buildings.

This approach can be extended to multi-storey buildings subjected to a lateral force vector **P** and torque **T**. If the pure translation and rotational displacement vectors of the diaphragms are represented by $\boldsymbol{\delta}$ and $\boldsymbol{\theta}$, the work experienced for the two sequences of loading are

$$W_1 = \frac{1}{2}\mathbf{P}^{\mathrm{T}}\boldsymbol{\delta} + \frac{1}{2}\mathbf{T}^{\mathrm{T}}\boldsymbol{\theta} + \mathbf{P}^{\mathrm{T}}(\boldsymbol{\Delta}_R - \boldsymbol{\Delta}_T)\boldsymbol{\theta} \tag{4.6}$$

$$W_2 = \frac{1}{2}\mathbf{T}^{\mathrm{T}}\boldsymbol{\theta} + \frac{1}{2}\mathbf{P}^{\mathrm{T}}\boldsymbol{\delta} \tag{4.7}$$

Where $\boldsymbol{\Delta}_{\mathbf{R}}$ and $\boldsymbol{\Delta}_{\mathrm{T}}$ are diagonal matrices whose elements correspond to the location of the centres of rigidity and twist with respect to an arbitrary origin, respectively. Comparison of Eqs (4.6) and (4.7) once more leads to the equivalent conclusion that

$$\mathbf{P}^{\mathrm{T}}(\boldsymbol{\Delta}_R - \boldsymbol{\Delta}_T)\boldsymbol{\theta} = 0 \tag{4.8}$$

Eq. (4.8) is a single linear equation with multiple unknown parameters so $(\boldsymbol{\Delta}_R - \boldsymbol{\Delta}_T) = \mathbf{0}$ is a sufficient, but not a necessary condition for the equation to be satisfied. Therefore, Eq. (4.8) can be satisfied without requiring the centres of rigidity and twist to be coincident.

4.2.2 Location of the centres of rigidity

In this section, a matrix method will be developed for determining the location of the centres of rigidity of multi-storey buildings using a two-dimensional approach. It requires

a knowledge of the distribution of lateral loads between resisting elements that satisfies the equations of equilibrium and compatibility of deformations.

Consider a typical floor plan of a multi-storey building comprising plane resisting elements (frames, columns, shearwalls or bracings) that run in two orthogonal directions, as shown in Figure 4.1. Plane resisting elements are assumed to have no out of plane rigidities and to be jointed to each other by rigid diaphragms at each floor level. The coordinate system Oxy is fixed at an arbitrary point on the plan, with the x and y axes running parallel to the orthogonal planes of the resisting elements. It is assumed that the building is subjected to a known set of lateral loads, defined by the vectors

$$\mathbf{V}_x^T = [V_{x1} \quad V_{x2} \quad V_{x3} \quad . \quad . \quad V_{xn}] \tag{4.9a}$$

and

$$\mathbf{V}_y^T = [V_{y1} \quad V_{y2} \quad V_{y3} \quad . \quad . \quad V_{yn}] \tag{4.9b}$$

where V_{xj} and V_{yj} (j=1,n) are the resultant lateral loads applied at j^{th} storey level in the x and y directions, respectively, and n is the number of storeys.

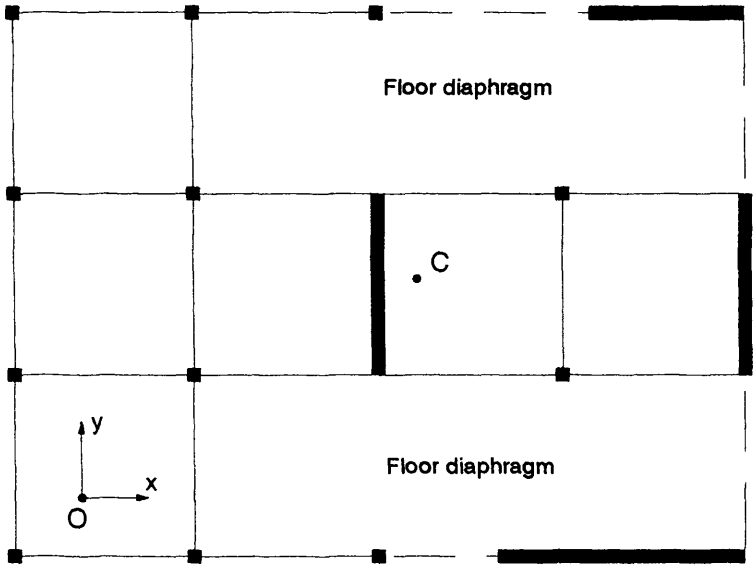

Figure 4.1 Floor plan of an asymmetric multi story building comprising resisting elements running in two orthogonal directions.

In similar fashion, the

$$\mathbf{X}_R^T = [X_{R1} \quad X_{R2} \quad X_{R3} \quad . \quad . \quad X_{Rn}] \tag{4.10a}$$

and

$$\mathbf{Y}_R^T = [Y_{R1} \quad Y_{R2} \quad Y_{R3} \quad . \quad . \quad Y_{Rn}] \tag{4.10b}$$

are assumed to contain, respectively, the unknown x and y coordinates, X_{Rj} and Y_{Rj} (j=1,n), that define the location of the centre of rigidity at floor level j. We now assume that the resultant lateral loads at each floor level are applied at their respective rigidity centres. Hence the building will undergo pure translation in both directions. Since the plane resisting elements have no out of plane stiffnesses, the structure can be analysed in the x and y directions separately.

From the definition of rigidity centres, the coordinates $\mathbf{X}_R$ and $\mathbf{Y}_R$ of rigidity centres can be interpreted as defining the load centres at floor levels. Therefore, if the loading on each resisting element at each floor level is known under the assumption of no rotational deformation, the load centre at each floor can be obtained by summing up the first moment of the element loads at that floor and dividing the moment by the total loading of the floor.

The loading on each resisting element can be calculated using equilibrium equations and the knowledge that the elements in either direction have equal deflections when the building is subjected to lateral loads applied through the centres of rigidity.

4.2.2.1 Equations of equilibrium

Consider the y direction first, where the building is subjected to lateral forces $\mathbf{V}_y$ only. If the loading on the i^{th} resisting element in the y direction is represented by $\mathbf{p}_y^{(i)}$, where

$$\mathbf{p}_y^{(i)T} = \begin{bmatrix} p_{y1}^{(i)} & p_{y2}^{(i)} & p_{y3}^{(i)} & . & . & p_{ym}^{(i)} \end{bmatrix} \tag{4.11}$$

in which $p_{yj}^{(i)}$ is the loading of the i^{th} element in the j^{th} floor, the equation of equilibrium in the y direction gives

$$\mathbf{V}_y = \sum_{i=1}^{m} \mathbf{p}_y^{(i)} \tag{4.12}$$

in which m is the number of resisting elements running in the y direction.

4.2.2.2 Equations of displacement compatibility

Applying lateral loads at the centres of rigidity of the building requires that the displacement vector of all resisting elements in the y direction be equal. This gives

$$\mathbf{d}_y^{(1)} = \mathbf{d}_y^{(2)} = \mathbf{d}_y^{(3)} = \cdots = \mathbf{d}_y^{(m)} = \mathbf{d}_y \tag{4.13}$$

in which $\mathbf{d}_y^{(i)}$ denotes the displacement vector of resisting element i, where

$$\mathbf{d}_y^{(i)T} = \begin{bmatrix} d_{y1}^{(i)} & d_{y2}^{(i)} & d_{y3}^{(i)} & . & . & d_{ym}^{(i)} \end{bmatrix} \tag{4.14}$$

and $d_{yj}^{(i)}$ gives the deflection of element i at the j^{th} floor.

Displacement vector $\mathbf{d}_y^{(i)}$ can now be written in terms of the stiffness matrix and lateral loading of the i^{th} resisting element as

$$\mathbf{d}_y^{(i)} = \mathbf{k}_y^{(i)^{-1}} \mathbf{p}_y^{(i)} \tag{4.16}$$

in which $\mathbf{k}_y^{(i)^{-1}}$ is the inverse of the stiffness matrix of the i^{th} element in the y direction.

The stiffness matrix of a resisting element however, is not always readily available. An alternative approach is therefore suggested that does not require its explicit use and as a result is more suitable for use in the design context.

Consider the i^{th} resisting element subjected to lateral load $\mathbf{p}_y^{(i)}$ as shown in Figure 4.2.

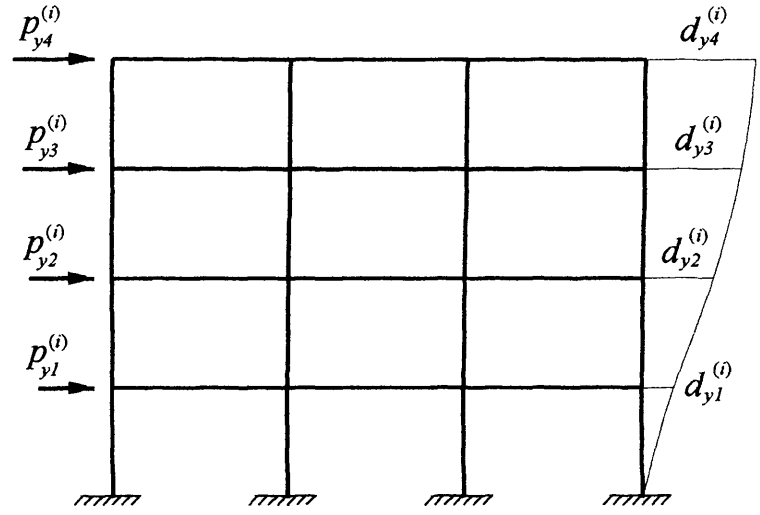

Figure 4.2 Resisting element i subjected to lateral loading $\mathbf{p}_y^{(i)}$ and the resulting displacement vector $\mathbf{d}_y^{(i)}$

The relationship between $\mathbf{p}_y^{(i)}$ and $\mathbf{d}_y^{(i)}$ can be established by using flexibility coefficients, $\delta_{yjk}^{(i)}$, which relates the deflection of the j^{th} floor of element i to a lateral unit force applied at level k. See Figure 4.3.

Since the behaviour of the building is assumed to be linear and elastic, the deflection of the j^{th} floor of element i subjected to $\mathbf{p}_y^{(i)}$ can be written as

$$d_{yj}^{(i)} = \sum_{k=1}^{n} \delta_{yjk}^{(i)} p_{yk}^{(i)} \tag{4.17}$$

or

$$\mathbf{d}_y^{(i)} = \boldsymbol{\delta}_y^{(i)} \mathbf{p}_y^{(i)} \tag{4.18}$$

where $\boldsymbol{\delta}_y^{(i)}$ is the flexibility matrix of element i in which $\delta_{yjk}^{(i)}$ is the coefficient of the matrix located at the intersection of row j and column k. Therefore the equation of compatibility of deflections can be written as

$$\boldsymbol{\delta}_y^{(i)}\mathbf{p}_y^{(i)} - \mathbf{d}_y = \mathbf{0} \tag{4.19}$$

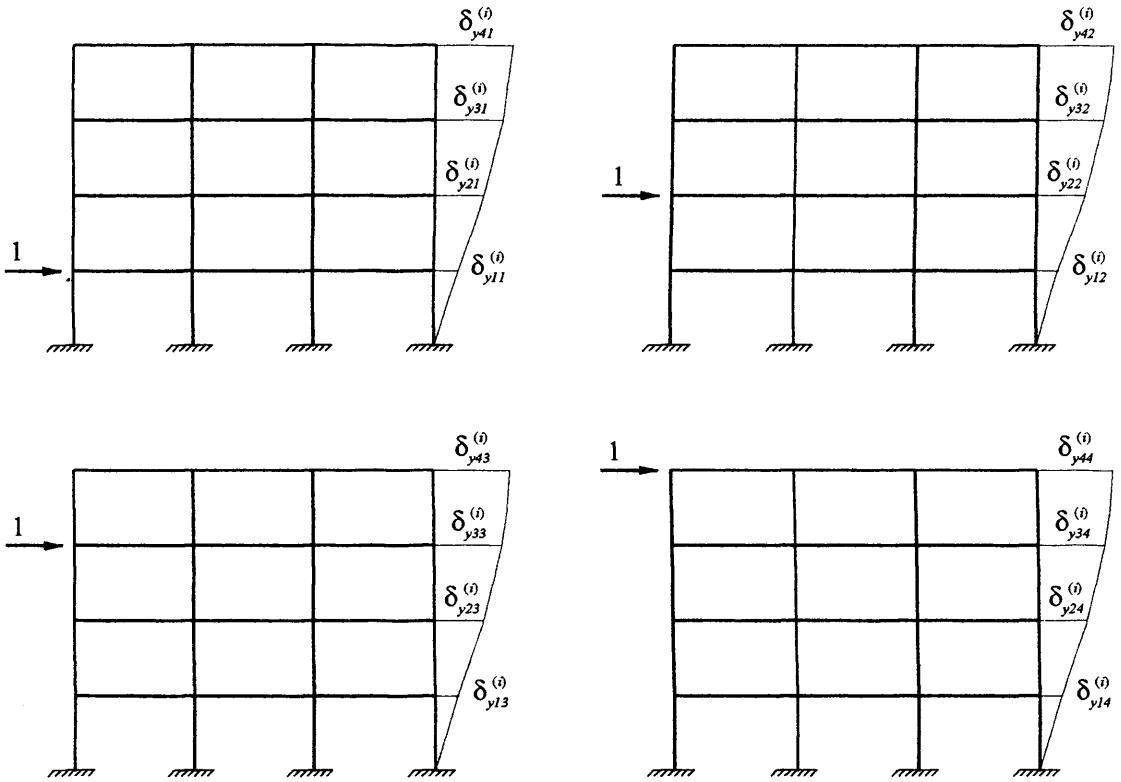

Figure 4.3 Resisting element i subjected to lateral unit forces at different floor levels

Eqs. (4.12) and (4.19) can be combined to give an $n(m+1)$ system of algebraic equations for calculating $\mathbf{p}_y^{(i)}$ and $\mathbf{d}_y$ as

$$\begin{bmatrix} \boldsymbol{\delta}_y^{(1)} & \mathbf{0} & \mathbf{0} & . & . & \mathbf{0} & \mathbf{I} \\ \mathbf{0} & \boldsymbol{\delta}_y^{(2)} & \mathbf{0} & . & . & \mathbf{0} & \mathbf{I} \\ \mathbf{0} & \mathbf{0} & \boldsymbol{\delta}_y^{(3)} & . & . & \mathbf{0} & \mathbf{I} \\ . & . & . & . & . & . & . \\ . & . & . & . & . & . & . \\ \mathbf{0} & \mathbf{0} & \mathbf{0} & . & . & \boldsymbol{\delta}_y^{(m)} & \mathbf{I} \\ \mathbf{I} & \mathbf{I} & \mathbf{I} & . & . & \mathbf{I} & \mathbf{0} \end{bmatrix} \begin{bmatrix} \mathbf{p}_y^{(1)} \\ \mathbf{p}_y^{(2)} \\ \mathbf{p}_y^{(3)} \\ . \\ . \\ \mathbf{p}_y^{(m)} \\ -\mathbf{d}_y \end{bmatrix} = \begin{bmatrix} \mathbf{0} \\ \mathbf{0} \\ \mathbf{0} \\ . \\ . \\ \mathbf{0} \\ \mathbf{V}_y \end{bmatrix} \tag{4.20}$$

Once $\mathbf{p}_y^{(i)}$ are determined, the location of the centres of rigidity $\mathbf{X}_R$ can be obtained as

$$X_{Rj} = \frac{\sum_{i=1}^{m} p_{yj}^{(i)} x_i}{V_{yj}} \tag{4.21}$$

in which x_i is the distance of element i from the y axis. Thus the vector $\mathbf{X}_R$, containing the x coordinates for each of the j centres of rigidity is obtained as

$$\mathbf{X}_R = \mathbf{V}_{yd}^{-1} \mathbf{P}_y \mathbf{X}_e \tag{4.22}$$

in which

$$\mathbf{V}_{yd} = \begin{bmatrix} V_{y1} & 0 & 0 & . & . & 0 \\ 0 & V_{y2} & 0 & . & . & 0 \\ 0 & 0 & V_{y3} & . & . & 0 \\ . & . & . & . & . & . \\ . & . & . & . & . & . \\ 0 & 0 & 0 & . & . & V_{yn} \end{bmatrix} \quad \mathbf{P}_y = \begin{bmatrix} p_{y1}^{(1)} & p_{y1}^{(2)} & p_{y1}^{(3)} & . & . & p_{y1}^{(m)} \\ p_{y2}^{(1)} & p_{y2}^{(2)} & p_{y2}^{(3)} & . & . & p_{y2}^{(m)} \\ p_{y3}^{(1)} & p_{y3}^{(2)} & p_{y3}^{(3)} & . & . & p_{y3}^{(m)} \\ . & . & . & . & . & . \\ . & . & . & . & . & . \\ p_{yn}^{(1)} & p_{yn}^{(2)} & p_{yn}^{(3)} & . & . & p_{yn}^{(m)} \end{bmatrix} \quad \mathbf{X}_e = \begin{bmatrix} x_1 \\ x_2 \\ x_3 \\ . \\ . \\ x_m \end{bmatrix}$$

(4.23a,b,c)

It can be seen that the location of the centres of rigidity are, in general, load dependent and do not lie on a vertical line through the building.

4.2.3 Proportional buildings

One special case would be a building with proportional resisting elements. In this case, the stiffness matrices of the resisting elements are proportional to one another in each of the co-ordinate directions. In other words, the stiffness matrix of resisting element *i* in the y direction , $\mathbf{k}_y^{(i)}$, can be expressed as

$$\mathbf{k}_y^{(i)} = \alpha_i \mathbf{K}_y \tag{4.24}$$

where α_i is a proportionality constant for element *i* and $\mathbf{K}_y$ is the sum of the stiffness matrices of the resisting elements in the y direction. i.e.

$$\mathbf{K}_y = \sum_{i=1}^{m} \mathbf{k}_y^{(i)} \tag{4.25}$$

and

$$\sum_{i=1}^{m} \alpha_i = 1 \tag{4.26}$$

The load-displacement relation for resisting element *i* can be written using Eqs. (4.13) and (4.16) as

$$\mathbf{p}_y^{(i)} = \mathbf{k}_y^{(i)} \mathbf{d}_y \tag{4.27}$$

and using Eq. (4.24) gives

$$\mathbf{p}_y^{(i)} = \alpha_i \mathbf{K}_y \mathbf{d}_y \tag{4.28}$$

Summation of Eq. (4.27) gives

$$\sum_{i=1}^{m} \mathbf{p}_y^{(i)} = \sum_{i=1}^{m} \mathbf{k}_y^{(i)} \mathbf{d}_y \tag{4.29}$$

Eq. (4.29) can be written in the following form using Eqs. (4.12) and (4.25)

$$\mathbf{V}_y = \mathbf{K}_y \mathbf{d}_y \tag{4.30}$$

Substituting Eq. (4.30) in Eq. (4.28) gives

$$\mathbf{p}_y^{(i)} = \alpha_i \mathbf{V}_y \tag{4.31}$$

Eq. (4.31) can be written in the following matrix format using the definition of $\mathbf{P}_y$ and $\mathbf{V}_{yd}$ in Eq. (4.23a,b)

$$\mathbf{P}_y = \mathbf{V}_{yd} \mathbf{u} \boldsymbol{\alpha} \tag{4.32}$$

where $\mathbf{u}$ is the $(n \times m)$ unitary matrix whose elements are all equal to 1 and $\boldsymbol{\alpha}$ is the diagonal $(m \times m)$ matrix given by

$$\boldsymbol{\alpha} = \begin{bmatrix} \alpha_1 & 0 & 0 & . & . & 0 \\ 0 & \alpha_2 & 0 & . & . & 0 \\ 0 & 0 & \alpha_3 & . & . & 0 \\ . & . & . & . & . & . \\ . & . & . & . & . & . \\ 0 & 0 & 0 & . & . & \alpha_m \end{bmatrix} \tag{4.33}$$

Substituting Eq. (4.32) in Eq. (4.22) gives

$$\mathbf{X}_R = \mathbf{u} \boldsymbol{\alpha} \mathbf{X}_e \tag{4.34}$$

Eq. (4.34) shows that the location of the centre of rigidity of the j^{th} floor can be expressed as

$$X_{Rj} = \sum_{i=1}^{m} \alpha_i x_i \qquad (4.35)$$

Eq. (4.35) clearly shows that in this particular case, the location of centres of rigidity are not load dependent and lie on a vertical line through the height of the structure. It also illustrates that these locations can be determined using relative stiffnesses of resisting elements in each direction independently. In the design profession, this is usually achieved by comparing the relative displacements at top floors of resisting elements under unit forces applied at the top floors.

An identical procedure can be used to determine the y components of the centres of rigidity of buildings by considering the motion of the structure in the x direction.

4.3 NUMERICAL RESULTS

Three singly asymmetric multi-storey buildings will be considered in this section to investigate the location of the centres of rigidity and shear centres of proportional and non-proportional structures using the proposed method. Each of these buildings has ten storeys with uniform storey height of 3 m and rectangular floor plan of dimensions 24m by 18m. The arrangement of resisting elements is such that each building is symmetric about the x axis and asymmetric about the y axis. The building of Example 4.1 consists of proportional plane frames running in the y direction where Examples 4.2 and 4.3 consider asymmetric, non-proprtional frame and wall-frame structures, respectively.

Young's modulus for all members is taken as E=2×10^{10} N/m^2 and the intensity of the distributed mass of the diaphragms is assumed to be m=360 kg/m^2. All buildings are considered to be located in seismic zone 1 (Paz 1994) in Iran and to be subjected to seismic lateral loading in the y-direction. The base shear and distributed lateral load along the height of the structures are determined according to the Iranian Earthquake Code (Paz 1994) and are given in Table 4.1.

Table 4.1 – The lateral load distribution of the buildings of Examples 4.1, 4.2 and 4.3

Storey	Height (m)	Mass (Kg)	$\mathbf{V}_x$ (KN)	$\mathbf{V}_y$ (KN)
10	30.00	155520	448.22	448.22
9	27.00	155520	294.75	294.75
8	24.00	155520	262.00	262.00
7	21.00	155520	229.25	229.25
6	18.00	155520	196.50	196.50
5	15.00	155520	163.75	163.75
4	12.00	155520	131.00	131.00
3	9.00	155520	98.25	98.25
2	6.00	155520	65.50	65.50
1	3.00	155520	32.75	32.75

Inextensible member theory is assumed.

4.3.1 Example 4.1

It is required to determine the location of centres of rigidity and shear centres of a ten-storey, three-dimensional, singly asymmetric building comprising five proportional plane frames running in the y direction (F1-F5), which are connected to each other by typical rigid diaphragms at each floor level with the arrangement shown in Figure 4.4

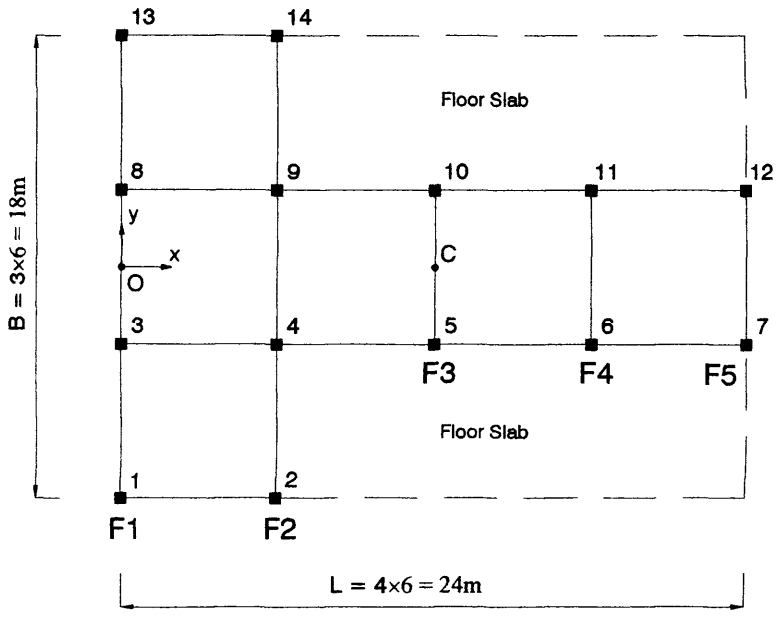

Figure 4.4 Floor plan of the building considerd in Example 4.1.

The properties of the structural elements do not change along the height of the structure and Table 4.2 shows the uniform second moment of area of columns and beams about the x and y axes.

Table 4.2 – The properties of columns and beams of the building of Example 4.1

1^{st} to 10^{th}	Columns				Beams
	1,2,7,12,13,14	5,6,10,11	3,8	4,9	all
$I_y(m^4)$	0.0035	0.007	0.0035	0.007	0.003
$I_x(m^4)$	0.0035	0.0035	0.007	0.007	0.003

All the plane frames in this example are proprtional, so according to Section 4.2.3 we would expect to determine a unique position for the centres of rigidity at different floor levels.

Table 4.3 shows the locations of the centres of mass, rigidity and shear of the building in the coordinate system Oxy shown in Figure 4.4 obtained using the proposed theory. It illustrates that the location of the centres of rigidity and shear are coincident and lie on a vertical line through the height of the structure.

Table 4.3 – The location of the rigidity and shear centres of the building of Examples 4.1

Storey	Height (m)	$\mathbf{X}_R$ (m)	$\mathbf{X}_S$ (m)	$\mathbf{e}_{Rx}$ (m)	$\mathbf{e}_{Sx}$ (m)
10	30.00	8.00	8.00	4.00	4.00
9	27.00	8.00	8.00	4.00	4.00
8	24.00	8.00	8.00	4.00	4.00
7	21.00	8.00	8.00	4.00	4.00
6	18.00	8.00	8.00	4.00	4.00
5	15.00	8.00	8.00	4.00	4.00
4	12.00	8.00	8.00	4.00	4.00
3	9.00	8.00	8.00	4.00	4.00
2	6.00	8.00	8.00	4.00	4.00
1	3.00	8.00	8.00	4.00	4.00

$\mathbf{X}_R$ and $\mathbf{X}_S$ are the vectors of the x coordinate of the centers of rigidity and shear relative to the coordinate system Oxy shown in Figure 4.4. $\mathbf{e}_{Rx}$ and $\mathbf{e}_{Sx}$ represent the static eccentricity vectors based on two definitions of eccentricity in different codes. The first definition, $\mathbf{e}_{Rx}$, specifies the eccentricity at floor levels based on the distance between the centers of mass and rigidity, where as the second definition, $\mathbf{e}_{Sx}$, defines it based on the distance between the centers of mass and shear rigidity.

4.3.2 Example 4.2

It is required to determine the location of the centres of rigidity and shear centres of the ten-storey building of Example 4.1, except that the properties of the columns are changed as shown in Table 4.4. Thus the plane frames running in the y direction are non-proportional

Table 4.4 – The properties of the columns and beams of the building of Example 4.2

1^{st} to 10^{th}	Columns (all)	Beams (all)
$I_y(m^4)$	0.0035	0.003
$I_x(m^4)$	0.0035	0.003

Table 4.5 shows the locations of the centres of mass, rigidity and shear of the building in the coordinate system Oxy shown in Figure 4.4. It illustrates that the location of the centres of rigidity and shear are not coincident and do not lie on a vertical line through the height of the structure.

Table 4.5 – The location of the rigidity and shear centres of the building of Examples 4.2

Storey	Height (m)	$\mathbf{X}_R$ (m)	$\mathbf{X}_S$ (m)	$\mathbf{e}_{Rx}$ (m)	$\mathbf{e}_{Sx}$ (m)
10	30.00	8.17	8.17	3.83	3.83
9	27.00	8.77	8.41	3.23	3.59
8	24.00	8.37	8.40	3.63	3.60
7	21.00	8.42	8.40	3.58	3.60
6	18.00	8.32	8.39	3.68	3.61
5	15.00	8.40	8.39	3.60	3.61
4	12.00	8.53	8.40	3.47	3.60
3	9.00	8.74	8.42	3.26	3.58
2	6.00	10.00	8.48	2.00	3.52
1	3.00	37.80	8.98	25.80	3.02

4.3.3 Example 4.3

It is now required to determine the centres of rigidity and shear of a ten-storey three-dimensional singly asymmetric, wall-frame building comprising 3 proportional plane frames (F1-F3) and two identical shear walls (W1-W2). These resisting elements run in the y direction and are connected to each other by a typical rigid diaphragm at each floor level with the arrangement shown in Figure 4.5.

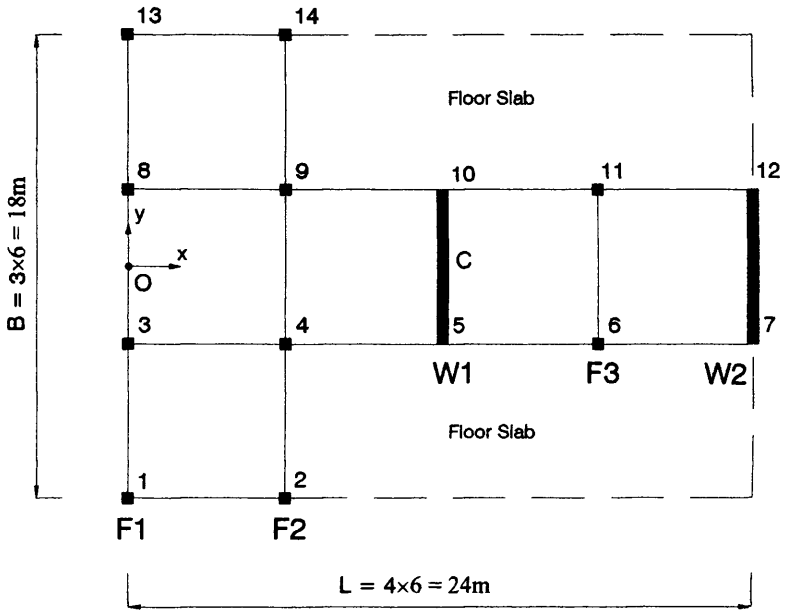

Figure 4.5 Floor plan of the building considerd in Example 4.3.

The properties of the structural elements do not change along the height of the building and Table 4.6 shows the uniform second moment of area of the columns and beams about the x and y directions. The shear walls have a uniform cross-section with second moment of area of 1.3333 m^4 about the x axis.

Table 4.6 – The properties of the columns and beams of the building of Example 4.3

1^{st} to 10^{th}	Columns				Beams
	1,2,13,14	6,11	3,8	4,9	all
$I_y(m^4)$	0.0035	0.007	0.0035	0.007	0.003
$I_x(m^4)$	0.0035	0.0035	0.007	0.007	0.003

Table 4.7 shows the locations of the centres of mass, rigidity and shear of the building in the coordinate system Oxy shown in Figure 4.5. It demonstrates that the location of the centres of rigidity and shear are not coincident and do not lie on a vertical line throughout the height of the structure. It can be concluded that even when the frames and walls of a wall-frame building are independently proportional, the whole building needs to be considered as a non proportional structure i.e. there is no proportional wall-frame structure.

Table 4.7 – The location of the rigidity and shear centres of the building of Examples 4.3

Storey	Height (m)	$\mathbf{X}_R$ (m)	$\mathbf{X}_S$ (m)	$\mathbf{e}_{Rx}$ (m)	$\mathbf{e}_{Sx}$ (m)
10	30.00	-9.89	-9.89	21.89	21.89
9	27.00	30.89	6.29	18.89	5.71
8	24.00	13.76	8.24	1.76	3.76
7	21.00	18.09	10.07	6.09	1.93
6	18.00	18.17	11.19	6.17	0.81
5	15.00	20.63	12.15	8.63	0.15
4	12.00	24.68	13.10	12.68	1.10
3	9.00	32.04	14.12	20.04	2.12
2	6.00	48.97	15.33	36.97	3.33
1	3.00	103.76	16.83	91.73	4.83

4.4 CONCLUSIONS

A practical method to locate the centers of rigidity, shear centers and hence static eccentricity has been given. The method is based on the use of a plane frame computer programme but does not need the explicit expressions for the stiffness matrix of the resisting elements. The method has the following advantages in comparison with the Cheung and Tso's method(Cheung and Tso 1986), which was explained in Section 4.1.

- Resisting elements are analyzed separately, so the input file is much smaller and there is no need for the modeling of pin-pin rigid beams in floor levels
- Identical plane elements are analyzed only once, since they all have a unique $\boldsymbol{\delta}^{(i)}$
- The method lends itself to simple data generation and programming
- The method is easily extendable to cover the static analysis of doubly asymmetric structures with rigid diaphragms, using the two-dimensional approach
- The method can be modified to account for the analysis of structures with flexible diaphragms.

It was shown that the centers of rigidity and shear centers of the floors of multi-storey buildings do not generally coincide. Their locations are not only dependent on the geometric and stiffness characteristics of the building, but also on the lateral forces. Also, their locations do not generally lie on a vertical line through the height of the structure. A particular class of buildings was distinguished, the so called proportional buildings, in which the centers of rigidity and shear of the floors are coincident, load independent and lie on a vertical line throughout their height. Buildings belonging to this special class comprise resisting elements that have proportional stiffness matrices along both their principal planes. The proportionality in the x and y directions are independent and it is not necessary that the resisting elements running in the x direction be proportional to those running in the y direction.

Torsional provision in most building codes is based on the evaluation of static eccentricity, usually given as the distance between the centers of mass and the centers of rigidity of a building. However it is applicable only to proportional structures where there is a unique eccentricity throughout the building. Since the diversion of location of shear centers along the height of the structures is smaller than that of centers of rigidity, it seems more practical for code provisions to give their rules based on eccentricity defined as the distance between the centers of mass and shear centers.

CHAPTER 5

VIBRATION ANALYSIS OF ASYMMETRIC THREE-DIMENSIONAL FRAME STRUCTURES

5.1 INTRODUCTION

It was shown in Chapter 3 that in a doubly symmetric structure in which the centres of mass and rigidity are coincident, the translational and torsional vibration of the structure could be treated separately. However, in the majority of buildings, the serviceability requirements lead to an asymmetric location of structural elements. In such asymmetric structures the translational and torsional behaviour of the building can no longer be treated independently and the governing equations are coupled.

This chapter presents two methods of analysis for determining the natural frequencies of asymmetric three-dimensional frame structures. Such structures comprise asymmetric arrangements of planar frame systems, which have been joined to each other by rigid diaphragms at floor level. Each method is able to analyse asymmetric, three-dimensional frame structures whose properties may vary through the height of the structure in a stepwise fashion at one or more storey levels.

The first method utilises a continuum approach so that an asymmetric, three-dimensional frame structure is divided into segments, by cutting through the structure horizontally at those storey levels corresponding to changes in storey properties. A typical segment is then considered in isolation. Initially, a primary frame in one direction is replaced by its shear substitute beam that has uniformly distributed mass and shear rigidity, thus utilising the continuum approach. In turn, each frame in the same direction is replaced by its own shear substitute beam and the effect of all these beams is summed to model the effect of the original frames. This leads directly to the differential equation governing the sway motion of the segment in the chosen direction. The same procedure is then adopted for those frames running in the orthogonal direction. Once both equations are available it requires little effort to write down the substitute expressions for the torsional motion.

The second method utilises the Principle of Multiples and extends its application to three-dimensional asymmetric structures. It will be shown that the substitute frame method can be used for the vibration analysis in a two-step procedure. First the analogous uncoupled system will be analysed using substitute frames then the relation between the uncoupled and coupled responses will be imposed through a cubic equation.

In order to validate the accuracy which might be expected from the proposed methods, it was deemed necessary to carry out a parametric study.

5.2 CONTINUUM METHOD

5.2.1 Coupled Vibration Analysis

Consider the hypothetical layout of a typical floor plan of the asymmetric, three-dimensional frame structure shown in Figure 5.1. The plane frames run in two orthogonal directions and are proportional to each other in any one direction, but the proportionality is not necessarily the same in both directions. The shear centre, S, at each floor level thus lies on a vertical line through the height of the structure.

It is assumed that the origin of the co-ordinate system is located at the shear centre, with the x and y co-ordinates running parallel to the plane frames. The z-axis runs vertically from the base of the building and therefore coincides with the rigidity axis. Point $C(x_c, y_c)$ denotes the centre of mass at a typical floor level. It is assumed that the floor system is rigid in its plane and that the centre of mass at each level lies on a vertical line, the mass axis, that runs through the height of the structure. When the rigidity and mass axes of a structure do not coincide, the lateral and torsional motion of the building will always be coupled in one or more planes.

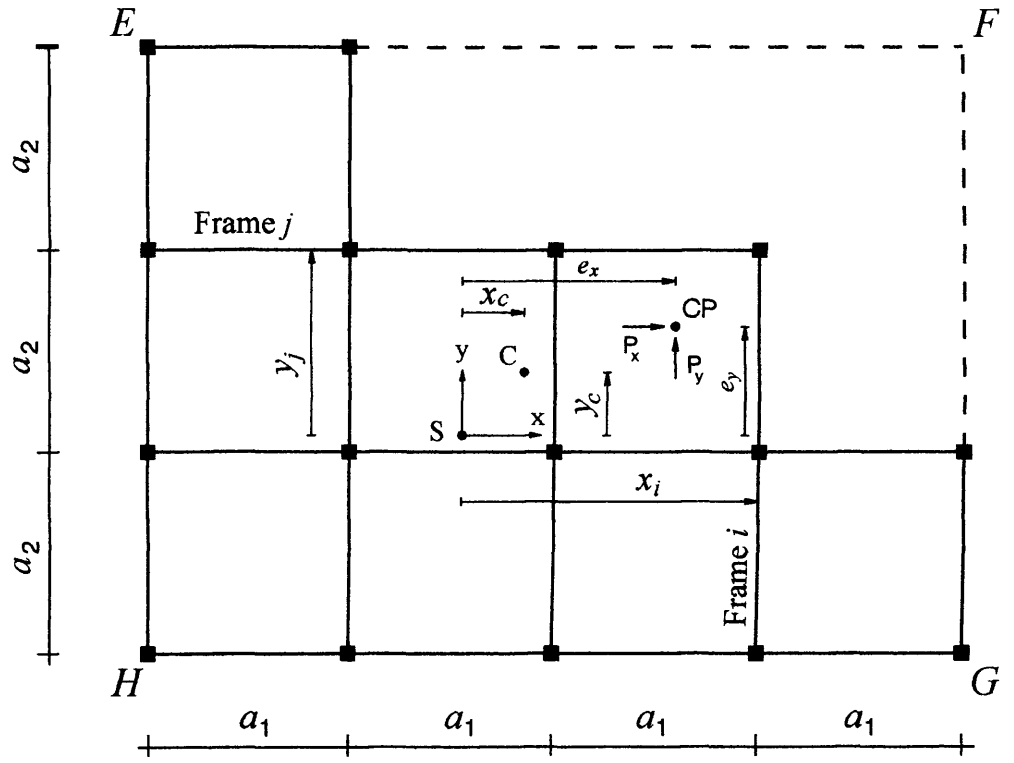

Figure 5.1 Typical floor plan of an asymmetric three-dimensional frame structure. S and C denote the locations of the shear and mass centres, respectively. The floor system *EFGH* is considered to be rigid in its plane.

During vibration, the displacement of the mass centre at any time t in the x-y plane can be determined as the result of a pure translation followed by a pure rotation about the shear centre, see Figure 5.2. During the translation phase the shear centre S moves to S′ and the mass centre C moves to C′, displacements in each case of $u(z,t)$ and $v(z,t)$ in the x and y directions, respectively. During rotation, the mass centre moves additionally from C′ to C″, an angular rotation of $\varphi(z,t)$ about S′. The resulting translations, u_c and v_c, of the mass centre in the x and y directions, respectively, are

$$u_c(z,t) = u(z,t) - y_c\varphi(z,t) \tag{5.1a}$$

$$v_c(z,t) = v(z,t) + x_c\varphi(z,t) \tag{5.1b}$$

More generally, it is clear that the displacements of a typical point (x_i,y_i) are given by Eqs. (5.1a) and (5.1b) when $c = i$.

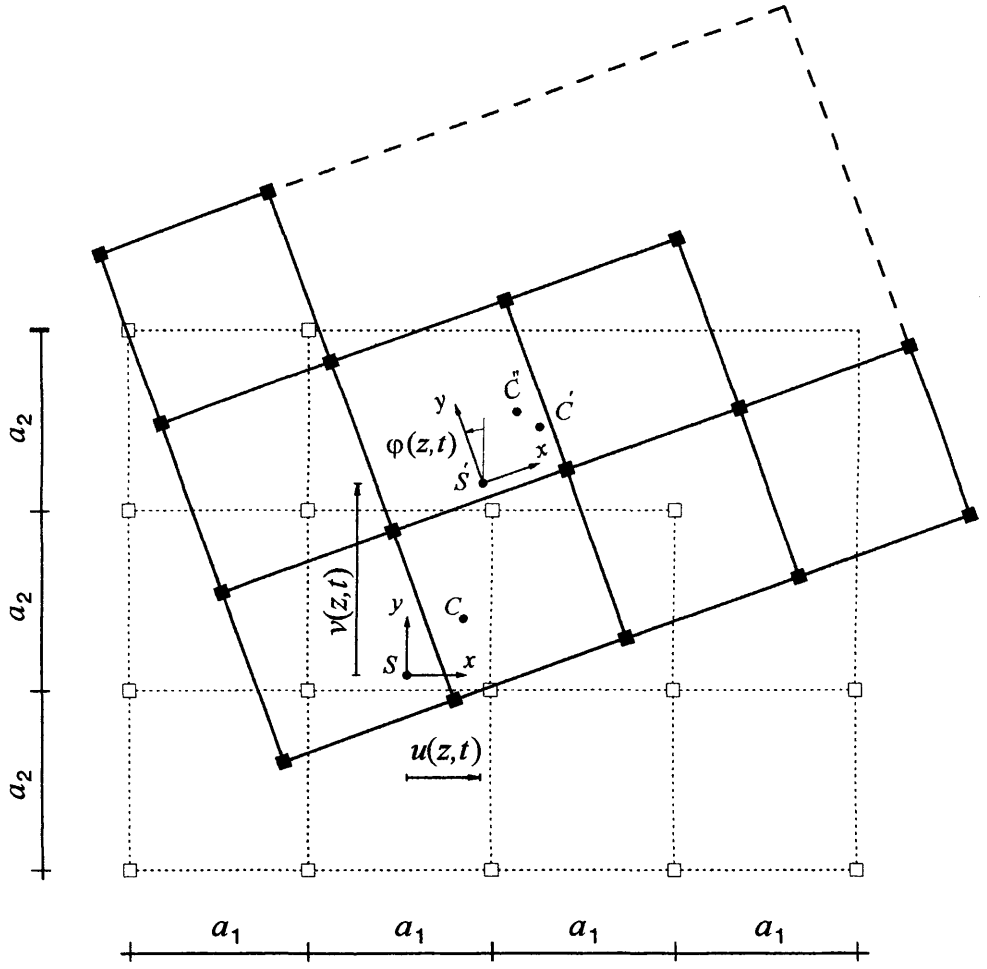

Figure 5.2 Coupled translational-torsional vibration of the structure. S and C move to S′ and C′, respectively, during translation and C′ moves additionally to C″ during rotation about S′.

The structure is now divided into segments along the z axis by notionally cutting the structure along horizontal planes at those storey levels corresponding to changes in storey properties. Figure 5.3 shows a typical segment formed by cutting the structure through planes $E_kF_kG_kH_k$ and $E_{k+1}F_{k+1}G_{k+1}H_{k+1}$ that correspond to the k^{th} and $k+1^{th}$ changes in storey properties. The number of storeys in any one segment can vary from one, to the total number of storeys in the structure if it is uniform throughout its height. However, in any one segment each storey must have the same properties.

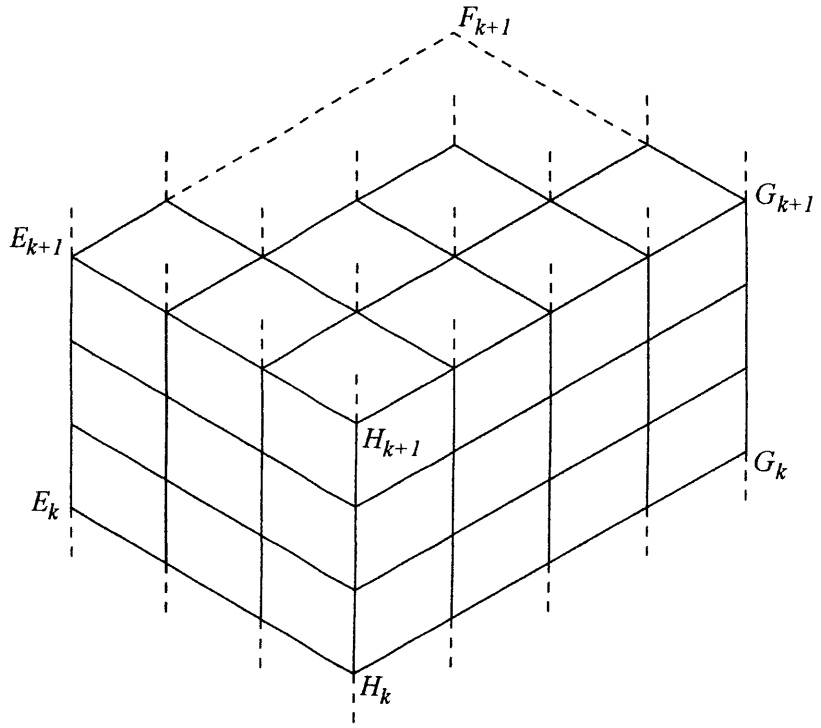

Figure 5.3 Typical segment formed by cutting the structure through planes $E_kF_kG_kH_k$ and $E_{k+1}F_{k+1}G_{k+1}H_{k+1}$ that correspond to the k^{th} and $k+1^{th}$ changes in storey properties. (Some column and beam members have been omitted for clarity.)

We now consider a typical segment in isolation and seek to replace each primary frame by a substitute shear beam that replicates its in-plane motion. We start by considering a typical frame, frame i, that runs parallel to the y-z plane, see Figure 5.1. This whole frame is replaced by the single substitute beam, beam i, shown in Figure 5.4. This beam is a two-dimensional shear beam of length L and has uniformly distributed mass and shear stiffness. The mass and elastic axes therefore coincide with the local z-axis and the elastic axis is only permitted shear deformation $v_i(z,t)$ in the y direction, where z and t denote distance from the local origin and time, respectively.

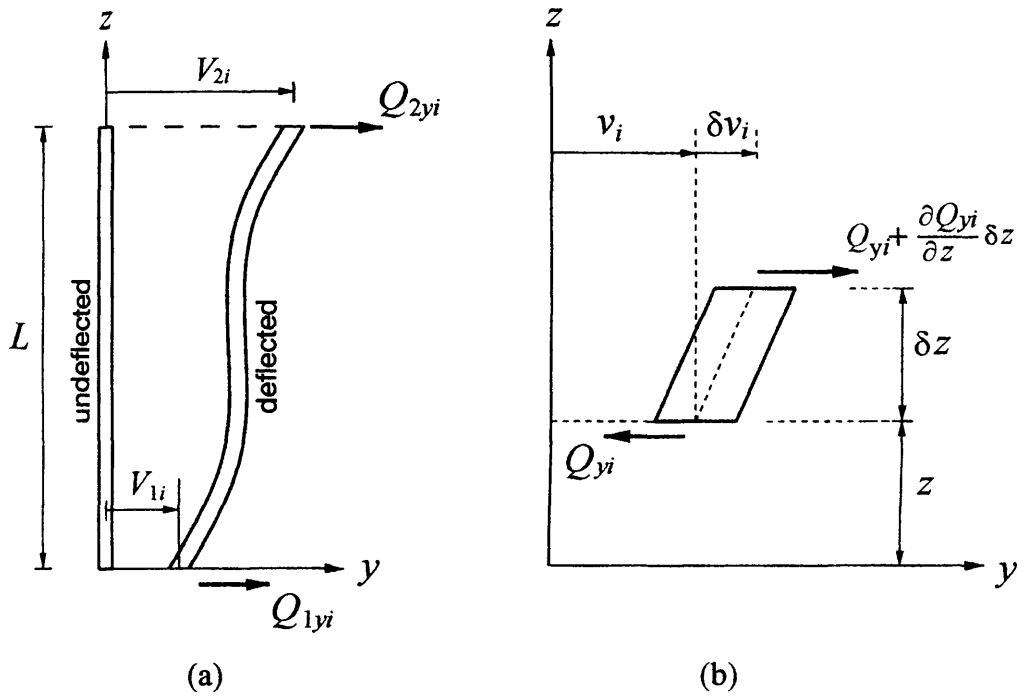

Figure 5.4 Coordinate system and sign convention for the substitute two-dimensional shear beam in the local *y*-*z* plane. a) Member convention. b) Element convention.

The equations of motion for the substitute beam can be developed by considering a typical elemental length of the beam, δz. Thus equating the resultant shear force to the mass acceleration gives

$$\frac{\partial Q_{yi}(z,t)}{\partial z} = m_{yi}\frac{\partial^2 v_i(z,t)}{\partial t^2} \tag{5.2}$$

where $Q_{yi}(z,t)$ is the shear force on the element and m_{yi} is the uniformly distributed mass per unit length.

The constitutive relationship for pure shear is given by

$$\frac{Q_{yi}(z,t)}{GA_{yi}} = \frac{\partial v_i(z,t)}{\partial z} \tag{5.3}$$

in which GA_{yi} is the effective shear rigidity in the y direction (Smith and Coull 1991).

Substituting the derivative of Eq. (5.3) into Eq. (5.2) gives

$$\frac{\partial^2 v_i(z,t)}{\partial z^2} - \frac{m_{yi}}{GA_{yi}} \frac{\partial^2 v_i(z,t)}{\partial t^2} = 0 \tag{5.4}$$

which is the required differential equation of motion for the shear beam element in the *y-z* plane.

If the equivalent procedure is carried out for all of the *i* frames that run parallel to the *y-z* plane, the dynamic equilibrium for motion in the *y-z* plane may be written as

$$\frac{\partial}{\partial z} \sum_{i=1}^{n_y} GA_{yi} \frac{\partial v_i(z,t)}{\partial z} = \sum_{i=1}^{n_y} m_{yi} \frac{\partial^2 v_i(z,t)}{\partial t^2} \tag{5.5}$$

where n_y is the number of frames.

Noting that GA_{yi} is constant over the length of the member and substituting for $v_i(z,t)$ from Eq. (5.1b) with *c* replaced by *i* gives

$$\sum_{i=1}^{n_y} GA_{yi} \frac{\partial^2 v(z,t)}{\partial z^2} + \sum_{i=1}^{n_y} GA_{yi} x_i \frac{\partial^2 \varphi(z,t)}{\partial z^2} - \sum_{i=1}^{n_y} m_{yi} \frac{\partial^2 v(z,t)}{\partial t^2} - \sum_{i=1}^{n_y} m_{yi} x_i \frac{\partial^2 \varphi(z,t)}{\partial t^2} = 0 \tag{5.6}$$

where x_i is the distance of frame *i* from the shear centre, S. The second term in Eq. (5.6) equals zero, since S is the centre of rigidity of the structure. As C is the centre of mass, $\sum_{i=1}^{n_y} m_{yi} x_i$ can be replaced with $m_y x_c$, where $m_y = \sum_{i=1}^{n_y} m_{yi}$, so Eq. (5.6) can be written as follows

$$GA_y \frac{\partial^2 v(z,t)}{\partial z^2} - m_y \frac{\partial^2 v(z,t)}{\partial t^2} - m_y x_c \frac{\partial^2 \varphi(z,t)}{\partial t^2} = 0 \tag{5.7}$$

in which

$$GA_y = \sum_{i=1}^{n_y} GA_{yi} \tag{5.8}$$

Since the total mass of the segment contributes to its vibration, including the mass of the frames running in the x direction and the rigid diaphragms, m_y should be replaced by m, where m is the equivalent distributed mass over the height of the segment. Therefore

$$GA_y \frac{\partial^2 v(z,t)}{\partial z^2} - m\frac{\partial^2 v(z,t)}{\partial t^2} - mx_c \frac{\partial^2 \varphi(z,t)}{\partial t^2} = 0 \tag{5.9}$$

In an identical fashion, the dynamic equilibrium relationship for motion in the x-z plane yields the second governing differential equation as

$$\sum_{j=1}^{n_x} GA_{xj} \frac{\partial^2 u(z,t)}{\partial z^2} + \sum_{j=1}^{n_x} GA_{xj} y_j \frac{\partial^2 \varphi(z,t)}{\partial z^2} - \sum_{j=1}^{n_x} m_{xj} \frac{\partial^2 u(z,t)}{\partial t^2} - \sum_{j=1}^{n_x} m_{xj} y_j \frac{\partial^2 \varphi(z,t)}{\partial t^2} = 0 \tag{5.10}$$

where n_x is the number of frames running in the x direction and y_j is the distance of frame j from the shear centre, S. GA_{xj} and m_{xj} are the effective shear rigidity in the x direction and uniformly distributed mass per unit length of the replacement beam for frame j, respectively. Once more the second term in Eq. (5.10) equals zero, since S is the centre of rigidity of the structure. This leads to

$$GA_x \frac{\partial^2 u(z,t)}{\partial z^2} - m\frac{\partial^2 u(z,t)}{\partial t^2} + my_c \frac{\partial^2 \varphi(z,t)}{\partial t^2} = 0 \tag{5.11}$$

in which

$$GA_x = \sum_{j=1}^{n_x} GA_{xj} \tag{5.12}$$

Finally, it should be noted that the plane frames running parallel to the x-z and y-z planes also provide the torsional stiffness of the building. Thus the required equation for torsion can be developed from a consideration of the torsional equilibrium about S, which yields

$$\sum_{i=1}^{n_y} GA_{yi} x_i \frac{\partial^2 (v(z,t) + x_i \varphi(z,t))}{\partial z^2} - \sum_{i=1}^{n_y} m_{yi} x_i \frac{\partial^2 (v(z,t) + x_i \varphi(z,t))}{\partial t^2} +$$

$$- \left[\sum_{j=1}^{n_x} GA_{xj} y_j \frac{\partial^2 (u(z,t) - y_j \varphi(z,t))}{\partial z^2} - \sum_{j=1}^{n_x} m_{xj} y_j \frac{\partial^2 (u(z,t) - y_j \varphi(z,t))}{\partial t^2} \right] = 0 \tag{5.13}$$

Eq. (5.13) can be simplified to

$$\left(\sum_{i=1}^{n_y} GA_{yi}x_i^2 + \sum_{j=1}^{n_x} GA_{xj}y_j^2\right)\frac{\partial^2\varphi(z,t)}{\partial z^2} - m_y x_c \frac{\partial^2 v(z,t)}{\partial t^2} + m_x y_c \frac{\partial^2 u(z,t)}{\partial t^2}$$

$$-\left(\sum_{i=1}^{n_y} m_{yi}x_i^2 + \sum_{j=1}^{n_x} m_{xj}y_j^2\right)\frac{\partial^2\varphi(z,t)}{\partial z^2} = 0 \qquad (5.14)$$

As before, the total mass of the frames running in the x and y directions, as well as that of the rigid diaphragms, should be taken into account. Thus, Eq. (5.14) can finally be written as

$$GJ\frac{\partial^2\varphi(z,t)}{\partial z^2} - mx_c\frac{\partial^2 v(z,t)}{\partial t^2} + my_c\frac{\partial^2 u(z,t)}{\partial t^2} - I_g\frac{\partial^2\varphi(z,t)}{\partial z^2} = 0 \qquad (5.15)$$

in which I_g is the polar second moment of mass of the system about the shear centre and

$$GJ = \left(\sum_{i=1}^{n_y} GA_{yi}x_i^2 + \sum_{j=1}^{n_x} GA_{xj}y_j^2\right) \qquad (5.16)$$

where GJ is the effective torsional rigidity of the structure about the shear centre S.

Eqs. (5.9), (5.11) and (5.15) are the required differential equations of motion and can be rearranged in the following form

$$GA_x\frac{\partial^2 u(z,t)}{\partial z^2} - m\frac{\partial^2 u(z,t)}{\partial t^2} + my_c\frac{\partial^2\varphi(z,t)}{\partial t^2} = 0 \qquad (5.17a)$$

$$GA_y\frac{\partial^2 v(z,t)}{\partial z^2} - m\frac{\partial^2 v(z,t)}{\partial t^2} - mx_c\frac{\partial^2\varphi(z,t)}{\partial t^2} = 0 \qquad (5.17b)$$

$$GJ\frac{\partial^2\varphi(z,t)}{\partial z^2} + my_c\frac{\partial^2 u(z,t)}{\partial t^2} - mx_c\frac{\partial^2 v(z,t)}{\partial t^2} - mr_m^2\frac{\partial^2\varphi(z,t)}{\partial z^2} = 0 \qquad (5.17c)$$

where r_m is the polar mass radius of gyration of the structure about shear centre S.

5.2.2 Member Dynamic Stiffness Matrix

Eqs. (5.17) are now solved and posed in dynamic stiffness form. Although each equation was developed individually from a consideration of the planar shear beam of Figure 5.4, they now describe the motion of a three-dimensional, shear-torsion coupled beam whose coordinate system and sign convention are shown in Figure 5.5. This beam (exact finite element) will replace a typical segment of the original, asymmetric, three-dimensional frame structure. The whole of the original structure can then be reconstituted by assembling the exact finite elements corresponding to each segment in the usual way.

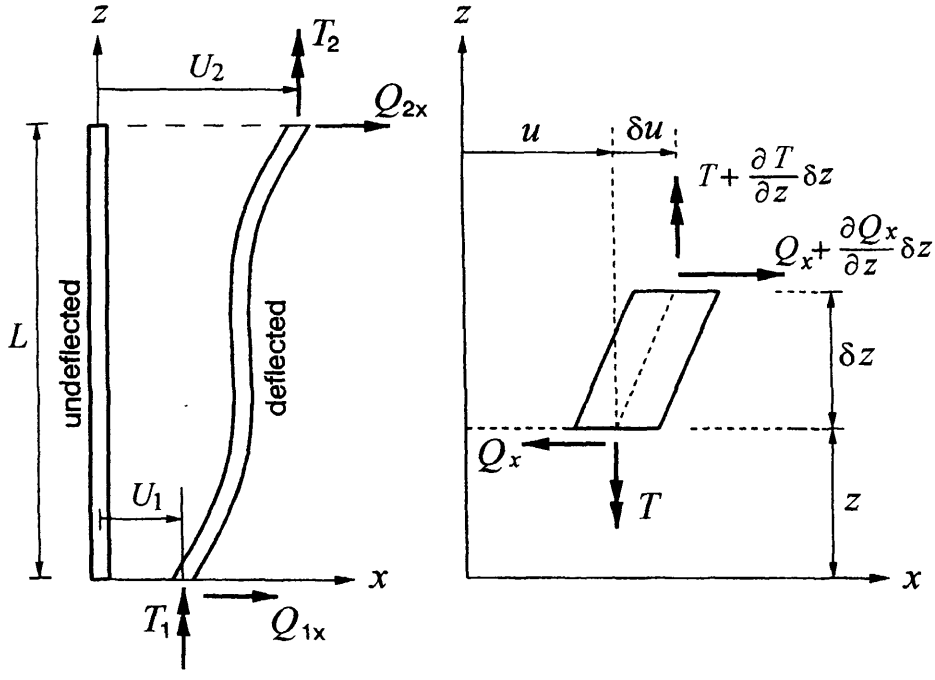

(a)

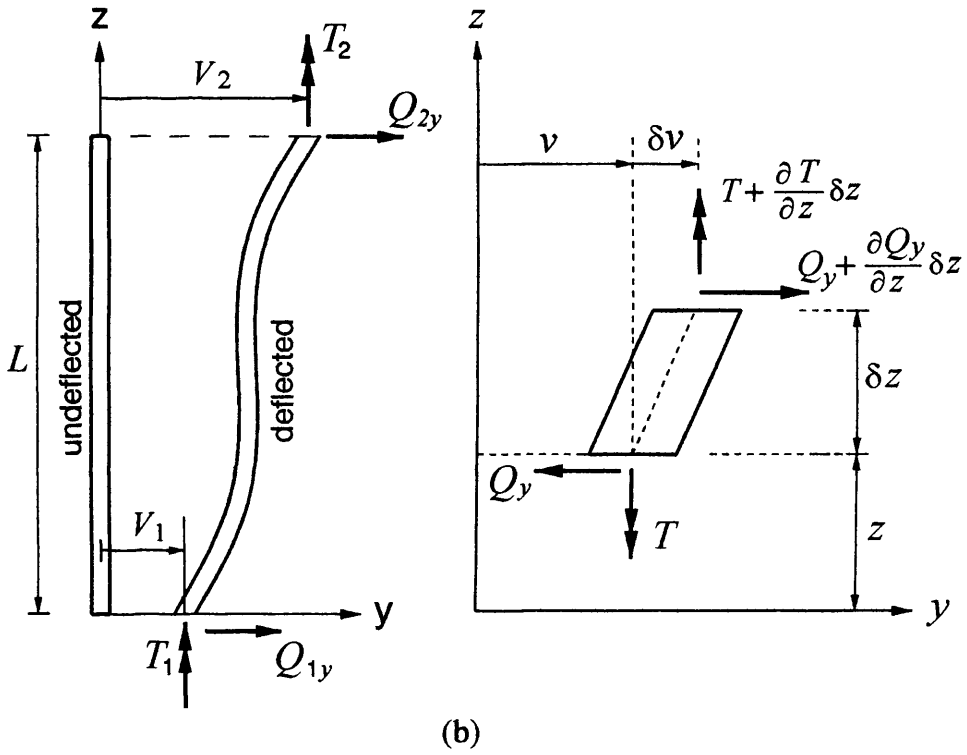

(b)

Figure 5.5 Coordinate system and sign convention for forces and displacements of the three-dimensional shear-torsion coupled beam. a) Member and element convention for the x-z plane. b) Member and element convention for the y-z plane

Eqs. (5.17) are solved on the assumption of harmonic motion, so that the instantaneous displacements can be written as

$$u(z,t) = U(z)\sin\omega t \qquad v(z,t) = V(z)\sin\omega t \qquad \varphi(z,t) = \Phi(z)\sin\omega t \qquad (5.18a,b,c)$$

where $U(z)$, $V(z)$ and $\Phi(z)$ are the amplitudes of the sinusoidally varying displacements and ω is the circular frequency.

Substituting Eqs. (5.18) into Eqs. (5.17) and re-writing in non-dimensional form gives

$$U''(\xi) + \omega^2\lambda_x^2 U(\xi) - y_c\omega^2\lambda_x^2\Phi(\xi) = 0 \qquad (5.19a)$$

$$V''(\xi) + \omega^2\lambda_y^2 V(\xi) + x_c\omega^2\lambda_y^2\Phi(\xi) = 0 \qquad (5.19b)$$

$$\Phi''(\xi) - (1/r_m^2)y_c\omega^2\lambda_\varphi^2 U(\xi) + (1/r_m^2)x_c\omega^2\lambda_\varphi^2 V(\xi) + \omega^2\lambda_\varphi^2\Phi(\xi) = 0 \qquad (5.19c)$$

where

$$\lambda_x^2 = mL^2/GA_x \quad \lambda_y^2 = mL^2/GA_y \quad \lambda_\varphi^2 = r_m^2(mL^2/GJ) \text{ and } \xi = (z/L) \qquad (5.20a,b,c,d)$$

Eqs. (5.19) can be re-written in the following matrix form

$$\begin{bmatrix} D^2+\omega^2\lambda_x^2 & 0 & -y_c\omega^2\lambda_x^2 \\ 0 & D^2+\omega^2\lambda_y^2 & x_c\omega^2\lambda_y^2 \\ -(1/r_m^2)y_c\omega^2\lambda_\varphi^2 & (1/r_m^2)x_c\omega^2\lambda_\varphi^2 & D^2+\omega^2\lambda_\varphi^2 \end{bmatrix} \begin{bmatrix} U(\xi) \\ V(\xi) \\ \Phi(\xi) \end{bmatrix} = 0 \qquad (5.21)$$

in which $D = d/d\xi$.

Eq. (5.21) can be combined into one equation by eliminating either U, V or Φ to give the sixth-order differential equation

$$\begin{vmatrix} D^2+\omega^2\lambda_x^2 & 0 & -y_c\omega^2\lambda_x^2 \\ 0 & D^2+\omega^2\lambda_y^2 & x_c\omega^2\lambda_y^2 \\ -(1/r_m^2)y_c\omega^2\lambda_\varphi^2 & (1/r_m^2)x_c\omega^2\lambda_\varphi^2 & D^2+\omega^2\lambda_\varphi^2 \end{vmatrix} W(\xi) = 0 \qquad (5.22)$$

where $W = U, V$ or Φ.

The solution of Eq. (5.22) is found by substituting the trial solution $W(\xi) = e^{s\xi}$ to yield the characteristic equation

$$\begin{vmatrix} b^2+\lambda_x^2 & 0 & -y_c\lambda_x^2 \\ 0 & b^2+\lambda_y^2 & x_c\lambda_y^2 \\ -y_c\lambda_\varphi^2 & x_c\lambda_\varphi^2 & r_m^2(b^2+\lambda_\varphi^2) \end{vmatrix} = 0 \qquad (5.23)$$

where $b^2 = (s/\omega)^2$.

Eq. (5.23) is a cubic equation in the frequency parameter b^2 and it can be proven (Appendix 5A) that it always has three negative real roots. Let these three roots be $-b_1^2, -b_2^2$ and $-b_3^2$, where b_j^2 (j=1,2,3) are all real and positive. Therefore

$$(\frac{s}{\omega})^2 = -b_j^2 \qquad \text{giving} \qquad s = \pm i\omega b_j \qquad (j=1,2,3) \qquad \text{where } i = \sqrt{-1} \tag{5.24}$$

It follows that the solution of Eq. (5.22) can be written in the form

$$\begin{aligned} W(\xi) &= C_1 \cos b_1\omega\xi + C_2 \sin b_1\omega\xi + C_3 \cos b_2\omega\xi \\ &+ C_4 \sin b_2\omega\xi + C_5 \cos b_3\omega\xi + C_6 \sin b_3\omega\xi \end{aligned} \tag{5.25}$$

Eq. (5.25) represents the solution for $U(\xi)$, $V(\xi)$ and $\Phi(\xi)$, since they are all related via Eq. (5.21). They can be written individually as

$$\begin{aligned} U(\xi) &= t_1^u(C_1 \cos b_1\omega\xi + C_2 \sin b_1\omega\xi) + t_2^u(C_3 \cos b_2\omega\xi \\ &+ C_4 \sin b_2\omega\xi) + t_3^u(C_5 \cos b_3\omega\xi + C_6 \sin b_3\omega\xi) \end{aligned} \tag{5.26a}$$

$$\begin{aligned} V(\xi) &= t_1^v(C_1 \cos b_1\omega\xi + C_2 \sin b_1\omega\xi) + t_2^v(C_3 \cos b_2\omega\xi \\ &+ C_4 \sin b_2\omega\xi) + t_3^v(C_5 \cos b_3\omega\xi + C_6 \sin b_3\omega\xi) \end{aligned} \tag{5.26b}$$

$$\begin{aligned} \Phi(\xi) &= C_1 \cos b_1\omega\xi + C_2 \sin b_1\omega\xi + C_3 \cos b_2\omega\xi \\ &+ C_4 \sin b_2\omega\xi + C_5 \cos b_3\omega\xi + C_6 \sin b_3\omega\xi \end{aligned} \tag{5.26c}$$

in which the constants t_j^u and t_j^v (j=1,2,3) are given by

$$t_j^u = \frac{y_c\lambda_x^2}{\lambda_x^2 - b_j^2} \quad , \quad t_j^v = \frac{-x_c\lambda_y^2}{\lambda_y^2 - b_j^2} \qquad (j=1,2,3) \tag{5.27a,b}$$

Substituting Eqs. (5.18) and (5.26) into Eq. (5.2) yields the equations for the lateral shear forces and torsional moment of the substitute shear beam as

$$Q_x(z) = GA_x\frac{dU(z)}{dz} = \frac{1}{L}GA_x\frac{dU(\xi)}{d\xi} \tag{5.28a}$$

$$Q_y(z) = GA_y \frac{dV(z)}{dz} = \frac{1}{L} GA_y \frac{dV(\xi)}{d\xi} \tag{5.28b}$$

$$T(z) = GJ \frac{d\Phi(z)}{dz} = \frac{1}{L} GJ \frac{d\Phi(\xi)}{d\xi} \tag{5.28c}$$

The nodal forces and displacements can now be defined in the member co-ordinate system of the substitute shear-torsion beam shown in Figures 5.5(a) and 5.5(b), as follows

At $\xi = 0$: $U=U_1$, $V=V_1$, $\Phi=\Phi_1$, $Q_x=-Q_{1x}$, $Q_y=-Q_{1y}$, $T=-T_1$ (5.29a)

At $\xi = 1$: $U=U_2$, $V=V_2$, $\Phi=\Phi_2$, $Q_x=Q_{2x}$, $Q_y=Q_{2y}$, $T=T_2$ (5.29b)

The nodal displacements can then be determined from Eqs. (5.26) as

$$\begin{bmatrix} \mathbf{d}_1 \\ \mathbf{d}_2 \end{bmatrix} = \begin{bmatrix} \mathbf{E} & \mathbf{0} \\ \mathbf{0} & \mathbf{E} \end{bmatrix} \begin{bmatrix} \mathbf{I} & \mathbf{0} \\ \mathbf{C} & \mathbf{S} \end{bmatrix} \begin{bmatrix} \mathbf{C}_o \\ \mathbf{C}_e \end{bmatrix} \tag{5.30}$$

where

$$\mathbf{d}_1 = \begin{bmatrix} U_1 \\ V_1 \\ \Phi_1 \end{bmatrix}, \mathbf{d}_2 = \begin{bmatrix} U_2 \\ V_2 \\ \Phi_2 \end{bmatrix}, \mathbf{C}_o = \begin{bmatrix} C_1 \\ C_3 \\ C_5 \end{bmatrix}, \mathbf{C}_e = \begin{bmatrix} C_2 \\ C_4 \\ C_6 \end{bmatrix}, \mathbf{E} = \begin{bmatrix} t_1^u & t_2^u & t_3^u \\ t_1^v & t_2^v & t_3^v \\ 1 & 1 & 1 \end{bmatrix},$$

$$\mathbf{C} = \begin{bmatrix} C_{b_1\omega} & 0 & 0 \\ 0 & C_{b_2\omega} & 0 \\ 0 & 0 & C_{b_3\omega} \end{bmatrix}, \mathbf{S} = \begin{bmatrix} S_{b_1\omega} & 0 & 0 \\ 0 & S_{b_2\omega} & 0 \\ 0 & 0 & S_{b_3\omega} \end{bmatrix},$$

$\mathbf{I}$ is the unit matrix, $S_{b_j\omega} = \sin(b_j\omega)$ and $C_{b_j\omega} = \cos(b_j\omega)$ (j=1,2,3) (5.31)

Hence the vector of constants $[\mathbf{C}_o\ \mathbf{C}_e]^T$ can be determined from Eq. (5.30) as

$$\begin{bmatrix} \mathbf{C}_o \\ \mathbf{C}_e \end{bmatrix} = \begin{bmatrix} \mathbf{I} & \mathbf{0} \\ \mathbf{C} & \mathbf{S} \end{bmatrix}^{-1} \begin{bmatrix} \mathbf{E} & \mathbf{0} \\ \mathbf{0} & \mathbf{E} \end{bmatrix}^{-1} \begin{bmatrix} \mathbf{d}_1 \\ \mathbf{d}_2 \end{bmatrix} \tag{5.32}$$

In similar fashion the vector of nodal forces can be determined from Eqs. (5.28) as

$$\begin{bmatrix}\mathbf{p}_1\\ \mathbf{p}_2\end{bmatrix}=\begin{bmatrix}\mathbf{DEb} & \mathbf{0}\\ \mathbf{0} & \mathbf{DEb}\end{bmatrix}\begin{bmatrix}\mathbf{0} & -\mathbf{I}\\ -\mathbf{S} & \mathbf{C}\end{bmatrix}\begin{bmatrix}\mathbf{C}_o\\ \mathbf{C}_e\end{bmatrix} \tag{5.33}$$

where

$$\mathbf{p}_1=\begin{bmatrix}Q_{1x}\\ Q_{1y}\\ T_1\end{bmatrix},\ \mathbf{p}_2=\begin{bmatrix}Q_{2x}\\ Q_{2y}\\ T_2\end{bmatrix},\ \mathbf{D}=\frac{\omega}{L}\begin{bmatrix}GA_x & 0 & 0\\ 0 & GA_y & 0\\ 0 & 0 & GJ\end{bmatrix}\ \text{and}\ \mathbf{b}=\begin{bmatrix}b_1 & 0 & 0\\ 0 & b_2 & 0\\ 0 & 0 & b_3\end{bmatrix} \tag{5.34}$$

Thus the required stiffness matrix can be developed by substituting Eqs. (5.32) into Eqs. (5.33) to give

$$\begin{bmatrix}\mathbf{p}_1\\ \mathbf{p}_2\end{bmatrix}=\begin{bmatrix}\mathbf{DEb} & \mathbf{0}\\ \mathbf{0} & \mathbf{DEb}\end{bmatrix}\begin{bmatrix}\mathbf{0} & -\mathbf{I}\\ -\mathbf{S} & \mathbf{C}\end{bmatrix}\begin{bmatrix}\mathbf{I} & \mathbf{0}\\ \mathbf{C} & \mathbf{S}\end{bmatrix}^{-1}\begin{bmatrix}\mathbf{E} & \mathbf{0}\\ \mathbf{0} & \mathbf{E}\end{bmatrix}^{-1}\begin{bmatrix}\mathbf{d}_1\\ \mathbf{d}_2\end{bmatrix} \tag{5.35}$$

or

$$\mathbf{p=kd} \tag{5.36}$$

5.2.2.1 Wittrick-Williams algorithm

The dynamic stiffness matrix, **K**, when assembled from the member stiffness matrices, yields the required natural frequencies as solutions of the equation

$$\mathbf{K\,D=0} \tag{5.37}$$

The Wittrick-Williams algorithm can then be used again to solve this transcendental eigenvalue problem. The algorithm has already been explained in Section 2.2.2.1.2 and here only two key equations for finding the natural frequencies of the structure exceeded by the trial frequency ω^* are given for convenience as

$$J = J_0 + s\,\{\mathbf{K}\} \tag{5.38}$$

where

$$J_0 = \sum J_m \tag{5.39}$$

In the present case it is possible to determine the value of J_m symbolically, using a direct approach, as follows

The end conditions for a clamped-clamped member are $\mathbf{d}_1 = \mathbf{d}_2 = \mathbf{0}$ (5.40)

If Eqs. (5.40) are substituted into Eq. (5.30) it is clear that the condition for non-trivial solutions is

$$\begin{vmatrix} \mathbf{E} & \mathbf{0} & \mathbf{I} & \mathbf{0} \\ \mathbf{0} & \mathbf{E} & \mathbf{C} & \mathbf{S} \end{vmatrix} = 0 \tag{5.41}$$

However, it is easy to show that the left-hand determinant can never be zero. Thus, noting that the right-hand determinant is that of a lower triangular matrix, Eq. (5.41) is only satisfied when the product of its significant leading diagonal terms is zero, i.e.

$$\prod_{j=1}^{3} S_{b_j\omega} = 0 \tag{5.42}$$

which is satisfied when $\omega_j^k = \dfrac{k\pi}{b_j}$ $\quad j$=1,2,3 ; $\quad k$=1,2,3,... (5.43)

so J_m for any trial frequency ω^* can be found from

$$J_m = \text{int}\left[\frac{\omega^*}{(\pi/b_1)}\right] + \text{int}\left[\frac{\omega^*}{(\pi/b_2)}\right] + \text{int}\left[\frac{\omega^*}{(\pi/b_3)}\right] \tag{5.44}$$

in which int represents the image integer function i.e. the greatest integer $< \omega^* / (\pi / b_j)$, j=1,2,3.

5.2.2.2 Special case: uniform structures

When all storeys of a frame are identical, the whole frame can be considered as a single segment and this can be modelled with a substitute shear beam, which is free at one end and clamped at the other end. The end conditions for such abeam are

$$\mathbf{d}_1 = 0 \tag{5.45}$$

$$\mathbf{p}_2 = 0 \tag{5.46}$$

Eq. (5.46) can be written in the following form using Eqs. (5.28)

$$\begin{bmatrix} U'(\xi = 1) \\ V'(\xi = 1) \\ \Phi'(\xi = 1) \end{bmatrix} = \mathbf{0} \quad \text{or} \quad \mathbf{d}_2' = 0 \tag{5.47}$$

where $\mathbf{d}_2'$ is the derivative of the vector of displacement functions when $\xi = 1$.

If Eqs. (5.45) and (5.47) are substituted in Eqs. (5.30) it is clear that the condition for non-trivial solutions is

$$b_1 b_2 b_3 \omega^3 \begin{vmatrix} \mathbf{E} & \mathbf{0} & \mathbf{I} & \mathbf{0} \\ \mathbf{0} & \mathbf{E} & \mathbf{S} & \mathbf{C} \end{vmatrix} = 0 \tag{5.48}$$

However, it is easy to show that the left-hand determinant as well as b_1, b_2, b_3 and ω are not generally zero. Thus, noting that the right-hand determinant is that of a lower triangular matrix, Eq. (5.48) is only satisfied when the product of its significant leading diagonal terms is zero, i.e.

$$\prod_{j=1}^{3} C_{b_j\omega} = 0 \tag{5.49}$$

which is satisfied when $\omega_j^k = (k - \frac{1}{2})\frac{\pi}{b_j}$ $\quad j$=1,2,3 ; $\quad k$=1,2,3,... (5.50)

Hence the required natural frequencies can conveniently be determined using Eqs. (5.50)

5.2.3 Alternative Method Using the Analogous Uncoupled System

In Section 5.2.1 the simultaneous differential Eqs. (5.17) were used to demonstrate the spatial behaviour of a three-dimensional shear beam with asymmetric cross-section. The nature of the behaviour depends on the relative position of the shear centre and the centre of mass. The torsion angle φ appears in all three equations, showing that the resulting deformation is composed of both translation and torsion. In the latter section the set of coupled Eqs. (5.17) were solved and the result posed in the form of a dynamic stiffness matrix for such an element. There is, however, a simpler way of producing the coupled natural frequencies. It will be proven in the following section that the system of differential equations (5.17) can be solved exactly with a simple two-step procedure if the frame is modelled as a single uniform cantilever.

In this method x_c and y_c are first set equal to zero. This yields the uncoupled natural frequencies, which are then used to determine the coupled natural frequencies by way of a cubic coupling relationship.

5.2.3.1 Analogous uncoupled system

The natural frequencies of the analogous uncoupled system can easily be calculated using Eqs. (5.23) and (5.50) with the assumption of $x_c = y_c = 0$. From Eq. (5.23) it is clear that

$$b^2 = -\lambda_x^2 \quad , \quad b^2 = -\lambda_y^2 \quad \text{and} \quad b^2 = -\lambda_\varphi^2 \tag{5.51}$$

or

$$b_1 = \lambda_x \quad , \quad b_2 = \lambda_y \quad \text{and} \quad b_3 = \lambda_\varphi \tag{5.52}$$

and hence from Eqs. (5.50)

$$\omega_x = \left(k - \frac{1}{2}\right)\frac{\pi}{\lambda_x} \tag{5.53a}$$

$$\omega_y = \left(k - \frac{1}{2}\right)\frac{\pi}{\lambda_y} \tag{5.53b}$$

$$\omega_\varphi = \left(k - \frac{1}{2}\right)\frac{\pi}{\lambda_\varphi} \tag{5.53c}$$

5.2.3.2 Coupling effect

Multiplying the first row of Eq. (5.23) by $1/(b^2\lambda_x^2)$, the second row by $1/(b^2\lambda_y^2)$ and the third row by $1/(b^2\lambda_\varphi^2)$ gives

$$\begin{vmatrix} \frac{1}{\lambda_x^2}+\frac{1}{b^2} & 0 & -\frac{y_c}{b^2} \\ 0 & \frac{1}{\lambda_y^2}+\frac{1}{b^2} & \frac{x_c}{b^2} \\ -\frac{y_c}{b^2} & \frac{x_c}{b^2} & r_m^2(\frac{1}{\lambda_\varphi^2}+\frac{1}{b^2}) \end{vmatrix} = 0 \tag{5.54}$$

Also, it is clear from Eqs. (5.50) and (5.53) that

$$\frac{1}{\lambda_x^2} = \frac{\omega_x^2}{\pi^2\left(k-\frac{1}{2}\right)^2} \tag{5.55a}$$

$$\frac{1}{\lambda_y^2} = \frac{\omega_y^2}{\pi^2\left(k-\frac{1}{2}\right)^2} \tag{5.55b}$$

$$\frac{1}{\lambda_\kappa^2} = \frac{\omega_\varphi^2}{\pi^2\left(k-\frac{1}{2}\right)^2} \tag{5.55c}$$

and

$$\frac{1}{b^2} = -\frac{\omega^2}{\pi^2\left(k-\frac{1}{2}\right)^2} \tag{5.56}$$

Substituting Eqs. (5.55) and (5.56) in Eq. (5.54) gives

$$\begin{vmatrix} \omega^2-\omega_x^2 & 0 & -y_c\omega^2 \\ 0 & \omega^2-\omega_y^2 & x_c\omega^2 \\ -y_c\omega^2 & x_c\omega^2 & r_m^2(\omega^2-\omega_\varphi^2) \end{vmatrix} = 0 \tag{5.57}$$

Eq. (5.57) is precise for the shear cantilever considered and can be used as a simpler way of calculating the natural frequencies of asymmetric systems using the natural frequencies of the analogous uncoupled systems. This equation has already been used by several authors(Ng and Kuang 2000; Zalka 1994; Zalka and Macleod 1996).

5.3 SUBSTITUTE FRAME METHOD

5.3.1 Application of the Substitute Frame Method in the Static and Dynamic Analysis of Asymmetric Three-dimensional Frame Structures

It was explained in Section 2.3.1 that any two-dimensional frame, may be simplified to an equivalent one bay substitute frame which has the same natural frequencies of vibration as the original frame if the original frame satisfies Principle of Multiples. If it does not, the substitute frame method can still be applied and the accuracy of the results will normally be satisfactory for engineering problems.

Nodal displacements of three-dimensional, multi-bay, multi-storey skeletal sway frames have already been investigated by Howson and Rafezy (Howson and Rafezy 2002) using the substitute frame method. In this section their method will be extended to calculate the coupled natural frequencies of asymmetric three-dimensional, multi -bay, multi-storey sway frames. Each substitute frame has a single bay and the same number of storeys and storey heights as the original frame, but is symmetric and comprises only in plane stiffnesses.

It is assumed that the original structure is doubly asymmetric and that the centre of rigidity of different floor levels coincides with the z-axis passing through the shear centre S. Point C on a typical floor denotes the centre of mass and its location in the coordinate system Sxy is given by x_c and y_c (Figure 5.1). When the centres of shear and mass do not coincide, the transverse vibration of the structure will always be coupled, i.e. the motion will be a combination of translation and torsion.

The centre of pressure CP, the point at which the resultant horizontal load acts at each floor level, lies on a vertical line through the building. Its location in the coordinate system Sxy is given by e_x and e_y. The three centres of shear, mass and pressure don't need to be coincident, but they have to be in three vertical lines that are parallel to each other. It is also assumed that inextensional member theory is used.

Consider Figure 5.1 again. It shows the plan view of a multi-storey structure that is idealised as a set of plane frames running in the x and y directions. If we consider only a typical frame, frame *i*, running in the y direction, it is clear that we can determine the material and geometric properties of each individual member of the equivalent substitute plane frame using the procedure described in Section 2.3.1. The substitute frame stiffness $\mathbf{s}_{yi}$ can then be assembled in the usual way from the member stiffness relationship given in Figure 5.4(a) and (b), where the stiffness elements are defined for both buckling and vibration theory in references (Howson 1979; Howson et al. 1983).

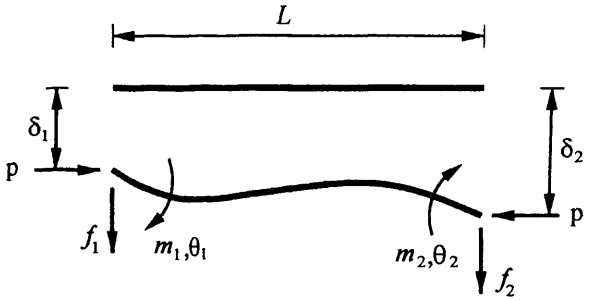

(a)

$$\begin{bmatrix} f_1 \\ m_1 \\ f_2 \\ m_2 \end{bmatrix} = \frac{EI}{L} \begin{bmatrix} \gamma/L^2 & \nu/L & -\varepsilon/L^2 & \delta/L \\ \nu/L & \alpha & -\delta/L & \beta \\ -\varepsilon/L^2 & -\delta/L & \gamma/L^2 & -\nu/L \\ \delta/L & \beta & -\nu/L & \alpha \end{bmatrix} \begin{bmatrix} \delta_1 \\ \theta_1 \\ \delta_2 \\ \theta_2 \end{bmatrix}$$

(b)

Figure 5.6 (a) Member end forces and displacements; (b) Member stiffness relationship.

Hence the stiffness relationship for the typical frame *i* is given by

$$\mathbf{p}_{yi} = \mathbf{s}_{yi}\mathbf{d}_{yi} \tag{5.58}$$

where $\mathbf{p}_{yi}$ is the vector of external forces and $\mathbf{d}_{yi}$ is the corresponding vector of nodal displacements. During vibration, the structure undergoes translation and torsion (Figure 5.2). Based on the assumption of a rigid diaphragm at each floor level, $\mathbf{d}_{yi}$ can be related to the vector of nodal displacement at the shear centre, $\mathbf{d}_{y0}$, through the following equation

$$\mathbf{d}_{yi} = \mathbf{d}_{y0} + x_i\boldsymbol{\theta} \tag{5.59}$$

in which $\boldsymbol{\theta}$ is the vector of torsional displacements and x_i is the distance of frame *i* from the shear centre S.

With an identical argument, the corresponding relationship for frames running in the x direction is

$$\mathbf{d}_{xi} = \mathbf{d}_{x0} - y_i\boldsymbol{\theta} \tag{5.60}$$

in which y_i is the distance of frame j from shear centre S.

Eqs. (5.59) and (5.60) show that the frames running in the x and y directions no longer share a unique displacement, so the substitute frame method cannot be applied in the way described for symmetric structures in Chapter 3. However, the study of asymmetric structures using the continuum method suggests that asymmetric structures can be treated in a two step process i.e. the analogous uncoupled system can be analysed first then the relation between the uncoupled and coupled response can be applied through Eq. (5.57).

5.3.1.1 The analogous uncoupled system

In the analogous uncoupled system it is assumed that the centre of mass and pressure are coincident with the centre of shear, therefore the structure would be in pure translation or torsion. In the following sections, the translational and torsional substitute frames for the vibration of the analogous uncoupled systems will be studied.

5.3.1.1.1. Substitute frame for translation

Considering the translational modes in the y direction first, and noting the fact that the displacement vector of all frames running in the y direction are the same, $\mathbf{d}_{y0}$, it is clear that we can add together the substitute frames arising from all such frames to obtain a further substitute frame whose stiffness is given by

$$\mathbf{S}_y = \sum_{i=1}^{n_y} \mathbf{s}_{yi} \tag{5.61}$$

where n_y is the number of plane frames running in the y direction i.e. the individual substitute frames have been notionally clamped together as described in Section 2.3.1. The corresponding force vector is given by

$$\mathbf{P}_y = \sum_{i=1}^{n_y} \mathbf{p}_{yi} \tag{5.62}$$

An identical argument enables us to write the equivalent expressions for the stiffness and force vector of the n_x frames running in the x direction as

$$\mathbf{S}_x = \sum_{j=1}^{n_x} \mathbf{s}_{xj} \tag{5.63}$$

and

$$\mathbf{P}_x = \sum_{j=1}^{n_x} \mathbf{p}_{xj} \tag{5.64}$$

The stiffness relationships in the x and y directions for the analogous uncoupled structure, respectively, can therefore be written as

$$\mathbf{P}_x = \mathbf{S}_x \mathbf{D}_x. \tag{5.65}$$

and

$$\mathbf{P}_y = \mathbf{S}_y \mathbf{D}_y \tag{5.66}$$

where $\mathbf{D}_x$ and $\mathbf{D}_y$ are the corresponding nodal displacement vectors. Noting that $\mathbf{P}_x = \mathbf{P}_y = \mathbf{0}$ when calculating natural frequencies, Eqs. (5.65) and (5.66) can be solved using the Wittrick-Williams algorithm (Wittrick and Williams 1971) which guarantees that no required eigenvalues can be missed. The modal vectors $\mathbf{D}_x$ and $\mathbf{D}_y$ then follow

directly in the usual way, A suitable computer program for such solution is freely available in the literature (Howson et al. 1983).

The out of plane contribution of plane frames running in the x direction to the translational vibration of the structure in the y direction should be taken into account, as in the case of three-dimensional symmetric structures. The same argument applies for the vibration of the structure in the x direction.

5.3.1.1.2. Substitute frame for torsion

The substitute frame for torsion of the analogous uncoupled structure can be obtained in a similar way to that for torsion for symmetric structures in Section 3.3.1.2. As pure torsion accurse about the shear centre S, it is enough to rewrite all equations with respect to the shear centre S.

Hence the corresponding force-displacement equation for torsional vibration of the structure can be obtained as

$$\mathbf{P}_y e_x - \mathbf{P}_x e_y = \left\{ \sum_{i=1}^{n_y} \mathbf{s}_{yi}\, x_i^2 + \sum_{j=1}^{n_x} \mathbf{s}_{xj}\, y_j^2 \right\} \boldsymbol{\theta} \qquad (5.67)$$

Once more $\mathbf{P}_x = \mathbf{P}_y = \mathbf{0}$ when calculating natural frequencies, hence equation (5.67) can be solved for the required eigenvalues in the same way as the previous section.

The modal displacements at specific points on the original frame follow from $\mathbf{D}_x$, $\mathbf{D}_y$ and $\boldsymbol{\theta}$ in a straightforward manner.

The out of plane effects should be taken into account in the same way as for the symmetric structures of Chapter 3.

5.3.1.2 Coupling effect

Once the natural frequencies of the analogous uncoupled system have been obtained, the final coupled natural frequencies of the asymmetric structure can be calculated using Eq. (5.57). As Eq. (5.57) has been obtained using continuum theory, its accuracy in the substitute frame method will be investigated by numerical examples in the following section.

5.4 NUMERICAL RESULTS

The vibrational behaviour of asymmetric three-dimentional frame structures are now investigated using the proposed methods. Examples 5.1 compare the results obtained from the continuum method with the results obtained from a finite element analysis of the whole structure using the vibration programme ETABS (Wilson et al. 1995) for a series of asymmetric concrete multi storey frame structures. Example 5.2 does the same thing for substitute frame method.

5.4.1 Example 5.1

The work of this section consolidates the foregoing theory by performing a small parametric study on four frames of varying slenderness and comparing the lower natural frequencies with those obtained from a full finite element analysis of the original structures. The frames, which have 5, 10, 20 and 30 storeys, respectively, all have the same doubly asymmetric floor plan and equal storey height of 3 m. Each structure consists of 5 plane frames in the y direction (F1-F5) and 4 plane frames in the x direction (F6-F9) which are connected to each other by typical rigid diaphragms at each floor level with the arrangement shown in Figure 5.7. In the 5 and 10 storey buildings, the properties of the structural elements do not change along the height of the structure, so each structure can be modelled using a single substitute beam element. In the 20 and 30 storey buildings, the properties of the structural elements change in a step-wise fashion every 10

storeys. Tables 5.1a to 5.1c shows the second moment of area of the columns and beams about the x and y directions for the 1^{st}-10^{th}, 11^{th}-20^{th} and 21^{st}-30^{th} floors of the buildings, respectively.

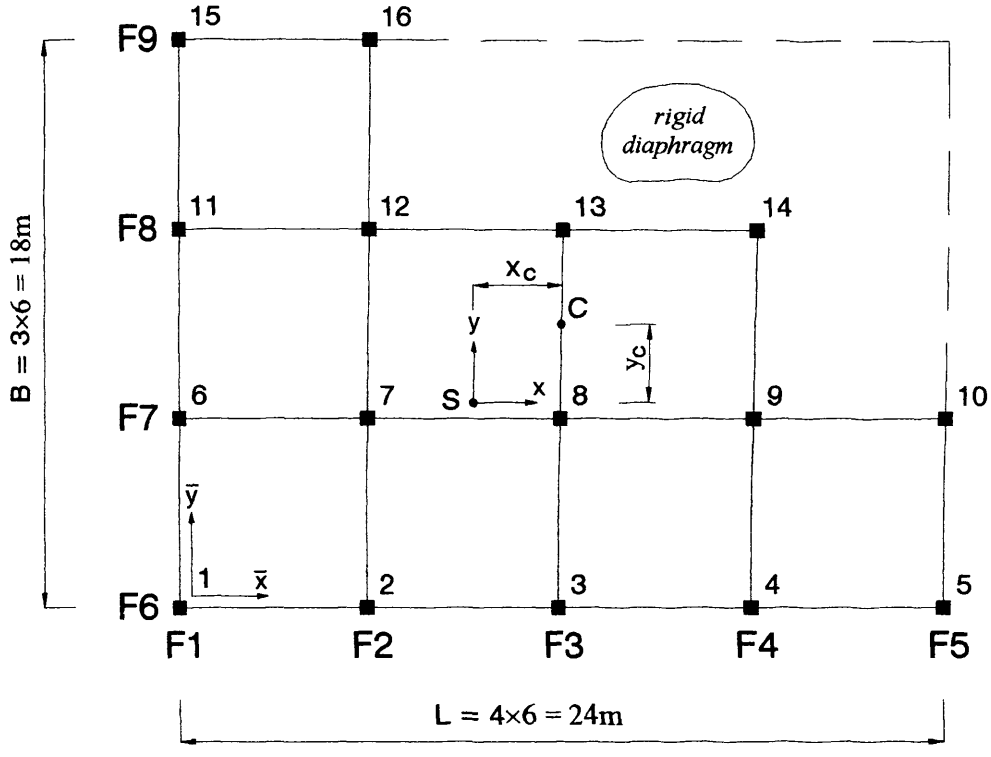

Figure 5.7 Floor plan of structures considerd in Examples 5.1 and 5.2

Table 5.1a – The properties of the columns and beams of the buildings from 1^{st} to 10^{th} floors

1^{st} to 10^{th}	Columns (members are defined in Figure 5.7)				Beams
	1,5,10,14,15,16	2,3,4,13	6,11	7,8,9,12	all
$I_y(m^4)$	0.0035	0.007	0.0035	0.007	0.003
$I_x(m^4)$	0.0035	0.0035	0.007	0.007	0.003

Table 5.1b – The properties of the columns and beams of the buildings from 11^{th} to 20^{th} floors

11^{th} to 20^{th}	Columns (members are defined in Figure 5.7)				Beams
	1,5,10,14,15,16	2,3,4,13	6,11	7,8,9,12	all
$I_y(m^4)$	0.0025	0.005	0.0025	0.0025	0.002143
$I_x(m^4)$	0.0025	0.0025	0.005	0.0025	0.002143

Table 5.1c – The properties of the columns and beams of the buildings from 21st to 30th floors

21st to 30th	Columns (members are defined in Figure 5.7)				Beams
	1,5,10,14,15,16	2,3,4,13	6,11	7,8,9,12	all
$I_y(m^4)$	0.0015	0.003	0.0015	0.003	0.001286
$I_x(m^4)$	0.0015	0.0015	0.003	0.003	0.001286

For simplicity in determining member masses, half the mass of the columns framing into and emanating from a floor diaphragm, together with the mass of the diaphragm and any associated beams, is stated as an equivalent uniformly distributed floor mass at that storey level. Thus the centre of mass is at the geometric centre of the floor plan. This corresponds precisely to the automatic idealisation process in ETABS (Wilson et al. 1995) and additionally only requires the total mass of the floor to be converted into the equivalent uniformly distributed mass of the member in the substitute beam approach. Arbitrarily the mass is assumed to have a constant value of 360 Kg/m^2 at each floor level, even where the stiffness properties of the member change. Young's modulus for all members is taken to be $E = 2\times10^{10}$ N/m^2 and inextensible member theory is assumed.

All the plane frames in this example are proprtional, so that the shear centre at each floor level lies in a vertical line through the building. The eccentricities in the x and y directions can then be calculated using Eq. (4.33) as follows

$$x_c = 2.727\text{m} \ , \ y_c = 2.5\text{m}$$

The effective distributed mass of the shear beam (smeared from the diaphragm) and the polar mass radius of gyration of the diaphragms about the shear centre can be calculated as follows

$$m = 18\times24\times360/3 = 51840 \text{ kg/m}$$

$$r_m^2 = \frac{18^2+24^2}{12} + 2.727^2 + 2.5^2 = 88.686 \text{ m}^2$$

Tables 5.2a, 5.2b and 5.2c show the effective shear rigidities of the plane frames in the x and y directions obtained using the formula presented by Smith and Coull (Smith and

Coull 1991) and the torsional rigidity of the buildings about the shear centre S, which was calculated using Eq. (5.16)

Table 5.2a – Translational and torsional rigidity of the buildings1st to 10th floors

Plane Frames	x_i	y_j	GA_{xj} - 10^6 N	GA_{yi} - 10^6 N	GJ -10^6 N
F1	-9.273	-	-	98.824	8497.69
F2	-3.273	-	-	98.824	1058.65
F3	2.727	-	-	65.882	489.936
F4	8.727	-	-	65.882	5017.64
F5	14.727	-	-	32.941	7144.43
F6	-	-6.50	131.764	-	5567.06
F7	-	-0.50	131.764	-	32.941
F8	-	5.50	98.824	-	2989.41
F9	-	11.50	32.941	-	4356.47
Σ			GA_x=395.294	GA_y=362.353	GJ=35154.231

Table 5.2b – Translational and torsional rigidity of the buildings11th to 20th floors

Plane Frames	x_i	y_j	GA_{xj} - 10^6 N	GA_{yi} - 10^6 N	GJ -10^6 N
F1	-9.273	-	-	70.589	6069.78
F2	-3.273	-	-	70.589	756.179
F3	2.727	-	-	45.059	349.954
F4	8.727	-	-	45.059	3584.03
F5	14.727	-	-	23.529	5103.17
F6	-	-6.50	94.177	-	3976.47
F7	-	-0.50	94.117	-	23.529
F8	-	5.50	70.589	-	2135.29
F9	-	11.50	23.529	-	3111.77
Σ			GA_x=282.353	GA_y=258.824	GJ=25110.165

Table 5.2c – Translational and torsional rigidity of the buildings21stto 30th floors

Plane Frames	x_i	y_j	GA_{xj} - 10^6N	GA_{yi} - 10^6N	GJ -10^6N
F1	-9.273	-	-	42.353	3641.87
F2	-3.273	-	-	42.353	453.707
F3	2.727	-	-	28.235	209.973
F4	8.727	-	-	28.235	2150.42
F5	14.727	-	-	14.118	3061.9
F6	-	-6.50	56.47	-	2385.88
F7	-	-0.50	56.47	-	14.117
F8	-	5.50	42.353	-	1281.18
F9	-	11.50	14.118	-	1867.06
Σ			GA_x=169.412	GA_y=155.294	GJ=15066.099

5.4.1.1 Results

Column 2 of Tables 5.3a to 5.3d show the coupled natural frequencies (Hz) of the 5, 10, 20 and 30 storey frames obtained from the three-dimensional shear beam theory respectively. The third column in each table shows the results of a full finite element analysis of the frames (3D model of the original frame), obtained using the vibration programme ETABS (Wilson et al. 1995). Finally, column 4 shows the difference between the results of the substitute beam method with those of ETABS. The following assumptions have been made in modelling buildings with ETABS.

- The floor diaphragm at each storey level is assumed to be rigid and its mass is uniformly distributed.
- The mass of the beams, columns and shearwalls is distributed into the floor diaphragm.
- No allowance has been made for the shear deformation and rotary inertia of beams and columns

- No $P-\Delta$ effect
- No reduction in the stiffness of columns due to compressive axial loads (no geometric rigidity)
- Inextensible member theory is imposed by multiplying the cross-sectional area of the beams and columns by a factor, typically 10^3.

Table 5.3a- Coupled natural frequencies of the 5-storey frame obtained from the continuum and FEM models

Frequency No.	3D Shear beam	ETABS (FEM)	Difference%
	frequency (Hz)	frequency (Hz)	
1	1.22	1.27	3.94
2	1.43	1.49	4.03
3	1.85	1.93	4.15
4	3.65	4.18	12.68
5	4.28	4.9	12.65
6	5.55	6.35	12.60
Average			8.34

Table 5.3b- Coupled natural frequencies of the 10-storey frame obtained from the continuum and FEM models

Frequency No.	3D Shear beam	ETABS (FEM)	Difference%
	frequency (Hz)	frequency (Hz)	
1	0.61	0.62	1.61
2	0.71	0.73	2.74
3	0.92	0.94	2.13
4	1.83	1.92	4.69
5	2.14	2.26	5.31
6	2.77	2.92	5.14
7	3.04	3.4	10.59
8	3.56	3.99	10.78
9	4.26	5.13	16.96
Average			6.66

Table 5.3c- Coupled natural frequencies of the 20-storey frame obtained from the continuum and FEM models

Frequency No.	3D Shear beam frequency (Hz)	ETABS (FEM) frequency (Hz)	Difference%
1	0.29	0.3	3.33
2	0.34	0.35	2.86
3	0.45	0.45	0.00
4	0.82	0.84	2.38
5	0.96	0.98	2.04
6	1.25	1.27	1.57
7	1.41	1.46	3.42
8	1.65	1.71	3.51
9	1.94	2.07	6.28
Average			2.82

Table 5.3d- Coupled natural frequencies of the 30-storey frame obtained from the continuum and FEM models

Frequency No.	3D Shear beam frequency (Hz)	ETABS (FEM) frequency (Hz)	Difference%
1	0.18	0.18	0.00
2	0.22	0.22	0.00
3	0.28	0.28	0.00
4	0.49	0.49	0.00
5	0.57	0.58	1.72
6	0.74	0.75	1.33
7	0.81	0.83	2.41
8	0.95	0.97	2.06
9	1.15	1.19	3.36
10	1.24	1.26	1.59
11	1.35	1.39	2.88
12	1.47	1.55	5.16
Average			1.71

The three-dimensional shear beam model shows very good agreement for all frames and the average difference (last row in the tables) never exceeds 10%. The model is less accurate for small numbers of storeys, since the model cannot consider the full height bending stiffness of individual columns (Figure 2.3(b)). The difference is perfectly acceptable (less than 4%) for the first three natural frequencies that play the most dominant role in the vibrational behaviour of structures. The results also show that the method presented has easily been able to model step changes in member properties along the height of the structure to equal accuracy i.e. the 20 and 30 storey frames (Figure 5.8).

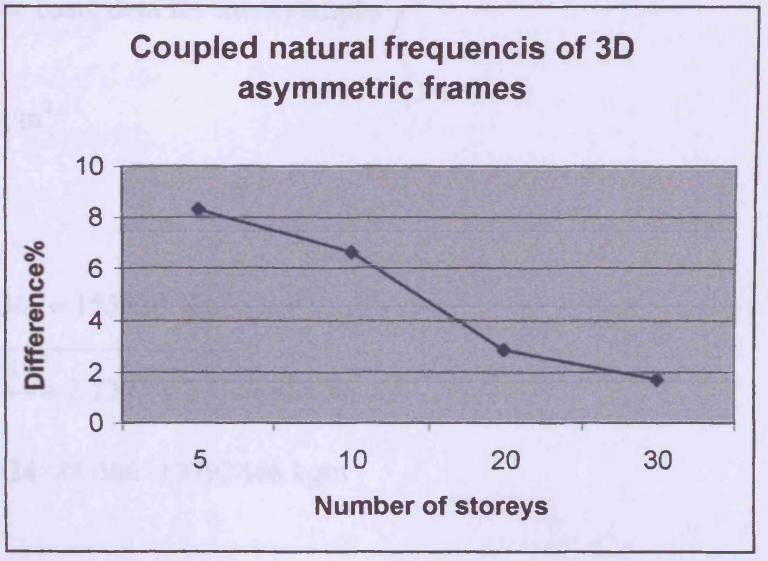

Figure 5.8 Average percentage difference between the continuum and FE models

A small parametric study has been undertaken to assess the effect of inextensible member theory when determining the natural frequencies of a series of three-dimensional, asymmetric, multi-storey buildings with the plan configuration of Figure 5.7. It shows that the difference between the results of extensible and inextensible member theory increases with increasing number of storeys. It also shows that the difference is less than 5% for buildings up to 20 storeys and less than 7.5% for buildings up to 40 storeys. Thus the model developed may be used for buildings up to 20 or 40 stories depending upon the required accuracy and for taller structures more investigations are necessary.

5.4.2 Example 5.2

To investigate the accuracy of the substitute frame method, the frames of Example 5.1 are analysed again, but this time using the substitute frame method. First, the substitute frames of the analogous uncoupled system in the x, y and torsional directions are modelled to yield the uncoupled natural frequencies. The effect of coupling is then imposed through Eq. (5.57).

Summary of the basic data for this example:

$E = 2\times10^{10}$ Kg/m^2

$x_c = 2.727m$

$y_c = 2.5m$

$m = 18\times24\times360 = 155520$ Kg

$$r_m^2 = \sqrt{\frac{18^2+24^2}{12}+2.727^2+2.5^2} = 88.686 \text{ m}^2$$

$I_{gf} = 360\times18\times24\times88.686 = 13792446$ kgm^2

5.4.2.1 Uncoupled system

5.4.2.1.1. Characteristics of the substitute frames that run in the x direction

The characteristics of the substitute frame can be calculated using Eqs. (5.63) and (5.65) as follows

a) 1st -10th floors

$I_{beam1}=12\times0.003=0.036m^4$

$I_{column1}=0.5\times(0.0035\times8+0.007\times8)=0.042m^4$

$m_{beam}=18\times24\times360/6=155520$ Kg

$m_{column}=0$

b) 11th-20th floors

$I_{beam2}=12\times0.002143=0.02571m^4$

$I_{column2}=0.5\times(0.0025\times8+0.005\times8)=0.03m^4$

$m_{beam}=18\times24\times360/6=155520$ Kg

$m_{column}=0$

c) 21st-30th floors

$I_{beam3}=12\times0.001286=0.01543m^4$

$I_{column3}=0.5\times(0.0015\times8+0.003\times8)=0.018m^4$

$m_{beam}=18\times24\times360/6=155520$ Kg

$m_{column}=0$

5.4.2.1.2. Characteristics of the substitute frames that run in the y direction

a) 1st -10th floors

$I_{beam1}=11\times0.003=0.033m^4$

$I_{column1}=0.5\times(0.0035\times10+0.007\times6)=0.0385m^4$

$m_{beam}=18\times24\times360/6=155520$ Kg

$m_{column}=0$

b) 11th-20th floors

$I_{beam2}=11\times0.002143=0.02357m^4$

$I_{column2}=0.5\times(0.0025\times10+0.005\times6)=0.0275m^4$

$m_{beam}=18\times24\times360/6=155520$ Kg

$m_{column}=0$

c) 21st-30th floors

$I_{beam3}=11\times0.001286=0.01414m^4$

$I_{column3}=0.5\times(0.0015\times10+0.003\times6)=0.0165m^4$

$m_{beam}=18\times24\times360=155520$ Kg

$m_{column}=0$

5.4.2.1.3. Characteristics of the substitute frames for torsion

The characteristics of the substitute frame for torsion can be calculated using Eq. (5.67) as follows

a) 1st -10th floors

$I_{beam1}=(4\times0.003\times6.5^2)+(4\times0.003\times0.5^2)+(3\times0.003\times5.5^2)+(1\times0.003\times11.5^2)+(3\times0.003\times9.273^2)+(3\times0.003\times3.273^2)+(2\times0.003\times2.727^2)+(2\times0.003\times8.727^2)+(1\times0.003\times14.727^2)=3.2015\ m^4$

$I_{column1}=0.5[(2\times0.0035+3\times0.007)\times6.5^2+(2\times0.0035+3\times0.007)\times0.5^2+(2\times0.003+2\times0.007)\times5.5^2+2\times0.0035\times11.5^2+(2\times0.0035+2\times0.007)\times9.273^2+(2\times0.0035+2\times0.007)\times3.273^2+2\times0.0035+0.007)\times2.727^2+(2\times0.0035+0.007)\times8.727^2+2\times0.0035\times14.727^2]=3.7351\ m^4$

$m_{beam}=360\times(18\times24^3/12+24\times18^3/12+24\times18\times(2.727^2+2.5^2))=13792529$ Kg

$m_{column}=0$

b) 11th-20th floors

$I_{beam2}=(4\times0.002143\times6.5^2)+(4\times0.002143\times0.5^2)+(3\times0.002143\times5.5^2)+(1\times0.002143\times11.5^2)+(3\times0.002143\times9.273^2)+(3\times0.002143\times3.273^2)+(2\times0.002143\times2.727^2)+(2\times0.002143\times8.727^2)+(1\times0.002143\times14.727^2)=2.2868\ m^4$

$I_{column2}=0.5[(2\times0.0025+3\times0.005)\times6.5^2+(2\times0.0025+3\times0.005)\times0.5^2+(2\times0.003+2\times0.005)\times5.5^2+2\times0.0025\times11.5^2+(2\times0.0025+2\times0.005)\times9.273^2+(2\times0.0025+2\times0.005)\times3.273^2+2\times0.0025+0.005)\times2.727^2+(2\times0.0025+0.005)\times8.727^2+2\times0.0025\times14.727^2]=2.6679\ m^4$

$m_{beam}=360\times(18\times24^3/12+24\times18^3/12+24\times18\times(2.727^2+2.5^2))=13792529$ Kg

$m_{column}=0$

c) 21st-30th floors

$I_{beam3}=(4\times0.001286\times6.5^2)+(4\times0.001286\times0.5^2)+(3\times0.001286\times5.5^2)+$
$(1\times0.001286\times11.5^2)+(3\times0.001286\times9.273^2)+(3\times0.001286\times3.273^2)+$
$(2\times0.001286\times2.727^2)+(2\times0.001286\times8.727^2)+(1\times0.001286\times14.727^2)=$
$1.3721\ m^4$

$I_{column3}=0.5[(2\times0.0015+3\times0.003)\times6.5^2+(2\times0.0015+3\times0.003)\times0.5^2+$
$(2\times0.003+2\times0.003)\times5.5^2+2\times0.0015\times11.5^2+(2\times0.0015+2\times0.003)\times9.273^2+$
$(2\times0.0015+2\times0.003)\times3.273^2+2\times0.0015+0.003)\times2.727^2+(2\times0.0015+0.003)\times$
$8.727^2+2\times0.0015\times14.727^2]=1.6008\ m^4$

$m_{beam}=360\times(18\times24^3/12+24\times18^3/12+24\times18\times(2.727^2+2.5^2))=13792529$ Kg

$m_{column}=0$

These values can then be used with other data in a general plane frame program, which in addition may be able to account for the destabilising effect of member axial force, shear deflection etc., to obtain the uncoupled natural frequencies of the frame. These are shown in columns 2-4 of Tables 5.4a-d below. The results can then be converted easily to the equivalent coupled natural frequencies of the frame using Eq. (5.57). These are shown in columns 5-7. Note that all results assume inextensible member theory that can be simulated in a general program by multiplying the cross-sectional area of the original member by 10^3.

Table 5.4a – The uncoupled and coupled natural frequencies of the 5 storey frame

Mode *k*	Uncoupled natural frequencies using one-bay multi-storey substitute frames (Hz)			Coupled natural frequencies using Eq. (5.57) (Hz)		
	x dir.	y dir.	torsion			
1	1.5211	1.4564	1.5232	1.2721	1.4923	1.9330
2	4.9938	4.7812	5.0006	4.1762	4.8992	6.3459
3	9.5596	9.1526	9.5727	7.9945	9.3784	12.1480

Table 5.4b – The uncoupled and coupled natural frequencies of the 10 storey frame

Mode k	Uncoupled natural frequencies using one-bay multi-storey substitute frames (Hz)			Coupled natural frequencies using Eq. (5.57) (Hz)		
	x dir.	y dir.	torsion			
1	0.7426	0.7109	0.7435	0.6209	0.7285	0.9436
2	2.3017	2.2037	2.3047	1.9248	2.258	2.9249
3	4.0679	3.8947	4.0734	3.4019	3.9908	5.1694
4	6.137	5.8757	6.1453	5.1322	6.0206	7.7986

Table 5.4c – The uncoupled and coupled natural frequencies of the 20 storey frame

Mode k	Uncoupled natural frequencies using one-bay multi-storey substitute frames (Hz)			Coupled natural frequencies using Eq. (5.57) (Hz)		
	x dir.	y dir.	torsion			
1	0.3538	0.3387	0.3541	0.2958	0.3471	0.4495
2	1.002	0.9593	1.0032	0.8379	0.9831	1.2732
3	1.7419	1.6678	1.7442	1.4567	1.709	2.2135
4	2.4761	2.3707	2.4794	2.0707	2.4292	3.1465

Table 5.4d – The uncoupled and coupled natural frequencies of the 30 storey frame

Mode k	Uncoupled natural frequencies using one-bay multi-storey substitute frames (Hz)			Coupled natural frequencies using Eq. (5.57) (Hz)		
	x dir.	y dir.	torsion			
1	0.2205	0.2112	0.2207	0.1844	0.2164	0.2802
2	0.5893	0.5642	0.59	0.4929	0.5782	0.7488
3	0.9917	0.9494	0.993	0.8293	0.9729	1.2602
4	1.4208	1.3603	1.4227	1.1882	1.3939	1.8055
5	1.8525	1.7736	1.855	1.5492	1.8174	2.3541

The results from the continuum and substitute frame methods are compared with finite element results in Tables 5.5a to 5.5d.

Table 5.5a- Coupled natural frequencies of the 5-storey frame obtained from the continuum, substitute and FEM methods

Frequency No.	3D Shear beam	Substitute Frame method	ETABS (FEM)
	frequency (Hz)	frequency (Hz)	frequency (Hz)
1	1.22	1.27	1.27
2	1.43	1.49	1.49
3	1.85	1.93	1.93
4	3.65	4.18	4.18
5	4.28	4.9	4.9
6	5.55	6.35	6.35

Table 5.5b- Coupled natural frequencies of the 10-storey frame obtained from the continuum, substitute and FEM methods

Frequency No.	3D Shear beam	Substitute Frame method	ETABS (FEM)
	frequency (Hz)	frequency (Hz)	frequency (Hz)
1	0.61	0.62	0.62
2	0.71	0.73	0.73
3	0.92	0.94	0.94
4	1.83	1.92	1.92
5	2.14	2.26	2.26
6	2.77	2.92	2.92
7	3.04	3.4	3.4
8	3.56	3.99	3.99
9	4.26	5.13	5.13

Table 5.5c- Coupled natural frequencies of the 20-storey frame obtained from the continuum, substitute and FEM methods

Frequency No.	3D Shear beam	Substitute Frame method	ETABS (FEM)
	frequency (Hz)	frequency (Hz)	frequency (Hz)
1	0.29	0.30	0.30
2	0.34	0.35	0.35
3	0.45	0.45	0.45
4	0.82	0.84	0.84
5	0.96	0.98	0.98
6	1.25	1.27	1.27
7	1.41	1.46	1.46
8	1.65	1.71	1.71
9	1.94	2.07	2.07

Table 5.5d- Coupled natural frequencies of the 30-storey frame obtained from the continuum, substitute and FEM methods

Frequency No.	3D Shear beam	Substitute Frame method	ETABS (FEM)
	frequency (Hz)	frequency (Hz)	frequency (Hz)
1	0.18	0.18	0.18
2	0.22	0.22	0.22
3	0.28	0.28	0.28
4	0.49	0.49	0.49
5	0.57	0.58	0.58
6	0.74	0.75	0.75
7	0.81	0.83	0.83
8	0.95	0.97	0.97
9	1.15	1.19	1.19
10	1.24	1.26	1.26
11	1.35	1.39	1.39
12	1.47	1.55	1.55

The results show that the substitute frame method gives precise results with no difference in comparison with the FEM method. It can be justified as follows. The plane frames obey the principle of multiples so there was no loss of accuracy in reducing multi-bay plane frames to a single-bay substitute frames. There is also no loss of accuracy in applying the coupling of modes, as Eq. (5.57) is precise for a uniform shear cantilever.

5.5 CONCLUSIONS

The following conclusions can be drawn from the parametric study presented in examples 5.1 and 5.2.

- The continuum method gives acceptable results for any number of storeys (difference<8%). The difference was less than 4% for the first three natural frequencies.

- Eq. (5.57) can take into account the coupling of modes and is precise for the shear cantilever presented. The results show that the effect of coupling between the natural frequencies of asymmetric buildings should be taken into account and ignoring it can lead to substantial inaccuracy

- The Substitute frame method gives very accurate results in proportional asymmetric 3D frames

Appendix 5A – The nature of the roots of the characteristic Eq. (5.21)

The nature of the roots of the characteristic Eq. (5.23) is investigated in this appendix. For this purpose, Eq. (5.23) is re-written again for convenience.

$$\begin{vmatrix} s^2+\omega^2\lambda_x^2 & 0 & -y_c\omega^2\lambda_x^2 \\ 0 & s^2+\omega^2\lambda_y^2 & x_c\omega^2\lambda_y^2 \\ -(1/r_m^2)y_c\omega^2\lambda_\varphi^2 & (1/r_m^2)x_c\omega^2\lambda_\varphi^2 & s^2+\omega^2\lambda_\varphi^2 \end{vmatrix} = 0 \qquad (5A.1)$$

Since λ_x^2, λ_y^2, λ_φ^2, x_c and y_c are all real constants, the coefficients in Eq. (5A.1) are all real. It will be convenient to note that the left-hand side of the Eq. (5A.1) is a 3rd order polynomial function $f(\varepsilon)$ in which $\varepsilon = \left(\frac{s}{\omega}\right)^2$. Therefore

$$f(\varepsilon) = \begin{vmatrix} \varepsilon+\lambda_x^2 & 0 & -y_c\lambda_x^2 \\ 0 & \varepsilon+\lambda_y^2 & x_c\lambda_y^2 \\ -y_c\lambda_\varphi^2 & x_c\lambda_\varphi^2 & r_m^2(\varepsilon+\lambda_\varphi^2) \end{vmatrix} \qquad (5A.2)$$

The quantity $f(\varepsilon)$ is a smooth continuous function, that becomes infinite and positive as ε tends to $+\infty$ and becomes infinite and negative as ε tends to $-\infty$. It is shown below that the quantity $f(\varepsilon)$ has a positive value as ε tends zero.

Substituting zero for ε in Eq. (5A.2) gives

$$f(0) = (r_m^2 - x_c^2 - y_c^2)\lambda_x^2\lambda_y^2\lambda_\varphi^2 \qquad (5A.3)$$

in which r_m is the polar mass radius of gyration about the shear centre and can be related to the polar mass radius of gyration about the centre of mass, r_{mc}, through the following equation

$$r_m^2 = r_{mc}^2 + x_c^2 + y_c^2 \qquad (5A.4)$$

therefore

$$(r_m^2 - x_c^2 - y_c^2) > 0 \qquad \text{(5A.5)}$$

The right side of Eq. (5A.3) is the product of four positive parameters and therefore $f(0)$ is always positive.

Before discussing the roots of $f(\varepsilon) = 0$ it is useful to calculate the quantity $f(\varepsilon)$ when $\varepsilon = -\lambda_x^2$ and $\varepsilon = -\lambda_y^2$ as follows

Replacing ε with $-\lambda_x^2$ and $-\lambda_y^2$ in Eq. (5A.2) gives, respectively,

$$f(-\lambda_x^2) = -y_c^2 \lambda_x^2 \lambda_\varphi^2 (\lambda_y^2 - \lambda_x^2) \qquad \text{(5A.6)}$$

and

$$f(-\lambda_y^2) = -x_c^2 \lambda_y^2 \lambda_\varphi^2 (\lambda_x^2 - \lambda_y^2) \qquad \text{(5A.7)}$$

It will be shown that $f(\varepsilon)$ has a constant sign at the four key points, which are $\varepsilon = 0$, $\varepsilon = -\lambda_x^2$, $\varepsilon = -\lambda_y^2$ and $\varepsilon = -\infty$.

Three main cases are distinguished and studied separately as follows

Case 1: $-\lambda_x^2 < -\lambda_y^2$

Eqs. (5A.6) and (5A.7) give,

$$f(0) > 0 \qquad \text{(5A.8a)}$$

$$f(-\lambda_y^2) < 0 \qquad \text{(5A.8b)}$$

$$f(-\lambda_x^2) > 0 \qquad \text{(5A.8c)}$$

$$f(-\infty) < 0 \qquad \text{(5A.8d)}$$

This implies that there are three negative real roots of the function $f(\varepsilon)$ in the intervals $(0,-\lambda_y^2)$, $(-\lambda_y^2,-\lambda_x^2)$ and $(-\lambda_x^2,-\infty)$. (Figure 5A.1(a))

Case 2: $-\lambda_y^2 < -\lambda_x^2$

Eqs. (5A.6) and (5A.7) give,

$$f(0) > 0 \qquad \text{(5A.9a)}$$

$$f(-\lambda_x^2) < 0 \qquad \text{(5A.9b)}$$

$$f(-\lambda_y^2) > 0 \qquad \text{(5A.9c)}$$

$$f(-\infty) < 0 \qquad \text{(5A.9d)}$$

This implies that there are three negative real roots of the function $f(\varepsilon)$ in the intervals $(0,-\lambda_x^2)$, $(-\lambda_x^2,-\lambda_y^2)$ and $(-\lambda_y^2,-\infty)$. (Figure 5A.1(b))

Case 3: $-\lambda_y^2 = -\lambda_x^2 = -\lambda^2$

By inspection it can be seen that if $\lambda_y = \lambda_x = \lambda^2$, Eq. (5A.2) becomes

$$f(\varepsilon) = (\varepsilon + \lambda^2)[r_m^2(\varepsilon + \lambda^2)(\varepsilon + \lambda_\varphi^2) - \lambda^2\lambda_\varphi^2(x_c^2 + y_c^2)] \qquad \text{(5A.10)}$$

and the roots may be calculated from

$$(\varepsilon + \lambda^2)[\varepsilon^2 + \beta\varepsilon + \gamma] = 0 \qquad \text{(5A.11)}$$

where

$$\beta = \lambda^2 + \lambda_\varphi^2 \text{ and } \gamma = \lambda^2\lambda_\varphi^2(r_m^2 - x_c^2 - y_c^2)/r_m^2 \qquad \text{(5A.12)}$$

The required roots ε_j (j=1,2,3) are therefore

$$\varepsilon_1 = -\lambda^2,\ 2\varepsilon_2 = -\beta - \Delta \text{ and } 2\varepsilon_3 = -\beta + \Delta \tag{5A.13}$$

$$\text{where } \Delta^2 = \beta^2 - 4\gamma = (\lambda^2 - \lambda_\varphi^2)^2 + 4\lambda^2\lambda_\varphi^2(x_c^2 + y_c^2)/r_m^2 \tag{5A.14}$$

ε_1 is clearly a negative root, as are ε_2 and ε_3, since

$$\Delta > 0,\ \gamma > 0 \text{ and } -\beta < 0 \tag{5A.15}$$

Cases 1, 2 and 3 include all possibilities, so $f(\varepsilon)$ always has three negative real roots i.e.

$$(s/\omega)^2 = -b_j^2 \qquad (j=1,2,3)$$

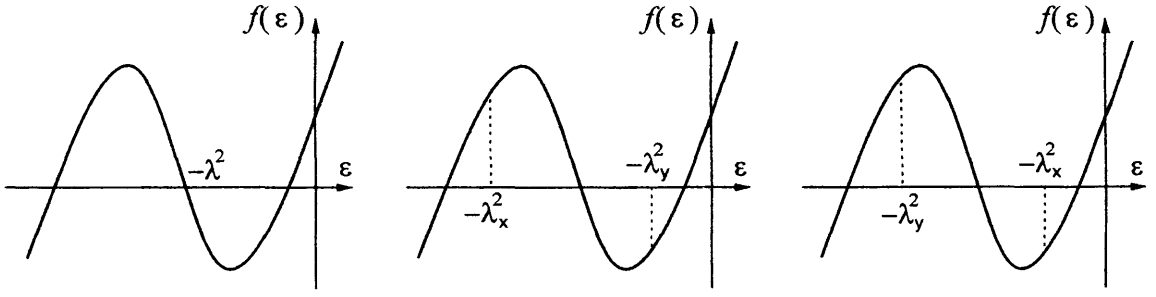

(a) (b) (c)

Figure 5A.1 The diagram of $f(\varepsilon)$ in terms of ε

(a) Case 1: $-\lambda_x^2 < -\lambda_y^2$

(b) Case 2: $-\lambda_y^2 < -\lambda_x^2$

(c) Case 3: $-\lambda_y^2 = -\lambda_x^2$

CHAPTER 6

VIBRATION ANALYSIS OF ASYMMETRIC THREE-DIMENSIONAL WALL-FRAME STRUCTURES

6.1 INTRODUCTION

Three dimensional vibration of symmetric wall-frame structures were studied in Chapter three and it was shown that the translational and torsional vibration of such structures can be treated independently. However, in most wall-frame structures the serviceability requirements lead to an asymmetric arrangement of walls and frames. In such structural configurations, the translational and torsional vibration of the structure can no longer be studied separately since the set of governing equations of motion are coupled.

This chapter presents two methods of analysis for determining the natural frequencies of asymmetric, three-dimensional wall-frame structures. Such structures comprise asymmetric arrangements of planar frames and walls, which have been joined to each other by rigid diaphragms at each floor level. Each method is able to analyse asymmetric, three-dimensional wall-frame structures whose properties may vary through the height of the structure in a stepwise fashion at one or more storey levels.

The first method utilises a continuum approach so that an asymmetric, three-dimensional wall-frame structure is divided into segments, by cutting through the structure horizontally at those storey levels corresponding to changes in storey properties. A typical segment is then considered in isolation. Initially, a primary frame and wall in one direction is replaced by its shear and flexural substitute beam, respectively, that have uniformly distributed mass and rigidity, thus utilising the continuum approach. In turn, each frame and wall in the same direction is replaced by their own substitute beams and the effect of all these beams is summed to model the effect of the original frames and walls. This leads directly to the differential equation governing the motion of the segment in the chosen direction. The same procedure is then adopted for those frames and walls running in the orthogonal direction. Once both equations are available it requires little effort to write down the substitute expressions for the torsional motion.

The second method utilises the Principle of Multiples and extends its application to three-dimensional asymmetric wall-frame structures. It will be shown that the substitute frame or wall-frame method can be used for the vibration analysis of asymmetric structures in a two-step procedure. First, the analogous uncoupled system will be analysed using the substitute frame or wall-frame method, then the relationship between the uncoupled and coupled frequencies will be determined via a cubic equation.

In order to validate the accuracy of the proposed methods, it was deemed necessary to carry out a parametric study.

6.2 CONTINUUM METHOD

6.2.1 Coupled Vibration Analysis

Consider the hypothetical layout of a typical floor plan of the asymmetric, three-dimensional wall-frame structure shown in Figure 6.1. The plane frames run in two orthogonal directions are proportional to each other in any one direction, as are the walls, but the proportionality is not necessarily the same in both directions. The shear centre, S, and flexural rigidity centre, O, at each floor level thus lie on a vertical line through the height of the structure.

It is assumed that the origin of the co-ordinate system is located at the flexural centre, with the x and y co-ordinates running parallel to the plane frames and walls. The z-axis runs vertically from the base of the building. Points $S(x_s, y_s)$ and $C(x_c, y_c)$ denote the shear rigidity centre and the centre of mass at a typical floor level, respectively. It is assumed that the floor system is rigid in its plane and that the centre of mass at each level lies on a vertical line, the mass axis, that runs through the height of the structure. When the rigidity and mass axes of a structure do not coincide, the lateral and torsional motion of the building will always be coupled in one or more planes. Since the aim is to find the natural frequencies of the structure, the externally applied forces $\mathbf{P}_x$ and $\mathbf{P}_y$ are zero.

The structure comprises n_{wy} walls and n_y frames running in the y direction and n_{wx} walls and n_x frames running in the x direction. The second moment of area and uniformly distributed mass of a typical wall i in the y direction are I_{wyi} and m_{wyi} respectively, while those of wall j running in the x direction are I_{wxj} and m_{wxj}. Likewise the effective shear rigidity and uniformly distributed mass of a typical frame i in the y direction are represented by GA_{yi} and m_{fyi} and those of frame j running in the x direction by GA_{xj} and m_{fxj}.

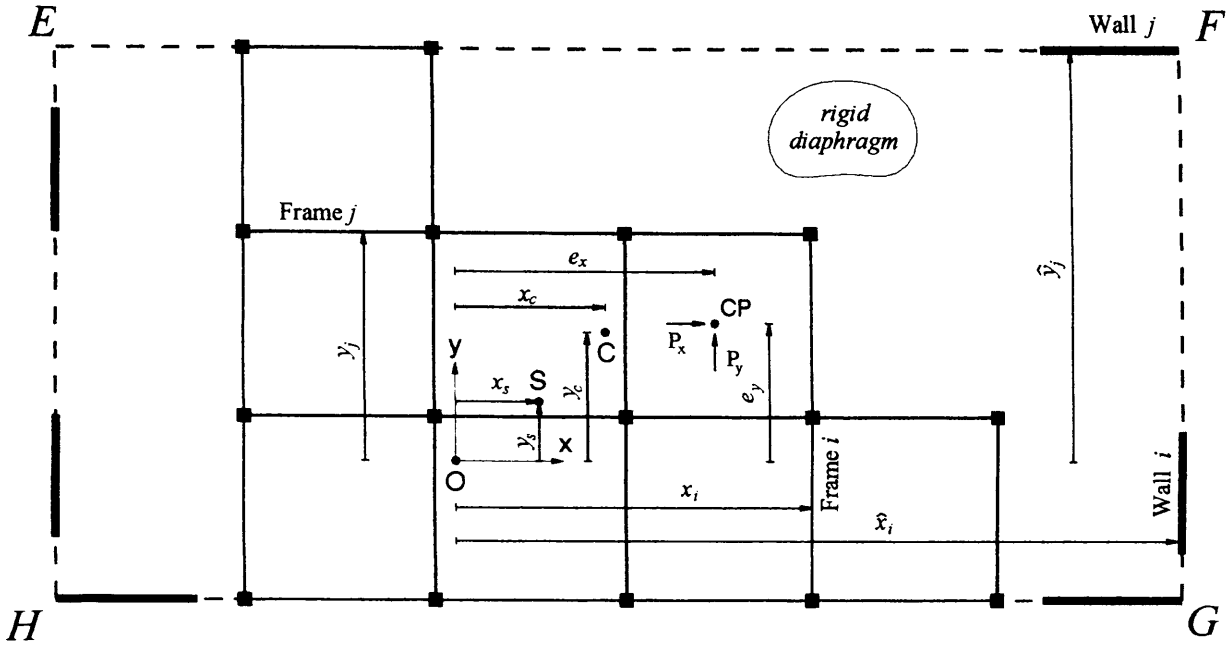

Figure 6.1 Typical floor plan of an asymmetric three-dimensional wall-frame structure. O, S and C denote the locations of the flexure, shear and mass centres, respectively. The floor system *EFGH* is considered to be rigid in its plane.

During vibration, the displacement of the shear rigidity and mass centres at any time t in the x-y plane can be determined as the result of a pure translation followed by a pure rotation about the flexural rigidity centre, see Figure 6.2. During the translation phase the flexural rigidity centre moves to O′, the shear rigidity centre S moves to S′ and the mass centre C moves to C′, displacements in each case of $u(z,t)$ and $v(z,t)$ in the x and y directions, respectively. During rotation, the shear and mass centres moves additionally from S′ and C′ to S″ and C″, respectively, an angular rotation of $\varphi(z,t)$ about O′. The resulting translations, (u_s, v_s) and (u_c, v_c) of the shear and mass centres in the x and y directions, respectively, are

$$u_s(z,t) = u(z,t) - y_s\varphi(z,t) \tag{6.1a}$$

$$v_s(z,t) = v(z,t) + x_s\varphi(z,t) \tag{6.1b}$$

and

$$u_c(z,t) = u(z,t) - y_c\varphi(z,t) \tag{6.1c}$$

$$v_c(z,t) = v(z,t) + x_c\varphi(z,t) \tag{6.1d}$$

More generally, it is clear that the displacements of a typical point (x_i, y_i) are given by Eqs. (6.1a) and (6.1b) when $s = i$.

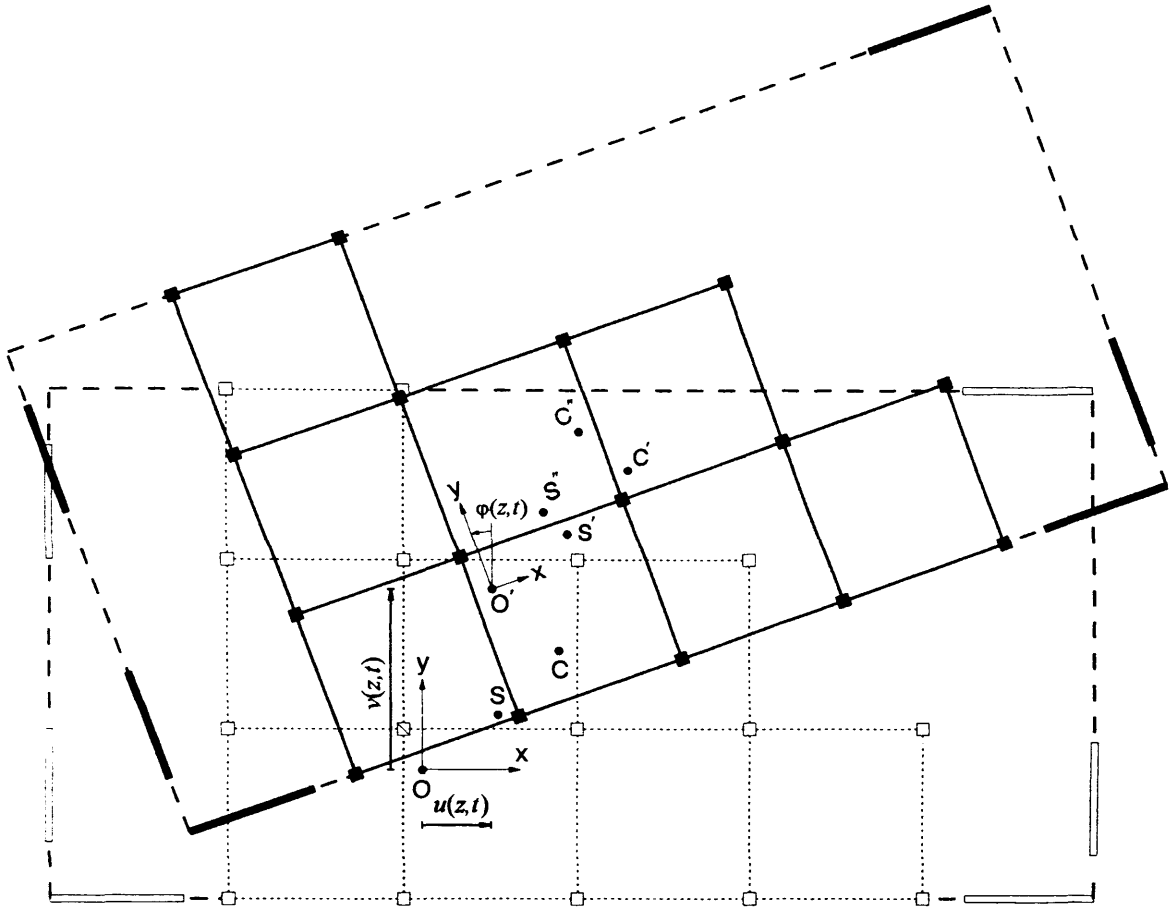

Figure 6.2 Coupled translational-torsional vibration of the structure. O, S and C move to O′, S′ and C′, respectively, during translation and S′ and C′ moves additionally to S″ and C″ during rotation about O′.

The structure is now divided into segments along the z axis by notionally cutting the structure along horizontal planes at those storey levels corresponding to changes in storey properties. Figure 6.3 shows a typical segment formed by cutting the structure through planes $E_kF_kG_kH_k$ and $E_{k+1}F_{k+1}G_{k+1}H_{k+1}$ that correspond to the k^{th} and $k+1^{th}$ changes in storey properties. The number of storeys in any one segment can vary from one, to the

total number of storeys in the structure if it is uniform throughout its height. However, in any one segment each storey must have the same properties.

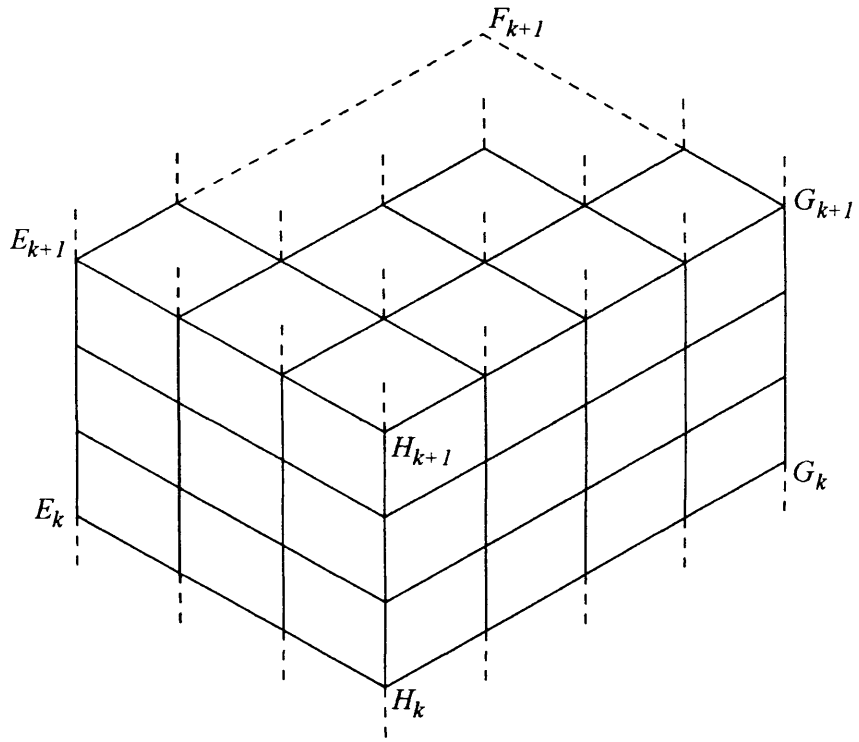

Figure 6.3 Typical segment formed by cutting the structure through planes $E_kF_kG_kH_k$ and $E_{k+1}F_{k+1}G_{k+1}H_{k+1}$ that correspond to the k^{th} and $k+1^{th}$ changes in storey properties. (Walls and some column and beam members have been omitted for clarity.)

We now consider a typical segment in isolation and seek to replace each primary frame with a substitute shear beam and each primary wall with a substitute flexural beam that replicate their in-plane motion. We start by considering a typical frame, frame i, that runs parallel to the y-z plane, see Figure 6.1. This whole frame is replaced by the single substitute shear beam, beam i, shown in Figure 6.4a. This beam is a two-dimensional shear beam of length L and has uniformly distributed mass and shear stiffness. The mass and elastic axes therefore coincide with the local z-axis and the elastic axis is only permitted shear deformation $v_i(z,t)$ in the y direction, where z and t denote distance from the local origin and time, respectively. Likewise, we consider a typical wall, wall i, running parallel to the y-z plane and replace it by the single flexural substitute beam, beam i, shown in Figure 6.4b. This beam is a two-dimensional flexural beam of length L and has uniformly distributed mass and flexural stiffness. The mass and elastic axes

therefore coincide with the local z-axis and the elastic axis is only permitted deformation $\hat{v}_i(z,t)$ in the y direction.

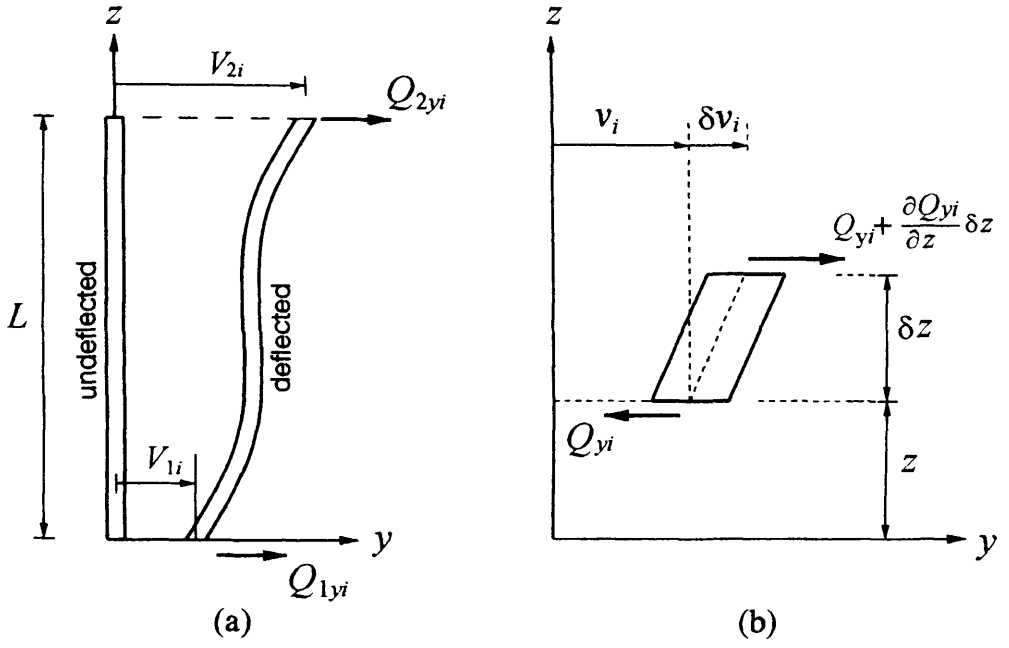

Figure 6.4a Coordinate system and sign convention for the substitute two-dimensional shear beam in the local y-z plane. a) Member convention b) Element convention.

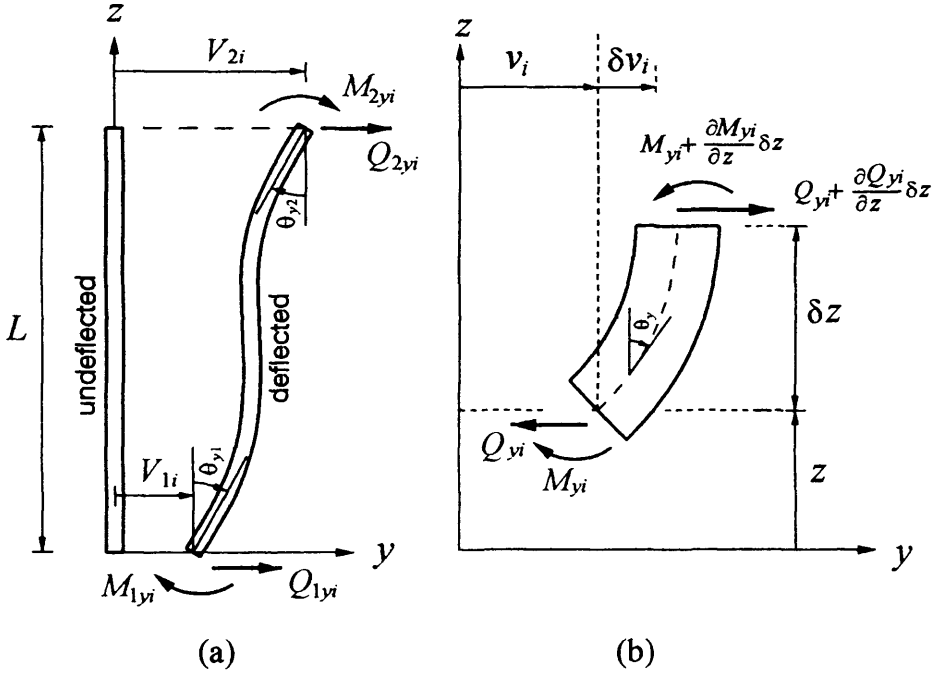

Figure 6.4b Coordinate system and sign convention for the substitute two-dimensional flexural beam in the local y-z plane. a) Member convention b) Element convention.

The motion of two-dimensional, shear and flexural beams have already been studied in Chapters 2 and 5. The transverse shear force for the substitute shear and flexural beams for frame and wall i running in the y-z plane, respectively, are

$$Q_{yi} = GA_{yi}\frac{\partial v_i(z,t)}{\partial z} \tag{6.2a}$$

$$Q_{wyi} = -EI_{yi}\frac{\partial^3 \hat{v}_i(z,t)}{\partial z^3} \tag{6.2b}$$

where v_i and $\hat{v}_i$ are the deformation of frame i and wall i in the y direction, respectively.

The dynamic equilibrium for motion of the structure in the y-z plane may then be written as

$$\frac{\partial}{\partial z}\left(\sum_{i=1}^{n_{wy}} -EI_{wyi}\frac{\partial^3 \hat{v}_i(z,t)}{\partial z^3} + \sum_{i=1}^{n_y} GA_{yi}\frac{\partial v_i(z,t)}{\partial z}\right)\delta z = \left(\sum_{i=1}^{n_{wy}} m_{wyi}\frac{\partial^2 \hat{v}_i(z,t)}{\partial t^2}\sum_{i=1}^{n_y} m_{fyi}\frac{\partial^2 v_i(z,t)}{\partial t^2}\right)\delta z \tag{6.3}$$

Noting that GA_{yi} and EI_{wyi} are constant over the length of the member and substituting for $v_i(z,t)$ and $\hat{v}_i(z,t)$ from Eq. (6.1b) with c replaced by i gives

$$\sum_{i=1}^{n_{wy}} -EI_{wyi}\frac{\partial^4 (v(z,t)+\hat{x}_i\varphi(z,t))}{\partial z^4} + \sum_{i=1}^{n_y} GA_{yi}\frac{\partial^2 (v(z,t)+x_i\varphi(z,t))}{\partial z^2}$$
$$-\sum_{i=1}^{n_y} m_{wyi}\frac{\partial^2 (v(z,t)+\hat{x}_i\varphi(z,t))}{\partial t^2} - \sum_{i=1}^{n_y} m_{fyi}\frac{\partial^2 (v(z,t)+x_i\varphi(z,t))}{\partial t^2} = 0 \tag{6.4}$$

where x_i and $\hat{x}_i$ are the distance of frame i and wall i from the flexure centre, O, respectively. Since O is the centre of flexural rigidity, $\sum_{i=1}^{n_{wy}} EI_{wyi}\hat{x}_i = 0$ and Eq. (6.4) can be simplified to

$$EI_{wy}\frac{\partial^4 v(z,t)}{\partial z^4} - GA_y\frac{\partial^2 v(z,t)}{\partial z^2} - x_s GA_y\frac{\partial^2 \varphi(z,t)}{\partial z^2} + m_y\frac{\partial^2 v(z,t)}{\partial t^2} + x_c m_y\frac{\partial^2 \varphi(z,t)}{\partial t^2} = 0 \tag{6.5}$$

in which

$$EI_{wy} = \sum_{i=1}^{n_{wy}} EI_{wyi} \tag{6.6a}$$

$$x_s GA_y = \sum_{i=1}^{n_y} x_i GA_{yi} \text{ where } GA_y = \sum_{i=1}^{n_y} GA_{yi} \tag{6.6b}$$

$$\text{and } x_c m_y = \sum_{i=1}^{n_{wy}} \hat{x}_i m_{wyi} + \sum_{i=1}^{n_y} x_i m_{fyi} \text{ where } m_y = \sum_{i=1}^{n_{wy}} m_{wyi} + \sum_{i=1}^{n_y} m_{fyi} \tag{6.7}.$$

Since the total mass of the segment contributes to its vibration, including the mass of the frames running in the x direction and the rigid diaphragms, m_y should be replaced by m, where m is the equivalent distributed mass over the height of the segment. Therefore Eq. (6.5) becomes

$$EI_{wy}\frac{\partial^4 v(z,t)}{\partial z^4} - GA_y\frac{\partial^2 v(z,t)}{\partial z^2} - x_s GA_y\frac{\partial^2 \varphi(z,t)}{\partial z^2} + m\frac{\partial^2 v(z,t)}{\partial t^2} + x_c m\frac{\partial^2 \varphi(z,t)}{\partial t^2} = 0 \tag{6.8}$$

In an identical fashion, the dynamic equilibrium relationship for motion in the x-z plane yields the second governing differential equation as

$$EI_{wx}\frac{\partial^4 u(z,t)}{\partial z^4} - GA_x\frac{\partial^2 u(z,t)}{\partial z^2} + y_s GA_x\frac{\partial^2 \varphi(z,t)}{\partial z^2} + m\frac{\partial^2 u(z,t)}{\partial t^2} - y_c m\frac{\partial^2 \varphi(z,t)}{\partial t^2} = 0 \tag{6.9}$$

in which

$$EI_{wx} = \sum_{j=1}^{n_{wx}} EI_{wxj} \tag{6.10}$$

$$y_s GA_x = \sum_{j=1}^{n_x} y_j GA_{xj} \text{ where } GA_x = \sum_{j=1}^{n_x} GA_{xj} \tag{6.11}$$

$$y_c m_x = \sum_{j=1}^{n_{wx}} \hat{y}_j m_{wxj} + \sum_{j=1}^{n_x} y_j m_{fxj} \text{ where } m_x = \sum_{j=1}^{n_{wx}} m_{wxj} + \sum_{j=1}^{n_x} m_{fxj} \tag{6.12}$$

where y_j and $\hat{y}_j$ are the distance of frame j and wall j from the flexural rigidity centre O, respectively.

Finally, it should be noted that the plane frames and walls running parallel to the x-z and y-z planes also provide the torsional stiffness of the building. Thus the required equation for torsion can be developed from a consideration of the torsional equilibrium about O, which yields

$$\sum_{i=1}^{n_{wy}} -EI_{wyi}\hat{x}_i \frac{\partial^4(v(z,t)+\hat{x}_i\varphi(z,t))}{\partial z^4} + \sum_{i=1}^{n_y} GA_{yi}x_i \frac{\partial^2(v(z,t)+x_i\varphi(z,t))}{\partial z^2}$$
$$-\sum_{i=1}^{n_y} m_{wyi}\hat{x}_i \frac{\partial^2(v(z,t)+\hat{x}_i\varphi(z,t))}{\partial t^2} - \sum_{i=1}^{n_y} m_{fyi}x_i \frac{\partial^2(v(z,t)+x_i\varphi(z,t))}{\partial t^2}$$
$$-\left[\sum_{j=1}^{n_{wx}} -EI_{wxj}\hat{y}_j \frac{\partial^4(u(z,t)-\hat{y}_i\varphi(z,t))}{\partial z^4} + \sum_{j=1}^{n_x} GA_{xj}y_j \frac{\partial^2(u(z,t)-y_i\varphi(z,t))}{\partial z^2}\right.$$
$$\left.-\sum_{j=1}^{n_{wx}} m_{wxj}\hat{y}_j \frac{\partial^2(u(z,t)-\hat{y}_j\varphi(z,t))}{\partial t^2} - \sum_{j=1}^{n_x} m_{fxj}y_j \frac{\partial^2(u(z,t)-y_j\varphi(z,t))}{\partial t^2}\right] = 0 \qquad (6.13)$$

or

$$EI_{ww}\frac{\partial^4\varphi(z,t)}{\partial z^4} - x_s GA_y \frac{\partial^2 v(z,t)}{\partial z^2} + y_s GA_x \frac{\partial^2 u(z,t)}{\partial z^2} - GJ_o \frac{\partial^2\varphi(z,t)}{\partial z^2}$$
$$+ m_y x_c \frac{\partial^2 v(z,t)}{\partial t^2} - m_x y_c \frac{\partial^2 u(z,t)}{\partial t^2} + I_g \frac{\partial^2\varphi(z,t)}{\partial t^2} = 0 \qquad (6.14)$$

in which

$$EI_{ww} = \sum_{i=1}^{n_{wy}} EI_{wyi}\hat{x}_i^2 + \sum_{j=1}^{n_{wx}} EI_{wxj}\hat{y}_j^2 \qquad (6.15)$$

$$GJ_o = \sum_{i=1}^{n_y} GA_{yi}x_i^2 + \sum_{j=1}^{n_x} GA_{xj}y_j^2 \qquad (6.16)$$

$$I_g = \sum_{i=1}^{n_{wy}} m_{wyi}\hat{x}_i^2 + \sum_{j=1}^{n_{wx}} m_{wxj}\hat{y}_j^2 + \sum_{i=1}^{n_y} m_{fyi}x_i^2 + \sum_{j=1}^{n_x} m_{fxj}y_j^2 \qquad (6.17)$$

EI_{ww} and GJ_o are the torsional rigidity of the walls and frames about the flexural rigidity O, respectively. Comparing Eq. (6.14) with the theory describing the torsion of members with thin walled cross-sections, EI_{ww} and GJ_o can be recognised as the warping and Saint-Venant torsional rigidity respectively. I_g is the polar second moment of mass about the flexural rigidity centre O.

As in the case of symmetric structures, the out of plane stiffness and inertia of the plane frames and walls running in the x and y directions, as well as that of the rigid diaphragms, should be taken into account. Thus Eqs. (6.8), (6.9) and (6.14) can be rearranged in the following form

$$EI_{wx}\frac{\partial^4 u(z,t)}{\partial z^4} - GA_x\frac{\partial^2 u(z,t)}{\partial z^2} + y_s GA_x\frac{\partial^2 \varphi(z,t)}{\partial z^2} + m\frac{\partial^2 u(z,t)}{\partial t^2} - y_c m\frac{\partial^2 \varphi(z,t)}{\partial t^2} = 0 \quad (6.18a)$$

$$EI_{wy}\frac{\partial^4 v(z,t)}{\partial z^4} - GA_y\frac{\partial^2 v(z,t)}{\partial z^2} - x_s GA_y\frac{\partial^2 \varphi(z,t)}{\partial z^2} + m\frac{\partial^2 v(z,t)}{\partial t^2} + x_c m\frac{\partial^2 \varphi(z,t)}{\partial t^2} = 0 \quad (6.18b)$$

$$EI_{ww}\frac{\partial^4 \varphi(z,t)}{\partial z^4} - GJ_o\frac{\partial^2 \varphi(z,t)}{\partial z^2} + y_s GA_x\frac{\partial^2 u(z,t)}{\partial z^2} - x_s GA_y\frac{\partial^2 v(z,t)}{\partial z^2}$$
$$+ I_g\frac{\partial^2 \varphi(z,t)}{\partial t^2} - y_c m\frac{\partial^2 u(z,t)}{\partial t^2} + x_c m\frac{\partial^2 v(z,t)}{\partial t^2} = 0 \quad (6.18c)$$

Eqs. (6.18a-c) are the governing differential equations of vibration of an asymmetric three-dimensional wall-frame structure.

6.2.2 Member Dynamic Stiffness Matrix

Eqs. (6.18) are now solved and posed in dynamic stiffness form. Although each equation was developed individually from a consideration of the planar flexural and shear beams of Figure 6.4, they now describe the motion of a three-dimensional, flexural-shear coupled substitute beam whose coordinate system and sign convention are shown in Figure 6.5. This beam (exact finite element) will replace a typical segment of the original, asymmetric, three-dimensional wall-frame structure. The whole of the original structure can then be reconstituted by assembling the exact finite elements corresponding to each segment in the usual way.

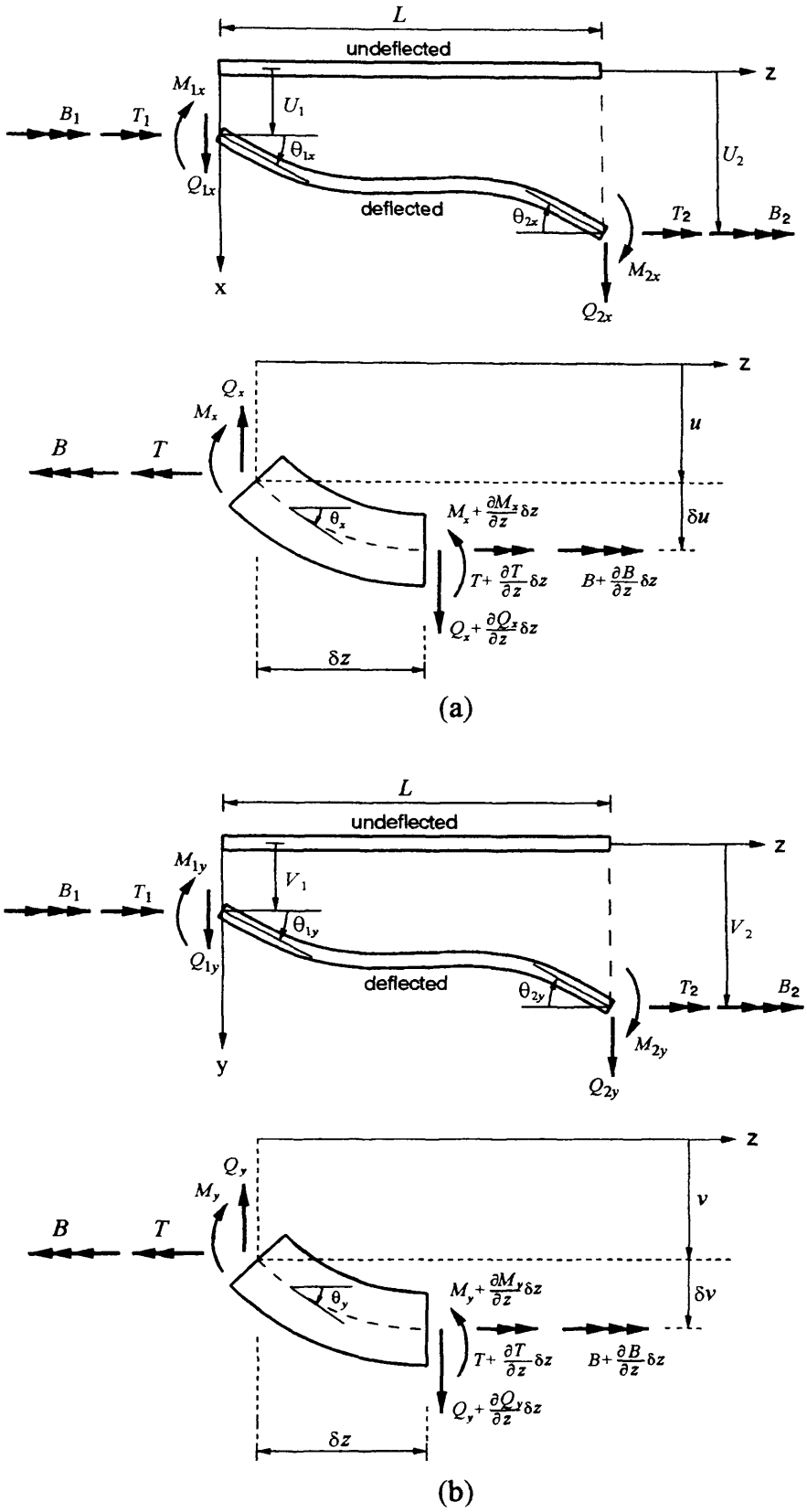

Figure 6.5 Coordinate system and sign convention for forces and displacements of the three-dimensional flexural-shear coupled substitute beam. a) Member and element convention for the x-z plane. b) Member and element convention for the y-z plane

Eqs. (6.18) are solved on the assumption of harmonic motion, so that the instantaneous displacements can be written as

$$u(z,t) = U(z)\sin\omega t \tag{6.19a}$$

$$v(z,t) = V(z)\sin\omega t \tag{6.19b}$$

$$\varphi(z,t) = \Phi(z)\sin\omega t \tag{6.19c}$$

where $U(z)$, $V(z)$ and $\Phi(z)$ are the amplitudes of the sinusoidally varying translations and torsion, respectively and ω is the circular frequency.

Substituting Eqs. (6.19a-c) into Eqs. (6.18a-c) gives:

$$EI_{wx}U''''(z) - GA_xU''(z) + y_sGA_x\Phi''(z) - m\omega^2U(z) + y_cm\omega^2\Phi(z) = 0 \tag{6.20a}$$

$$EI_{wy}V''''(z) - GA_yV''(z) - x_sGA_y\Phi''(z) - m\omega^2V(z) - x_cm\omega^2\Phi(z) = 0 \tag{6.20b}$$

$$\begin{aligned} &EI_{ww}\Phi''''(z) - GJ_o\Phi''(z) + y_sGA_xU''(z) - x_sGA_yV''(z) \\ &\quad - I_g\omega^2\Phi(z) + y_cm\omega^2U(z) - x_cm\omega^2V(z) = 0 \end{aligned} \tag{6.20c}$$

Eqs. (6.20a-c) can be written in the following non-dimensional form

$$U''''(\xi) - \alpha_x^2U''(\xi) + y_s\alpha_x^2\Phi''(\xi) - \beta_x^2\omega^2U(\xi) + y_c\omega^2\beta_x^2\Phi(\xi) = 0 \tag{6.21a}$$

$$V''''(\xi) - \alpha_y^2V''(\xi) - x_s\alpha_y^2\Phi''(\xi) - \beta_y^2\omega^2V(\xi) - x_c\omega^2\beta_y^2\Phi(\xi) = 0 \tag{6.21b}$$

$$\begin{aligned} &\Phi''''(\xi) - \alpha_\varphi^2\Phi''(\xi) + y_s\frac{\alpha_x^2}{\gamma_x^2}U''(\xi) - x_s\frac{\alpha_y^2}{\gamma_y^2}V''(\xi) \\ &\quad - \omega^2\beta_\varphi^2\Phi(\xi) + y_c\omega^2\frac{\beta_x^2}{\gamma_x^2}U(\xi) - x_c\omega^2\frac{\beta_y^2}{\gamma_y^2}V(\xi) = 0 \end{aligned} \tag{6.21c}$$

in which $\xi = (z/L)$, L is the length of the element, and

$$\alpha_x^2 = \frac{GA_x}{EI_x}L^2, \quad \alpha_y^2 = \frac{GA_y}{EI_y}L^2 \quad \text{and} \quad \alpha_\varphi^2 = \frac{GJ_o}{EI_{ww}}L^2 \tag{6.22a,b,c}$$

$$\beta_x^2 = \frac{mL^4}{EI_x}, \quad \beta_y^2 = \frac{mL^4}{EI_y} \quad \text{and} \quad \beta_\varphi^2 = \frac{mL^4}{EI_{ww}} r_m^2 \tag{6.23a,b,c}$$

$$\gamma_x^2 = \frac{EI_{ww}}{EI_x} \quad \text{and} \quad \gamma_y^2 = \frac{EI_{ww}}{EI_y} \tag{6.24a,b}$$

where r_m is the polar mass radius of gyration about O i.e.

$$I_g = mr_m^2 \tag{6.24c}$$

Eqs. (6.21a-c) can be rewritten in matrix form as

$$\begin{bmatrix} D^4 - \alpha_x^2 D^2 - \omega^2 \beta_x^2 & 0 & y_s \alpha_x^2 D^2 + y_c \omega^2 \beta_x^2 \\ 0 & D^4 - \alpha_y^2 D^2 - \omega^2 \beta_y^2 & -x_s \alpha_y^2 D^2 - x_c \omega^2 \beta_y^2 \\ y_s \frac{\alpha_x^2}{\gamma_x^2} D^2 + y_c \omega^2 \frac{\beta_x^2}{\gamma_x^2} & -x_s \frac{\alpha_y^2}{\gamma_y^2} D^2 - x_c \omega^2 \frac{\beta_y^2}{\gamma_y^2} & D^4 - \alpha_\varphi^2 D^2 - \omega^2 \beta_\varphi^2 \end{bmatrix} \begin{bmatrix} U(\xi) \\ V(\xi) \\ \Phi(\xi) \end{bmatrix} = 0 \tag{6.25}$$

in which $D = d/d\xi$.

Eq. (6.25) can be combined into one equation by eliminating all but one of the displacements to give the twelfth-order differential equation

$$\begin{vmatrix} D^4 - \alpha_x^2 D^2 - \omega^2 \beta_x^2 & 0 & y_s \alpha_x^2 D^2 + y_c \omega^2 \beta_x^2 \\ 0 & D^4 - \alpha_y^2 D^2 - \omega^2 \beta_y^2 & -x_s \alpha_y^2 D^2 - x_c \omega^2 \beta_y^2 \\ y_s \frac{\alpha_x^2}{\gamma_x^2} D^2 + y_c \omega^2 \frac{\beta_x^2}{\gamma_x^2} & -x_s \frac{\alpha_y^2}{\gamma_y^2} D^2 - x_c \omega^2 \frac{\beta_y^2}{\gamma_y^2} & D^4 - \alpha_\varphi^2 D^2 - \omega^2 \beta_\varphi^2 \end{vmatrix} W(\xi) = 0 \tag{6.26}$$

where $W = U$, V or Φ

The solution of the differential Eq. (6.26) can be obtained by substituting the trial solution $W(\xi) = e^{s\xi}$ to give the characteristic equation

$$\begin{vmatrix} \tau^2-\alpha_x^2\tau-\omega^2\beta_x^2 & 0 & y_s\alpha_x^2\tau+y_c\omega^2\beta_x^2 \\ 0 & \tau^2-\alpha_y^2\tau-\omega^2\beta_y^2 & -x_s\alpha_y^2\tau-x_c\omega^2\beta_y^2 \\ y_s\dfrac{\alpha_x^2}{\gamma_x^2}\tau+y_c\omega^2\dfrac{\beta_x^2}{\gamma_x^2} & -x_s\dfrac{\alpha_y^2}{\gamma_y^2}\tau-x_c\omega^2\dfrac{\beta_y^2}{\gamma_y^2} & \tau-\alpha_\varphi^2\tau-\omega^2\beta_\varphi^2 \end{vmatrix} W(\xi)=0 \qquad (6.27)$$

or

$$\begin{aligned}
&\tau^6-(\alpha_x^2+\alpha_y^2+\alpha_\varphi^2)\tau^5+(-\omega^2\beta_x^2-\omega^2\beta_y^2-\omega^2\beta_\varphi^2+\alpha_x^2\alpha_y^2+\alpha_x^2\alpha_\varphi^2+\alpha_y^2\alpha_\varphi^2-x_s^2\frac{\alpha_y^2}{\gamma_y^2}-y_s^2\frac{\alpha_x^2}{\gamma_x^2})\tau^4\\
&+(\omega^2\alpha_x^2\beta_y^2+\omega^2\alpha_x^2\beta_\varphi^2+\omega^2\alpha_y^2\beta_x^2+\omega^2\alpha_y^2\beta_\varphi^2+\omega^2\alpha_\varphi^2\beta_x^2+\omega^2\alpha_\varphi^2\beta_y^2-\alpha_x^2\alpha_y^2\alpha_\varphi^2\\
&-2y_cy_s\omega^2\alpha_x^2\frac{\beta_x^2}{\gamma_x^2}-2x_cx_s\omega^2\alpha_y^2\frac{\beta_y^2}{\gamma_y^2}+x_s^2\alpha_x^2\frac{\alpha_y^4}{\gamma_y^2}+y_s^2\alpha_y^2\frac{\alpha_x^4}{\gamma_x^2})\tau^3\\
&+(\omega^4\beta_x^2\beta_y^2+\omega^4\beta_x^2\beta_\varphi^2+\omega^4\beta_y^2\beta_\varphi^2-\omega^2\alpha_x^2\alpha_y^2\beta_\varphi^2-\omega^2\alpha_x^2\alpha_\varphi^2\beta_y^2-\omega^2\alpha_y^2\alpha_\varphi^2\beta_x^2\\
&-x_c^2\omega^4\frac{\beta_y^4}{\gamma_y^2}-y_c^2\omega^4\frac{\beta_x^4}{\gamma_x^2}+2x_sx_c\omega^2\alpha_x^2\alpha_y^2\frac{\beta_y^2}{\gamma_y^2}+2y_sy_c\omega^2\alpha_x^2\alpha_y^2\frac{\beta_x^2}{\gamma_x^2}+x_s^2\omega^2\beta_x^2\frac{\alpha_y^2}{\gamma_y^2}+y_s^2\omega^2\beta_y^2\frac{\alpha_x^2}{\gamma_x^2})\tau^2\\
&+(-\omega^4\alpha_x^2\beta_y^2\beta_\varphi^2-\omega^4\alpha_y^2\beta_x^2\beta_\varphi^2-\omega^4\alpha_\varphi^2\beta_x^2\beta_y^2+x_c^2\omega^4\alpha_x^2\frac{\beta_y^2}{\gamma_y^2}+y_c^2\omega^4\alpha_y^2\frac{\beta_x^2}{\gamma_x^2}\\
&+2x_sx_c\omega^4\beta_x^2\beta_y^2\frac{\alpha_y^2}{\gamma_y^2}+2y_sy_c\omega^4\beta_x^2\beta_y^2\frac{\alpha_x^2}{\gamma_x^2})\tau\\
&+(-\omega^6\beta_x^2\beta_y^2\beta_\varphi^2+x_c^2\omega^6\beta_x^2\frac{\beta_y^2}{\gamma_y^2}+y_c^2\omega^6\beta_y^2\frac{\beta_x^2}{\gamma_x^2})=0 \qquad (6.28)
\end{aligned}$$

in which $\tau = s^2$ (6.29)

Eq. (6.28) is a sixth order equation in terms of τ and it can be proved (Appendix 6A) that it always has three negative and three positive real roots. Let these six roots be τ_1, τ_2, τ_3, $-\tau_4$, $-\tau_5$ and $-\tau_6$, where τ_j (j=1,6) are all real and positive. Therefore the twelve roots of Eq. (6.27) are

$\alpha,-\alpha \quad \beta,-\beta \quad \gamma,-\gamma \quad i\delta,-i\delta \quad i\eta,-i\eta \quad i\mu,-i\mu$

where $i = \sqrt{-1}$ and

$$\alpha = \sqrt{\tau_1}\ ,\ \beta = \sqrt{\tau_2}\ ,\ \gamma = \sqrt{\tau_3}\ ,\ \delta = \sqrt{\tau_4}\ ,\ \eta = \sqrt{\tau_5} \text{ and } \mu = \sqrt{\tau_6} \tag{6.30}$$

It follows that the solution of Eq. (6.26) is of the form

$$W(\xi) = C_1 \cosh\alpha\xi + C_2 \sinh\alpha\xi + C_3 \cosh\beta\xi + C_4 \sinh\beta\xi + C_5 \cosh\gamma\xi + C_6 \sinh\gamma\xi +$$
$$C_7 \cos\delta\xi + C_8 \sin\delta\xi + C_9 \cos\eta\xi + C_{10} \sin\eta\xi + C_{11} \cos\mu\xi + C_{12} \sin\mu\xi \tag{6.31}$$

Eq. (6.31) represents the solution for both displacements $U(\xi)$, $V(\xi)$ and torsion $\Phi(\xi)$. Since $U(\xi)$, $V(\xi)$ and $\Phi(\xi)$ are related via Eq. (6.26), they can be written as

$$U(\xi) = C_1^u \cosh\alpha\xi + C_2^u \sinh\alpha\xi + C_3^u \cosh\beta\xi + C_4^u \sinh\beta\xi + C_5^u \cosh\gamma\xi + C_6^u \sinh\gamma\xi +$$
$$C_7^u \cos\delta\xi + C_8^u \sin\delta\xi + C_9^u \cos\eta\xi + C_{10}^u \sin\eta\xi + C_{11}^u \cos\mu\xi + C_{12}^u \sin\mu\xi \tag{6.32a}$$
$$V(\xi) = C_1^v \cosh\alpha\xi + C_2^v \sinh\alpha\xi + C_3^v \cosh\beta\xi + C_4^v \sinh\beta\xi + C_5^v \cosh\gamma\xi + C_6^v \sinh\gamma\xi +$$
$$C_7^v \cos\delta\xi + C_8^v \sin\delta\xi + C_9^v \cos\eta\xi + C_{10}^v \sin\eta\xi + C_{11}^v \cos\mu\xi + C_{12}^v \sin\mu\xi \tag{6.32b}$$
$$\Phi(\xi) = C_1 \cosh\alpha\xi + C_2 \sinh\alpha\xi + C_3 \cosh\beta\xi + C_4 \sinh\beta\xi + C_5 \cosh\gamma\xi + C_6 \sinh\gamma\xi +$$
$$C_7 \cos\delta\xi + C_8 \sin\delta\xi + C_9 \cos\eta\xi + C_{10} \sin\eta\xi + C_{11} \cos\mu\xi + C_{12} \sin\mu\xi \tag{6.32c}$$

in which the constants C_j^u, C_j^v and C_j (j=1,12) can be related through Eq. (6.26) as

$$C_j^u = t_j^u C_j \text{ and } C_j^v = t_j^v C_j \quad (j\text{=}1,12) \tag{6.33a,b}$$

where

$$t_{2j-1}^u = t_{2j}^u = \frac{-y_s\alpha_x^2\tau_j - y_c\omega^2\beta_x^2}{\tau_j^2 - \alpha_x^2\tau_j - \omega^2\beta_x^2} \quad (j\text{=}1,2,3) \tag{6.34a}$$

$$t_{2j-1}^u = t_{2j}^u = \frac{y_s\alpha_x^2\tau_j - y_c\omega^2\beta_x^2}{\tau_j^2 + \alpha_x^2\tau_j - \omega^2\beta_x^2} \quad (j\text{=}4,5,6) \tag{6.34b}$$

$$t^{v}_{2j-1} = t^{v}_{2j} = \frac{x_s\alpha_y^2\tau_j + x_c\omega^2\beta_y^2}{\tau_j^2 - \alpha_y^2\tau_j - \omega^2\beta_y^2} \qquad (j=1,2,3) \tag{6.34c}$$

$$t^{v}_{2j-1} = t^{v}_{2j} = \frac{-x_s\alpha_y^2\tau_j + x_c\omega^2\beta_y^2}{\tau_j^2 + \alpha_y^2\tau_j - \omega^2\beta_y^2} \qquad (j=4,5,6) \tag{6.34d}$$

Following the sign convention of Figures 6.5(a) and 6.5(b), the expressions for the bending rotations $\theta_x(\xi)$ and $\theta_y(\xi)$, bending moments $M_x(\xi)$ and $M_y(\xi)$ and the shear forces $Q_x(\xi)$ and $Q_y(\xi)$ in the x and y directions, the torque $T(\xi)$ and the bi-moment $B(\xi)$ can be obtained from the appropriate stress/strain relationships as

$$\theta_x(\xi) = \frac{U'(\xi)}{L} = (\frac{1}{L})\big(C_1^u\alpha\sinh\alpha\xi + C_2^u\alpha\cosh\alpha\xi + C_3^u\beta\sinh\beta\xi + C_4^u\beta\cosh\beta\xi + C_5^u\gamma\sinh\gamma\xi$$
$$C_6^u\gamma\cosh\gamma\xi - C_7^u\delta\sin\delta\xi + C_8^u\delta\cos\delta\xi - C_9^u\eta\sin\eta\xi + C_{10}^u\eta\cos\eta\xi - C_{11}^u\mu\sin\mu\xi + C_{12}^u\mu\cos\mu\xi\big) \tag{6.35a}$$

$$\theta_y(\xi) = \frac{V'(\xi)}{L} = (\frac{1}{L})\big(C_1^v\alpha\sinh\alpha\xi + C_2^v\alpha\cosh\alpha\xi + C_3^v\beta\sinh\beta\xi + C_4^v\beta\cosh\beta\xi + C_5^v\gamma\sinh\gamma\xi$$
$$C_6^v\gamma\cosh\gamma\xi - C_7^v\delta\sin\delta\xi + C_8^v\delta\cos\delta\xi - C_9^v\eta\sin\eta\xi + C_{10}^v\eta\cos\eta\xi - C_{11}^v\mu\sin\mu\xi + C_{12}^v\mu\cos\mu\xi\big) \tag{6.35b}$$

$$\Phi'(\xi) = \frac{1}{L}(\frac{d\Phi}{d\xi}) = (\frac{1}{L})\big(C_1\alpha\sinh\alpha\xi + C_2\alpha\cosh\alpha\xi + C_3\beta\sinh\beta\xi + C_4\beta\cosh\beta\xi + C_5\gamma\sinh\gamma\xi$$
$$C_6\gamma\cosh\gamma\xi - C_7\delta\sin\delta\xi + C_8\delta\cos\delta\xi - C_9\eta\sin\eta\xi + C_{10}\eta\cos\eta\xi - C_{11}\mu\sin\mu\xi + C_{12}\mu\cos\mu\xi\big) \tag{6.35c}$$

in which θ_x, θ_y and Φ' are the gradient of U, V and Φ with respect to z, respectively.

The expressions for the corresponding forces are

$$M_x(\xi) = \frac{-EI_x}{L^2}U''(\xi) \tag{6.36}$$

$$M_y(\xi) = \frac{-EI_y}{L^2}V''(\xi) \tag{6.37}$$

$$Q_x(\xi) = \frac{-EI_x}{L^3}U'''(\xi) + \frac{GA_x}{L}\big(U(\xi) - y_s\Phi(\xi)\big)' \tag{6.38}$$

$$Q_y(\xi) = \frac{-EI_y}{L^3}V'''(\xi) + \frac{GA_y}{L}\big(V(\xi) + x_s\Phi(\xi)\big)' \tag{6.39}$$

$$B(\xi) = \frac{-EI_{ww}}{L^2}\Phi''(\xi) \tag{6.40}$$

$$T(\xi) = \frac{-EI_{ww}}{L^3}\Phi'''(\xi) + \frac{GJ_s}{L}\Phi'(\xi) + \frac{GA_y}{L}\left(V(\xi) + x_s\Phi(\xi)\right)' x_s - \frac{GA_x}{L}\left(U(\xi) - y_s\Phi(\xi)\right)' y_s \tag{6.41}$$

in which GJ_s is the torsional rigidity of the walls about the shear rigidity centre S. Eq. (6.41) can be simplified to

$$T(\xi) = \frac{-EI_{ww}}{L^3}\Phi'''(\xi) + \frac{GJ_o}{L}\Phi'(\xi) + \frac{GA_y}{L}V'(\xi) - \frac{GA_x}{L}U'(\xi) \tag{6.42}$$

The nodal displacements and forces can now be defined in the member co-ordinate system of Figures 6.5(a) and 6.5(b), as follows

At $\xi = 0$ $\quad U = U_1,\ \theta_x = \theta_{1x},\ V = V_1,\ \theta_y = \theta_{1y},\ \Phi = \Phi_1,\ \Phi' = \Phi'_1$ (6.43)

At $\xi = 1$ $\quad U = U_2,\ \theta_x = \theta_{2x},\ V = V_2,\ \theta_y = \theta_{2y},\ \Phi = \Phi_2,\ \Phi' = \Phi'_2$ (6.44)

At $\xi = 0$ $\quad Q_x = -Q_{1x},\ M_x = M_{1x},\ Q_y = -Q_{1y},\ M_y = M_{1y},\ T = -T_1,\ B = B_1$ (6.45)

At $\xi = 1$ $\quad Q_x = Q_{2x},\ M_x = -M_{2x},\ Q_y = Q_{2y},\ M_y = -M_{2y},\ T = T_2,\ B = -B_2$ (6.46)

The nodal displacements can then be determined from Eqs. (6.32) and (6.35) as

$$\begin{bmatrix} U_1 \\ \theta_{1x} \\ V_1 \\ \theta_{1y} \\ \Phi_1 \\ \Phi'_1 \\ U_2 \\ \theta_{2x} \\ V_2 \\ \theta_{2y} \\ \Phi_2 \\ \Phi'_2 \end{bmatrix} = \begin{bmatrix} t_1^u & 0 & t_3^u & 0 & t_5^u & 0 & t_7^u & 0 & t_9^u & 0 & t_{11}^u & 0 \\ 0 & \frac{\alpha}{L}t_2^u & 0 & \frac{\beta}{L}t_4^u & 0 & \frac{\gamma}{L}t_6^u & 0 & \frac{\delta}{L}t_8^u & 0 & \frac{\eta}{L}t_{10}^u & 0 & \frac{\mu}{L}t_{12}^u \\ t_1^v & 0 & t_3^v & 0 & t_5^v & 0 & t_7^v & 0 & t_9^v & 0 & t_{11}^v & 0 \\ 0 & \frac{\alpha}{L}t_2^v & 0 & \frac{\beta}{L}t_4^v & 0 & \frac{\gamma}{L}t_6^v & 0 & \frac{\delta}{L}t_8^v & 0 & \frac{\eta}{L}t_{10}^v & 0 & \frac{\mu}{L}t_{12}^v \\ 1 & 0 & 1 & 0 & 1 & 0 & 1 & 0 & 1 & 0 & 1 & 0 \\ 0 & \frac{\alpha}{L} & 0 & \frac{\beta}{L} & 0 & \frac{\gamma}{L} & 0 & \frac{\delta}{L} & 0 & \frac{\eta}{L} & 0 & \frac{\mu}{L} \\ t_1^u Ch_\alpha & t_2^u Sh_\alpha & t_3^u Ch_\beta & t_4^u Sh_\beta & t_5^u Ch_\gamma & t_6^u Sh_\gamma & t_7^u C_\delta & t_8^u S_\delta & t_9^u C_\eta & t_{10}^u S_\eta & t_{11}^u C_\mu & t_{12}^u S_\mu \\ \frac{\alpha}{L}t_1^u Sh_\alpha & \frac{\alpha}{L}t_2^u Ch_\alpha & \frac{\beta}{L}t_3^u Sh_\beta & \frac{\beta}{L}t_4^u Ch_\beta & \frac{\gamma}{L}t_5^u Sh_\gamma & \frac{\gamma}{L}t_6^u Ch_\gamma & \frac{-\delta}{L}t_7^u S_\delta & \frac{\delta}{L}t_8^u C_\delta & \frac{-\eta}{L}t_9^u S_\eta & \frac{\eta}{L}t_{10}^u C_\eta & \frac{-\mu}{L}t_{11}^u S_\mu & \frac{\mu}{L}t_{12}^u C_\mu \\ t_1^v Ch_\alpha & t_2^v Sh_\alpha & t_3^v Ch_\beta & t_4^v Sh_\beta & t_5^v Ch_\gamma & t_6^v Sh_\gamma & t_7^v C_\delta & t_8^v S_\delta & t_9^v C_\eta & t_{10}^v S_\eta & t_{11}^v C_\mu & t_{12}^v S_\mu \\ \frac{\alpha}{L}t_1^v Sh_\alpha & \frac{\alpha}{L}t_2^v Ch_\alpha & \frac{\beta}{L}t_3^v Sh_\beta & \frac{\beta}{L}t_4^v Ch_\beta & \frac{\gamma}{L}t_5^v Sh_\gamma & \frac{\gamma}{L}t_6^v Ch_\gamma & \frac{-\delta}{L}t_7^v S_\delta & \frac{\delta}{L}t_8^v C_\delta & \frac{-\eta}{L}t_9^v S_\eta & \frac{\eta}{L}t_{10}^v C_\eta & \frac{-\mu}{L}t_{11}^v S_\mu & \frac{\mu}{L}t_{12}^v C_\mu \\ Ch_\alpha & Sh_\alpha & Ch_\beta & Sh_\beta & Ch_\gamma & Sh_\gamma & C_\delta & S_\delta & C_\eta & S_\eta & C_\mu & S_\mu \\ \frac{\alpha}{L}Sh_\alpha & \frac{\alpha}{L}Ch_\alpha & \frac{\beta}{L}Sh_\beta & \frac{\beta}{L}Ch_\beta & \frac{\gamma}{L}Sh_\gamma & \frac{\gamma}{L}Ch_\gamma & \frac{-\delta}{L}S_\delta & \frac{\delta}{L}C_\delta & \frac{-\eta}{L}S_\eta & \frac{\eta}{L}C_\eta & \frac{-\mu}{L}S_\mu & \frac{\mu}{L}C_\mu \end{bmatrix} \begin{bmatrix} C_1 \\ C_2 \\ C_3 \\ C_4 \\ C_5 \\ C_6 \\ C_7 \\ C_8 \\ C_9 \\ C_{10} \\ C_{11} \\ C_{12} \end{bmatrix} \tag{6.47}$$

i.e.

$$\mathbf{d=sc} \tag{6.48}$$

where

$$Ch_\alpha = \cosh\alpha,\ Ch_\beta = \cosh\beta,\ Ch_\gamma = \cosh\gamma,\ C_\delta = \cos\delta,\ C_\eta = \cos\eta,\ C_\mu = \cos\mu$$
$$Sh_\alpha = \sinh\alpha,\ Sh_\beta = \sinh\beta,\ Sh_\gamma = \sinh\gamma,\ S_\delta = \sin\delta,\ S_\eta = \sin\eta,\ S_\mu = \sin\mu \tag{6.49}$$

Hence the vector of constants **c** can be determined from Eq. (6.47) as

$$\mathbf{c=s^{-1}d} \tag{6.50}$$

In similar fashion the vector of nodal forces can be determined from Eqs. (6.36-42) and (6.45-46) as

$$\begin{bmatrix} Q_{1x} \\ M_{1x} \\ Q_{1y} \\ M_{1y} \\ T_1 \\ B_1 \\ Q_{2x} \\ M_{2x} \\ Q_{2y} \\ M_{2y} \\ T_2 \\ B_2 \end{bmatrix} = \begin{bmatrix} 0 & B_{1,2} & 0 & B_{1,4} & 0 & B_{1,6} & 0 & B_{1,8} & 0 & B_{1,10} & 0 & B_{1,12} \\ B_{2,1} & 0 & B_{2,3} & 0 & B_{2,5} & 0 & B_{2,7} & 0 & B_{2,9} & 0 & B_{2,11} & 0 \\ 0 & B_{3,2} & 0 & B_{3,4} & 0 & B_{3,6} & 0 & B_{3,8} & 0 & B_{3,10} & 0 & B_{3,12} \\ B_{4,1} & 0 & B_{4,3} & 0 & B_{4,5} & 0 & B_{4,7} & 0 & B_{4,9} & 0 & B_{4,11} & 0 \\ 0 & B_{5,2} & 0 & B_{5,4} & 0 & B_{5,6} & 0 & B_{5,8} & 0 & B_{5,10} & 0 & B_{5,12} \\ B_{6,1} & 0 & B_{6,3} & 0 & B_{6,5} & 0 & B_{6,7} & 0 & B_{6,9} & 0 & B_{6,11} & 0 \\ B_{7,1} & B_{7,2} & B_{7,3} & B_{7,4} & B_{7,5} & B_{7,6} & B_{7,7} & B_{7,8} & B_{7,9} & B_{7,10} & B_{7,11} & B_{7,12} \\ B_{8,1} & B_{8,2} & B_{8,3} & B_{8,4} & B_{8,5} & B_{8,6} & B_{8,7} & B_{8,8} & B_{8,9} & B_{8,10} & B_{8,11} & B_{8,12} \\ B_{9,1} & B_{9,2} & B_{9,3} & B_{9,4} & B_{9,5} & B_{9,6} & B_{9,7} & B_{9,8} & B_{9,9} & B_{9,10} & B_{9,11} & B_{9,12} \\ B_{10,1} & B_{10,2} & B_{10,3} & B_{10,4} & B_{10,5} & B_{10,6} & B_{10,7} & B_{10,8} & B_{10,9} & B_{10,10} & B_{10,11} & B_{10,12} \\ B_{11,1} & B_{11,2} & B_{11,3} & B_{11,4} & B_{11,5} & B_{11,6} & B_{11,7} & B_{11,8} & B_{11,9} & B_{11,10} & B_{11,11} & B_{11,12} \\ B_{12,1} & B_{12,2} & B_{12,3} & B_{12,4} & B_{12,5} & B_{12,6} & B_{12,7} & B_{12,8} & B_{12,9} & B_{12,10} & B_{12,11} & B_{12,12} \end{bmatrix} \begin{bmatrix} C_1 \\ C_2 \\ C_3 \\ C_4 \\ C_5 \\ C_6 \\ C_7 \\ C_8 \\ C_9 \\ C_{10} \\ C_{11} \\ C_{12} \end{bmatrix} \tag{6.51}$$

i.e.

$$\mathbf{f=bc} \tag{6.52}$$

where

$$B_{1,2} = t_2^u(\alpha^3 B_x - \alpha C_x) + y_s \alpha C_x \tag{6.53}$$

$$B_{1,4} = t_4^u(\beta^3 B_x - \beta C_x) + y_s \beta C_x \tag{6.54}$$

$$B_{1,6} = t_6^u(\gamma^3 B_x - \gamma C_x) + y_s \gamma C_x \tag{6.55}$$

$$B_{1,8} = t_8^u(-\delta^3 B_x - \delta C_x) + y_s \delta C_x \tag{6.56}$$

$$B_{1,10} = t_{10}^u(-\eta^3 B_x - \eta C_x) + y_s \eta C_x \tag{6.57}$$

$$B_{1,12} = t_{12}^u(-\mu^3 B_x - \mu C_x) + y_s \mu C_x \tag{6.58}$$

$$B_{2,1} = -t_1^u(\alpha^2 A_x) \tag{6.59}$$

$$B_{2,3} = -t_3^u(\beta^2 A_x) \tag{6.60}$$

$$B_{2,5} = -t_5^u(\gamma^2 A_x) \tag{6.61}$$

$$B_{2,7} = t_7^u(\delta^2 A_x) \tag{6.62}$$

$$B_{2,9} = t_9^u(\eta^2 A_x) \tag{6.63}$$

$$B_{2,11} = t_{11}^u(\mu^2 A_x) \tag{6.64}$$

$$B_{3,2} = t_2^v(\alpha^3 B_y - \alpha C_y) - x_s \alpha C_y \tag{6.65}$$

$$B_{3,4} = t_4^v(\beta^3 B_y - \beta C_y) - x_s \beta C_y \tag{6.66}$$

$$B_{3,6} = t_6^v(\gamma^3 B_y - \gamma C_y) - x_s \gamma C_y \tag{6.67}$$

$$B_{3,8} = t_8^v(-\delta^3 B_y - \delta C_y) - x_s \delta C_y \tag{6.68}$$

$$B_{3,10} = t_{10}^v(-\eta^3 B_y - \eta C_y) - x_s \eta C_y \tag{6.69}$$

$$B_{3,12} = t_{12}^v(-\mu^3 B_y - \mu C_y) - x_s \mu C_y \tag{6.70}$$

$$B_{4,1} = -t_1^v(\alpha^2 A_y) \tag{6.71}$$

$$B_{4,3} = -t_3^v(\beta^2 A_y) \tag{6.72}$$

$$B_{4,5} = -t_5^v(\gamma^2 A_y) \tag{6.73}$$

$$B_{4,7} = t_7^v(\delta^2 A_y) \tag{6.74}$$

$$B_{4,9} = t_9^v(\eta^2 A_y) \tag{6.75}$$

$$B_{4,11} = t_{11}^v(\mu^2 A_y) \tag{6.76}$$

$$B_{5,2} = t_2^u(y_s \alpha C_x) - t_2^v(x_s \alpha C_y) + \alpha^3 E_o - \alpha F_o \tag{6.77}$$

$$B_{5,4} = t_4^u(y_s \beta C_x) - t_4^v(x_s \beta C_y) + \beta^3 E_o - \beta F_o \tag{6.78}$$

$$B_{5,6} = t_6^u(y_s\gamma C_x) - t_6^v(x_s\gamma C_y) + \gamma^3 E_o - \gamma F_o \quad (6.79)$$

$$B_{5,8} = t_8^u(y_s\delta C_x) - t_8^v(x_s\delta C_y) - \delta^3 E_o - \delta F_o \quad (6.80)$$

$$B_{5,10} = t_{10}^u(y_s\eta C_x) - t_{10}^v(x_s\eta C_y) - \eta^3 E_o - \eta F_o \quad (6.81)$$

$$B_{5,12} = t_{12}^u(y_s\mu C_x) - t_{12}^v(x_s\mu C_y) - \mu^3 E_o - \mu F_o \quad (6.82)$$

$$B_{6,1} = -\alpha^2 D_o \quad (6.83)$$

$$B_{6,3} = -\beta^2 D_o \quad (6.84)$$

$$B_{6,5} = -\gamma^2 D_o \quad (6.85)$$

$$B_{6,7} = \delta^2 D_o \quad (6.86)$$

$$B_{6,9} = \eta^2 D_o \quad (6.87)$$

$$B_{6,11} = \mu^2 D_o \quad (6.88)$$

$$B_{7,1} = t_1^u(-\alpha^3 B_x Sh_\alpha + \alpha C_x Sh_\alpha) - y_s\alpha C_x Sh_\alpha \quad (6.89)$$

$$B_{7,2} = t_2^u(-\alpha^3 B_x Ch_\alpha + \alpha C_x Ch_\alpha) - y_s\alpha C_x Ch_\alpha \quad (6.90)$$

$$B_{7,3} = t_3^u(-\beta^3 B_x Sh_\beta + \beta C_x Sh_\beta) - y_s\beta C_x Sh_\beta \quad (6.91)$$

$$B_{7,4} = t_4^u(-\beta^3 B_x Ch_\beta + \beta C_x Ch_\beta) - y_s\beta C_x Ch_\beta \quad (6.92)$$

$$B_{7,5} = t_5^u(-\gamma^3 B_x Sh_\gamma + \gamma C_x Sh_\gamma) - y_s\gamma C_x Sh_\gamma \quad (6.93)$$

$$B_{7,6} = t_6^u(-\gamma^3 B_x Ch_\gamma + \gamma C_x Ch_\gamma) - y_s\gamma C_x Ch_\gamma \quad (6.94)$$

$$B_{7,7} = t_7^u(-\delta^3 B_x S_\delta - \delta C_x S_\delta) + y_s\delta C_x S_\delta \quad (6.95)$$

$$B_{7,8} = t_8^u(\delta^3 B_x C_\delta + \delta C_x C_\delta) - y_s\delta C_x C_\delta \quad (6.96)$$

$$B_{7,9} = t_9^u(-\eta^3 B_x S_\eta - \eta C_x S_\eta) + y_s\eta C_x S_\eta \quad (6.97)$$

$$B_{7,10} = t_{10}^u(\eta^3 B_x C_\eta + \eta C_x C_\eta) - y_s\eta C_x C_\eta \quad (6.98)$$

$$B_{7,11} = t_{11}^u(-\mu^3 B_x S_\mu - \mu C_x S_\mu) + y_s\mu C_x S_\mu \quad (6.99)$$

$$B_{7,12} = t_{12}^u(\mu^3 B_x C_\mu + \mu C_x C_\mu) - y_s\mu C_x C_\mu \quad (6.100)$$

$$B_{8,1} = t_1^u(\alpha^2 A_x Ch_\alpha) \quad (6.101)$$

$$B_{8,2} = t_2^u(\alpha^2 A_x Sh_\alpha) \quad (6.102)$$

$$B_{8,3} = t_3^u(\beta^2 A_x Ch_\beta) \quad (6.103)$$

$$B_{8,4} = t_4^u(\beta^2 A_x Sh_\beta) \quad (6.104)$$

$$B_{8,5} = t_5^u(\gamma^2 A_x Ch_\gamma) \tag{6.105}$$

$$B_{8,6} = t_6^u(\gamma^2 A_x Sh_\gamma) \tag{6.106}$$

$$B_{8,7} = -t_7^u(\delta^2 A_x C_\delta) \tag{6.107}$$

$$B_{8,8} = -t_8^u(\delta^2 A_x S_\delta) \tag{6.108}$$

$$B_{8,9} = -t_9^u(\eta^2 A_x C_\eta) \tag{6.109}$$

$$B_{8,10} = -t_{10}^u(\eta^2 A_x S_\eta) \tag{6.110}$$

$$B_{8,11} = -t_{11}^u(\mu^2 A_x C_\mu) \tag{6.111}$$

$$B_{8,12} = -t_{12}^u(\mu^2 A_x S_\mu) \tag{6.112}$$

$$B_{9,1} = t_1^v(-\alpha^3 B_y Sh_\alpha + \alpha C_y Sh_\alpha) + x_s \alpha C_y Sh_\alpha \tag{6.113}$$

$$B_{9,2} = t_2^v(-\alpha^3 B_y Ch_\alpha + \alpha C_y Ch_\alpha) + x_s \alpha C_y Ch_\alpha \tag{6.114}$$

$$B_{9,3} = t_3^v(-\beta^3 B_y Sh_\beta + \beta C_y Sh_\beta) + x_s \beta C_y Sh_\beta \tag{6.115}$$

$$B_{9,4} = t_4^v(-\beta^3 B_y Ch_\beta + \beta C_y Ch_\beta) + x_s \beta C_y Ch_\beta \tag{6.116}$$

$$B_{9,5} = t_5^v(-\gamma^3 B_y Sh_\gamma + \gamma C_y Sh_\gamma) + x_s \gamma C_y Sh_\gamma \tag{6.117}$$

$$B_{9,6} = t_6^v(-\gamma^3 B_y Ch_\gamma + \gamma C_y Ch_\gamma) + x_s \gamma C_y Ch_\gamma \tag{6.118}$$

$$B_{9,7} = t_7^v(-\delta^3 B_y S_\delta - \delta C_y S_\delta) - x_s \delta C_y S_\delta \tag{6.119}$$

$$B_{9,8} = t_8^v(\delta^3 B_y C_\delta + \delta C_y C_\delta) + x_s \delta C_y C_\delta \tag{6.120}$$

$$B_{9,9} = t_9^v(-\eta^3 B_y S_\eta - \eta C_y S_\eta) - x_s \eta C_y S_\eta \tag{6.121}$$

$$B_{9,10} = t_{10}^v(\eta^3 B_y C_\eta + \eta C_y C_\eta) + x_s \eta C_y C_\eta \tag{6.122}$$

$$B_{9,11} = t_{11}^v(-\mu^3 B_y S_\mu - \mu C_y S_\mu) - x_s \mu C_y S_\mu \tag{6.123}$$

$$B_{9,12} = t_{12}^v(\mu^3 B_y C_\mu + \mu C_y C_\mu) + x_s \mu C_y C_\mu \tag{6.124}$$

$$B_{10,1} = t_1^v(\alpha^2 A_y Ch_\alpha) \tag{6.125}$$

$$B_{10,2} = t_2^v(\alpha^2 A_y Sh_\alpha) \tag{6.126}$$

$$B_{10,3} = t_3^v(\beta^2 A_y Ch_\beta) \tag{6.127}$$

$$B_{10,4} = t_4^v(\beta^2 A_y Sh_\beta) \tag{6.128}$$

$$B_{10,5} = t_5^v(\gamma^2 A_y Ch_\gamma) \tag{6.129}$$

$$B_{10,6} = t_6^v(\gamma^2 A_y Sh_\gamma) \tag{6.130}$$

$$B_{10,7} = -t_7^v(\delta^2 A_y C_\delta) \tag{6.131}$$

$$B_{10,8} = -t_8^v(\delta^2 A_y S_\delta) \tag{6.132}$$

$$B_{10,9} = -t_9^v(\eta^2 A_y C_\eta) \tag{6.133}$$

$$B_{10,10} = -t_{10}^v(\eta^2 A_y S_\eta) \tag{6.134}$$

$$B_{10,11} = -t_{11}^v(\mu^2 A_y C_\mu) \tag{6.135}$$

$$B_{10,12} = -t_{12}^v(\mu^2 A_y S_\mu) \tag{6.136}$$

$$B_{11,1} = t_1^u(-y_s \alpha C_x Sh_\alpha) + t_1^v(x_s \alpha C_y Sh_\alpha) - \alpha^3 E_o Sh_\alpha + \alpha F_o Sh_\alpha \tag{6.137}$$

$$B_{11,2} = t_2^u(-y_s \alpha C_x Ch_\alpha) + t_2^v(x_s \alpha C_y Ch_\alpha) - \alpha^3 E_o Ch_\alpha + \alpha F_o Ch_\alpha \tag{6.138}$$

$$B_{11,3} = t_3^u(-y_s \beta C_x Sh_\beta) + t_3^v(x_s \beta C_y Sh_\beta) - \beta^3 E_o Sh_\beta + \beta F_o Sh_\beta \tag{6.139}$$

$$B_{11,4} = t_4^u(-y_s \beta C_x Ch_\beta) + t_4^v(x_s \beta C_y Ch_\beta) - \beta^3 E_o Ch_\beta + \beta F_o Ch_\beta \tag{6.140}$$

$$B_{11,5} = t_5^u(-y_s \gamma C_x Sh_\gamma) + t_5^v(x_s \gamma C_y Sh_\gamma) - \gamma^3 E_o Sh_\gamma + \gamma F_o Sh_\gamma \tag{6.141}$$

$$B_{11,6} = t_6^u(-y_s \gamma C_x Ch_\gamma) + t_6^v(x_s \gamma C_y Ch_\gamma) - \gamma^3 E_o Ch_\gamma + \gamma F_o Ch_\gamma \tag{6.142}$$

$$B_{11,7} = t_7^u(y_s \delta C_x S_\delta) + t_7^v(-x_s \delta C_y S_\delta) - \delta^3 E_o S_\delta - \delta F_o S_\delta \tag{6.143}$$

$$B_{11,8} = t_8^u(-y_s \delta C_x C_\delta) + t_8^v(x_s \delta C_y C_\delta) + \delta^3 E_o C_\delta + \delta F_o C_\delta \tag{6.144}$$

$$B_{11,9} = t_9^u(y_s \eta C_x S_\eta) + t_9^v(-x_s \eta C_y S_\eta) - \eta^3 E_o S_\eta - \eta F_o S_\eta \tag{6.145}$$

$$B_{11,10} = t_{10}^u(-y_s \eta C_x C_\eta) + t_{10}^v(x_s \eta C_y C_\eta) + \eta^3 E_o C_\eta + \eta F_o C_\eta \tag{6.146}$$

$$B_{11,11} = t_{11}^u(y_s \mu C_x S_\mu) + t_{11}^v(-x_s \mu C_y S_\mu) - \mu^3 E_o S_\mu - \mu F_o S_\mu \tag{6.147}$$

$$B_{11,12} = t_{12}^u(-y_s \mu C_x C_\mu) + t_8^v(x_s \mu C_y C_\mu) + \mu^3 E_o C_\mu + \mu F_o C_\mu \tag{6.148}$$

$$B_{12,1} = \alpha^2 D_o Ch_\alpha \tag{6.149}$$

$$B_{12,2} = \alpha^2 D_o Sh_\alpha \tag{6.150}$$

$$B_{12,3} = \beta^2 D_o Ch_\beta \tag{6.151}$$

$$B_{12,4} = \beta^2 D_o Sh_\beta \tag{6.152}$$

$$B_{12,5} = \gamma^2 D_o Ch_\gamma \tag{6.153}$$

$$B_{12,6} = \gamma^2 D_o Sh_\gamma \tag{6.154}$$

$$B_{12,7} = -\delta^2 D_o C_\delta \tag{6.155}$$

$$B_{12,8} = -\delta^2 D_o S_\delta \tag{6.156}$$

$$B_{12,9} = -\eta^2 D_o C_\eta \tag{6.157}$$

$$B_{12,10} = -\eta^2 D_o S_\eta \tag{6.158}$$

$$B_{12,11} = -\mu^2 D_o C_\mu \tag{6.159}$$

$$B_{12,12} = -\mu^2 D_o S_\mu \tag{6.160}$$

and

$$A_x = \frac{EI_x}{L^2},\ A_y = \frac{EI_y}{L^2} \tag{6.161a,b}$$

$$B_x = \frac{EI_x}{L^3},\ B_y = \frac{EI_y}{L^3} \tag{6.162a,b}$$

$$C_x = \frac{GA_x}{L},\ C_y = \frac{GA_y}{L} \tag{6.163a,b}$$

$$D_O = \frac{EI_{ww}}{L^2},\ E_o = \frac{EI_{ww}}{L^3},\ F_o = \frac{GJ_o}{L} \tag{6.164a,b,c}$$

Thus the required stiffness matrix **K** can be formed by substituting Eq.(6.50) into Eq. (6.52) as

$$\mathbf{k=bs^{-1}} \tag{6.165}$$

6.2.3 Wittrick-Williams Algorithm

The dynamic stiffness matrix, **K,** when assembled from the member stiffness matrices, yields the required natural frequencies as solutions of the equation

$$\mathbf{K\,D = 0} \tag{6.166}$$

The Wittrick-Williams algorithm can then be used again to solve this transcendental eigenvalue problem. The algorithm has already been explained in Section 2.2.2.1.2 and

here only two key equations for finding the natural frequencies of the structure exceeded by trial frequency ω^* are given for convenience as

$$J = J_0 + s\,\{\mathbf{K}\} \tag{6.167}$$

where

$$J_0 = \sum J_m \tag{6.168}$$

In the present case due to complicity of the expression it is impractical to determine the value of J_m for a structural member symbolically using direct approach. However the result is achieved by an argument based on Eq. (6.167) and applied Wittrick-Williams algorithm (Wittrick and Williams 1971) in reverse. The procedure corresponds to the one originally proposed by Howson and Williams (Howson and Williams 1973) and was described in Section 2.2.2.1.2.

The stiffness relationship for this single member with simply supported ends can be obtained by deleting appropriate rows and columns from Eq. (6.165) as

$$\begin{bmatrix} M_{1x} \\ M_{1y} \\ B_1 \\ M_{2x} \\ M_{2y} \\ B_2 \end{bmatrix} = \begin{bmatrix} K_{2,2} & K_{2,4} & K_{2,6} & K_{2,8} & K_{2,10} & K_{2,12} \\ K_{4,2} & K_{4,4} & K_{4,6} & K_{4,8} & K_{4,10} & K_{4,12} \\ K_{6,2} & K_{6,4} & K_{6,6} & K_{6,8} & K_{6,10} & K_{6,12} \\ K_{8,2} & K_{8,4} & K_{8,6} & K_{8,8} & K_{8,10} & K_{8,12} \\ K_{10,2} & K_{10,4} & K_{10,6} & K_{10,8} & K_{10,10} & K_{10,12} \\ K_{12,2} & K_{12,4} & K_{12,6} & K_{12,8} & K_{12,10} & K_{12,12} \end{bmatrix} \begin{bmatrix} \theta_{1x} \\ \theta_{1y} \\ \Phi_1' \\ \theta_{2x} \\ \theta_{2y} \\ \Phi_2' \end{bmatrix} \tag{6.169}$$

or

$$\mathbf{m_{ss}} = \mathbf{k_{ss}}\,\boldsymbol{\theta}_{ss} \tag{6.170}$$

where $\mathbf{k_{ss}}$ is the required 6×6 stiffness matrix of this simple one-member structure .

Application of the Wittrick-Williams algorithm to this simple structure gives

$$J_{ss} = J_m + s\{\mathbf{k}_{ss}\} \tag{6.171}$$

or

$$J_m = J_{ss} - s\{\mathbf{k}_{ss}\} \tag{6.172}$$

Where J_m, J_{ss}, and $s\{\mathbf{k}_{ss}\}$ have already been defined in Section 2.2.2.1.2.

Evaluation of J_{ss} relates to the boundary conditions that yield a simple exact solution, as explained below.

For the simply supported case, the boundary conditions are defined for

$$\xi = 0 \text{ and } \xi = 1 \text{ as } U = V = \Phi = 0 \text{ and } M_x = M_y = B = 0 \tag{6.173}$$

Based on Eqs. (6.32a-c), (6.36-37) and (6.40), these conditions are satisfied by assuming solutions for the displacements $U(\xi)$, $V(\xi)$ and $\Phi(\xi)$ of the form

$$U(\xi) = C_i \sin(i\pi\xi) \qquad (i = 1,2,3,\ldots,\infty) \tag{6.174a}$$

$$V(\xi) = D_i \sin(i\pi\xi) \qquad (i = 1,2,3,\ldots,\infty) \tag{6.174b}$$

$$\Phi(\xi) = E_i \sin(i\pi\xi) \qquad (i = 1,2,3,\ldots,\infty) \tag{6.174c}$$

where C_i, D_i and E_i are constants.

Substituting Eqs. (6.174a-c) into Eq. (6.25) gives

$$\begin{bmatrix} (i\pi)^4+\alpha_x^2(i\pi)^2-\omega^2\beta_x^2 & 0 & -y_s\alpha_x^2(i\pi)^2+y_c\omega^2\beta_x^2 \\ 0 & (i\pi)^4+\alpha_y^2(i\pi)^2-\omega^2\beta_y^2 & x_s\alpha_y^2(i\pi)^2-x_c\omega^2\beta_y^2 \\ -y_s\dfrac{\alpha_x^2}{\gamma_x^2}(i\pi)^2+y_c\omega^2\dfrac{\beta_x^2}{\gamma_x^2} & x_s\dfrac{\alpha_y^2}{\gamma_y^2}(i\pi)^2-x_c\omega^2\dfrac{\beta_y^2}{\gamma_y^2} & (i\pi)^4+\alpha_\varphi^2(i\pi)^2-\omega^2\beta_\varphi^2 \end{bmatrix} \begin{bmatrix} C_i \\ D_i \\ E_i \end{bmatrix} = 0 \tag{6.175}$$

in which ω represents the coupled natural frequencies of the member with simply supported ends. The non-trivial solution of Eq. (6.175) is obtained when

$$\begin{vmatrix} (i\pi)^4+\alpha_x^2(i\pi)^2-\omega^2\beta_x^2 & 0 & -y_s\alpha_x^2(i\pi)^2+y_c\omega^2\beta_x^2 \\ 0 & (i\pi)^4+\alpha_y^2(i\pi)^2-\omega^2\beta_y^2 & x_s\alpha_y^2(i\pi)^2-x_c\omega^2\beta_y^2 \\ -y_s\dfrac{\alpha_x^2}{\gamma_x^2}(i\pi)^2+y_c\omega^2\dfrac{\beta_x^2}{\gamma_x^2} & x_s\dfrac{\alpha_y^2}{\gamma_y^2}(i\pi)^2-x_c\omega^2\dfrac{\beta_y^2}{\gamma_y^2} & (i\pi)^4+\alpha_\varphi^2(i\pi)^2-\omega^2\beta_\varphi^2 \end{vmatrix} = 0 \tag{6.176}$$

Eq. (6.176) is a cubic equation in ω^2 and yields three positive values of ω for each value of i. It is then possible to calculate J_{ss} for any trial value of ω^*. Once J_{ss} is known, J_m can be calculated from Eq. (6.172).

However, a very helpful simplification can be made to Eq. (6.176), based on the fact that the theory stems from the use of planar elements. It was shown in Chapter 2 that Eq. (2.61)yields the natural frequencies of a two-dimensional shear-flexural element with both ends simply supported as

$$\omega_{ss}^2=\frac{(i\pi)^2}{\beta^2}\left(\alpha^2+(i\pi)^2\right) \tag{6.177}$$

in which α and β are the parameters of the shear-flexural element defined in Section 2.2.2.1.2 as

$$\alpha=\frac{GA}{EI}L^2 \quad \text{and} \quad \beta=\frac{mL^4}{EI} \tag{6.178a,b}$$

Eq. (6.176) can then be rewritten in the following form

$$\begin{vmatrix} \frac{(i\pi)^2}{\beta_x^2}\left(\alpha_x^2+(i\pi)^2\right)-\omega^2 & 0 & -y_s\frac{GA_x}{mL^2}(i\pi)^2+y_c\omega^2 \\ 0 & \frac{(i\pi)^2}{\beta_y^2}\left(\alpha_y^2+(i\pi)^2\right)-\omega^2 & x_s\frac{GA_y}{mL^2}(i\pi)^2-x_c\omega^2 \\ -y_s\frac{GA_x}{mL^2}(i\pi)^2+y_c\omega^2 & x_s\frac{GA_y}{mL^2}(i\pi)^2-x_c\omega^2 & r_m^2\left(\frac{(i\pi)^2}{\beta_\varphi^2}\left(\alpha_\varphi^2+(i\pi)^2\right)-\omega^2\right) \end{vmatrix} = 0 \quad (6.179)$$

which reduces to

$$\begin{vmatrix} \omega_x^2-\omega^2 & 0 & -y_s\omega_{xf}^2+y_c\omega^2 \\ 0 & \omega_y^2-\omega^2 & x_s\omega_{yf}^2-x_c\omega^2 \\ -y_s\omega_{xf}^2+y_c\omega^2 & x_s\omega_{yf}^2-x_c\omega^2 & r_m^2\left(\omega_\varphi^2-\omega^2\right) \end{vmatrix} = 0 \quad (6.180)$$

where

$$\omega_x^2=\frac{(i\pi)^2}{\beta_x^2}\left(\alpha_x^2+(i\pi)^2\right) \quad (6.181a)$$

$$\omega_y^2=\frac{(i\pi)^2}{\beta_y^2}\left(\alpha_y^2+(i\pi)^2\right) \quad (6.181b)$$

$$\omega_\varphi^2=\frac{(i\pi)^2}{\beta_\varphi^2}\left(\alpha_\varphi^2+(i\pi)^2\right) \quad (6.181c)$$

where ω_x, ω_y and ω_φ are the natural frequencies of the analogous uncoupled member with both ends simply supported and

$$\omega_{xf}^2=\frac{(i\pi)^2 GA_x}{mL^2} \quad (6.182a)$$

$$\omega_{yf}^2=\frac{(i\pi)^2 GA_y}{mL^2} \quad (6.182b)$$

ω_{xf}^2 and ω_{yf}^2 are the natural frequencies of the equivalent planar shear beam when both ends are simply supported. See Eq. (2.97).

This again leads to the fact that the frequencies of a member with asymmetric cross-section may be obtained precisely by using the frequencies of the analogous uncoupled system in certain cases.

6.3 SUBSTITUTE FRAME METHOD

6.3.1 Application of the Substitute Frame Method in the Static and Dynamic Analysis of Asymmetric Three-Dimensional Wall-Frame Structures

The application of the substitute frame method in the analysis of symmetric three-dimensional wall-frame structures was studied in Section 3.3.2. In this section the method will be extended to cover the dynamic analysis of asymmetric three-dimensional wall-frame structures. In such structures the asymmetric arrangement of walls and frames results in different locations for the centres of mass and rigidity and hence the transverse response of the structure will always be coupled, i.e. the motion will be a combination of translation and torsion.

Consider Figure 6.1 again. It shows the plan view of a multi-storey wall-frame structure that is idealised as a set of plane walls and frames running in the x and y directions, as described in Section 6.2.1. The substitute frame method can be applied to the vibration analysis of such structures, in a similar way to the case of three-dimensional asymmetric frame structures. This means that such structures can be treated in a two step process i.e. the analogous uncoupled system can be analysed first then the relation between the uncoupled and coupled response may be applied through Eq. (5.57).

6.3.1.1 The analogous uncoupled system

In the analogous uncoupled system it is assumed that the centre of mass is coincident with the centre of rigidity, therefore the structure would be in pure translation or pure torsion. However in a wall-frame structure, due to the non proportional mode shapes of the walls and frames, the centres of rigidity of the floors inevitably do not lie on a common vertical line throughout the height of the structure. Hence it is not straightforward to define the analogous uncoupled system. Nevertheless the structure can be perceived as an equivalent proportional one, in which the centres of rigidity of the floors are considered to be located along a fictitious single vertical line.

In deciding how to estimate the location of the fictitious centre of rigidity R, i.e. the centre of torsional rotation, it is reasonable to approach it in terms of the likely significance of the centres of flexure and shear rigidity. It means that when the wall system is predominant in the lateral behaviour of the structure, the fictitious centre of rigidity will be close to the centre of flexural rigidity of the wall system O. On the other hand, the fictitious centre of rigidity will be close to the centre of shear rigidity of the frame system S when the frame system dominates the lateral motion. In the case where neither the wall nor the frame system is predominant, the fictitious centre of rigidity will be located between the centres of flexural rigidity O and shear rigidity S.

Wang et al. (Wang et al. 2000) has presented a method in which the position of the fictitious centre of rigidity can be determined from the ratio of the second natural frequency to the fundamental frequency of the structure, as follows.

Theoretically, the frequency ratio for a pure flexure cantilever is 6.27 and 3 for a pure shear cantilever. Since a frame system of regular shape is dominated by shear-type lateral deformation, it would be expected that its lateral modal frequency ratio will be close to the value of 3. On the other hand, a slender wall system is expected to have a frequency ratio close to the value of 6.27. This suggests that if the frequency ratio of a uniform multi-storey wall-frame structure in lateral motion is close to 6.27, the wall system in the building will be predominant in the lateral behaviour and the fictitious centre of rigidity will be close to the centre of flexural rigidity of the wall system. In contrast, the frame system in a building will be predominant in the lateral behaviour and the fictitious centre

of rigidity will be close to the centre of shear rigidity of the frame system if the frequency ratio approaches the value of 3. Therefore, the fictitious centre of rigidity may be determined from the frequency ratio of the lateral vibration modes by linear interpolation. In this study the frequency ratio of the structure will be obtained using the analogous uncoupled system in the x and y directions.

Three other options can be considered for determining the location of the fictitious centre of rigidity that makes the definition of the analogous uncoupled system much simpler. In the first case it would be assumed that the fictitious centre of rigidity coincides with the centre of flexural rigidity O. In the second case it would be assumed that it coincides with the centre of shear rigidity S. The third case assumes that the fictitious centre of rigidity is located at the middle point of the straight line connecting the centres of flexural and shear rigidities. Wang's method is termed as case 4.

Once the analogous uncoupled wall-frame system is defined, the uncoupled natural frequencies can be obtained using the three one-bay, multi-storey substitute planar wall-frames presented in Section 3.3.2. The final substitute wall-frames can be further simplified using the theory of Section 2.3.3 and be replaced by one-bay multi-storey substitute frames.

6.3.1.2 Coupling effect

Once the natural frequencies of the analogous uncoupled system are obtained, the final coupled natural frequencies of the asymmetric structure can be calculated using Eq. (5.57). In the numerical results section an extensive parametric study is undertaken to investigate the accuracy of the substitute frame method in the frequency analysis of asymmetric wall-frame structures using the analogous uncoupled system for the four cases defined earlier.

6.4 NUMERICAL RESULTS

The vibrational behaviour of asymmetric three-dimensional wall-frame structures is now investigated using the proposed methods. Example 6.1 compares the results obtained from the continuum method with those obtained from a full finite element analysis of the original structure using ETABS (Wilson et al. 1995). The structure considered is a 20 storey, multi-bay, asymmetric concrete wall-frame building. Examples 6.2 to 6.4 investigate the accuracy of the subtitute frame method. Example 6.2 considers a series of asymmetric wall-frame structures in which the walls and frames have almost equal rigidities. In Example 6.3 the frames make the most significant contribution, while in example 6.4 the wall system is predominant

6.4.1 Example 6.1

It is required to determine the coupled natural frequencies of a 20 storey building which has equal storey heights of 3m. The structure consist of 5 plane frames (F1-F5) and three shearwalls (W1-W3) in the y direction and also 4 plane frames (F6-F9) and three shearwalls (W4-W6) in the x direction, which are connected to each other by typical rigid diaphragms at each floor level with the arrangement shown in Figure 6.6.

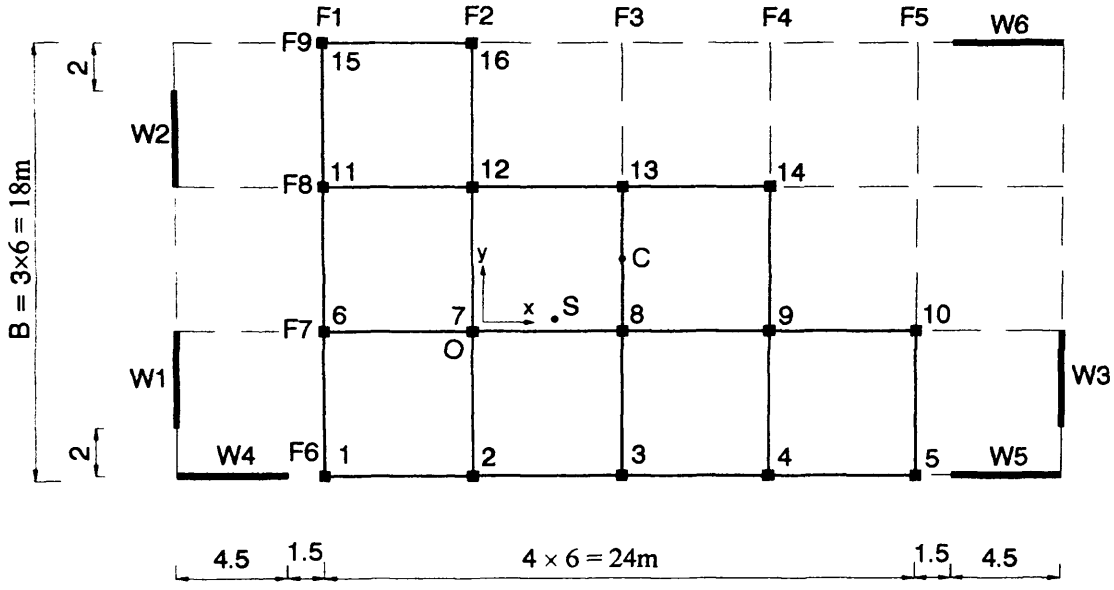

Figure 6.6 Floor plan of the 20 storey wall-frame structure considered in Example 6.1

For simplicity in determining member masses, half the mass of the walls and columns framing into and emanating from a floor diaphragm, together with the mass of the diaphragm and any associated beams, is stated as an equivalent uniformly distributed floor mass at that storey level. Thus the centre of mass is at the geometric centre of the floor plan. This corresponds precisely to the automatic idealisation process in ETABS (Wilson et al. 1995) and additionally only requires the total mass of the floor to be converted into the equivalent uniformly distributed mass of the member in the substitute beam approach. Arbitrarily the mass is assumed to have a constant value of 360 Kg/m^2 at each floor level, even where the stiffness properties of the member change. Young's modulus for all members is taken to be $E = 2 \times 10^{10}$ N/m^2 and inextensible member theory is assumed.

The properties of the structural elements change in a step-wise fashion every 10 storeys. Tables 6.1a and 6.1b show the second moment of area of the columns and beams about the x and y axes between the 1st-10th and 11th-20th floors of the building respectively. Also Tables 6.2a and 6.2b show the properties of the walls in the x and y directions between 1st-10th and 11th-20th floors respectively. Inextensible member theory is assumed.

Table 6.1a – The properties of the columns and beams of the building from the 1st to 10th floors

Ex. 6.1	Columns (members are defined in Figure 6.6)				Beams
	1,5,10,14,15,16	2,3,4,13	6,11	7,8,9,12	all
I_y(m^4)	0.0035	0.007	0.0035	0.007	0.003
I_x(m^4)	0.0035	0.0035	0.007	0.007	0.003

Table 6.1b – The properties of the columns and beams of the building from the 11th to 20th floors

Ex. 6.1	Columns (members are defined in Figure 6.6)				Beams
	1,5,10,14,15,16	2,3,4,13	6,11	7,8,9,12	all
I_y(m^4)	0.0025	0.005	0.0025	0.0025	0.002143
I_x(m^4)	0.0025	0.0025	0.005	0.0025	0.002143

Table 6.2a – The properties of the walls of the building from the 1st to 10th floors

Ex. 6.1	Shearwalls	Length (m)	Thickness (m)
Shearwalls in the y direction	W1, W2 and W3	4.0	0.2
Shearwalls in the x direction	W4, W5 and W6	4.5	0.2

Table 6.2b – The properties of the walls of the building from the 11th to 20th floors

Ex. 6.1	Shearwalls	Length (m)	Thickness (m)
Shearwalls in the y direction	W1, W2 and W3	4.0	0.15
Shearwalls in the x direction	W4, W5 and W6	4.5	0.15

All the plane frames and walls in this example are independently proprtional, so that the flexure and shear centre at each floor level lies in a vertical line through the building. The eccentricities in the x and y directions can then be calculated as follows

$$\begin{vmatrix} x_s = 3.273m \\ y_s = 0.500m \end{vmatrix}, \qquad \begin{vmatrix} x_c = 6m \\ y_c = 3m \end{vmatrix}$$

The effective distributed mass of the substitute beam (smeared from the diaphragm) and the polar mass radius of gyration of the diaphragms about the flexural rigidity centre O can be calculated as follows

$$m = 18 \times 36 \times 360/3 = 77760 \text{ kg/m}$$

$$r_m^2 = \frac{18^2 + 36^2}{12} + 6^2 + 3^2 = 180 \text{ m}^2$$

Tables 6.3a and 6.3b show the effective shear rigidities of the plane frames in the x and y directions obtained using the formula presented by Smith and Coull (Smith and Coull 1991) and the torsional rigidity of the buildings about the flexure centre O was calculated using Eq. (6.16).

Table 6.3a – Translational and torsional rigidities of the building from 1st to 10th floors

Plane Frames	x_i	y_j	GA_{xj} - 10^6 N	GA_{yi} - 10^6 N	GJ -10^6 Nm^2
F1	-6	-	-	98.824	3557.66
F2	0	-	-	98.824	0
F3	6	-	-	65.882	2371.75
F4	12	-	-	65.882	9487.01
F5	18	-	-	32.941	10672.88
F6	-	-6	131.764	-	4743.50
F7	-	0	131.764	-	0
F8	-	6	98.824	-	3557.66
F9	-	12	32.941	-	4743.50
Σ			GA_x=395.294	GA_y=362.353	GJ=39134

Table 6.3b – Translational and torsional rigidities of the building from 11th to 20th floors

Plane Frames	x_i	y_j	GA_{xj} - 10^6 N	GA_{yi} - 10^6 N	GJ -10^6 Nm^2
F1	-6	-	-	70.589	2541.20
F2	0	-	-	70.589	0
F3	6	-	-	45.059	1622.12
F4	12	-	-	45.059	6488.50
F5	18	-	-	23.529	7623.40
F6	-	-6	94.177	-	3390.37
F7	-	0	94.117	-	0
F8	-	6	70.589	-	2541.20
F9	-	12	23.529	-	3388.18
Σ			GA_x=282.353	GA_y=258.824	GJ=27594

Tables 6.4a and 6.4b show the translational and warping torsional rigidities of the plane walls about the flexural rigidity centre O.

Table 6.4a – Translational and warping rigidities of the building from the 1st to 10th floors

Walls	$\hat{x}_i$	$\hat{y}_j$	EI_{wxj} - 10^9 Nm^2	EI_{wyi} – 10^9 Nm^2	EI_{ww} -10^9 Nm^4
W1	-12	-	-	21.333	3071.95
W2	-12	-	-	21.333	3071.95
W3	24	-	-	21.333	12287.81
W4	-	-6	30.375	-	1093.5
W5	-	-6	30.375	-	1093.5
W6	-	12	30.375	-	4374
Σ			EI_x=91.125	EI_y=64.00	EI_{ww}=24992.7

Table 6.4b – Translational and warping rigidities of the building from the 11th to 20th floors

Walls	$\hat{x}_i$	$\hat{y}_j$	EI_{wxj} - 10^9 Nm^2	EI_{wyi} – 10^9 Nm^2	EI_{ww} -10^9 Nm^4
W1	-12	-	-	16	2303.96
W2	-12	-	-	16	2303.96
W3	24	-	-	16	9215.86
W4	-	-6	22.781	-	820.13
W5	-	-6	22.781	-	820.13
W6	-	12	22.781	-	3280.5
		Σ	EI_x=91.125	EI_y=64.00	EI_{ww}=18744.5

6.4.1.1 Results

Column 2 of Table 6.5 shows the coupled natural frequencies (Hz) of the 20 storey building obtained from the proposed continuum theory. For every ten storeys of the building, one element has been used and the final natural frequencies have been calculated using a Qbasic code that assembles the two elements. The third column in the table shows the results of a full finite element analysis of the structure (3D model of whole frame), obtained using the finite element programme ETABS (Wilson et al. 1995). Finally the fourth column shows the difference between the two, which never exceeds 7%. The difference is quite low (less than 5%) for the first three natural frequencies that play the most dominant role in the vibrational behaviour of structures. The results also show that the method presented has easily been able to model varying properties along the height of the structure with no additional loss of accuracy. The basic assumptions in modelling the structure with ETABS have been given in Section 5.4.1.1.

Table 6.5 - The coupled natural frequencies of the structure of Example 6.1 obtained from the continuum and FEM methods

Frequency No.	Continuum method	FEM (ETABS)	Difference%
	frequency(Hz)	frequency(Hz)	
1	0.30	0.29	3.45
2	0.36	0.35	2.86
3	0.44	0.42	4.70
4	1.12	1.08	3.57
5	1.33	1.27	4.51
6	1.79	1.70	5.29
7	2.53	2.40	5.41
8	3.06	2.88	6.25
9	4.50	4.22	6.63

6.4.2 Example 6.2

It is required to determine the coupled natural frequencies of a series of wall-frame structures using the substitute frame method and to investigate the accuracy of the method in the vibrational analsis of such structures. Twelve asymmetric wall-frame structures are considered and catagorised in the three groups labelled Groups 2a, 2b and 2c. Figures 6.6a, 6.6b and 6.6c show the arrangment of the frames, walls and rigid diaphragm for each group, respectively. Each group consists of a series of 5, 10, 20 and 30 storey asymmetric wall-frame structures with equal storey heights of 3m and uniform properties along the height of the structure. All the structures in this example consist of 5 plane frames and three shearwalls in the y direction and four plane frames and three shearwalls in the x direction, which are connected to each other by rigid diaphragms at each floor level. It is seen that in the structures of group 2a, the frames and walls have almost symmetric distribution around the centre of mass, while groups 2b and 2c include structures in which the walls or frames are mainly on one side of the centre of mass, C.

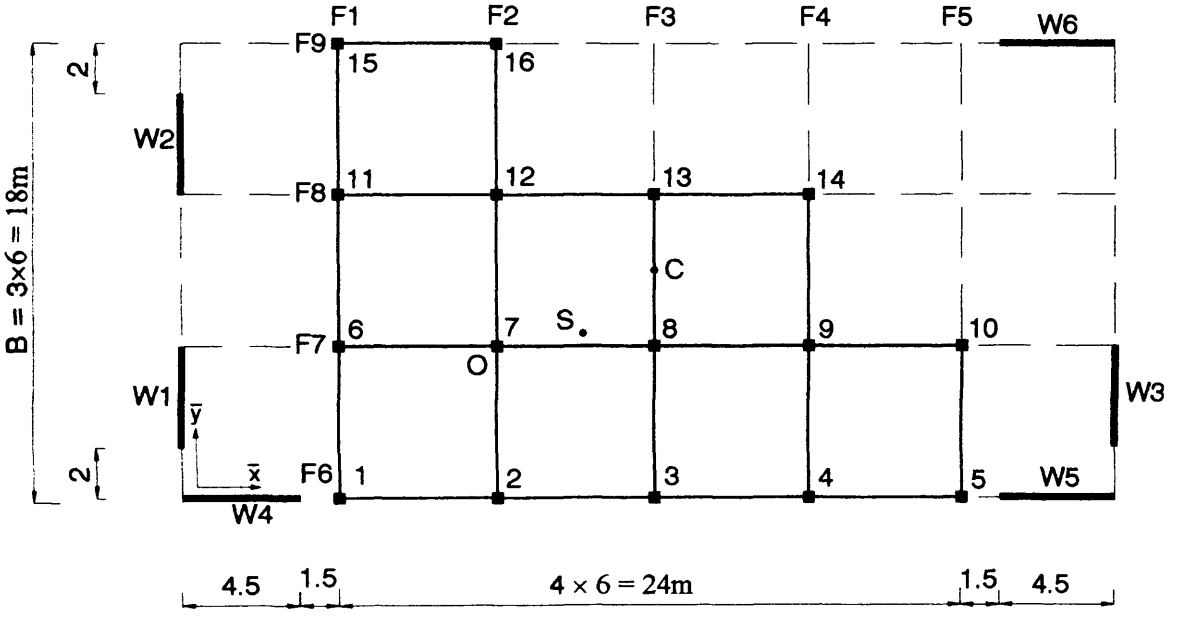

Figure 6.6a Floor plan of the structures considerd in groups 2a, 3a and 4a in Examples 6.2, 6.3 and 6.4 respectively

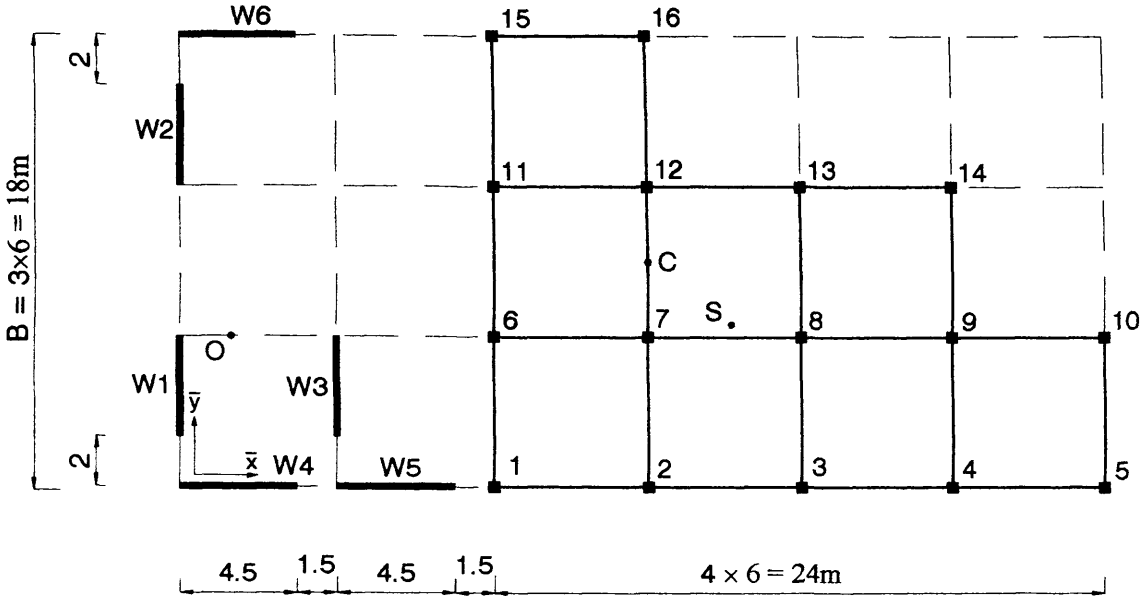

Figure 6.6b Floor plan of the structures considerd in groups 2b, 3b and 4b in Examples 6.2, 6.3 and 6.4 respectively

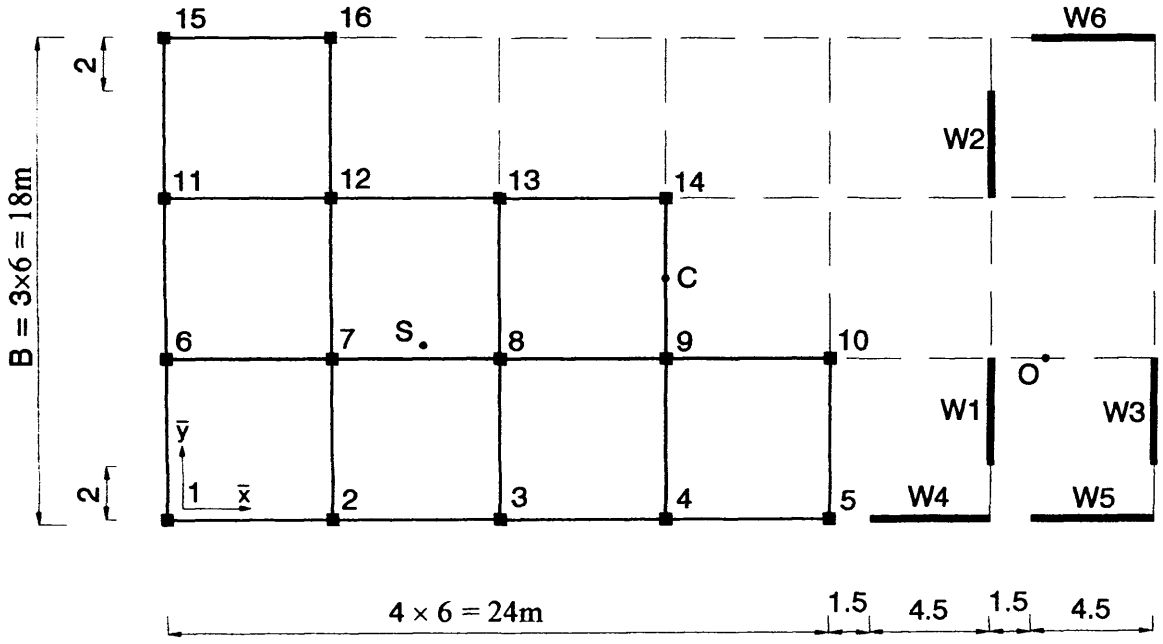

Figure 6.6c Floor plan of the structures considerd in groups 2c, 3c and 4c in Examples 6.2, 6.3 and 6.4 respectively

For simplicity in determining member masses, half the mass of the walls and columns framing into and emanating from a floor diaphragm, together with the mass of the diaphragm and any associated beams, is stated as an equivalent uniformly distributed floor mass at that storey level. Thus the centre of mass is at the geometric centre of the floor plan. This corresponds precisely to the automatic idealisation process in ETABS (Wilson et al. 1995) and additionally only requires the total mass of the floor to be converted into the equivalent uniformly distributed mass of the member in the substitute beam approach. Arbitrarily the mass is assumed to have a constant value of 360 Kg/m^2 at each floor level, even where the stiffness properties of the member change. Young's modulus for all members is taken to be $E = 2 \times 10^{10}$ N/m^2 and inextensible member theory is assumed.

Table 6.6 shows the second moment of area of the columns and beams about the x and y directions and Table 6.7 shows the characteristics of the shearwalls in the x and y directions..

Table 6.6 – The properties of the columns and beams of the structures in groups 2a, 2b and 2c

Groups 2a, 2b and 2c	Columns (members are defined in Figure 6.6a,b and c)				Beams
	1,5,10,14,15,16	2,3,4,13	6,11	7,8,9,12	all
$I_y(m^4)$	0.0035	0.007	0.0035	0.007	0.003
$I_x(m^4)$	0.0035	0.0035	0.007	0.007	0.003

Table 6.7 – The properties of the shearwalls of the structures in groups 2a, 2b and 2c

Groups 2a, 2b and 2c	Shearwalls	Length (m)	Thickness (m)
Shearwalls in the y direction	W1, W2 and W3	4.0	0.2
Shearwalls in the x direction	W4, W5 and W6	4.5	0.2

Once more, the plane frames and walls in this example are proprtional, so that the flexure and shear centre at each floor level lies in a vertical line through the building. The eccentricities for the structures of Groups 2a, 2b and 2c in the x and y directions of Figures 6.6a, 6.6b and 6.6c, respectively, can then be calculated as follows

Group 2a:

$$\begin{vmatrix} x_s = 3.273m \\ y_s = 0.500m \end{vmatrix}, \qquad \begin{vmatrix} x_c = 6m \\ y_c = 3m \end{vmatrix}$$

Group 2b:

$$\begin{vmatrix} x_s = 19.273m \\ y_s = 0.500m \end{vmatrix}, \qquad \begin{vmatrix} x_c = 16m \\ y_c = 3m \end{vmatrix}$$

Group 2c:

$$\begin{vmatrix} x_s = -22.727m \\ y_s = 0.500m \end{vmatrix}, \qquad \begin{vmatrix} x_c = -14m \\ y_c = 3m \end{vmatrix}$$

The structures will be analysed in a two step process i.e. first the analogous uncoupled system will be analysed using the substitute frame method assuming no eccentricities, then the relation between the uncoupled and coupled response will be obtained through Eq. (5.57).

Four cases can be assumed for determining the location of the fictitious centre of rigidity R (the centre of torsional rotation), which makes the definition of the analogous uncoupled system feasible. These four cases were described previously and are summarised as follows

Case 1: The fictitious centre of rigidity is at the centre of flexural rigidity (O)
Case 2: The fictitious centre of rigidity is at the centre of shear rigidity (S)
Case 3: The centre of fictitious rigidity is at the middle of a line connecting O and S
Case 4: The centre of fictitious rigidity is somewhere between O and S
based on the ratio of the 2nd to the 1st natural frequency

Table 6.8a shows the natural frequencies of the 10 storey wall-frame of Group 2a obtained from the substitute frame method of case 1 and compares it with the result of a full finite element analysis of the wall-frames, obtained using the finite element program ETABS (Wilson et al. 1995). Like the symmetric, three-dimensional, wall-frame

structures of Section 3.3.2, the final substitute frames are classified as type W-F and type F-F as shown in Figure 6.7.

In Table 6.8a, *i* in column 1 represents the mode of vibration and columns 3 and 6 show the uncoupled natural frequencies of the analogous uncoupled system in the x, y and torsional directions using substitute frame type W-F and F-F, respectively. Columns 4 and 7 in the table show the coupled natural frequencies obtained using Eq. (5.57), while columns 5 and 8 show the difference between W-F and F-F types, respectively, when compared to the finite element results in column 10. Column 9 shows the Importance Factor of the modes of vibration, which shows the contribution of every mode in the total response of the structure and has been explained in Appendix 6B. In the last row of the table, the average difference between the natural frequencies has been given after applying the importance factor to every mode.

Tables 6.8b, 6.8c and 6.8d show the same information for the 10 storey wall-frame for cases 2, 3 and 4 respectively.

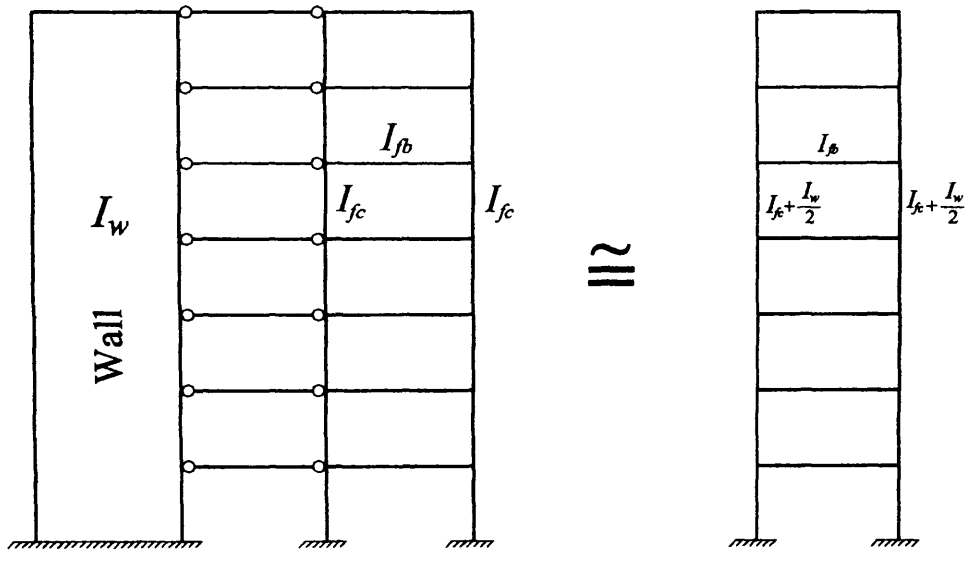

Figure 6.7 (a) Substitute wall-frame type W-F (b) Substitute frame type F-F

Table 6.8a – Uncoupled and Coupled natural frequencies of the 10 storey wall-frame structure of **Group 2a & Case 1**

Mode	Dir.	Uncoupled SF (W-F)	Coupled Eq.(5.57) (W-F)	Diff.% (W-F)	Uncoupled SF (F-F)	Coupled Eq.(5.57) (F-F)	Diff.% (F-F)	Imp. Factor	FEM ETABS
$i=1$	1(x)	5.9857	4.877	-1.26	6.2151	5.0644	2.58	0.847	4.9423
	2(y)	5.4268	5.8962	1.2	5.6562	6.1239	5.14	0.847	5.8302
	3(z)	6.7899	8.8568	17.19	6.9941	9.1542	21.16	0.847	7.5602
$i=2$	1(x)	26.3869	21.6923	0.78	26.0362	21.5146	-0.06	0.131	21.5324
	2(y)	23.1098	26.0169	0.59	22.9587	25.6792	-0.73	0.131	25.8682
	3(z)	34.8845	43.5235	13.84	34.3495	42.9141	12.25	0.131	38.2362
$i=3$	1(x)	64.5314	53.2893	1.51	60.9593	50.5942	-3.63	0.022	52.5043
	2(y)	56.2669	63.7002	0.44	53.396	60.1978	-5.07	0.022	63.4232
	3(z)	89.9343	111.0807	12.61	85.6788	105.7331	7.18	0.022	98.6467
Av. Diff.%		(W-F) : 6.32			(F-F) : 8.83				

Table 6.8b – Uncoupled and Coupled natural frequencies of the 10 storey wall-frame structure of **Group 2a & Case 2**

Mode	Dir.	Uncoupled SF (W-F)	Coupled Eq.(5.57) (W-F)	Diff.% (W-F)	Uncoupled SF (F-F)	Coupled Eq.(5.57) (F-F)	Diff.% (F-F)	Imp. Factor	FEM ETABS
$i=1$	1(x)	5.9857	5.196	5.22	6.2151	5.3994	9.26	0.847	4.9423
	2(y)	5.4268	5.8189	-0.17	5.6562	6.0409	3.77	0.847	5.8302
	3(z)	6.7331	7.5916	0.53	6.9208	7.8281	3.57	0.847	7.5602
$i=2$	1(x)	26.3869	22.6729	5.33	26.0362	22.5084	4.54	0.131	21.5324
	2(y)	23.1098	25.892	0.13	22.9587	25.5495	-1.23	0.131	25.8682
	3(z)	35.1527	38.3213	0.24	34.5927	37.7355	-1.3	0.131	38.2362
$i=3$	1(x)	64.5314	55.3962	5.51	60.9593	52.5787	0.16	0.022	52.5043
	2(y)	56.2669	63.501	0.13	53.396	60.0158	-5.37	0.022	63.4232
	3(z)	90.9653	98.5389	-0.11	86.6911	93.8463	-4.86	0.022	98.6467
Av. Diff.%		(W-F) : 1.96			(F-F) : 5.07				

Table 6.8c – Uncoupled and Coupled natural frequencies of the 10 storey wall-frame structure of **Group 2a & Case 3**

Mode	Dir.	Uncoupled SF (W-F)	Coupled Eq.(5.57) (W-F)	Diff.% (W-F)	Uncoupled SF (F-F)	Coupled Eq.(5.57) (F-F)	Diff.% (F-F)	Imp. Factor	FEM ETABS
$i=1$	1(x)	5.9857	5.0128	1.57	6.2151	5.2052	5.42	0.847	4.9423
	2(y)	5.4268	5.8654	0.68	5.6562	6.0915	4.63	0.847	5.8302
	3(z)	6.7158	8.1177	7.41	6.9083	8.3801	10.98	0.847	7.5602
$i=2$	1(x)	26.3869	22.1699	2.96	26.0362	21.996	2.17	0.131	21.5324
	2(y)	23.1098	25.9489	0.32	22.9587	25.6103	-1	0.131	25.8682
	3(z)	34.8638	40.4328	5.76	34.3157	39.8397	4.22	0.131	38.2362
$i=3$	1(x)	64.5314	54.3428	3.51	60.9593	51.5878	-1.73	0.022	52.5043
	2(y)	56.2669	63.5798	0.26	53.396	60.0879	-5.25	0.022	63.4232
	3(z)	90.1005	103.5971	5.03	85.8567	98.6385	0	0.022	98.6467
Av. Diff.%		(W-F) : 3.19			(F-F) : 6.31				

Table 6.8d – Uncoupled and Coupled natural frequencies of the 10 storey wall-frame structure of **Group 2a & Case 4**

Mode	Dir.	Uncoupled SF (W-F)	Coupled Eq.(5.57) (W-F)	Diff.% (W-F)	Uncoupled SF (F-F)	Coupled Eq.(5.57) (F-F)	Diff.% (F-F)	Imp. Factor	FEM ETABS
$i=1$	1(x)	5.9857	5.0436	2.18	6.2151	5.2374	6.02	0.847	4.9423
	2(y)	5.4268	5.8581	0.51	5.6562	6.0836	4.46	0.847	5.8302
	3(z)	6.712	8.0038	5.95	6.9032	8.2607	9.39	0.847	7.5602
$i=2$	1(x)	26.3869	22.2645	3.43	26.0362	22.0919	2.64	0.131	21.5324
	2(y)	23.1098	25.9364	0.28	22.9587	25.5974	-1.03	0.131	25.8682
	3(z)	34.8939	39.965	4.53	34.3435	39.3739	2.99	0.131	38.2362
$i=3$	1(x)	64.5314	54.5452	3.89	60.9593	51.7784	-1.37	0.022	52.5043
	2(y)	56.2669	63.5599	0.22	53.396	60.0697	-5.28	0.022	63.4232
	3(z)	90.2078	102.4702	3.88	85.9616	97.5704	-1.09	0.022	98.6467
Av. Diff.%		(W-F) : 2.86			(F-F) : 5.96				

Similar tables have been produced for the 12 wall-frame structures of Example 6.2, which are not presented here due to lack of space. However Figures 6.8a to 6.8c show the

average differnce in the application of the substitute frame metehod (type W-F) on the structures of Groups 2a, 2b and 2c. Thus the data of Tables 6.8a-d corresponds to the second bar group of Figure 6.8a.. Figure 6.8d shows the average differences for the groups 2a, 2b and 2c in one graph. Figures 6.9a to 6.9d comprise the same information resulting from the application of the substitute frame method (type F-F). Finally Figure 6.10 compares the final average difference from the application of the substitute frame method (types W-F and F-F) on the structures of Example 6.2.

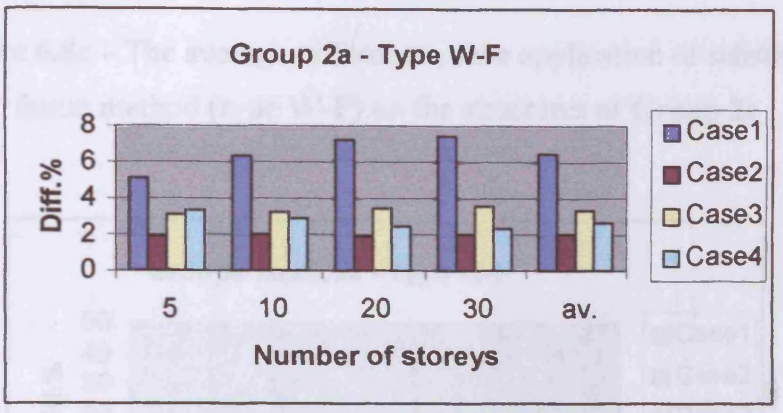

Figure 6.8a – The average difference in the application of substitute frame method **(type W-F)** on the structures of **Group 2a**

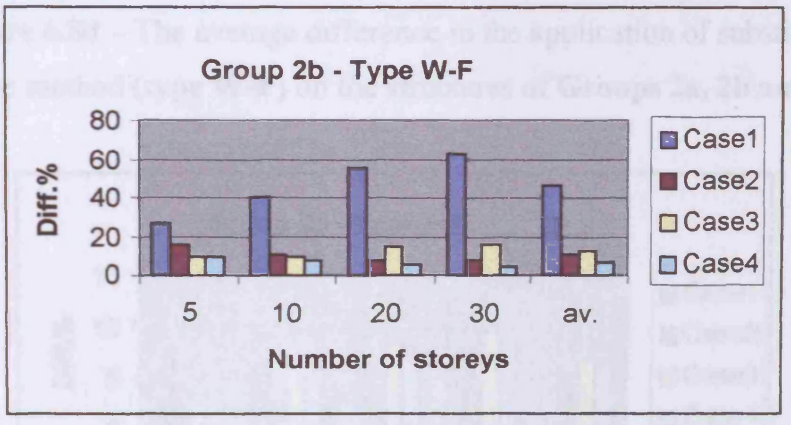

Figure 6.8b – The average difference in the application of substitute frame method **(type W-F)** on the structures of **Group 2b**

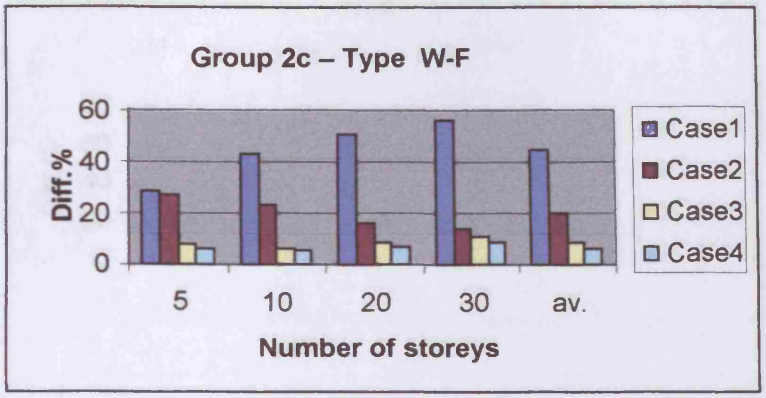

Figure 6.8c – The average difference in the application of substitute frame method **(type W-F)** on the structures of **Group 2c**

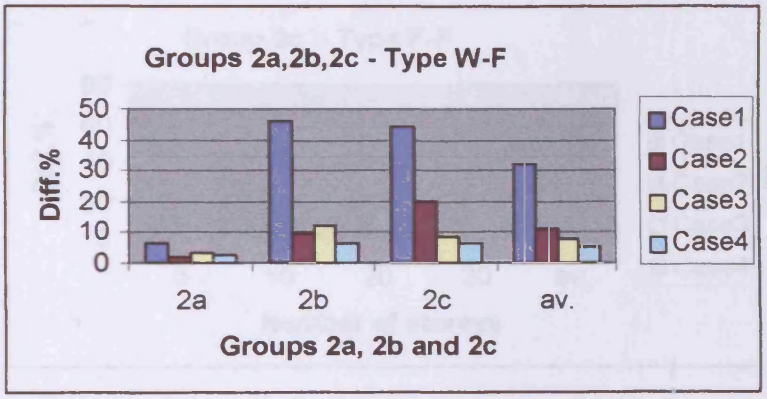

Figure 6.8d – The average difference in the application of substitute frame method **(type W-F)** on the structures of **Groups 2a, 2b and 2c**

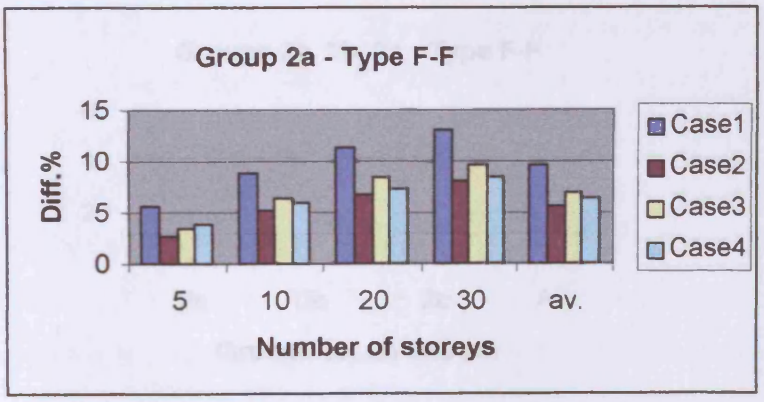

Figure 6.9a – The average difference in the application of substitute frame method **(type F-F)** on the structures of **Group 2a**

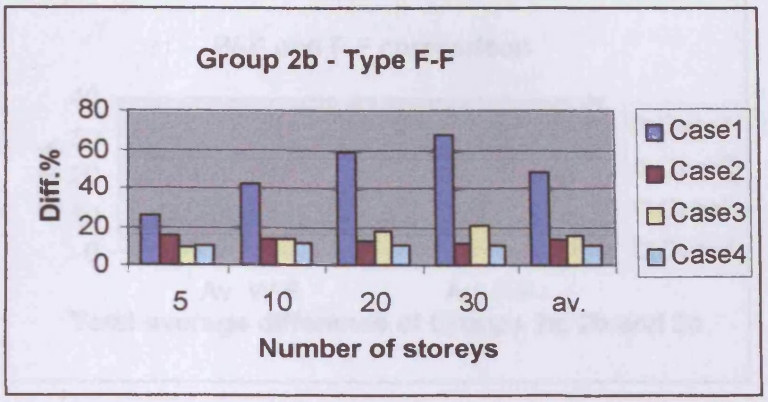

Figure 6.9b – The average difference in the application of substitute frame method **(type F-F)** on the structures of **Group 2b**

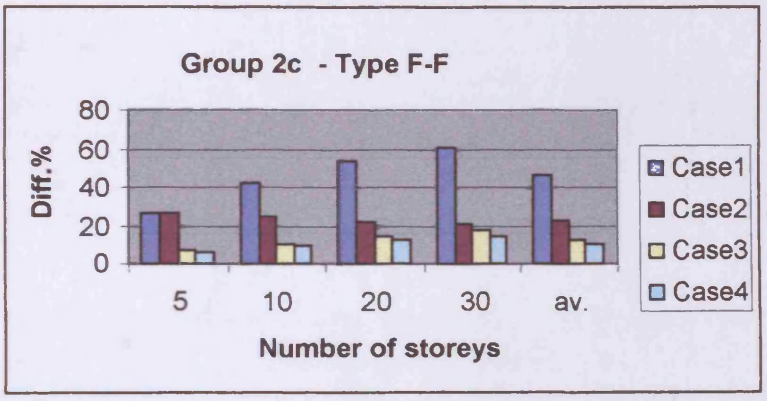

Figure 6.9c – The average difference in the application of substitute frame method **(type F-F)** on the structures of **Group 2c**

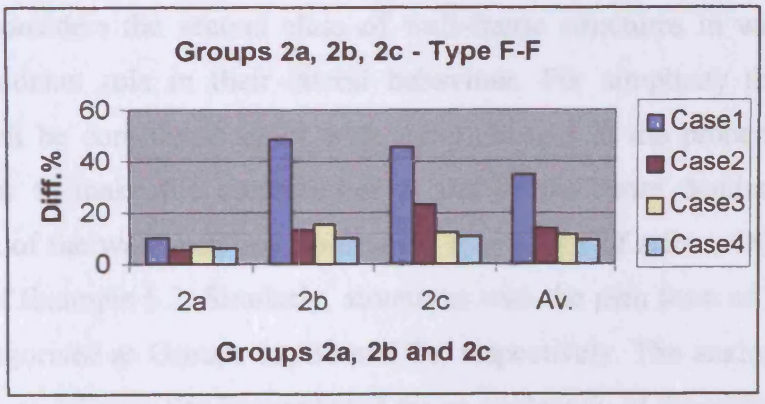

Figure 6.9d – The average difference in the application of substitute frame method **(type F-F)** on the structures of **Group 2a, 2b and 2c**

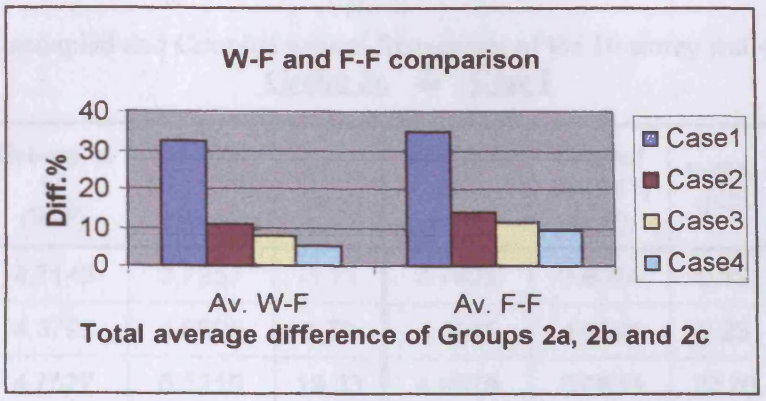

Figure 6.10 – The final average difference comparison in the application of the substitute frame method on the structures of Example 6.2

(Type W-F) & (Type F-F)

6.4.3 Example 6.3

This example considers the second class of wall-frame structures in which the frames provide the dominant role in their lateral behaviour. For simplicity the structures of Example 6.2 will be considered again with some changes in the properties of the wall system. In order to make the contribution of the frames more dominant, the second moment of area of the walls has been weakened by a factor of a four. Other data are the same as those of Example 6.2. Similarly, structures with the plan form of Figures 6.4, 6.5 and 6.6 are catagorised as Groups 3a, 3b and 3c, respectively. The analogous tables and graphs are given as follows. See Example 6.2 for an explanatio of the tables and graphs.

Table 6.9a – Uncoupled and Coupled natural frequencies of the 10 storey wall-frame structure of **Group 3a & Case 1**

Mode	Dir.	Uncoupled SF (W-F)	Coupled Eq.(5.57) (W-F)	Diff.% (W-F)	Uncoupled SF (F-F)	Coupled Eq.(5.57) (F-F)	Diff.% (F-F)	Imp. Factor	FEM ETABS
$i=1$	1(x)	4.7143	3.7357	-1.71	4.7422	3.8074	0.13	0.87	3.8052
	2(y)	4.3795	4.6505	1.79	4.4045	4.6798	2.23	0.87	4.5779
	3(z)	4.7527	6.5219	19.33	4.9379	6.6838	22.26	0.87	5.4721
$i=2$	1(x)	17.0946	14.0447	-1.19	16.5551	13.7274	-3.44	0.103	14.2191
	2(y)	15.5383	16.8517	1.01	15.1183	16.3349	-2.1	0.103	16.6914
	3(z)	19.8458	25.7185	16.69	19.6514	25.3277	14.92	0.103	22.041
$i=3$	1(x)	37.0957	30.835	0.14	33.8883	28.4774	-7.52	0.027	30.7964
	2(y)	33.1667	36.5948	0.6	30.4801	33.4679	-8	0.027	36.3816
	3(z)	47.63	59.9671	14.67	44.9712	56.2782	7.62	0.027	52.3031
Av. Diff.%		(W-F) : 7.41			(F-F) : 8.05				

Table 6.9b – Uncoupled and Coupled natural frequencies of the 10 storey wall-frame structure of **Group 3a & Case 2**

Mode	Dir.	Uncoupled SF (W-F)	Coupled Eq.(5.57) (W-F)	Diff.% (W-F)	Uncoupled SF (F-F)	Coupled Eq.(5.57) (F-F)	Diff.% (F-F)	Imp. Factor	FEM ETABS
$i=1$	1(x)	4.7143	3.9866	4.86	4.7422	4.0636	6.96	0.87	3.8052
	2(y)	4.3795	4.5679	-0.17	4.4045	4.6031	0.7	0.87	4.5779
	3(z)	4.6272	5.5058	0.69	4.812	5.639	3.07	0.87	5.4721
$i=2$	1(x)	17.0946	14.9382	5.07	16.5551	14.5717	2.54	0.103	14.2191
	2(y)	15.5383	16.657	-0.19	15.1183	16.1651	-3.12	0.103	16.6914
	3(z)	19.7388	22.1136	0.36	19.5443	21.7939	-1.09	0.103	22.041
$i=3$	1(x)	37.0957	32.4013	5.24	33.8883	29.8408	-3.07	0.027	30.7964
	2(y)	33.1667	36.3611	-0.03	30.4801	33.2893	-8.5	0.027	36.3816
	3(z)	47.8557	52.4481	0.29	45.2565	49.3857	-5.57	0.027	52.3031
Av. Diff.%		(W-F) :1.90			(F-F) :3.50				

Table 6.9c – Uncoupled and Coupled natural frequencies of the 10 storey wall-frame structure of **Group 3a & Case 3**

Mode	Dir.	Uncoupled SF (W-F)	Coupled Eq.(5.57) (W-F)	Diff.% (W-F)	Uncoupled SF (F-F)	Coupled Eq.(5.57) (F-F)	Diff.% (F-F)	Imp. Factor	FEM ETABS
$i=1$	1(x)	4.7143	3.8287	0.65	4.7422	3.9043	2.75	0.87	3.8052
	2(y)	4.3795	4.6222	1.14	4.4045	4.6531	1.79	0.87	4.5779
	3(z)	4.6462	5.9306	8.55	4.8304	6.076	11.11	0.87	5.4721
$i=2$	1(x)	17.0946	14.4327	1.56	16.5551	14.0972	-0.84	0.103	14.2191
	2(y)	15.5383	16.7723	0.53	15.1183	16.2649	-2.52	0.103	16.6914
	3(z)	19.6668	23.6109	7.17	19.474	23.2576	5.53	0.103	22.041
$i=3$	1(x)	37.0957	31.5763	2.55	33.8883	29.1315	-5.38	0.027	30.7964
	2(y)	33.1667	36.4803	0.3	30.4801	33.3781	-8.25	0.027	36.3816
	3(z)	47.5109	55.521	6.16	44.9058	52.1918	-0.2	0.027	52.3031
Av. Diff.%		(W-F) : 3.40			(F-F) :4.97				

Table 6.9d – Uncoupled and Coupled natural frequencies of the 10 storey wall-frame structure of **Group 3a & Case 4**

Mode	Dir.	Uncoupled SF (W-F)	Coupled Eq.(5.57) (W-F)	Diff.% (W-F)	Uncoupled SF (F-F)	Coupled Eq.(5.57) (F-F)	Diff.% (F-F)	Imp. Factor	FEM ETABS
$i=1$	1(x)	4.7143	3.9218	3.28	4.7422	3.9989	5.12	0.87	3.8052
	2(y)	4.3795	4.5916	0.48	4.4045	4.6248	1.14	0.87	4.5779
	3(z)	4.6237	5.6379	3.07	4.808	5.775	5.63	0.87	5.4721
$i=2$	1(x)	17.0946	14.7478	3.74	16.5551	14.394	1.27	0.103	14.2191
	2(y)	15.5383	16.7022	0.11	15.1183	16.2039	-2.88	0.103	16.6914
	3(z)	19.684	22.5746	2.45	19.4904	22.2432	0.95	0.103	22.041
$i=3$	1(x)	37.0957	32.1085	4.27	33.8883	29.5914	-3.88	0.027	30.7964
	2(y)	33.1667	36.4007	0.08	30.4801	33.3179	-8.41	0.027	36.3816
	3(z)	47.6789	53.3785	2.07	45.083	50.2318	-3.95	0.027	52.3031
Av. Diff.%		(W-F) : 2.26			(F-F) :3.77				

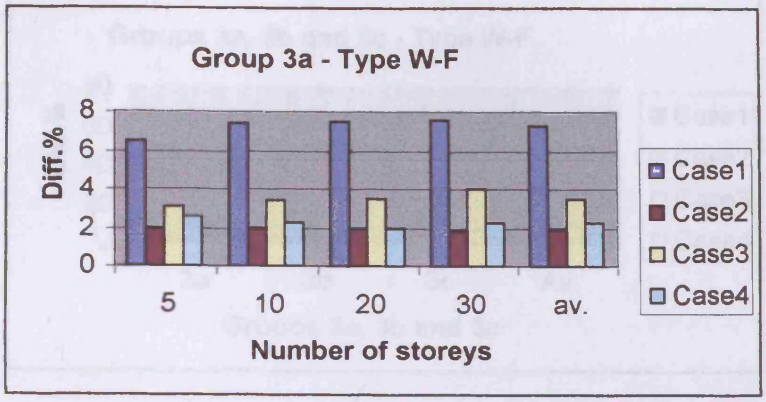

Figure 6.11a – The average difference in the application of substitute frame method **(type W-F)** on the structures of **Group 3a**

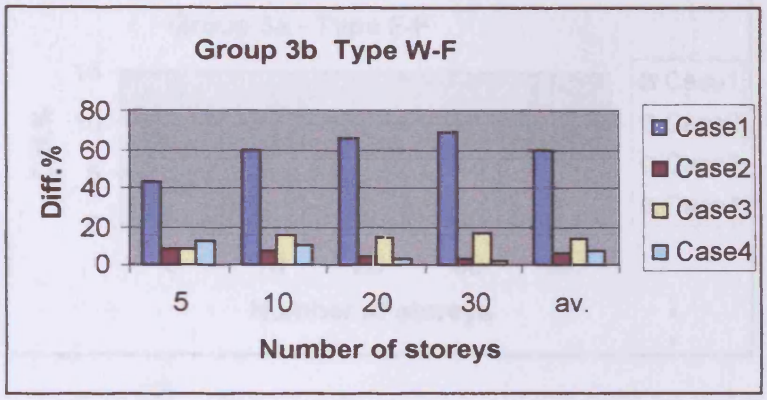

Figure 6.11b – The average difference in the application of substitute frame method **(type W-F)** on the structures of **Group 3b**

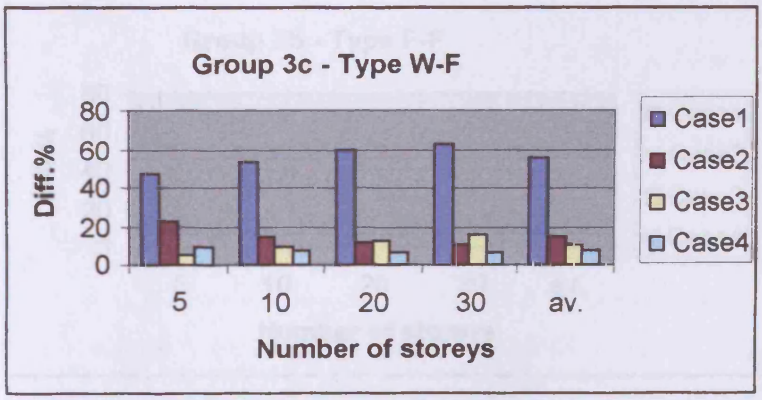

Figure 6.11c – The average difference in the application of substitute frame method **(type W-F)** on the structures of **Group 3c**

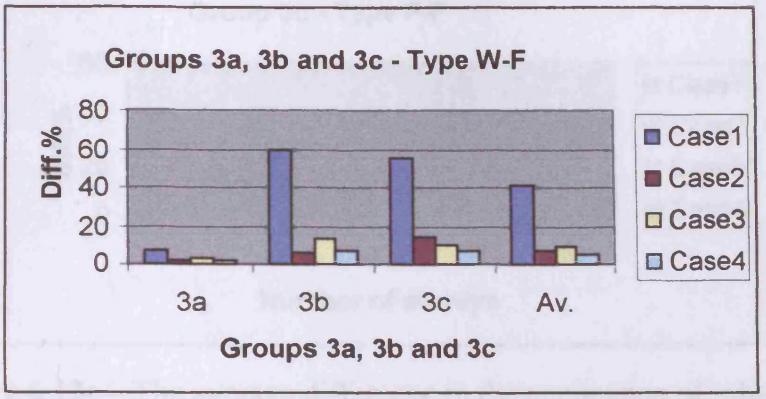

Figure 6.11d – The average difference in the application of substitute frame method **(type W-F)** on the structures of **Groups 3a, 3b and 3c**

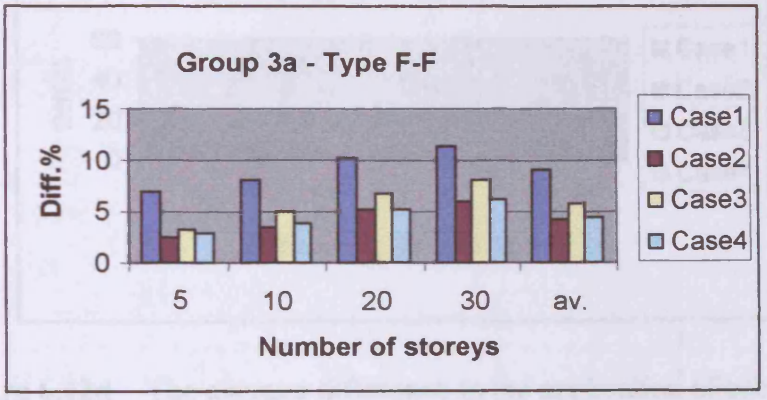

Figure 6.12a – The average difference in the application of substitute frame method **(type F-F)** on the structures of **Group 3a**

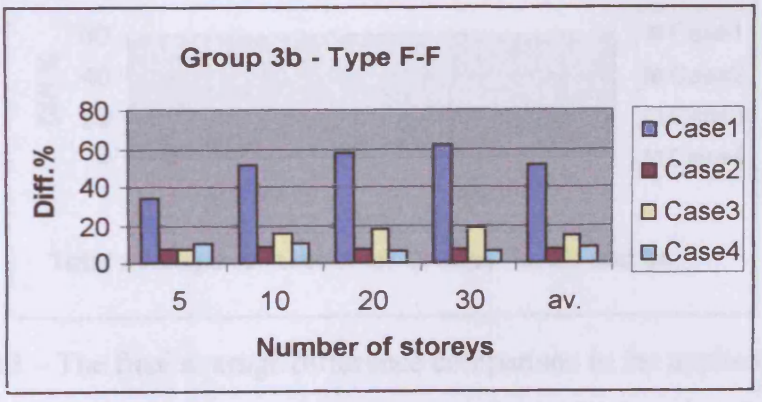

Figure 6.12b – The average difference in the application of substitute frame method **(type F-F)** on the structures of **Group 3b**

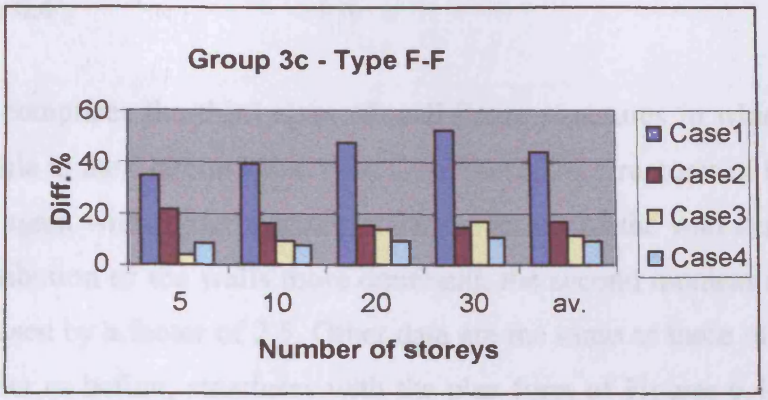

Figure 6.12c – The average difference in the application of substitute frame method **(type F-F)** on the structures of **Group 3c**

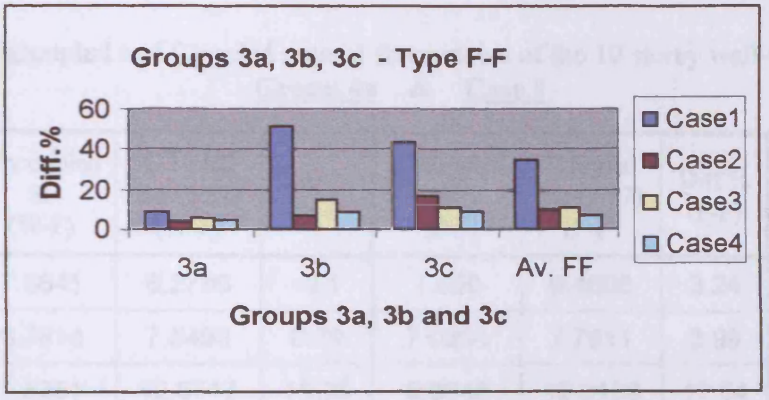

Figure 6.12d – The average difference in the application of substitute frame method **(type F-F)** on the structures of **Group 3a, 3b and 3c**

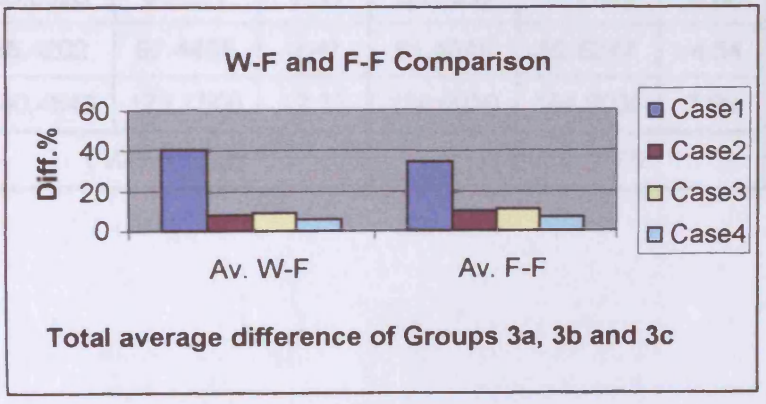

Figure 6.13 – The final average difference comparison in the application of the substitute frame method on the structures of Example 6.3

(Type W-F) & (Type F-F)

6.4.4 Example 6.4

This example comprises the third class of wall-frame structures in which walls provide the dominant role in their lateral behaviour. Once more, the structures of Example 6.2 will be considered again with some changes in the properties of the wall system. In order to make the contribution of the walls more dominant, the second moment area of the walls has been increased by a factor of 2.5. Other data are the same as those of Example 6.2. In the same manner as before, structures with the plan form of Figures 6.4, 6.5 and 6.6 are catagorised as groups 4a, 4b and 4c, respectively. The analogous tables and graphs are given bellow, but see Example 6.2 for an explanations of the tables and graphs.

Table 6.10a – Uncoupled and Coupled natural frequencies of the 10 storey wall-frame structure of **Group 4a & Case 1**

Mode	Dir.	Uncoupled SF (W-F)	Coupled Eq.(5.57) (W-F)	Diff.% (W-F)	Uncoupled SF (F-F)	Coupled Eq.(5.57) (F-F)	Diff.% (F-F)	Imp. Factor	FEM ETABS
$i=1$	1(x)	7.6641	6.2798	-0.1	7.899	6.4806	3.24	0.875	6.2861
	2(y)	6.7814	7.5493	0.79	7.0306	7.7811	3.99	0.875	7.4909
	3(z)	9.5361	12.0717	15.25	9.6848	12.3159	17.54	0.875	10.4815
$i=2$	1(x)	38.6811	31.5812	1.52	38.0396	31.1808	0.23	0.11	31.1177
	2(y)	33.3192	38.1568	0.5	32.9318	37.5293	-1.16	0.11	37.9687
	3(z)	53.4869	66.0556	12.94	52.4954	64.8911	10.95	0.11	58.489
$i=3$	1(x)	98.6925	81.221	1.85	93.7995	77.4617	-2.86	0.015	79.7501
	2(y)	85.4202	97.4455	0.42	81.4645	92.6347	-4.54	0.015	97.0458
	3(z)	140.4546	172.7506	12.22	134.0259	164.8035	7.06	0.015	153.943
Av. Diff.%		(W-F) : 5.33			(F-F) : 7.75				

Table 6.10b – Uncoupled and Coupled natural frequencies of the 10 storey wall-frame structure of **Group 4a & Case 2**

Mode	Dir.	Uncoupled SF (W-F)	Coupled Eq.(5.57) (W-F)	Diff.% (W-F)	Uncoupled SF (F-F)	Coupled Eq.(5.57) (F-F)	Diff.% (F-F)	Imp. Factor	FEM ETABS
$i=1$	1(x)	7.6641	6.6126	5.31	7.899	6.8393	8.81	0.875	6.2861
	2(y)	6.7814	7.492	0.12	7.0306	7.7152	3.06	0.875	7.4909
	3(z)	9.5582	10.5235	0.46	9.6898	10.7026	2.18	0.875	10.4815
$i=2$	1(x)	38.6811	32.8134	5.47	38.0396	32.4191	4.19	0.11	31.1177
	2(y)	33.3192	38.0402	0.21	32.9318	37.4084	-1.47	0.11	37.9687
	3(z)	54.0941	58.6164	0.23	53.0743	57.5355	-1.63	0.11	58.489
$i=3$	1(x)	98.6925	84.2193	5.6	93.7995	80.32	0.73	0.015	79.7501
	2(y)	85.4202	97.2041	0.17	81.4645	92.4065	-4.78	0.015	97.0458
	3(z)	142.2811	153.7675	-0.11	135.7869	146.7134	-4.69	0.015	153.943
Av. Diff.%		(W-F) :1.97			(F-F) :4.42				

Table 6.10c – Uncoupled and Coupled natural frequencies of the 10 storey wall-frame structure of **Group 4a & Case 3**

Mode	Dir.	Uncoupled SF (W-F)	Coupled Eq.(5.57) (W-F)	Diff.% (W-F)	Uncoupled SF (F-F)	Coupled Eq.(5.57) (F-F)	Diff.% (F-F)	Imp. Factor	FEM ETABS
$i=1$	1(x)	7.6641	6.4352	2.45	7.899	6.6457	5.79	0.875	6.2861
	2(y)	6.7814	7.5216	0.52	7.0306	7.7505	3.59	0.875	7.4909
	3(z)	9.4974	11.1575	6.48	9.6343	11.3651	8.48	0.875	10.4815
$i=2$	1(x)	38.6811	32.1986	3.48	38.0396	31.7993	2.19	0.11	31.1177
	2(y)	33.3192	38.0843	0.32	32.9318	37.4557	-1.34	0.11	37.9687
	3(z)	53.5818	61.6149	5.35	52.5776	60.5025	3.45	0.11	58.489
$i=3$	1(x)	98.6925	82.7371	3.75	93.7995	78.9071	-1.06	0.015	79.7501
	2(y)	85.4202	97.289	0.25	81.4645	92.4876	-4.69	0.015	97.0458
	3(z)	140.8541	161.4014	4.85	134.4189	153.9881	0.03	0.015	153.943
Av. Diff.%		(W-F) : 3.13			(F-F) : 5.49				

Table 6.10d – Uncoupled and Coupled natural frequencies of the 10 storey wall-frame structure of **Group 4a & Case 4**

Mode	Dir.	Uncoupled SF (W-F)	Coupled Eq.(5.57) (W-F)	Diff.% (W-F)	Uncoupled SF (F-F)	Coupled Eq.(5.57) (F-F)	Diff.% (F-F)	Imp. Factor	FEM ETABS
$i=1$	1(x)	7.6641	6.3995	1.81	7.899	6.6073	5.15	0.875	6.2861
	2(y)	6.7814	7.528	0.52	7.0306	7.7576	3.59	0.875	7.4909
	3(z)	9.4972	11.3286	8.1	9.6362	11.5432	10.2	0.875	10.4815
$i=2$	1(x)	38.6811	32.0634	3.06	38.0396	31.6636	1.78	0.11	31.1177
	2(y)	33.3192	38.0987	0.34	32.9318	37.4705	-1.29	0.11	37.9687
	3(z)	53.5268	62.4395	6.76	52.5256	61.3178	4.85	0.11	58.489
$i=3$	1(x)	98.6925	82.4076	3.33	93.7995	78.5931	-1.44	0.015	79.7501
	2(y)	85.4202	97.3194	0.29	81.4645	92.5162	-4.66	0.015	97.0458
	3(z)	140.6836	163.5069	6.21	134.2542	155.9947	1.34	0.015	153.943
Av. Diff.%		(W-F) : 3.46			(F-F) : 5.85				

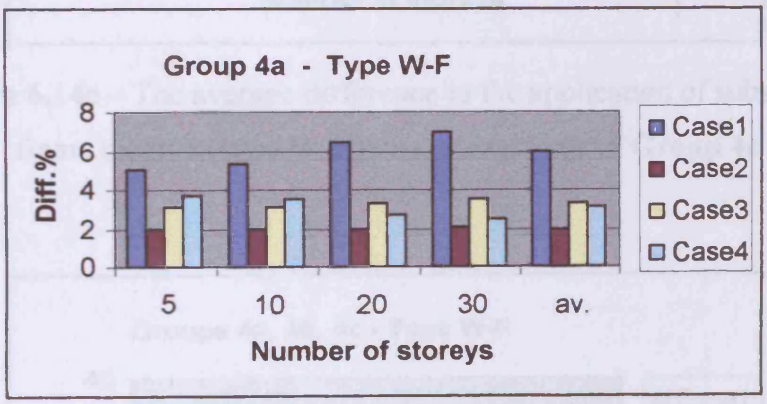

Figure 6.14a – The average difference in the application of substitute frame method **(type W-F)** on the structures of **Group 4a**

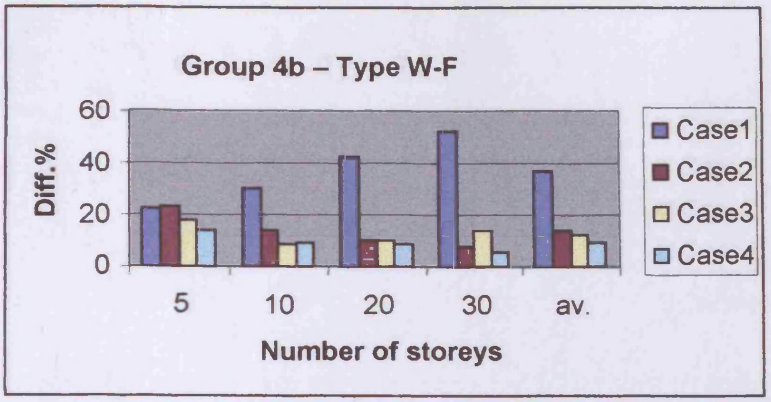

Figure 6.14b – The average difference in the application of substitute frame method **(type W-F)** on the structures of **Group 4b**

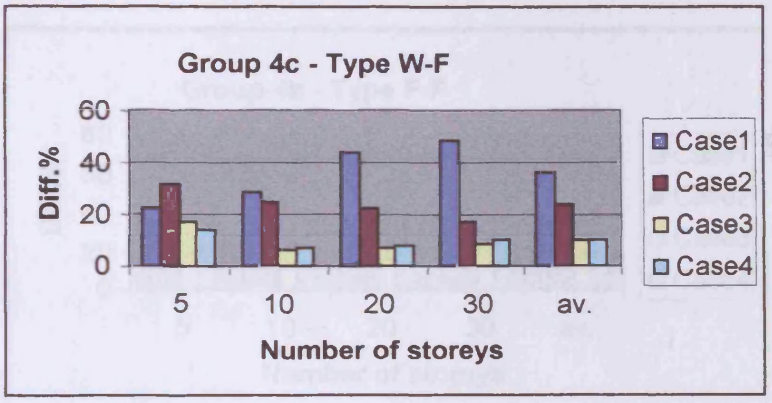

Figure 6.14c – The average difference in the application of substitute frame method **(type W-F)** on the structures of **Group 4c**

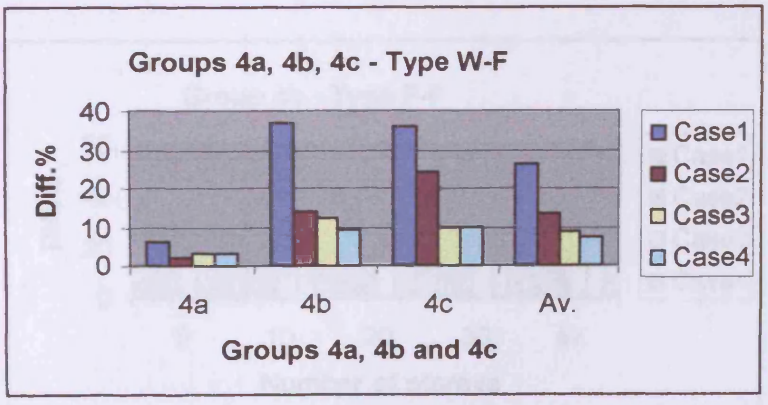

Figure 6.14d – The average difference in the application of substitute frame method **(type W-F)** on the structures of **Groups 4a, 4b and 4c**

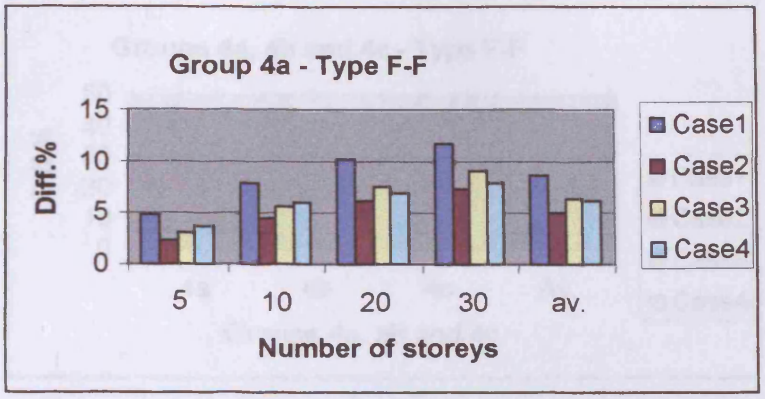

Figure 6.15a – The average difference in the application of substitute frame method **(type F-F)** on the structures of **Group 4a**

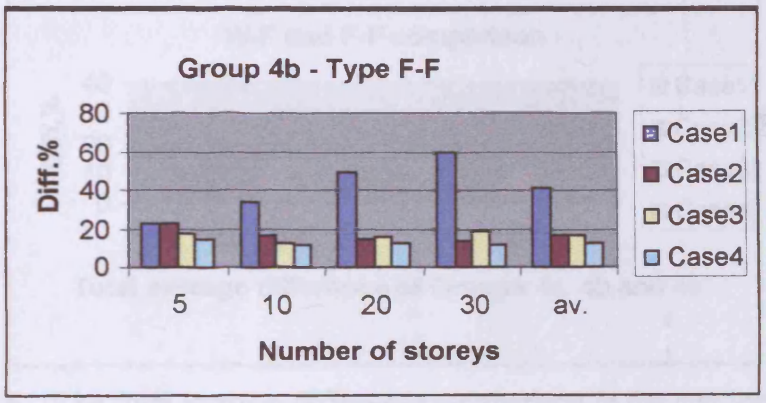

Figure 6.15b – The average difference in the application of substitute frame method **(type F-F)** on the structures of **Group 4b**

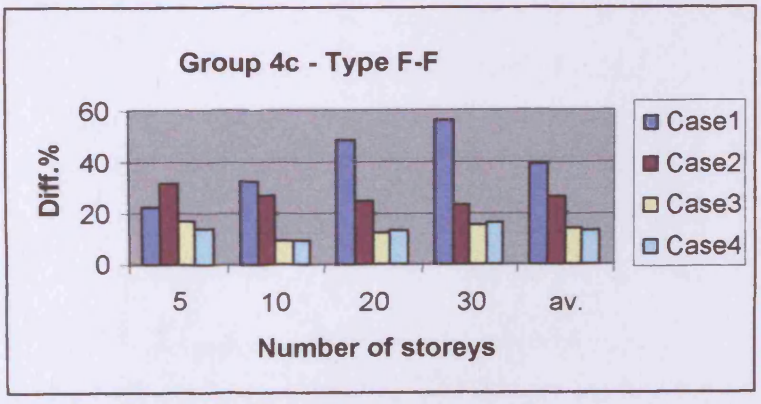

Figure 6.15c – The average difference in the application of substitute frame method **(type F-F)** on the structures of **Group 4c**

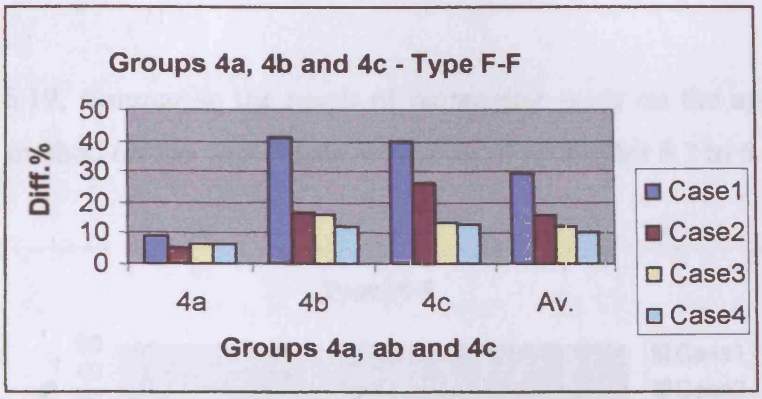

Figure 6.15d – The average difference in the application of substitute frame method **(type F-F)** on the structures of **Groups 4a, 4b and 4c**

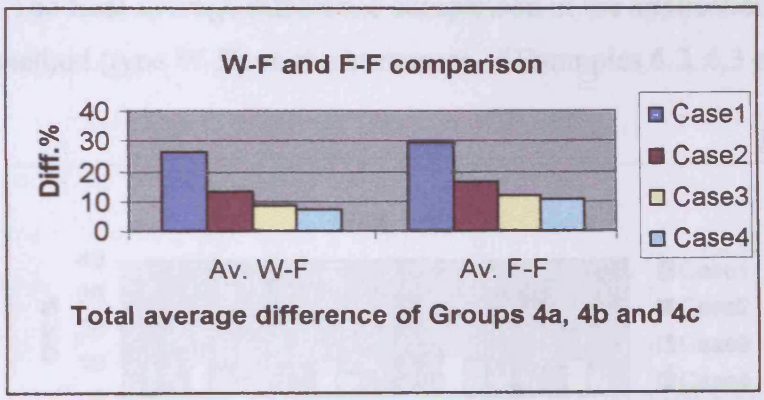

Figure 6.16 – The final average difference comparison in the application of the substitute frame method on the structures of Example 6.4

(Type W-F) & (Type F-F)

6.5 CONCLUSIONS

Figures 6.17 to 6.19, summarise the result of parametric study on the application of the substitute frame method on the wall-frame structures of Examples 6.2 to 6.4

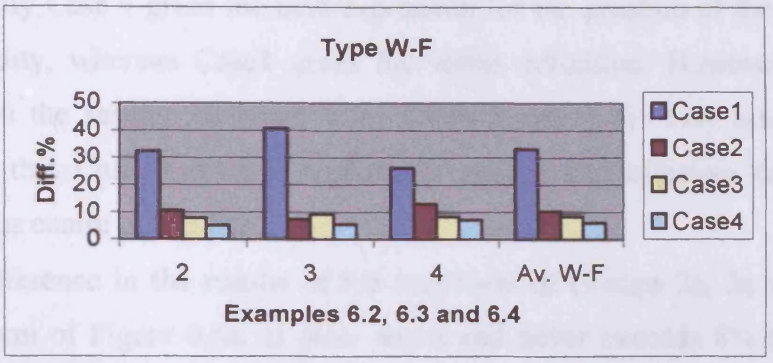

Figure 6.17 – The final average difference comparison in the application of substitute frame method (type W-F) on the structures of Examples 6.2, 6.3 and 6.4

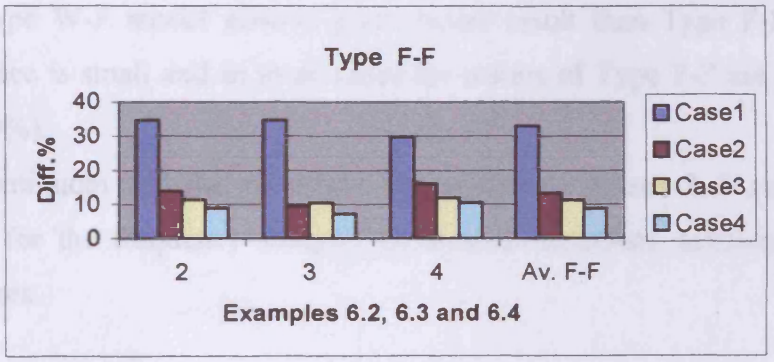

Figure 6.18 – The final average difference comparison in the application of substitute frame method (type F-F) on the structures of Examples 6.2, 6.3 and 6.4

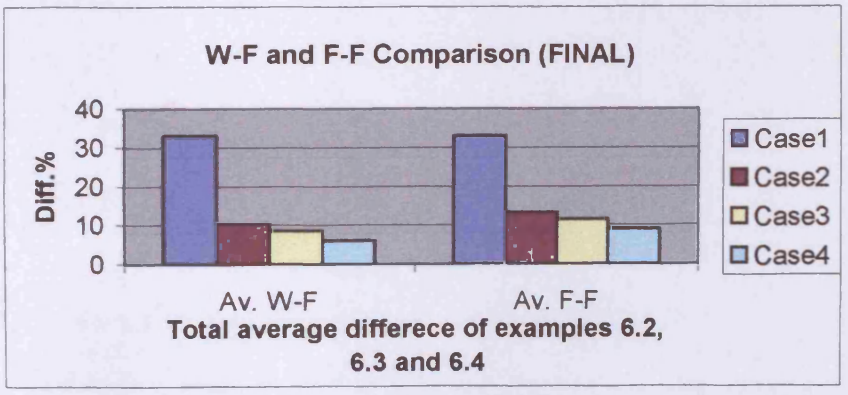

Figure 6.19 – The final average difference for types W-F and F-F

The following conclusions can be drawn from the parametric study of Examples 6.2-6.4.

- The substitute frame method gives better result when the frames and walls have an almost symmetric distribution around the centre of mass e.g. Figure 6.6a. See Figures 6.8d, 6.9d, 6.11d, 6.12d, 6.14d, 6.15d.
- Generally Case 4 gives the best expression for the position of the fictitious centre of rigidity, whereas Case1 gives the worst definition. However the difference between the results, obtained from Cases 3 and 4 are very small, so it would appear that Case 3 gives a reasonably simple and effective definition for the fictitious centre of rigidity.
- The difference in the results of the structures of Groups 2a, 3a and 4a, with the plan form of Figure 6.6a, is quite small and never exceeds 8% (Type W-F) and 12% (Type F-F). See Figures 6.8a, 6.9a, 6.11a, 6.12a, 6.14a, 6.15a.
- The examples show that the substitute frame method may be used for the analysis of wall-frame structures with acceptable accuracy (Figures 6.8a-d to 6.15a-d)
- The Type W-F model always gives better result than Type F-F. However the difference is small and in most cases the results of Type F-F are acceptable (less than 10%).
- The continuum and the substitute frame method (Cases 2, 3 and 4) give good results for the frequency analysis of three-dimensional, asymmetric wall-frame structures

Appendix 6A – The nature of the roots of the characteristic Eq. (6.27)

The nature of the roots of the characteristic Eq. (6.27) is investigated in this appendix. For this purpose, Eq. (6.27) is re-written again for convenience.

$$\begin{vmatrix} \tau^2 - \alpha_x^2\tau - \omega^2\beta_x^2 & 0 & y_s\alpha_x^2\tau + y_c\omega^2\beta_x^2 \\ 0 & \tau^2 - \alpha_y^2\tau - \omega^2\beta_y^2 & -x_s\alpha_y^2\tau - x_c\omega^2\beta_y^2 \\ y_s\dfrac{\alpha_x^2}{\gamma_x^2}\tau + y_c\omega^2\dfrac{\beta_x^2}{\gamma_x^2} & -x_s\dfrac{\alpha_y^2}{\gamma_y^2}\tau - x_c\omega^2\dfrac{\beta_y^2}{\gamma_y^2} & \tau - \alpha_\varphi^2\tau - \omega^2\beta_\varphi^2 \end{vmatrix} W(\xi) = 0 \qquad (6A.1)$$

Since α_x^2, α_y^2, λ_φ^2, β_x^2, β_y^2, β_φ^2, γ_x^2, γ_y^2, x_c, y_c, x_s and y_s are all real constants, the coefficients in Eq. (6A.1) are all real. It will be convenient to note that the left-hand side of Eq. (6A.1) is a 6th order polynomial function $f(\tau)$ so that

$$f(\tau) = \begin{vmatrix} A(\tau) & 0 & D(\tau) \\ 0 & B(\tau) & E(\tau) \\ \dfrac{1}{\gamma_x^2}D(\tau) & \dfrac{1}{\gamma_y^2}E(\tau) & C(\tau) \end{vmatrix} \qquad (6A.2)$$

in which

$$A(\tau) = \tau^2 - \alpha_x^2\tau - \omega^2\beta_x^2 \qquad (6A.3)$$

$$B(\tau) = \tau^2 - \alpha_y^2\tau - \omega^2\beta_y^2 \qquad (6A.4)$$

$$C(\tau) = \tau^2 - \alpha_\varphi^2\tau - \omega^2\beta_\varphi^2 \qquad (6A.5)$$

$$D(\tau) = y_s\alpha_x^2\tau + y_c\omega^2\beta_x^2 \qquad (6A.6)$$

$$E(\tau) = -x_s\alpha_y^2\tau - x_c\omega^2\beta_y^2 \qquad (6A.7)$$

The quantity $f(\tau)$ is a smooth continuous function that becomes infinite and positive as τ tends to $+\infty$ and $-\infty$ (Figure 6A.2). It is shown below that the quantity $f(\tau)$ has a negative value as τ tends zero.

Substituting zero for τ in Eq. (6A.2) gives

$$f(0)=\begin{vmatrix} -\omega^2\beta_x^2 & 0 & y_c\omega^2\beta_x^2 \\ 0 & -\omega^2\beta_y^2 & -x_c\omega^2\beta_y^2 \\ y_c\omega^2\frac{\beta_x^2}{\gamma_x^2} & -x_c\omega^2\frac{\beta_y^2}{\gamma_y^2} & -\omega^2\beta_\varphi^2 \end{vmatrix} \tag{6A.8}$$

or

$$f(0)=-\omega^2\beta_x^2(\omega^4\beta_y^2\beta_\varphi^2-\frac{1}{\gamma_y^2}x_c^2\omega^4\beta_y^2)+y_c\omega^2\beta_x^2(\frac{1}{\gamma_x^2}y_c\omega^2\beta_x^2\beta_y^2) \tag{6A.9}$$

Eq. (6A.9) can be simplified to

$$f(0)=-(1/r_m^2)(r_m^2-x_c^2-y_c^2)\beta_x^2\beta_y^2\beta_\varphi^2\omega^6 \tag{6A.10}$$

in which r_m is the polar mass radius of gyration about the flexural rigidity centre O and can be related to the polar mass radius of gyration about the centre of mass, r_{mc}, through the following equation

$$r_m^2=r_{mc}^2+x_c^2+y_c^2 \tag{6A.11}$$

Therefore

$$(r_m^2-x_c^2-y_c^2)>0 \tag{6A.12}$$

The right hand side of Eq. (6A.10) is the product of six positive parameters multiplied by a negative sign and therefore $f(0)$ is always negative.

$A(\tau)$ is a second order equation in terms of τ and always has one positive (x_1) and one negative (x_2) root as follows

$$x_1 = \frac{\alpha_x^2}{2} + \frac{1}{2}\sqrt{\alpha_x^4 + 4\omega^2\beta_x^2} \qquad (6A.13)$$

$$x_2 = \frac{\alpha_x^2}{2} - \frac{1}{2}\sqrt{\alpha_x^4 + 4\omega^2\beta_x^2} \qquad (6A.13)$$

Also $B(\tau)$ is a second order equation in terms of τ with one positive (y_1) and one negative (y_2) root as follows

$$y_1 = \frac{\alpha_y^2}{2} + \frac{1}{2}\sqrt{\alpha_y^4 + 4\omega^2\beta_y^2} \qquad (6A.13)$$

$$y_2 = \frac{\alpha_y^2}{2} - \frac{1}{2}\sqrt{\alpha_y^4 + 4\omega^2\beta_y^2} \qquad (6A.13)$$

Before discussing the roots of $f(\tau) = 0$ it is useful to calculate the quantity $f(\tau)$ when $\tau = x_1$ as follows

$$f(x_1) = -\frac{1}{\gamma_x^2} D^2(x_1) B(x_1) \qquad (6A.14)$$

Since γ_x^2 and $D^2(x_1)$ always have positive values, the sign of $f(x_1)$ only depends on the sign of $B(x_1)$.

Also the quantity $f(\tau)$ when $\tau = y_1$ can be written as

$$f(y_1) = -\frac{1}{\gamma_y^2} E^2(y_1) A(y_1) \qquad (6A.15)$$

Since γ_y^2 and $E^2(y_1)$ are always positive, the sign of $f(y_1)$ depends on the sign of $A(y_1)$

Eq. (6A.3) and Figure 6A.1(a) show that

$$A(\tau) < 0 \text{ when } x_2 < \tau < x_1 \tag{6A.16}$$

and

$$A(\tau) > 0 \text{ when } \tau > x_1 \text{ or } \tau < x_2. \tag{6A.17}$$

Similarly, Eq. (6A.4) and Figure 6A.1b show that

$$B(\tau) < 0 \text{ when } y_2 < \tau < y_1 \tag{6A.18}$$

and

$$B(\tau) > 0 \text{ when } \tau > y_1 \text{ or } \tau < y_2. \tag{6A.19}$$

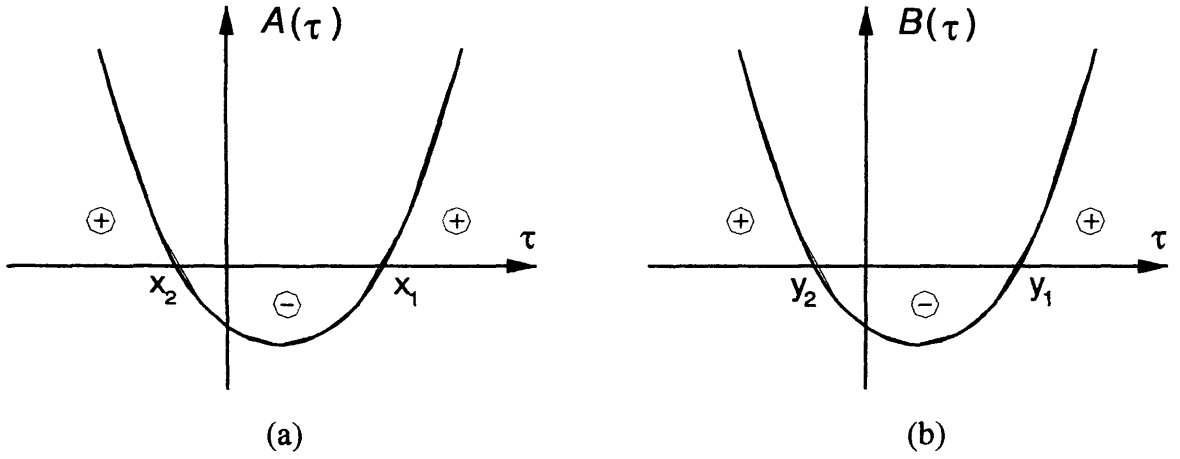

(a) (b)

Figure 6A.1 a) Graph of $A(\tau)$ versus τ b) Graph of $B(\tau)$ versus τ

We now wish to consider the two cases in which $x_1 < y_1$ and $x_1 > y_1$.

Figures 6A.1(a) and 6A.1(b) show that when $x_1 < y_1$ then $B(x_1) < 0$ and $A(y_1) > 0$ so that

$$f(x_1) > 0 \tag{6A.20}$$

$$f(y_1) < 0 \tag{6A.21}$$

The Figures also show that when $x_1 > y_1$ then $B(x_1) > 0$ and $A(y_1) < 0$ so that

$$f(x_1) < 0 \tag{6A.22}$$

$$f(y_1) > 0 \tag{6A.23}$$

If λ_1 represents the minimum value of x_1 and y_1, i.e. $\lambda_1 = \text{Min}[x_1, y_1]$, and λ_2 represents the maximum value of x_1 and y_1, i.e. $\lambda_2 = \text{Max}[x_1, y_1]$, then

$$f(0) < 0 \tag{6A.24}$$

$$f(\lambda_1) > 0 \tag{6A.25}$$

$$f(\lambda_2) < 0 \tag{6A.26}$$

$$f(\infty) > 0 \tag{6A.27}$$

This implies that there are at least three positive real roots of the function $f(\tau)$ in the intervals $(0, \lambda_1)$, (λ_1, λ_2) and (λ_2, ∞). See Figure 6A.2.

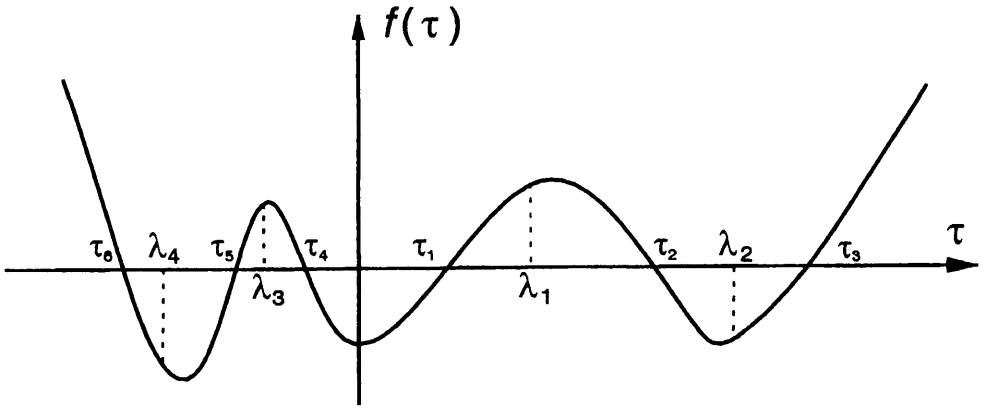

Figure 6A.2 Graph of $f(\tau)$ versus τ

With a similar argument, the nature of the roots of $f(\tau)$ for negative values of τ can be considered as follows

$$f(x_2) = -\frac{1}{\gamma_x^2} D^2(x_2) B(x_2) \tag{6A.28}$$

Since γ_x^2 and $D^2(x_2)$ always have positive values, the sign of $f(x_2)$ only depends on the sign of $B(x_2)$. In similar fashion
and

$$f(y_2) = -\frac{1}{\gamma_y^2} E^2(y_2) A(y_2) \tag{6A.29}$$

and γ_y^2 and $E^2(y_2)$ are always positive, thus the sign of $f(y_2)$ depends on the sign of $A(y_2)$

We now wish to consider the two cases in which $x_2 < y_2$ and $x_2 > y_2$.

Figures 6A.1 and 6A.2 show that when $x_2 < y_2$, $B(x_2) > 0$ and $A(y_2) < 0$ so that

$$f(x_2) < 0 \tag{6A.20}$$

$$f(y_2) > 0 \tag{6A.21}$$

The Figures also show that when $x_2 > y_2$, $B(x_2) < 0$ and $A(y_2) > 0$ so that

$$f(x_2) > 0 \tag{6A.22}$$

$$f(y_2) < 0 \tag{6A.23}$$

If λ_3 represents the maximum value of x_2 and y_2, i.e. $\lambda_3 = \text{Max}[x_2, y_2]$ and λ_4 represents the minimum value of x_2 and y_2, i.e. $\lambda_4 = \text{Min}[x_2, y_2]$, then

$$f(0) < 0 \tag{6A.24}$$

$$f(\lambda_3) > 0 \tag{6A.25}$$

$$f(\lambda_4) < 0 \tag{6A.26}$$

$$f(-\infty) > 0 \tag{6A.27}$$

This implies that there are at least three negative real roots of the function $f(\tau)$ in the intervals $(-\infty, \lambda_4)$, (λ_4, λ_3) and $(\lambda_3, 0)$. See Figure 6A.3.

Since Eq. (6A.1) is a six order equation in terms of τ, it has been proved that it will always have three negative and three positive real roots.

Appendix 6B – Importance factor of modes of vibration

The contribution of the lower natural frequencies on the overall response of a structure is greater than the higher frequencies, so it is reasonable to define an importance factor for every mode of vibration when calculating the average difference of the models. For this purpose, the contribution of every mode to the total base shear of the structure in the RSA method (Response Spectra Analysis) is defined as the importance factor of that mode.

Based on the theory of RSA, the base shear due to the n^{th} mode of vibration is given by (Paz 1994)

$$V_n = \frac{W_n}{g} S_{an} \tag{6B.1}$$

in which g is the acceleration due to gravity, S_{an} is the value of pseudo-acceleration response for the n^{th} natural frequency and W_n is the effective weight of the structure in the n^{th} mode of vibration. W_n can be calculated as follows

$$W_n = \frac{L_n^2}{M_n} g \tag{6B.2}$$

where L_n and M_n for the n^{th} natural mode are

$$L_n = \boldsymbol{\varphi}_n^T \mathbf{M} \mathbf{r} \tag{6B.3}$$

and

$$M_n = \boldsymbol{\varphi}_n^T \mathbf{M} \boldsymbol{\varphi}_n \tag{6B.4}$$

M_n is defined as the generalised mass and $\boldsymbol{\varphi}_n$ is the vector of the n^{th} mode shape, $\mathbf{M}$ is the mass matrix and $\mathbf{r}$ is the influence factor, in which the components that have the same direction as the ground motion are 1 and the rest are zero.

Based on the SRSS (Square Root of Sum Squares) method, the final base shear is obtained as

$$V = \sqrt{\sum V_n^2} \tag{6B.5}$$

The ratio of the base shear due to the n^{th} mode of vibration to the total base shear of the structure will be used as the importance factor of the n^{th} mode, e_n, and can be calculated as follows.

$$e_n = \frac{(W_n S_{an})^2}{\sum (W_n S_{an})^2} \tag{6B.6}$$

In this study, the "Iranian code of practice for seismic resistance design of buildings" (Paz 1994) has been used for S_{an}.

CHAPTER 7

SUMMARY, CONCLUSIONS AND FUTURE WORK

7.1 SUMMARY

This thesis presents two global analysis approaches to the calculation of the natural frequencies of high rise buildings. The structures are proportional and their component members are repeated at each storey level unless there is a step change of properties. Within this scope many geometric configurations can be encompassed, ranging from uniform structures with doubly symmetric floor plans to doubly asymmetric ones comprising plane frame and wall structures running in two orthogonal directions.

The first method utilises a continuum element approach in which the structure is divided into segments by cutting through the structure horizontally at those storey levels corresponding to changes in storey properties. A typical segment is then replaced by an appropriate substitute beam that has uniformly distributed mass and stiffness. Subsequently, the governing differential equations of the substitute beam are formulated using the continuum approach and posed in the form of a dynamic member stiffness matrix that is precise to small deflection theory. Since the formulation allows for the

distributed mass and stiffness of the member, it necessitates the solution of transcendental eigenvalue problem. The required natural frequencies are thus determined using a simple cantilever model in conjunction with the Wittrick-Williams algorithm (Wittrick and Williams 1971), which ensures that no natural frequencies can be missed. Also, a cubic equation has been derived for imposing the relationship between the uncoupled and coupled frequencies which enables that the coupled three-dimensional vibration problems can be dealt using a two dimensional approach in certain cases.

The second method utilises the Principle of Multiples which, when applicable, enables any frame, regardless of the number of storeys or bays, to be simplified to an equivalent one bay frame, that had precisely the same natural frequencies. If the original frame does not satisfy the Principle, the same process can still be obtained, but the resulting substitute frame will yield approximate frequencies, although they will normally be acceptable engineering accuracy. Like the first method, it can also be used for the vibration analysis of asymmetric, three-dimensional frame and wall-frame structures in a two-step procedure. First the analogous uncoupled system is analysed using substitute frames then the relationship between the uncoupled and coupled responses is imposed through a cubic equation.

In general, the computation of the coupled vibration of building structures may be done by using appropriate finite element software. However, the analytical technique of continuum modelling, as well as using the substitute frame method, not only provide a simple and convenient means for the analysis of coupled vibrations, but also permit direct and easy visualisation of the dynamic performance of building structures. In turn this leads to a qualitative understanding of how the natural frequencies and corresponding mode shapes of uncoupled and coupled vibration are related to the structural parameters through the use of quick and effective parametric studies.

Finally, the proposed methods require relatively little effort, offer clear and concise output and can sometimes yield solutions of sufficient accuracy for definitive checks, but more usually provide engineering accuracy for intermediate checks during tasks such as scheme development or remedial work. This claim is supported by the results of relatively extensive parametric studies done in the "Numerical Results" section of Chapters 2 to 6 of this thesis. In examples of Chapters 3,5 and 6, the results from the proposed methods have

been compared with the results of a full finite element analysis of the original structure obtained using the vibration programme ETABS (Wilson et al. 1995). The exercise confirms that the proposed methods can yield results of sufficient accuracy for engineering calculations.

7.2 CONCLUSIONS

The principle objectives of the investigation into the coupled vibration of asymmetric structures have been achieved, as described above. Also, since every chapter of this thesis has its own conclusions, it is now appropriate to bind these together and emphasise the major conclusions, as follows

1. The thesis systematically describes the calculation of the natural frequencies for both uncoupled and coupled vibration of symmetric and asymmetric structures. Structure properties may be uniform throughout the height of the structure or may have step changes of properties at one or more storey levels.
2. This is achieved using two global analysis approaches to the vibration analysis of symmetric and asymmetric structures. The first method is based on the well-established and well-known continuum approach in which a building structure may be replaced by a cantilever continuum representing both structural characteristics and geometric properties. The second method is based on the Principle of Multiples and offers the possibility of replacing the original structure by substitute frames that normally yield solutions of engineering accuracy, but under certain conditions provide precise solutions.
3. A cubic equation has been derived for imposing the relationship between the uncoupled and coupled frequencies of asymmetric, three-dimensional structures. It was shown that this relation is precise for a uniform shear cantilever and can also yield results of good accuracy for other cases.
4. The results of parametric studies on asymmetric structures show that the effect of coupling between the natural frequencies should be taken into account, since ignoring it can lead to substantial inaccuracy.

5. Results from the continuum method improves as the building height increases. It always gives results of sufficient accuracy for engineering calculations in building structures with more than 10 storeys.
6. The Substitute Frame method normally yields results to acceptable engineering accuracy for most regular buildings with any number of storeys. It was shown in Chapter 6 that a one-bay substitute frame (Type F-F) can still lead to results of sufficient accuracy for wall-frame structures.
7. A practical method to locate the centers of rigidity, shear centers and hence static eccentricity has been given. It was shown that the method has major advantages in comparison with Cheung and Tso's method (Cheung and Tso 1986). It was also shown that the centers of rigidity and shear centers of the floors of multi-storey buildings do not generally coincide. Their locations are not only dependent on the geometric and stiffness characteristics of the building, but also on the lateral forces. Also, their locations rarely lie on a vertical line through the height of the structure. A particular class of buildings was distinguished, the so called proportional buildings, in which the centers of rigidity and shear of the floors are coincident, load independent and lie on a vertical line throughout the height of the structure.
8. The research carried out in this thesis can be considered as a second basis for the development of a more general theoretical approach to the coupled vibration analysis of a variety of tall buildings.

7.3 FUTURE WORK

The following suggestions are made as to how the current work may be extended.

1. A more detailed study into the vibration analysis of two-dimensional structures with cladding
2. Developing the substitute beam approach for plane coupled shearwalls
3. Study of the vibration of symmetric and asymmetric structures comprising walls and/or cores

4. Extending substitute beam method to cover asymmetric structures comprising walls, frames, cores and coupled shear walls.
5. Extending the proposed methods to include structures with an arbitrary configuration of plane resisting elements i.e. frames, walls, cores and coupled shear walls (not running in two orthogonal directions)
6. A further investigation into the accuracy of the cubic equation that imposes the relationship between the uncoupled and coupled natural frequencies of the asymmetric, three-dimensional structures
7. Investigating the vibration of three-dimensional shear and flexural beams with asymmetric cross-section using the two-dimensional approach
8. Assessing the affect of axial deformation of columns and beams on overall behaviour of the structures (no inextensible member theory assumption)
9. Investigating the relationship between the uncoupled and coupled natural frequencies end assessing the accuracy of Eq. (6.180) for variety of end conditions
10. Extending the method of Chapter 4 for analysing three-dimensional asymmetric structures using two-dimensional approach.
11. The method of Chapter 4 can also be extended to cover the analysis of symmetric and asymmetric structures with flexible floor diaphragms.
12. More study is also required on the definitions of centres of shear and rigidity of non-proportional buildings in earthquake codes.
13. Investigating the analogous buckling problem for those cases that have been identified in this thesis or have been suggested above

REFERENCES

Anderson, M. S., and Williams, F. W. (1986). ""BUNVIS-RG: an exact buckling and vibration program for latice structures , with repetitive geometry and substructuring options." *Structural dynamics and materials conference paper No AIAA 86-0868-CP*, San Antonio, Texas, 211-220.

Armstrong, I. D. (1969a). "The natural frequencies of multi-storey frames." *The Structural Engineer*, 47.

Armstrong, I. D. (1969b). *Tables of dynamic stiffnesses and carry-over factors*, Civil Engineering Department, Heriot-Watt University, Edinburgh.

Banerjee, J. R. (1989). "Coupled Bending Torsional Dynamic Stiffness Matrix for Beam Elements." *International Journal for Numerical Methods in Engineering*, 28(6), 1283-1298.

Banerjee, J. R. (1997). "Dynamic stiffness formulation for structural elements: A general approach." *Computers & Structures*, 63(1), 101-103.

Banerjee, J. R., Guo, S., and Howson, W. P. (1996). "Exact dynamic stiffness matrix of a bending-torsion coupled beam including warping." *Computers & Structures*, 59(4), 613-621.

Banerjee, J. R., and Williams, F. W. (1985). "Exact Bernoulli-Euler Dynamic Stiffness Matrix for a Range of Tapered Beams." *International Journal for Numerical Methods in Engineering*, 21(12), 2289-2302.

Banerjee, J. R., and Williams, F. W. (1992). "Coupled Bending-Torsional Dynamic Stiffness Matrix for Timoshenko Beam Elements." *Computers & Structures*, 42(3), 301-310.

Banerjee, J. R., and Williams, F. W. (1994a). "Clamped Clamped Natural Frequencies of a Bending Torsion Coupled Beam." *Journal of Sound and Vibration*, 176(3), 301-306.

Banerjee, J. R., and Williams, F. W. (1994b). "Coupled Bending-Torsional Dynamic Stiffness Matrix of an Axially Loaded Timoshenko Beam Element." *International Journal of Solids and Structures*, 31(6), 749-762.

Banerjee, J. R., and Williams, F. W. (1995). "Free-Vibration of Composite Beams - an Exact Method Using Symbolic Computation." *Journal of Aircraft*, 32(3), 636-642.

Basu, A. K. (1983). "Seismic design charts for coupled shear walls." *Journal of Structural Engineering - ASCE*, 109(2), 335-352.

Blaszkowiak, S., and Kaczkowski, Z. (1966). *Iterative methods in structural analysis*, Pergamon Press, Oxford, England.

Bolton, A. (1955). "The critical load of portal frames when sidesway is permitted." *The Structural Engineer*, 33.

Bolton, A. (1969). "The natural frequencies of continuous beams." *The Structural Engineer*, 47.

Bolton, A. (1976). "A simple understanding of elastic critical loads." *Struct. Engr.*, 54(6), 213-218.

Bolton, A. (1978). "Natural Frequencies of Structures for Designers." *The Structural Engineer*, 56A(9), 245-253.

Capron, M. D., and Williams, F. W. (1988). "Exact dynamic stiffnesses for an axially loaded uniform timoshenko member embedded in an elastic medium." *Journal of Sound and Vibration*, 124(3), 453-466.

Cheng, F. Y. (1970). "Vibrations of Timoshenko beams and frameworks." *Journal of Structural Engineering-Asce*, 96(ST3), 551-571.

Cheung, V. W. T., and Tso, W. K. (1986). "Eccentricity in Irregular Multi-storey Buildings." *Canadian Journal of Civil Engineering*, 13(1), 46-52.

Chopra, A. K. (2000). *Dynamics of Structures, Theory and applications to Earthquake Engineering*, Prentice Hall.

Coull, A., and Smith, B. S. (1973). "Torsion analysis of symmetric building structures." *Journal of Structural Engineering-Asce*, 99(ST1), 229-233.

Delpak, R., Howson, W. P., and Richards, V. M. (1997). "Comparison Between Measured and Predicted Natural Frequencies of a Full Scale Building." *Proc of 5th International Conference on Modern Building Materials, Structures and Techniques*, Vilnius, Llthuania, 161-166.

Dokumaci, E. (1987). "An Exact Solution for Coupled Bending and Torsion Vibrations of Uniform Beams Having Single Cross-Sectional Symmetry." *Journal of Sound and Vibration*, 119(3), 443-449.

Falco, M., and Gasparetto, M. (1973). "Flexural-torsional vibration of thin-walled beams." *Meccanica*, 8, 181-189.

Friberg, P. O. (1983). "Coupled Vibrations of Beams - an Exact Dynamic Element Stiffness Matrix." *International Journal for Numerical Methods in Engineering*, 19(4), 479-493.

Friberg, P. O. (1985). "Beam Element Matrices Derived from Vlasovs Theory of Open Thin- Walled Elastic Beams." *International Journal for Numerical Methods in Engineering*, 21(7), 1205-1228.

Gere, J. M., and Lin, Y. K. (1958). "Coupled vibrations of thin-walled beams of open cross-section." *Journal of Applied Mechanics*, 25, 373-378.

Grinter, L. E. (1937). *Theory of modern steel structures*, Macmillan, N.Y.

Gupta, K. K. (1970). "Vibration of frames and other structures with banded stiffness matrix." *International Journal for Numerical Methods in Engineering*, 2.

Hallauer, W. L., and Liu, Y. L. (1982). "Beam bending-torsion dynamic stiffness method for calculation of exact vibration modes." *Journal of Sound and Vibration*, 85(1), 105-113.

Hejal, R., and Chopra, A. K. (1987). "Earthquake Response of Torsionally Coupled Buildings." Earthquake Engineering Research Centre, University of California at Berkeley, Report No. UCB/EERC-87/20.

Henshell, R. D., and Warburton, G. B. (1969). "Transmission of vibration in beam systems." *International Journal for Numerical Methods in Engineering*, 1, 47-66.

Horne, M. R. (1975). "An Approximate Method for Calculating the Elastic Critical Loads of Multi-Storey Plane Frames." *The Structural Engineer*, 53(6).

Horne, M. R., and Merchant, W. (1965). *The stability of frames*, Pergamon, Oxford.

Howson, W. P. (1979). "A Compact Method for Computing the Eigenvalues and Eigenvectors of Plane Frames." *Advances in Engineering Software and Workstations*, 1(4), 181-190.

Howson, W. P. (1985). "A Teaching, Analysis and Design Program for the Complete Eigensolution of Plane Frames Using Microcomputers." *International Conference on Education, Practice and Promotion of Computational Methods in Engineering Using Small Computers (EPMESC)*, Macau.

Howson, W. P., Banerjee, J. R., and Williams, F. W. (1983). "Concise Equations and Program for Exact Eigensolutions of Plane Frames Including Member Shear." *Advances in Engineering Software and Workstations*, 5(3), 137-141.

Howson, W. P., and Jemah, A. K. (1999a). "Exact dynamic stiffness method for planar natural frequencies of curved Timoshenko beams." *Proceedings of the Institution*

of Mechanical Engineers Part C- Journal of Mechanical Engineering Science, 213(7), 687-696.

Howson, W. P., and Jemah, A. K. (1999b). "Exact out-of-plane natural frequencies of curved Timoshenko beams." *Journal of Engineering Mechanics-ASCE*, 125(1), 19-25.

Howson, W. P., Jemah, A. K., and Zhou, J. Q. (1995). "Exact Natural Frequencies for out-of-Plane Motion of Plane Structures Composed of Curved Beam Members." *Computers & Structures*, 55(6), 989-995.

Howson, W. P., and Rafezy, B. (2002). "Torsional analysis of asymmetric proportional building structures using substitute plane frames." *Advances in steel structures*, Hong Kong, 1177-1184.

Howson, W. P., and Williams, F. W. (1973). "Natural frequencies of frames with axially loaded Timoshenko members." *Journal of Sound and Vibration*, 26(4), 503-515.

Howson, W. P., and Williams, F. W. (1999). "A unified principle of multiples for lateral deflection, buckling and vibration of multi-storey, multi-bay, sway frames." *Advances in Steel Structures, Vols 1 and 2*, 87-98.

Humar, J. L., and Awad, A. M. (1983). "Design of seismic torsional forces." *4th Canadian Conference on Earthquake Engineering*, Vancouver, Canada, 251-260.

Japan Earthquake Code, International Association for Earthquake Engineering, Earthquake resistant regulations. (1980). Tokyo." 503-519.

Issa, M. S. (1988). "Natural frequencies of continuous curved beams on Winkler-type foundation." *Journal of Sound and Vibration*, 127, 291-301.

Jiang, W., Hutchinson, G. L., and Chandler, A. M. (1993). "Definitions of static eccentricity for design of asymmetric shear buildings." *Engng Struct.*, 15(3), 167-178.

Kollar, L. P. (1991). "Calculation of plane frames braced by shear walls for seismic load." *Acta Technica Academiae Scientiarum Hungaricae*, 104(1-3), 187-209.

Kopecsiri, A., and Kollar, L. P. (1999a). "Approximate seismic analysis of building structures by the continuum method." *Acta Technica Academiae Scientiarum Hungaricae*, 108(3-4), 417-446.

Kopecsiri, A., and Kollar, L. P. (1999b). "Simple formulas for the analysis of symmetric (plane) bracing structures subjected to earthquakes." *Acta Technica Academiae Scientiarum Hungaricae*, 108(3-4), 447-473.

Kuang, J. S., and Ng, S. C. (2000). "Coupled lateral-torsion vibration of asymmetric shear-wall structures." *Thin-Walled Structures*, 38(2), 93-104.

Kuang, J. S., and Ng, S. C. (2001). "Dynamic coupling of asymmetric shear wall structures: an analytical solution." *International Journal of Solids and Structures*, 38(48-49), 8723-8733.

Laursen, H. I., Shubinski, R. P., and Clough, R. W. (1962). "Dynamic matrix analysis of framed structures." *Proceedings of the Forth U.S. National Congress on Applied Mechanics 1*.

Lightfoot, E. (1956a). "The analysis of wind loading of rigid-jointed multi-storey building frames (1)." *Civil Engineering and Public Works Review*, 51(601), 757-759.

Lightfoot, E. (1956b). "The analysis of wind loading of rigid-jointed multi-storey building frames (2)." *Civil Engineering and Public Works Review*, 51(602), 887-889.

Lightfoot, E. (1957). "Substitute frames in the analysis of rigid jointed structures (Part 1)." *Civil Engineering and Public Works Review*, 52(618), 1381-1383.

Lightfoot, E. (1958). "Substitute frames in the analysis of rigid jointed structures (Part 2)." *Civil Engineering and Public Works Review*, 53(619), 70-72.

Macleod, I. A. (1970). "Shear Wall-Frame Interaction - a design aid." Portland cement association PCA.

Macleod, I. A. (1990). *Analytical modeling of structural systems*, Ellis Horwood Limited, Great Britain.

Macleod, I. A., and Zalka, K. A. (1996). "The global critical load ratio approach to stability of building structures." *The Structural Engineer*, 74(15), 249-254.

Mohsin, M. E., and Sadek, E. A. (1968). "The distributed mass-stiffness technigue for the dynamical analysis of complex frameworks." *The Structural Engineer*, 46, 345-351.

Ng, S. C., and Kuang, J. S. (2000). "Triply coupled vibration of asymmetric wall-frame structures." *Journal of Structural Engineering-Asce*, 126(8), 982-987.

Paz, M. (1994). "International handbook of earthquake engineering." Chapman & Hall.

Peters, G., and Wilkinson, J. H. (1969). "Eigenvalues of $Ax=\lambda Bx$ with band symmetric A and B." *The Computer Journal*, 12.

Poole, R. A. (1977). "Analysis for torsion employing provisions of NZRS 4203." *Bulletin of the Newzelan national society for earthquake engineering*, 10(4), 219-225.

Popper, K. R. (1977). *The logic of scientific discovery*, Hutchison.

Potzta, G., and Kollar, L. P. (2003). "Analysis of building structures by replacement sandwich beams." *International Journal of Solids and Structures*, 40, 535-553.

Rafezy, B., and Howson, W. P. (2003). "Natural frequencies of plane sway frames: An overview of two simple models." *Proceedings of ICCES2003: International Conference on computational and Expermental Engineering and Sciences*, Corfu, Greece, 1-6.

Rafezy, B., and Howson, W. P. (2004). "Exact dynamic stiffness matrix of a three-dimensional shear beam with doubly asymmetric cross-section." *J. Sound Vib.*, Submitted in April 2004.

Rayleigh, J. W. S. (1877). *Theory of sound*, Dover Publications, 1945 re-issue, New York.

Riddell, R., and Vásquez, J. (1984). "Existence of Centers of Resistance and Torsional Uncoupling of Earthquake Response of Buildings." *Proceedings of the 8th World Conference on Earthquake Engineering*, San Francisco, 187-194.

Roberts, E. H., and Wood, R. H. (1981). "A Simplified Method for Evaluation the Natural Frequencies and Corresponding Modal Shapes of Multistorey Frames." *The Structural Engineer*, 59B(1), 1-9.

Rosman, R. (1974). "Stability and dynamics of shear wall frame structures." *Build. Sci.*, 9, 55-63.

Rutenberg, A. (1975). "Approximate natural frequencies for coupled shear walls." *Earthquake engineering and structural dynamics*, 4, 95-100.

Skattum, S. K. (1971). "Dynamic analysis od coupled shear walls and sandwich beams."

Smith, B. S., and Coull, A. (1991). *Tall building structures*, John Wiley & Sons, Inc., New York.

Smith, B. S., and Crowe, E. (1986). "Estimating Periods of Vibration of Tall Buildings." *Journal of Structural Engineering-Asce*, 112(5), 1005-1019.

Smith, B. S., and Vezina, S. (1985). "Evaluation of Centres of Resistance in Multi-storey Building Structures." *Proceedings of the Institution of Civil Engineers Part 2-Research and Theory*, 79(DEC), 623-635.

Smith, B. S., and Yoon, Y. S. (1991). "Estimating seismic base shears of tall wall-frame buildings." *Journal of Structural Engineering - ASCE*, 117(10), 3026-3041.

Tarani, T. (1999). "Summation theorems concerning critical loads of Bi-furcation"." *Structural Stability in Engineering Practice*, Spon, 23-58.

Tarjan, G., and Kollar, L. P. (2004). "Approximate analysis of building structures with identical stories subjected to earthquakes." *International Journal of Solids and Structures*, 41, 1411-1433.

Timoshenko, S. P. (1921). "On the correction for shear of the differential equation for transverse vibrations of prismatic bars." *Philosophical Magazine*, 41.

Timoshenko, S. P., Young, D. H., and Weaver, W. (1974). *Vibration problems in engineering*, Wiley, New York.

Tso, W. K. (1984). "Torsions in multi-storey buildings." *3rd Int. Conf. on Tall Buildings.*

Veletsos, A. S., and Newmark, N. M. (1955). "Natural frequencies of continuous flexural members." *Journal of the structural division - ASCE*, 81.

Wang, T. M., and Kinsman, T. A. (1971). "Vibration of frame structures according to the Timoshenko theory." *Journal of Sound and Vibration*, 14, 215-227.

Wang, Y., Arnaouti, C., and Guo, S. (2000). "A simple approximate formulation for the first two frequencies of asymmetric wall-frame multi-storey building structures." *Journal of Sound and Vibration*, 236(1), 141-160.

Wilkinson, J. H. (1965). *The algebric eigenvalue problem*, Clarendon Press, Oxford.

Williams, F. W. (1977). "Simple Design Procedures for Unbraced Multi-Storey Frames." *Proc. Instn Civ. Engrs*, 63, 475-479.

Williams, F. W. (1979). "Consistent, exact, wind and stability calculationsfor substitute sway frames with cladding." *Proc. Instn Civ. Engrs*,.

Williams, F. W., Bond, M. D., and Fergusson, L. (1983). "Accuracy of natural frequencies given by substitute sway frames with cladding." *Proc. Instn Civ. Engrs.*, 129-135.

Williams, F. W., and Butler, R. (1988). "Simple Calculation for Wind Deflection of Multi-Storey Rigid Sway Frames." *Proc. Instn Civ. Engrs*, 551-565.

Williams, F. W., and Howson, W. P. (1977). "Accuracy of Critical Loads Obtained Using Substitute Frames." *Stability of Steel Structures*, Liege, 511-515.

Williams, F. W., and Kennedy, D. (1987). "Exact dynamic member stiffness for a beam on an elastic foundation." *Earthquake Engineering & Structural Dynamics*, 15, 133-136.

Williams, F. W., and Wittrick, W. H. (1983). "Exact Buckling and Frequency Calculations Surveyed." *Journal of Structural Engineering - ASCE*, 109(1), 169-187.

Wilson, E. L., Hollings, J. P., and Dovey, H. H. (1995). "ETABS version 6, three-dimensional analysis of building structures." Berkeley, California.

Wittrick, W. H., and Williams, F. W. (1971). "A General Algorithm for Computing Natural Frequencies of Elastic Structures." *The Quarterly Journal of Mechanics and Applied Mathematics*, 24(3), 263-284.

Wood, R. H. (1974a). "Effective Lengths of Columns in Multi-Storey Buildings - Part 1." *The Structural Engineer*, 52(7), 235-244.

Wood, R. H. (1974b). "Effective Lengths of Columns in Multi-Storey Buildings - Part 2." *The Structural Engineer*, 52(8), 295-302.

Wood, R. H. (1974c). "Effective Lengths of Columns in Multi-Storey Buildings - Part 3." *The Structural Engineer*, 52(9), 341-346.

Zalka, K. A. (1979). "Buckling of a cantilever subjected to distributed normal loads, taking shearing deformation into account." *Acta Technica Academiae Scientiarum Hungaricae*, 89(3-4), 497-508.

Zalka, K. A. (2001a). *Global structural analysis of buildings*, E&FN Spon, London.

Zalka, K. A. (2001b). "A simplified method for calculation of the natural frequencies of wall-frame buildings." *Engineering Structures*, 23(12), 1544-1555.

Zalka, K. A., and Macleod, I. A. (1996). "The equivalant column concept in stability analysis of buildings." *The structural Engineer*, 74(23&24), 405-411.